



HAL
open science

Dual-arm robotic manipulation inspired by human skills

Marija Tomic

► **To cite this version:**

Marija Tomic. Dual-arm robotic manipulation inspired by human skills. Automatic. École centrale de Nantes; Univerzitet u Beogradu, 2018. English. NNT : 2018ECDN0017 . tel-01959569

HAL Id: tel-01959569

<https://theses.hal.science/tel-01959569>

Submitted on 18 Dec 2018

HAL is a multi-disciplinary open access archive for the deposit and dissemination of scientific research documents, whether they are published or not. The documents may come from teaching and research institutions in France or abroad, or from public or private research centers.

L'archive ouverte pluridisciplinaire **HAL**, est destinée au dépôt et à la diffusion de documents scientifiques de niveau recherche, publiés ou non, émanant des établissements d'enseignement et de recherche français ou étrangers, des laboratoires publics ou privés.

THESE DE DOCTORAT DE

L'ÉCOLE CENTRALE DE NANTES

COMUE UNIVERSITE BRETAGNE LOIRE

Et l'UNIVERSITÉ DE BELGRADE

FACULTE DE GENIE ELECTRIQUE

ECOLE DOCTORALE N° 601

*Mathématiques et Sciences et Technologies
de l'Information et de la Communication*

Spécialité : Automatique, productique et robotique

Par

Marija TOMIĆ

Manipulation robotique à deux mains inspirée des aptitudes humaines

Thèse présentée et soutenue à Faculté de Génie Electrique de Belgrade, le 04/07/2018

Unité de recherche : Laboratoire des Sciences du Numérique de Nantes et Faculté de Génie Electrique

Rapporteurs avant soutenance :

Philippe FRAISSE

Professeur des Universités, Université Montpellier, Laboratoire d'Informatique, de Robotique et de Microélectronique de Montpellier

Željko ĐUROVIĆ

Professeur des Universités, Université de Belgrade, Faculté de Génie Electrique

Composition du Jury :

Président :

Željko ĐUROVIĆ

Professeur titulaire, Université de Belgrade, Faculté de Génie Electrique

Examineurs :

Aleksandar RODIĆ

Conseiller scientifique, Université de Belgrade, Institut Mihailo Pupin

Yannick Aoustin

Professeur titulaire, Université de Nantes, Laboratoire des Sciences du Numérique de Nantes

Dir. de thèse :

Christine CHEVALLEREAU

Directeur de Recherche, CNRS, Laboratoire des Sciences du Numérique de Nantes

Kosta JOVANOVIĆ

Professeur adjoint, Université de Belgrade, Faculté de Génie Electrique

Titre : Manipulation robotique à deux mains inspirée des aptitudes humaines

Mots clés : habileté humaine, commande optimale inverse, cinématique inverse, imitation de mouvements humains, robots humanoïdes.

Résumé : Le nombre de robot humanoïde s'est accru ces dernières années pour pouvoir collaborer avec l'homme ou le remplacer dans des tâches fastidieuses. L'objectif de cette thèse est de transférer aux robots humanoïdes, des habiletés ou compétences humaines, en particulier pour des mouvements impliquant une coordination entre les deux bras. Dans la première partie de la thèse, un processus de conversion d'un mouvement humain vers un mouvement de robot, dans un objectif d'imitation est proposé. Comme les humains possèdent beaucoup plus de degrés de liberté qu'un robot humanoïde, les mouvements identiques ne peuvent pas être produits, les caractéristiques (longueurs des corps) peuvent aussi être différentes. Notre processus de conversion prend en compte l'enregistrement des

des localisations de marqueurs attachés aux corps de l'humain et des articulations pour améliorer les processus d'imitation.

La deuxième partie de la thèse vise à analyser les stratégies de génération du mouvement utilisées par l'homme. Les mouvements humains sont supposés optimaux et notre objectif est de trouver un critère à minimiser pendant les manipulations. Nous faisons l'hypothèse que ce critère est une combinaison de critères classiquement utilisés en robotique et nous recherchons les poids de chaque critère qui représente au mieux le mouvement humain. De cette façon, une approche de commande cinématique optimale peut ensuite être utilisée pour générer des mouvements du robot humanoïde.

Title : Dual-arm robotic manipulation inspired by human skills

Keywords : human motion skills, inverse optimal control algorithm, inverse kinematics algorithm, human motion imitation, humanoid robots.

Abstract : The number of humanoid robots has increased in recent years to be able to collaborate with humans or replace them in tedious tasks. The objective of this thesis is to transfer to humanoid robots, skills or human competences, in particular for movements involving coordination between the two arms. In the first part of the thesis, a process of conversion from a human movement to a robot movement, with the aim of imitation is proposed. Since humans have much more freedom than a humanoid robot, identical movements cannot be produced, the characteristics (body lengths) can also be different. Our conversion process takes into account the recording of marker locations attached to human bodies and joints to improve the imitation processes.

The second part of the thesis aims at analyzing the strategies used by humans to generate movement. Human movements are assumed to be optimal and our goal is to find criteria minimized during manipulations. We hypothesize that this criterion is a combination of classical criteria used in robotics and we look for the weights of each criterion that best represents human movement. In this way, an optimal kinematic control approach can then be used to generate movements of the humanoid robot.

Acknowledgments

Firstly, I would like to express my sincere gratitude to my advisors Dr. Christine Chevallereau, Dr. Kosta Jovanović and Dr. Veljko Potkonjak for their patience and guidance.

I would like to thank the Institut "Mihajlo Pupin" and LS2N, ECN, for all the support I received during my PhD. Also, thanks to the Institut Francais Serbie, for providing me the means to complete my doctorate studies.

I would like to thank the members of my thesis committee and express my gratitude for all the support they gave me during the development of this work. In addition, a very special thank you to Dr. Mirjana Filipović, Dr. Yannick Aoustin, Dr. Philippe Lemoine, Dr. Philippe Wenger and Dr. Wisama Khalil for their valuable comments and discussions.

My sincere thanks to my friends and colleges Vesna, Ljubinko, Zarko, Nemanja, Marijana, Jelena, Rada, Anastasia, Natalia, Oscar, Eduardo, Loriane, Ivanka and Sebastian for their invaluable help and friendship. Also I would like to thank to my friends who participate in my experiments: Guillaume, Hendry, Sahab, Taghit, Narek, Maxime, Vincent, Bertrand, Joan, Kosta, Luis, Misbah, Tiago, Arun.

Finally, thanks to my family Miroslav, Ljubica, Nebojša, Dušan for their trust, their love, and for being my greatest motivation and inspiration. Thank you!

Dissertation title: Dual-arm robotic manipulation inspired by human skills

Abstract: Man's desire to shape the world to fit his ideas (or vision) has led to major technological achievements. Many machines have been inspired by biological systems and processes observed in nature. The greatest challenge for the research engineer is to develop a human-like mechanical system that has the skills of a human being. The shape of the human body has largely inspired the mechanical structure of humanoid robots. Current efforts of researchers in humanoid robotics and cognitive sciences are aimed at translating models of human behavior to humanoid robots. Modeling of human movement has been extensively studied and explored in the literature, to design and control a humanoid robot inspired by human movement in daily human activities. Various scientific disciplines analyze human movement in different ways. There are many techniques and strategies for imitating and analyzing human motions, such as the motion imitation process, imitation learning, and optimization approaches.

The objectives of this thesis are to:

- improve the conversion process for the imitation of human upper-body movement by a humanoid, for a task with and/or without contact between hands and equipment;
- define an objective function optimized by human movement, in order to transfer human skills to humanoid robots; and
- execute humanoid robot motion similar to human motion, by minimizing the same criteria.

Since the human model is complex and has many degrees of freedom, the goal is to imitate human motion and transfer human skills to a humanoid robot with fewer degrees of freedom. To this end, a kinematic model of the robot ROMEO was used as the kinematic model of a human body. The motions of a human being that uses both arms to perform a task, including contact with the environment, are analyzed in the thesis. This type of motion has not been sufficiently explored in the literature.

A conversion process for the imitation of human motion by a humanoid robot is proposed in the first part of the thesis. This conversion process enhances existing techniques and was developed to imitate human motion and have a humanoid robot perform a task with and/or without contact between hands and equipment. The proposed conversion process takes into account the situation of marker frames and the position of joints and

ensures more precise imitation than previously proposed methods. Precise imitation of hand motion in Cartesian space is essential for the task where the hands come into contact with the environment. The conversion process is based on the analytical expression of the kinematic model and is able to define the motion generated by the robot in real time. The results were tested on the robot ROMEO, which performed complex dual-arm manipulation tasks.

The second part of the thesis analyzes strategies for the generation of human motion. Based on the assumption that human movement is optimal, the aim was to define an unknown objective function, minimized during the manipulation tasks. Consequently, the inverse optimal control approach was used. The objective function is written as a weighted sum of well-known basic criterion functions of process optimization in robotics, such as the minimization of kinetic energy, minimization of joint velocity, improved manipulability, and minimization of deviations from the ergonomic position of the human. The optimal combination of criteria, which best represented the recorded human motion, was sought. For that purpose, the motion resulting from the minimization of the weighted criteria was compared to the motion recorded during human manipulations. A genetic algorithm suitable for solving global optimization problems was used in the task. Several manipulation tasks were analyzed and several people performed the same tasks. The objective was to study how the optimized criteria vary depending on the tasks and the people. The optimized criteria are shown to vary and be contingent upon the type of motion and the amplitude of the shoulder, elbow and wrist movement. The effect of the characteristics of the human body and the environment (involved equipment) on the achievement of motions was also examined.

This study produced optimized criteria, which could be used to generate motion of the humanoid robot inspired by human motion. In order to generate the same motion as that of a human, the humanoid robot can minimize the same criteria using the inverse kinematics algorithm. Experimental tests were conducted for the opening/closing drawer task. It was noted that adaptation of the motion was necessary, to take into account the size of the robot and its working space. This thesis aims to better integrate robots in human environments. In addition, the proposed algorithm is applicable in rehabilitation medicine.

The analysis of human motions made it possible to establish rules that, based on observed joint motions, define the minimized criteria. This approach is followed in the third and final part of the thesis, where a fuzzy logic algorithm is proposed and tested for the transfer of human skills to humanoid robots. The fuzzy algorithm estimates the weights of the criteria defined in the objective function, according to the human motion recorded in the joint space. The fuzzy logic algorithm should be able to generate an objective function for each type of dual-arm human motion, regardless of whether it had previously been analyzed or not. An inverse kinematic model, adapted to minimize criteria, can be used to generate humanoid robot motion.

Keywords: human motion skills, inverse optimal control algorithm, inverse kinematics algorithm, human motion imitation, humanoid robots.

Scientific field: Electrical and Computer Engineering

Research area: Robotics and Control Systems

UDC number: 621.3

Naslov teze: Dvoručna manipulacija inspirisana ljudskim veštinama

Rezime: Čovekova želja da stvori svet po svojoj zamisli (ili viziji) dovela je do razvoja velikih tehničkih dostignuća. Inspiracije za stvaranje brojnih mašina istraživači su pronašli posmatranjem bioloških sistema i procesa u prirodi. Najveći izazov za istraživača je razvoj mehaničkog sistema nalik čoveku koji ima karakteristike ljudskog bića. Mehanička struktura ljudskog tela u velikoj meri je mapirana u model humanoidnih robota. Sadašnji naponi istraživača u oblasti humanoidne robotike i kognitivnih nauke su da transformišu modele ljudskog ponašanja i procesa u model humanoidnih robota. Modeliranje ljudskog pokreta široko je proučavano i istraživano u literaturi sa ciljem da se dizajnira humanoidni robot i definiše njegovo upravljanje inspirisano karakteristikama ljudskog pokreta u svakodnevnim ljudskim aktivnostima. Razne discipline nauke analiziraju ljudsko kretanje na različite načine. Postoje brojne tehnike i strategije koje imitiraju i analiziraju ljudsko kretanje, kao što su imitacioni proces, učenje iz imitacije i optimizacioni pristupi.

Cilj ove teze je:

- da unapredi konverzione procese za imitaciju pokreta gornjeg dela tela čoveka sa humanoidnim robotom za zadatke sa ili bez kontakata između ruku i opreme;
- da definiše objektivnu funkciju koja predstavlja optimizirano ljudsko kretanje sa ciljem prenošenja ljudskih veština na humanoidne robote; i
- da humanoidni robot izvršava pokret na isti način kao čovek minimiziranjem istih kriterijuma

S obzirom da je model čoveka kompleksan i obuhvata mnogo stepeni slobode, naš cilj je da se ljudski pokret i veštine kretanja prenesu na kretanje humanoidnog robota sa manje stepeni slobode. U tu svrhu, kinematski model robota ROMEO je korišćen za predstavljanje kinematskog model ljudskog tela. Pokreti dvoručne manipulacije koji uključuju kontakt sa okruženjem su predmet istraživanja u tezi. Ova vrsta kretanja nije dovoljno istražena u literaturi.

U prvom delu teze predložen je konverzioni proces za imitaciju ljudskog kretanja sa humanoidnim robotom. Ovaj konverzioni proces poboljšava postojeće tehnike i razvijen je za imitaciju ljudskog kretanja sa humanoidnim robotom za izvođenje zadataka sa ili/i bez kontakata između ruku i opreme. Predstavljeni konverzioni proces uzima u obzir poziciju i orijentaciju markera i poziciju zglobova i pruža precizniju imitaciju ljudskih

pokreta od prethodno predloženih metoda. Precizna imitacija kretanja ruku u Kartezijanskom prostoru je od suštinskog značaja za zadatak gde ruke dolaze u dodir sa opremom. Konverzion proces je zasnovan na analitičkoj predstavi kinematskog modela čoveka i generiše očekivano kretanje robota u realnom vremenu. Dobijeni rezultati našeg konverzionog procesa su testirani na robotu ROMEO kroz obavljanje kompleksnih zadataka dvoručne manipulacije.

Drugi deo teze analizira strategije generisanja ljudskih pokreta. Na osnovu pretpostavke da je ljudski pokret optimalan, cilj je definisati nepoznatu objektivnu funkciju, koja je minimizirana tokom zadatka manipulacije. Shodno tome, inverzan optimalni pristup upravljanja je korišćen. Objektivna funkcija je napisana kao ponderisana suma poznatih osnovnih kriterijumskih funkcija u robotici, kao što je minimizacija kinetičke energije, minimizacija brzine zglobova, povećanje manipulabilnosti i minimizacija razlike između trenutne i ergonomične pozicije čoveka. Optimalna kombinacija kriterijuma, koja najbolje predstavljaju snimljeno ljudsko kretanje je predmet istraživanja. Kretanje koje je dobijeno minimiziranjem ponderisanih kriterijuma upoređivano je sa snimljenim ljudskim kretanjem tokom manipulacija. Genetski algoritam, pogodan za rešavanje globalnih problema optimizacije, je korišćen u tu svrhu. Analizirano je nekoliko manipulacionih zadataka izvršenih od strane više ljudi. Cilj je proučiti kako se optimizacioni kriterijumi razlikuju u zavisnosti od zadataka i ljudi. Pokazano je da optimizacioni kriterijumi variraju u zavisnosti od vrste kretanja i amplitude pokreta ramena, laktova i zgloba. Ispitivan je i efekat karakteristika ljudskog tela i životne sredine (uključujući i opremu) na ostvarljivost pokreta.

Ovo istraživanje definiše optimizacione kriterijume koji mogu biti korišćeni za generisanje pokreta humanoidnog robota inspirisanog kretanjem čoveka. Da bi generisao isti pokret kao čovečiji, humanoidni robot može minimizirati iste kriterijume koristeći algoritam inverzne kinematike. Eksperimentalni testovi su urađeni za zadatak "otvaranje/zatvaranje fioke". Primećeno je da je prilagođavanje kretanja neophodno, uzimajući u obzir veličinu robota i njegovog radnog prostora. Ova teza ima za cilj da bolje integriše robote u ljudskom okruženju. Pored toga, predloženi algoritam može naći primenu u medicinskoj rehabilitaciji.

Analiza ljudskih pokreta u prostoru unutrašnjih koordinata omogućila je predstavljanje pravila koja definišu minimizirane kriterijume. Ovaj pristup je predstavljen u trećem i završnom delu teze, gde je predložen i ispitivan algoritam fazi logike za prenos ljudskih veština na humanoidne robote. Algoritam fazi logike estimira težinske koeficijente kriterijuma definisanih u objektivnoj funkciji, u skladu sa ljudskim kretanjem zabeleženim u prostoru unutrašnjih koordinata. Algoritam fazi logičke je u mogućnosti da generiše objektivnu funkciju za svaki tip pokreta dvoručne manipulacije, bez obzira da li je ranije analiziran ili ne. Inverzni kinematski model, prilagođen da minimiziranje kriterijuma, može se koristiti za generisanje istih pokreta na humanoidnom robotu.

Ključne reči: veštine ljudskog kretanja, inverzni optimalni algoritam upravljanja, algori-

tam inverznej kinematike, imitacija ljudskih pokreta, humanoidni roboti.

Naučna oblast: Electrical and Computer Engineering

Uža naučna oblast: Robotics and Control Systems

UDK broj: 621.3

Titre de la thèse: Manipulation robotique à deux mains inspirée des aptitudes humaines

Résumé: Le désir de l'homme de créer un monde à son idée (ou image) a conduit au développement de grandes réalisations techniques. De nombreuses machines sont inspirées des systèmes et des processus biologiques observés dans la nature. Le plus grand défi pour le chercheur est de mettre au point un système mécanique, ressemblant à l'homme, et qui présente les aptitudes d'un être humain. La forme du corps humain a largement inspiré la structure mécanique des robots humanoïdes. Les efforts actuels des chercheurs dans le domaine de la robotique humanoïde et des sciences cognitives visent à transposer les modèles du comportement humain vers les robots humanoïdes. La modélisation du mouvement humain a été largement étudiée et explorée dans la littérature dans le but de concevoir et de contrôler un robot humanoïde inspiré par le mouvement humain dans les activités humaines quotidiennes. Les différentes disciplines scientifiques analysent le mouvement humain de différentes manières. Il existe de nombreuses techniques et stratégies pour imiter et analyser le mouvement humain, comme le processus d'imitation du mouvement, l'apprentissage par imitation et les approches d'optimisation.

Le but de cette thèse est :

- d'améliorer le processus de conversion pour l'imitation du mouvement humain du haut du corps par un humanoïde, pour une tâche avec ou/et sans contact entre les mains et l'équipement.
- de définir la fonction objective optimisée par un mouvement humain dans le but de transférer les habiletés humaines aux robots humanoïdes.
- de faire exécuter au robot humanoïde des mouvements similaires au mouvement humain, c'est à dire minimisant les mêmes critères.

Comme le modèle humain est complexe et comporte de nombreux degrés de liberté, l'objectif est de faire imiter un mouvement et de transférer les habiletés humaines à un robot humanoïde avec moins de degrés de liberté. A cette fin, le modèle cinématique du robot ROMEO est utilisé comme modèle cinématique du l'humain. Des mouvements d'un humain utilisant ses deux bras pour une tâche incluant le contact avec l'environnement sont analysées ici. Ce type de mouvement a été peu étudié dans la littérature.

Dans la première partie de la thèse, un processus de conversion pour l'imitation du mouvement humain par un robot humanoïde est proposé. Ce processus de conversion améliore les techniques existantes et est développé dans le but de permettre l'imitation

du mouvement humain avec un robot humanoïde pour effectuer une tâche avec ou/et sans contact entre les mains et l'équipement. Notre processus de conversion tient compte de la situation de marqueurs et de la position des articulations et fournit une imitation plus précise que les méthodes proposées précédemment. L'imitation précise du mouvement des mains dans l'espace cartésien est essentielle pour la tâche où les mains entrent en contact avec l'environnement. Notre processus de conversion est basé sur l'expression analytique d'un modèle cinématique et peut permettre de définir le mouvement à générer par le robot en temps réel. Les résultats obtenus de notre processus de conversion ont été testés sur le robot ROMEO lors de l'exécution de manipulations à deux bras.

La deuxième partie de la thèse vise à analyser les stratégies de génération du mouvement par l'homme. En partant de l'hypothèse que le mouvement humain est optimal, on cherche à définir la fonction-objectif inconnue minimisée pendant les manipulations. L'approche du contrôle optimal inverse est utilisée. Nous écrivons la fonction-objectif recherchée comme une somme pondérée de fonctions de base bien connues dans l'optimisation des processus en robotique, telles que la minimisation de l'énergie cinétique, la minimisation de la vitesse articulaire, l'augmentation de la manipulabilité et la minimisation des écarts par rapport à la position ergonomique de l'homme. Puis nous cherchons la combinaison optimale de critères pour représenter au mieux le mouvement humain enregistré. Pour ceci nous comparons le mouvement résultant de la minimisation du critère pondéré, et le mouvement enregistré lors de manipulations humaines. Un algorithme génétique, qui convient pour résoudre les problèmes d'optimisation globale, est utilisé dans cette tâche. Plusieurs tâches sont considérées, et plusieurs personnes exécutent les mêmes tâches. Notre objectif étant d'étudier comment varient les critères optimisés en fonction des tâches et des personnes. Nous montrons que selon le type de mouvement obtenus et l'amplitude des mouvements d'épaule, de coude et de poignet, les critères optimisés varient. L'effet sur les caractéristiques corporelles des humains et les caractéristiques de l'environnement (équipement impliqué) pour réaliser des mouvements sont également analysés.

Cette étude nous permet d'obtenir pour une tâche, le critère optimisé et ensuite ce critère peut être utilisé pour générer des mouvements du robot humanoïde inspiré des mouvements humains car minimisant le même critère, en s'appuyant sur un modèle cinématique inverse. Des tests expérimentaux ont été menés pour une tâche d'ouverture de tiroir. On peut noter que des adaptations peuvent être nécessaires pour tenir compte de la taille du robot et des limites de son espace de travail. Cette étude a pour objectif une meilleure intégration des robots dans les environnements humains. De plus, notre algorithme peut trouver des applications en médecine de réadaptation.

Cette analyse des mouvements humains nous a permis de définir des règles qui à partir des mouvements articulaires observés nous permettant de connaître le critère minimisé. Celles-ci ont été utilisées dans la troisième et dernière parties de la thèse, dans laquelle un algorithme de logique floue est proposé comme la voie universelle pour le transfert de

l'habilité des humains vers les robots humanoïdes. L'algorithme permet, pour un mouvement humain enregistré dans l'espace articulaire, d'estimer les poids définissant le critère optimisé. Cet algorithme est capable de générer des fonctions-objectif pour chaque type de mouvement humain à deux bras, qu'ils aient été analysés ou non. Un modèle cinématique inverse adapté au critère à minimiser peut alors être utilisé pour générer les mouvements du robot humanoïde.

Mots clés: habileté humaine, commande optimal inverse, cinématique inverse, imitation de mouvements humains, robots humanoïdes.

Domaine scientifique: Génie électrique et informatique

Espace de recherche: Robotique et systèmes de contrôle

UDC nombre: 621.3

List of Tables

| | | |
|-----|--|-----|
| 2.1 | The kinematic model of the humanoid robots with human motion functionalities | 14 |
| 4.1 | The average values of the fitness function in one time sample of all actors for the all tasks. | 74 |
| 4.2 | The generalized combination of criteria functions calculated for each experiment. | 84 |
| 5.1 | Fuzzy rules which describe the energy criterion as dominant | 96 |
| 5.2 | Fuzzy rules which define the velocity criterion as dominant | 96 |
| 5.3 | Fuzzy rules which define the ergonomy as dominant | 96 |
| 5.4 | Fuzzy rule which provides equal domination of energy and ergonomy criteria | 96 |
| A.1 | The information of robot ROMEO motors | 131 |
| B.1 | Anthropometric parameters used in the Modified Hanavan model | 132 |
| B.2 | Mass prediction equations | 133 |
| B.3 | Geometric Shapes and Arguments of the BSP Functions | 134 |
| D.1 | Modified DH parameters for the extended upper body model of the robot ROMEO | 143 |

List of Figures

| | | |
|-----|---|----|
| 2.1 | Examples of humanoid robots (part 1). | 9 |
| 2.2 | Examples of humanoid robots (part 2). | 10 |
| 2.3 | a) Hanavan model; b) The arm's axes of rotations (Zanchettin, Rocco, Bascetta, Symeonidis, and Peldschus (2011)); c) kinematic model of the shoulder and shoulder girdle. | 11 |
| 2.4 | a) Santos, a Complete Virtual Human by (J. Yang, Marler, Kim, Arora, & Abdel-Malek, 2004) ; b) Skeleton model with 75 bones and 846 muscle model by (S. H. Lee, 2008). | 13 |
| 3.1 | Overview of the conversion from human to humanoid motions. | 26 |
| 3.2 | Classification of dual-arm coordinates motions. | 27 |
| 3.3 | a) Kinematic model of Master Motor Map (Azad, Asfour, & Dillmann, 2007); b) Kinematic model of the robot ROMEO. | 34 |
| 3.4 | Scaling process: a) extended kinematic model of robot ROMEO in a basic configuration; b) Intermediate model - scaled extended kinematic model of the robot ROMEO to the dimensions of the human in the initial configuration with markers and marker frames. | 35 |
| 3.5 | The displacement of the shoulder joints and Real Markers attached to the shoulders during the motion. | 38 |
| 3.6 | Human body segmentation according to the modified Hanavan notation. | 39 |
| 3.7 | The position and orientation errors in matching actor's initial configuration with the scaled model of the ROMEO robot generated by our Initial configuration algorithm: (a), (b) and (c) represent average position errors of the arm joints $\mu(E_j)$ for the 19 actors in millimetres; (d) represents average normed orientation errors $\mu(\ \Delta\vec{e}_{hand}\)$ of the hand joints in quaternion. | 49 |
| 3.8 | The orientation and position errors between the recorded and obtained motion generated by our analytical (blue scale, dashed line) and numerical (blue scale, solid line) imitation algorithms and the numerical imitation algorithm proposed by Ude (Ude, Atkeson, & Riley, 2004) (red scale): a) the normed orientation errors $\Delta\vec{e}_{rvmRightHd}$ and $\Delta\vec{e}_{rvmLeftHd}$ of the right and left hand markers in quaternion; b) represents the normed position errors $P_{aj}(t_i) - P_{rj}(t_i)$ of the arm joints in meters. | 50 |

| | | |
|------|--|----|
| 3.9 | The normed position errors in following Real Marker P_{rm} with Virtual Marker P_{vm} obtained with our analytical (blue scale, dashed line) and numerical (blue scale, solid line) imitation algorithms and the numerical imitation algorithm proposed by Ude (Ude, Man, Riley, & Atkeson, 2000) (red scale) in meters. | 51 |
| 3.10 | Quality of the imitations of the right and left hand motions, expressed by $\mu(E)$, for the 19 actors obtained by our analytical (blue color) and numerical (green color) algorithms and the numerical algorithm proposed by Ude (red color). | 52 |
| 3.11 | The motion "Open/close drawer" performed by the actor and robot: a) Actor during the task. Simulation model of the robot and the calculated trajectories of the robot hands, b) in the imitation algorithm, c) in the algorithm for generation of humanoid motion. | 57 |
| 3.12 | Snapshot of the "Open/close drawer" motion performed by: (a) the actor; (b) and robot ROMEO. The robot is able to perform the same task under the same conditions as the actor. | 58 |
| 4.1 | The integral errors per sample calculated according to the results of each IK algorithms for different experiments in the case of all actors. | 67 |
| 4.2 | The "Opening/closing a drawer" task performed by the robot ROMEO. The pose obtained with a) IK algorithm with velocity criterion; b) IK algorithm with manipulability criterion; c) IK algorithm with energy criterion; d) IK algorithm with ergonomic criterion. | 68 |
| 4.3 | The actor and the robot ROMEO joint velocities during the "Opening/closing a drawer" task. The robot ROMEO joint velocities obtained by IK algorithm with velocity criterion and IK algorithm with manipulability criterion are similar and near the actor joint velocities. | 69 |
| 4.4 | a) "Opening/closing drawer" task b) Resulting weight factors defining the objective function - criterion minimization of joint velocity prevail c) Joint motions - shoulder and elbow motions dominate. | 75 |
| 4.5 | a) "Rotation of the valves" task b) Resulting weight factors defining the objective function - criterion maximization of manipulability prevail c) Joint motions - shoulder and elbow motions dominate. | 77 |
| 4.6 | a) "Rotation of a steering wheel" task b) Resulting weight factors defining the objective function - criterion minimization of kinetic energy prevail c) Joint motions - shoulder and wrist motions dominate. | 78 |
| 4.7 | a) "Inflating a mattress using a pump" task b) Resulting weight factors defining the objective function - criterion minimization of kinetic energy prevail c) Joint motions - elbow and wrist motions dominate | 79 |

| | | |
|------|---|-----|
| 4.8 | a) "Cutting with a knife" task b) Resulting weight factors defining the objective function - criterion minimization of joint velocity prevail c) Joint motions - shoulder and elbow motions dominate | 80 |
| 4.9 | a) "Grating of food" task b) Resulting weight factors defining the objective function - criterion minimization of kinetic energy prevail c) Joint motions - elbow motions dominate | 81 |
| 4.10 | a) "Rotation of the canoe paddles" task b) Resulting weight factors defining the objective function - criterion minimization of joint velocity prevail although all other criteria is present depending of the actors characteristic c) Joint motions - shoulder and elbow motions dominate. | 82 |
| 4.11 | "Opening/closing a drawer" task performed by the actor and the robot ROMEO. The motion of the robot obtained for the generalized combination of the weight coefficients (b) tends to be more similar to the actor motion (a), compared to the motion of the robot obtained with the criterion minimization of the kinetic energy (c). | 85 |
| 5.1 | Basic configuration of fuzzy logic system. | 90 |
| 5.2 | The linguistic variables and membership functions of the fuzzy input: a) $vShoulderPitch$; b) $ergonomyShoulderYaw$; and c) $vTrunckPitch$ | 94 |
| 5.3 | The linguistic variables and membership functions of the fuzzy output $Kenergy$ | 94 |
| 5.4 | "Grating of food" task: Fuzzy inputs, fuzzy rule and fuzzy outputs. | 98 |
| 5.5 | "Grating of food" task: Comparative analysis of weight coefficients obtained by optimization and fuzzy algorithms. | 98 |
| 5.6 | "Grating of food" task: Fuzzy rules, linguistic variables and membership functions. | 99 |
| 5.7 | "Grating of food" task: Comparative analysis of fitness functions obtained by optimization and fuzzy algorithms. | 101 |
| 5.8 | "Rotation of a steering wheel" task: Comparative analysis of weight coefficients obtained by optimization and fuzzy algorithms. | 102 |
| 5.9 | "Rotation of a steering wheel" task: Comparative analysis of fitness functions obtained by optimization and fuzzy algorithms. | 102 |
| 5.10 | "Rotation of the canoe paddles" task: Comparative analysis of weight coefficients obtained by optimization and fuzzy algorithms. | 103 |
| 5.11 | "Rotation of the canoe paddles" task: Comparative analysis of fitness functions obtained by optimization and fuzzy algorithms. | 104 |
| 5.12 | "Rotation of the valves" task: Comparative analysis of weight coefficients obtained by optimization and fuzzy algorithms. | 105 |
| 5.13 | "Rotation of the valves" task: Comparative analysis of fitness functions obtained by optimization and fuzzy algorithms. | 105 |

| | | |
|------|--|-----|
| 5.14 | "Opening/closing drawer" task: Comparative analysis of weight coefficients obtained by optimization and fuzzy algorithms. | 106 |
| 5.15 | "Opening/closing drawer" task: Comparative analysis of fitness functions obtained by optimization and fuzzy algorithms. | 106 |
| 5.16 | "Inflating a mattress using a pump" task: Comparative analysis of weight coefficients obtained by optimization and fuzzy algorithms. | 107 |
| 5.17 | "Inflating a mattress using a pump" task: Comparative analysis of fitness functions obtained by optimization and fuzzy algorithms. | 108 |
| 5.18 | "Cutting with a knife" task: Comparative analysis of weight coefficients obtained by optimization and fuzzy algorithms. | 109 |
| 5.19 | "Cutting with a knife" task: Comparative analysis of fitness functions obtained by optimization and fuzzy algorithms. | 109 |
| 5.20 | a) "Turning a hand drill" test task, b) Comparative analysis of weight coefficients obtained by optimization and fuzzy algorithms. | 110 |
| D.1 | The transformations described by the modified DH parameters between two joints. First a rotation α is performed around the x axis, followed by a translation a along the x axis; then, a rotation θ is done around the z axis, followed by a translation d along the z (Adorno, 2011). | 139 |
| D.2 | Kinematic model of for the extended upper body model of the robot ROMEO. 3 translation and 3 rotation joints into the trunk are included in order to estimate motions of legs. | 141 |

Contents

| | | |
|----------|--|-----------|
| 1 | Introduction | 1 |
| 1.1 | Contribution | 5 |
| 1.2 | Organization of the thesis | 5 |
| 2 | State of the art | 7 |
| 2.1 | Humanoid robots as replica of the human | 7 |
| 2.1.1 | Kinematic model of the human vs humanoid | 10 |
| 2.2 | Human motions as inspiration for the research | 15 |
| 2.2.1 | Algorithm for the human motion imitation | 17 |
| 2.2.2 | Algorithm for description of human motions | 19 |
| 2.3 | Humans strategies for performing tasks | 21 |
| 2.3.1 | Motion distribution through the arm joints | 21 |
| 2.3.2 | Ergonomy configuration of the human body | 22 |
| 2.3.3 | Feasibility measure of the task | 23 |
| 3 | Human to humanoid motion conversion for dual–arm manipulation tasks | 25 |
| 3.1 | Dual-arm manipulation | 25 |
| 3.1.1 | Segmentation of the human motion in the motion primitives | 31 |
| 3.1.2 | Our approach-phases of motion and normalized circle motion | 31 |
| 3.1.3 | Conclusion | 31 |
| 3.2 | Motion capture systems and recording human motions | 32 |
| 3.2.1 | ART motion capture system | 33 |
| 3.3 | Kinematic model of the humanoid as a human model | 33 |
| 3.3.1 | Robot ROMEO | 35 |
| 3.3.2 | Scaling process | 36 |
| 3.3.3 | Un-modeled kinematics of the human body | 37 |
| 3.3.4 | Estimation of the human body segments parameters | 38 |
| 3.4 | Initialization process | 39 |
| 3.5 | Imitation algorithms as optimization approach | 41 |
| 3.5.1 | Numerical approach for solving inverse optimal imitation problem | 43 |
| 3.5.2 | Analytical approach for solving inverse optimal imitation problem based on the Jacobian matrix | 44 |

| | | |
|----------|--|-----------|
| 3.6 | The simulation results of the imitation algorithms | 47 |
| 3.7 | From the Imitation Results to the Motion of Robot ROMEO | 53 |
| 3.7.1 | The inverse kinematic algorithm as a tool for generation of human like motion | 54 |
| 3.7.2 | Motion of the robot hands without a contact | 55 |
| 3.7.3 | The transition strategy connecting the motions without and with contact | 56 |
| 3.7.4 | Handling collision | 56 |
| 3.8 | The simulation and experimental results of the motion of robot ROMEO . | 57 |
| 3.9 | Conclusion | 59 |
| 4 | Dual-arm manipulation inspired by human skills | 60 |
| 4.1 | Mathematical representation of the human motion behaviors using criteria functions | 61 |
| 4.1.1 | Criterion minimization of joint velocities | 61 |
| 4.1.2 | Criterion minimization of the kinetic energy | 61 |
| 4.1.3 | Criterion minimization of distance between the current position and the ergonomic configuration of human | 62 |
| 4.1.4 | Criterion maximization of the manipulability | 62 |
| 4.2 | Inverse Kinematic algorithm as a tool for identification of human motion skills | 63 |
| 4.2.1 | Moore-Penrose pseudoinverse algorithm | 63 |
| 4.2.2 | Weighted pseudoinverse algorithm | 64 |
| 4.2.3 | Inverse Kinematic algorithm with optimization term | 65 |
| 4.2.4 | Inverse Kinematic algorithm and the criteria functions | 65 |
| 4.2.5 | Results | 66 |
| 4.2.6 | Conclusion | 70 |
| 4.3 | The inverse optimal control algorithm | 71 |
| 4.3.1 | Genetic algorithm for calculation of the weight coefficients | 73 |
| 4.3.2 | Human motion strategy as a result of the inverse optimal control algorithm | 74 |
| 4.3.3 | “Opening/closing a drawer” | 75 |
| 4.3.4 | “Rotation of the valves” | 76 |
| 4.3.5 | “Rotation of a steering wheel” and “Inflating a mattress using a pump” | 78 |
| 4.3.6 | “Cutting with a knife” and “Grating of food” | 80 |
| 4.3.7 | “Rotation of the canoe paddles” | 81 |
| 4.3.8 | Discussion | 82 |
| 4.4 | Human like dual-arm motion of the robot ROMEO | 83 |
| 4.5 | Conclusion | 87 |

| | | |
|----------|--|------------|
| 5 | Fuzzy logic algorithms for the analysis of human motion behaviors | 89 |
| 5.1 | Fuzzy logic and fuzzy logic system | 89 |
| 5.2 | Fuzzy system as the tool for modeling human motion strategy | 92 |
| 5.2.1 | Human motion parameters as a fuzzy inputs and output variables | 92 |
| 5.2.2 | Human motion strategy presented through the fuzzy rules | 95 |
| 5.3 | Optimization algorithm vs. fuzzy algorithm | 97 |
| 5.3.1 | “Grating of food” task | 97 |
| 5.3.2 | “Rotation of a steering wheel” task | 101 |
| 5.3.3 | “Rotation of the canoe paddles” task | 103 |
| 5.3.4 | “Rotation of the valves” task | 104 |
| 5.3.5 | “Opening/closing drawer” task | 105 |
| 5.3.6 | “Inflating a mattress using a pump” task | 107 |
| 5.3.7 | “Cutting with a knife” task | 108 |
| 5.4 | Implementation fuzzy algorithm for a new motion | 109 |
| 5.5 | Conclusion | 110 |
| 6 | Conclusion | 112 |
| | Reference | 130 |
| | Appendices | 131 |
| A | ROMEEO robot motor information | 131 |
| | Appendices | 132 |
| B | Hanavan model of the human body | 132 |
| B.1 | Modified Hanavan parameters | 132 |
| B.2 | Geometrical shape | 135 |
| | Appendices | 137 |
| C | Quaternions | 137 |
| | Appendices | 139 |
| D | Modified DH parameters of the ROMEEO robot | 139 |

Introduction

In recent years, the development of humanoid robotics has been oriented towards the integration of robots in human environments and helping the human in his daily activities. Accordingly, the tendency through generations is that humanoid robots increasingly take on the physical characteristics as well as the behavioral models of the human. Thanks to the development of biomechanics, medicine, physiology, robotics and neurophysiology, scientists have made a significant contribution to the modeling of the human body. However, humanoid robots still are far from having human characteristics. The human has around 206 bones connected to different types of elastic joints, so human motion is achieved with about 640 skeletal muscles. On the other hand, the humanoid robot has a rigid series of kinematic chains with rigid joints equipped with a limited number of sensors.

In order to increase the acceptability of humanoid robots in human environments, humanoid robots must have "closely" human motion and/or inspired human skills. Since the humanoid robot has the redundant structures as a human, it is able to imitate human motion. Imitation of human motion can be achieved by a motion imitation process (Do, Azad, Asfour, & Dillmann, 2008) or the imitation learning process. The imitation learning process aims to analyze the characteristics of human motion based on data obtained by recording human motions. On the other hand, the motion imitation process is based on imitation of the human motions without any analysis of the human motions characteristics. The research in this thesis is based on both approaches of the human motion imitation.

Looking at the state of the art in the field of human motion imitation, we can see that the "Programming by Demonstration" is the most commonly used method for transfer of human motion into the motion of humanoids (Calinon & Billard, 2004, 2007; Calinon, Guenter, & Billard, 2005). The imitation of the human motion can also be solved using

optimization algorithms on the dynamic and kinematic level. Imitation of the upper body human motion using the dynamic equations and data obtained by motion capture system is analyzed in (Ott, Lee, & Nakamura, 2008; Suleiman, Yoshida, Kanehiro, Laumond, & Monin, 2008). The human motion imitation problem is solved on the kinematic level in (Ude et al., 2004, 2000). A method for transforming the recorded 3D position of markers into the trajectory of joints is proposed. The human body is modeled as a scaled model of the humanoids. Optimization techniques such as "B-spline wavelets" and "large-scale optimization" are used to generate the motion of joints. Those algorithms are not able to achieve the imitation of the human motion in real time. Our objective will be to propose a imitation algorithm that is able to provide human motion imitation in real time. Whatever imitation process is used, verification of the results of the imitation algorithm on a humanoid robot requires taking into account the properties of the robots such as limiting joint, robot working space...

The process of studying the characteristics of human motion is linked to the process of the imitation of the human motion. Trajectories of human motion obtained by imitation algorithm are used to analyze the characteristics of human motion. During the motion, the human uses probably an optimal solution for the motion generation, trying to minimize the criterion function which is unknown to us. Therefore, for the analysis of the characteristics of motion, the inverse optimization approaches can be used to find the criterion used. Unfortunately, the apparent criterion function that the human minimizes during the motion may depend on the manner in which the motion is analyzed. In the field of biomechanics, criteria function that is most commonly used for the analysis of human motion is minimization of muscle effort (Khatib et al., 2009). In the field of robotics, minimization the moment in the joints is the most used criterion function (Zheng & Yamane, 2013). During our research, we analyzed the influence of the individual criterion function on the human motion imitation (Tomić, Vassallo, Chevallereau, Rodić, & Potkonjak, 2016). Criteria functions are defined in the kinematic level, such as minimization of kinetic energy, minimization of joint velocity, maximization of manipulability and minimization of deviations from the ergonomic position of the human.

Looking at the ways in which human performs tasks, it is a logical understanding that human uses a combination of criteria functions instead of just one criterion. In the works (Mombaur, Laumond, & Yoshida, 2008; Mombaur, Truong, & Laumond, 2010) imitation of the human motion is presented as an optimization problem with the objective function that adjusts the weighted sum of criterion function: minimization of the total time, minimization of components of acceleration during motion, minimization of errors in orientation and direction during the motion to the goal. The main goal of their research is to find the optimum combination of weight factors that would be able to describe any human motion. In the paper (A. G. Billard, Calinon, & Guenter, 2006) the optimization algorithm based on inverse kinematics pseudo inverse is extended and minimization of deviations from the desired position of the hand and wrist were taken as criteria functions. In the

presented optimization algorithms, criterion function is defined in task space. Analysis of the characteristics of human motion in joint space is presented in (J. Yang et al., 2004). The combination of criterion function such as minimization displacement of the joints, minimization changes of potential energy and minimization discomfort is defined in the optimization algorithm. For each criterion function a weighted factor is proposed which takes into account the influence of each joint on achieving motions.

The research objectives of the thesis will be organized into three connected parts: generation of the conversion process for imitation of recorded human motions in real time by humanoid robots; development of optimization algorithms for analysis of the characteristics of human motion in order to transfer the human motion skills into the motion of the humanoid; and development of the algorithm for detection of human motion skills based on artificial intelligence algorithms. In this study, dual-arm manipulation tasks will be analyzed that are less analyzed in literature. Each task consists of two phases: the phase of motion that involves contact between hands and equipment and the phase of the motion without contact. The dual-arm manipulation tasks will be classified as translational and rotational motions, with an additional classification defined according to the relations position between the arms, proposed in the papers (Krüger, Schreck, & Surdilovic, 2011; Zöllner, Asfour, & Dillmann, 2004). Each of the motions will be carried out by healthy subjects and recorded with the help of Vicon motion capture system.

In the first part of the research, the algorithms for conversion of human motion to the motion of the humanoids will be defined. The human to humanoid motion conversion is divided into two phases. In the first phase, we used the information given by the motion capture system and analytically defined the imitation algorithm to acquire the desired motion of the humanoid in the task and joint spaces. The algorithm is based on the markers positioned on a scaled model of the humanoid (Virtual Markers) that follow the motion of the marker (Real Markers) placed on the human. The intermediate use of a scaled model of the humanoid presented by Ude et al. (Ude et al., 2004) permits adapting size of the robot to size of the human that has achieved the task and thus able to record coherent joint and Cartesian motions. Since the task of our imitation algorithm is to generate the motion where hands and the environment are in contact, a precise imitation of the hands' motions is important. Our imitation algorithm incorporates not only the marker motion but also the joint motions measurement obtained via Advanced Realtime Tracking Human (ART Human) software, provided by the ART capture motion system, in order to increase the robot imitation accuracy. Instead of using twists, in our kinematic model, the modified Denavit and Hartenberg (DH) convention is used to simplify the modeling process (Khalil & Kleinfinger, 1986). The imitation algorithm is based on the kinematic structure of the humanoid and can be used in real time. In the second phase of the conversion, the motion imitation of the scaled robot model is used to generate a human-like motion on the ROMEO robot with its real size (1.40m height) in the same environments. Depending on whether a contact with the environment does or does not

exist during the phase of the motion studied, the strategy is different. During the phase in contact with the environment, the hands motions are defined to achieve the contact and the robot hand motions must be the same as those of the human. During the phase without contact, the priority is given to the motion that appears visually close to the human motion and is based on similar joint motions of the humanoid robot with respect to the human. Hand motions can be modified since they are not constrained by equipment. In particular, it can be very useful to deal with hand motion that can be unreachable for the robot due to the difference in segments lengths and/or joint limits. Conversion from the human to humanoid motion is analyzed for a complex task that consists of both types of the motion. A transition strategy between the motion with and without contact is introduced. Since our task is the motion imitation with a contact between hand and equipment, the technique proposed by Ude is unable to generate these types of motions for the robot. The advantage of the proposed conversion algorithm, over existing algorithms is precise imitation of the position and orientation of the human hand motions which is necessary to perform the task. The results of the conversion algorithm are tested on the ROMEO robot within the same environment as those of human.

In the second part of the thesis, we explore human motion skills in the dual-arm manipulation tasks using the inverse optimal control approaches. Since human motion is optimal, we assume that humans try to minimize unknown objective function during the manipulation of tasks. Accordingly, human motion can be analyzed using optimization approaches with the objective function. Unlike some other studies where criteria functions are defined in the task space ([Mombaur et al., 2008, 2010](#)), we have decided to observe human motion characteristics based on the criteria functions in the joint space. More precisely, the basic criteria functions defined in the joint space (minimization of the kinetic energy, minimization of joint velocities, minimization of the distance between the current position and ergonomic configuration of humans while keeping the arm away from the singularity (maximization manipulability)) which are well known in the optimization process in robotics are taken into the analysis. We combine all these criteria in order to define the combination of criteria which best describes human motion. The optimization process is represented at the kinematic level due to the simplicity of the approach and the fact that humanoid robots are often controlled in position, while the torque information is not directly controlled (especially in the case of multiple contacts with the environment as in the present study). The results obtained from the optimization process are confirmed with our a priori knowledge about the activation of the upper body joints during the task. The effects of the actors' body characteristics and the characteristics of the environment on the choice of criteria functions are additionally analyzed. The objective function minimized by the inverse optimization approach is used in the inverse kinematics algorithm to transfer human motion skills to humanoid robots. The recorded human motion and the motion of the humanoid robot ROMEO (obtained with the same strategy used by the human) for the dual-arm manipulation tasks are assessed visually and quantitatively.

In the third part of the thesis, the fuzzy logic is defined as an approach for detection of human motion strategy. Based on the knowledge about human motion obtained in the previous chapter, this algorithm is able to define a combination of criterion functions for an inverse optimization algorithm for any recorded human movement. The obtained results can be used for describing the characteristics of the dual-arm human motion and its generation of the humanoid robot.

1.1 Contribution

According to the state of the art in the field of human motion imitation and imitation learning processes, we have additionally explored:

- Imitation of the upper body human motion by the humanoid, where the motion consists of the phases without contact with the environment and/or phases with contact with the environment and a transition strategy between these two types of motion. The publication that have come out of this work is (Tomić, Chevallereau, Potkonjak, Jovanović, & Rodić, 2018).
- An analytical imitation algorithm based on the Jacobian matrix (instead of the standard optimization algorithm presented in our previous research (Tomić et al., 2016)) which is capable of real time extraction of the Cartesian motions and joint motions that can be used by the humanoid. Paper related to these contributions include (Tomić, Chevallereau, et al., 2018).
- The criteria functions, defined in the joint space, which are able to describe the motion performed by a healthy human. Topic related publications include:(Tomić et al., 2016) and (Tomić, Jovanović, Chevallereau, Potkonjak, & Rodić, 2018)
- The human motion as an optimization process analyzed with the combination of basic criteria functions using the inverse optimal control approach (Tomić, Jovanović, et al., 2018).
- The influence of the human body size and the characteristics of the environment on the human motion strategy for performing the task.
- The generation of a good imitation of the analyzed human motion with a redundant humanoid robot using the generated human motion strategy obtained by the inverse optimal control approach. Paper related to these contributions include (Tomić, Jovanović, et al., 2018)

1.2 Organization of the thesis

The thesis is organized into six chapters, summarized as follows:

Chapter 2 presents some of the most recent developments in the analysis of dual-arm manipulations. Detailed overview in the fields of human motion imitation and the analysis of human motion strategy is given.

Chapter 3 presents a novel conversion process for imitation of the human dual-arm manipulation tasks with a humanoid robot. The dual-arm manipulation tasks consist of the motion with and without contact between hands and equipment. These types of motions are chosen for the analysis in this thesis since they are less studied in literatures. The conversion process consists of an imitation algorithm and an algorithm for generation of human like motion on the humanoid. The conversion from the human to the humanoid motion is analyzed for complex dual-arm tasks that consists of the motion with and without contact between hands and equipment. A transition strategy between motion with and without contact is introduced.

Chapter 4 proposes a new approach in analysis of human motion skills in dual-arm manipulation tasks. Human motion is analyzed using a combination of well-known criteria functions defined in the joint space is considered: minimization of kinetic energy, minimization of joint velocities, and minimization of the distance between the current and ergonomic positions, and maximization manipulability, which are well known in the optimization process in robotics. The effects of the actors' body characteristics and the characteristics of the environment on the choice of criteria functions are additionally analyzed. The objective function minimized by the inverse optimization approach is used in the inverse kinematics algorithm to transfer human motion skills to humanoid robot ROMEO.

Chapter 5 presents new approach for detection of human motion strategies based on artificial intelligence algorithm. The fuzzy logic algorithm is formulated in order to find the combination of criteria functions which describe new dual-arm motions in the optimal way. The inference rules are defined according to the knowledge about dual-arm human motion analyzed in Chapter 4.

Chapter 6 presents concluding remarks and perspectives for future works.

State of the art

2.1 Humanoid robots as replica of the human

At the beginning of our research, we ask the basic question: Why do people want to develop humanoid robots? This idea is the result of human's aspirations to make the world according to his imagination. Based to that, humans want to make a machine, such as a robot. This robot would be able to do tasks that we do not want to do and could be our partners in enjoyable communication. To sum up, humans desire to have a replica of himself who would be able to carry out his wishes and orders.

The idea of how the robot should look like arose at the beginning of the twentieth-century. Karel Capek's play, Rossum's Universal Robots, provided the first concrete vision of how a robot should look: "it should look like a human being". In that time, science fiction stories took this as inspiration and have created sophisticated superhuman machines. However, research has not been able to create a robot close to the product of such human imaginations that are depicted in these science fiction stories. This dream is hampered by many obstacles, including ethical, religious, and psychological concerns, but especially by technological limitations. Nevertheless, it seems that dreams about machine-like humans are becoming a reality.

The development of humanoid robots is based on the following requests. First, humanoid robots should be able to work in environments suitable for humans, as well as be able to use tools that are for humans. Second, humanoid robots should have a human-like shape. Consequently, it is more logical to make a robot with human characteristics rather than to modify the human environment and tools according to robotic characteristic. Moreover, a human-like shape of the robot would be more enjoyable for human to

robot interaction. For example, humanoid robot HRP-1 was able to execute tasks in an industrial plant, such as going down stairs and ramps. HRP-1S was able to drive an industrial vehicle, teleguided by a human operator, while the robot HRP-2 was able to perform a traditional Japanese dance. All of these requirements have been gradually realized during decades of development in humanoid robotics. In fact, the goal of 2010 in humanoid robotics was to make it possible for humanoids to walk, pass obstacles, and manipulate objects with both hands. In 2015, the goal was to develop an autonomous humanoid robot who could have variable dimensional perception, such as being able to recognize object's shape, position, or orientation, all through the use of a dexterous hand that can manipulate various kinds of objects. By 2020, the dream is to have a robot that can work cooperatively with humans within a human environment and that has the intelligence to make decisions and perform actions as a human.

The challenge in the development of human-like robots is strongly linked with the level of the state of technology today. Construction of robotic parts comparable to the human skeleton, muscular actuators, neural system senses, etc. is clearly a challenging feat to overcome. In the following, we will present a general overview of the tendency for scientists to make machine, humanoid robots like a human. The first humanoid robots WABOT-1 was developed at Waseda University in 1973. WABOT-1 was able to recognize objects by vision with a camera, understand spoken language and to speak with artificial voice, manipulate objects with two hands, and to walk on biped legs. The same team extended its research and in 1984 developed WABOT-2, which was also able to play piano (Koganezawa, Takanishi, and Sugano (1991)). The epoch of the humanoids continues with the development of the Honda humanoids P2 in 1996. P2, which is 180 cm by height and 210 kg by weight, is the first humanoid robot that can stably walk with a battery and computer connected to its body. The next upgrade to the humanoid P2 is reflected through the robot P3 (160 cm height and 130 kg weight) in 1997, and ASIMO (120 cm height and 43 kg weight) in 2000. The latest ASIMO from 2011 can run at 9 km/min, run backward, hop on one leg. . . As can be noted, a gap of 20 years has been made between the development of the robots WABOT and the Honda robots series. The reason for this is the level of technical development at that time. The first robots had a structure that was not rigid enough and has heavy gears with large backlash. In contrast, Honda humanoid robots use casted mechanical link with high rigidity and light weight. Honda developed the harmonic drives which have no backlash with high torque capacity. Compared with the first humanoid robot which did not have necessary sensors, the Honda humanoid robots have accelerometers, gyroscopes, and force/torque sensors. After Honda P2, the most advanced humanoid robots have compatible configurations with those of Honda humanoid robots. In 2002, the University of Tokyo developed humanoid robot HRP-1 which was able to execute the tasks in a mockup of an industrial plant. This includes stairs, ramps and pits. They continued the development of the humanoids series HRP and in the next robot HRP-2 they implemented algorithms for imitation of the human motion, such as

the example of the Japanese dance (Kaneko, Kanehiro, and Kajita (2004)). Still, HRP-2 robot has limitations in its manipulation ability and practical working environment, such as a construction site. To address these limitations, a new humanoid robot HRP-3 (1.60 m height, 68 kg weight, and 42 total DoF) was developed in 2007 by Kawada Industries Inc and AIST with better manipulation ability and hardware designed to be dust proof and splash proof in consideration of various environments (Kaneko, Harada, Kanehiro, Miyamori, and Akachi (2008)). In 2009 the tendency on the imitation of the human body and the human motion came back and AIST developed the Cybernetic human HRP-4C. Robot is designed to have body dimensions close to an average Japanese young female. The purpose of the robot has been made for the entertainment industry. HRP-4C is able to realize the human like walk with toe supporting period. Since 2009 the robot HRP-4C has been modified and its current specifications are 1.60m height, 46kg weight and total 44 DoF (Kaneko et al. (2009)). In 2010, AIST made HRP-4 (1.51 m height and 39kg weight) robot which is lightweight and slim body compared to the former platform. Some of these robots are shown in Fig. 2.1.



Figure 2.1: Examples of humanoid robots (part 1).

The last 10 years has been a fruitful period for the development of humanoid robotics also in other countries. Technische Universitat of Munchen developed robot LOLA in 2009 (Lohmeier, Buschmann, and Ulbrich (2009)); Korea Advanced Institute of Science and Technology in the same year developed robot HUBO2 (Cho, Park, and Oh (2009)); Italian Institute of Technology, the University of Genoa developed robot iCub in 2008 (Metta, Sandini, Vernon, Natale, and Nori (2008)); Virginia Polytechnic Institute and State University developed robot CHARLI in 2009-2010 (Lahr and Hong (2008)); robot Romeo was developed by Aldebaran in 2013 (Aldebaran (2013)); German Aerospace Center (DLR) developed robot TORO in 2013 (Englsberger et al. (2014)). In 2012 Boston Dynamics developed humanoid robot PETMAN, which is powered by hydraulic actuators and can perform squats while turning, sidesteps with its arms raised overhead, as well as natural human-like walking of up to 4.8 km/h (Nelson et al. (2012)). An upgrade of the PETMAN robot is the Atlas (1.75 m height and 150kg weight and 28 DoF) robot produced in 2013 by the same company (BostonDynamics (2013)). Atlas has four hydraulically-actuated limbs, two vision systems – a laser range finder and stereo cameras, fine motor skill capabilities at the hands, and is constructed of aluminum and titanium. Atlas can navigate through rough terrain, climb independently using its arms and legs, withstand

being hit by projectiles, and balance on one leg. In 2015, NASA announced that they are currently producing the most expensive robot under the name Valkyrie ([IEEE Spectrum \(2016\)](#)). Valkyrie will be able to perform the most common tasks that astronauts perform in space. The NASA researcher team will focus on validating relevant space tasks that will involve both manipulation and locomotion. Some of these robots can be seen in Fig. 2.2.

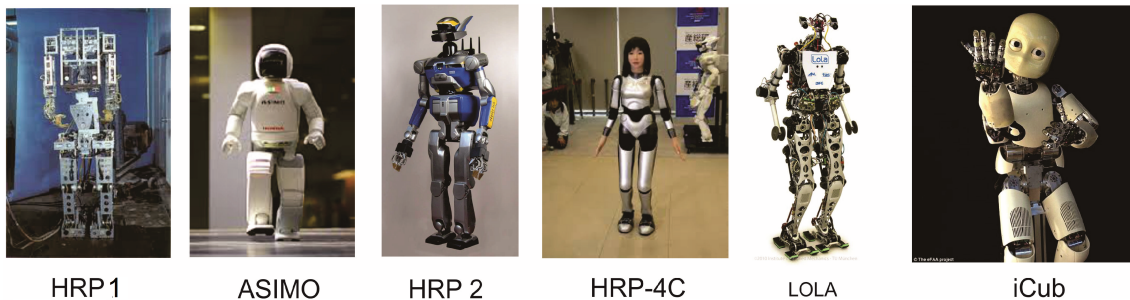


Figure 2.2: Examples of humanoid robots (part 2).

In this moment, we should not forget about autonomous humanoid robots, such as the robots Justin introduced in 2009 by DLR ([Wimböck, Nenchev, Albu-Schäffer, and Hirzinger \(2009\)](#)), Robonaut introduced in 2011 by the Dextrous Robotics Laboratory at NASA ([Bluethmann et al. \(2003\)](#)), and Pepper introduced in 2014 by Aldebaran which all have wheels instead of legs.

2.1.1 Kinematic model of the human vs humanoid

According to the need of human to create a faithful copy of himself, the analysis of human body characteristics represents the first step in creating humanoid robots. Similar to a machine, the human body was viewed as a system of levers (skeletal bones and joints), pulleys (tendons around bones), and movement actuators (muscles). Using the knowledge from different fields of the science, especially from medicine and biomechanics, we can obtain a simple or complex model of the human body.

At the beginning of the research of the human body, scientists used geometry to simplify the shape of body segments. Spherical and cylindrical objects, from which the mass and inertial parameters could be mathematically derived, are represented in models of the human limbs. One of these models was devised by Hanavan ([Pearsall & Reid, 1994](#)) who defined 15 segments of the human body and the mathematical equations for calculating mass, position vector of the center of mass, as well as the inertial matrix of them (see Fig 2.3 a). The trunk was divided into three segments: upper, middle, and lower trunk. The hand was defined as an ellipsoid of revolution, while the foot was defined as an elliptical solid with the base being circular. The thigh was defined as an elliptical solid with the top being circular. A total of 41 anthropometric parameters are needed for this model. This approach was significant because it permitted the body segment parameters of living persons to be approximated, and it reinforced the mechanical interpretation of the body. With

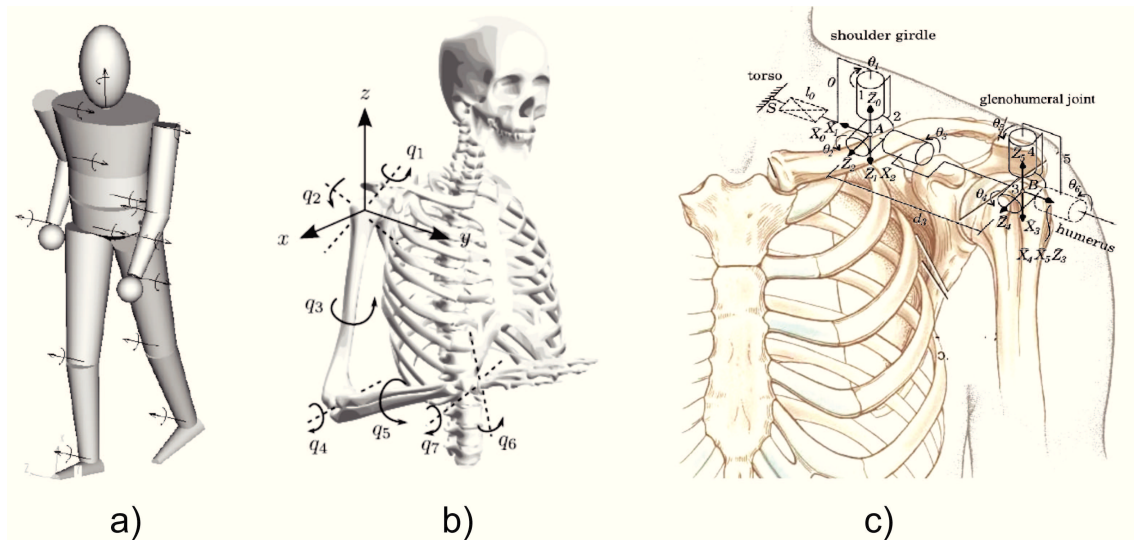


Figure 2.3: a) Hanavan model; b) The arm's axes of rotations (Zanchettin et al. (2011)); c) kinematic model of the shoulder and shoulder girdle.

the development of these techniques, researchers have been able to obtain a more complex model. For this purpose, many systems have been developed to capture human movement and the estimation of human skeletal parameters. Kohler et al. (Koehler, Pruzinec, Feldmann, & Wörner, 2008) proposed an approach for automatically estimating the skeleton of individual subjects and for transforming them into a human body model by preserving its relative configuration. They reconstruct the human motion of the different subjects from a set of 3D marker data, captured with a Vicon system, using a method known as interior-reflective Newton optimization. Kirk et al. (Kirk, O'Brien, & Forsyth, 2005) proposed an automatic method for estimation of skeletal parameters, which determines the length of each segment in the skeleton and reconstruct of the segment's orientation over time. The skeleton representation of the human body is very useful in the computer animation and the visualization of the human motion.

The skeletal model of the human body is not enough for modeling nor detailed analyses of human motion, especially if the task is to transfer the human motion to a humanoid. Thus, the kinematic model of the human body should be defined. The kinematic model of the human body is characterized by joints and segments which form five kinematic chains connected to each other. The bones or the set of the several bones connected to each other (for example, the ulna and the radius) represent segment of the kinematic model. The segments are connected by joints which define mutual rotation between them. The coordinate systems and axes of rotation for the ankle, hip, spine, shoulder, elbow, wrist, and hand joints are analyzed in detail by Wu et al. (Wu et al., 2002, 2005). Their approach of analysis for characterizing the joints and segments is taken as a recommendation for standardization in the reporting of kinematic data of the human body. In the same way, the anthropometric data for describing the kinematics of the human hand is given by (Buchholz, Armstrong, & Goldstein, 1992).

From a biomechanical point of view, the human upper body mechanism, particularly

the shoulder joints and spine, are the most complex part of the human body. The most common upper limb model integrates the thorax, the upper-arm, the forearm and the hand as rigid body segments. These segments are connected by the shoulder, the elbow, and the wrist, modeled as hinge or spherical joints (Naaim, 2016)(see Fig.2.3.b). The shoulder joint is usually modeled as a spherical joint. Additional features of the shoulder girdle must be considered if we want to achieve the functionality that it has. According to this, the shoulder girdle can be modeled as an equivalent mechanism: Lenarcic and Umek (Lenarcic & Umek, 1994) used a simple universal joint; Yang (J. Yang, Abdel-Malek, & Nebel, 2003) used 2 prismatic joints; Klopčar and Lenarcic (Klopčar & Lenarčič, 2006) proposed a more complex model where a universal joint was coupled with a prismatic joint; Lenarcic and Stanistic (Lenarcic & Stanistic, 2003) replaced the universal joint by a spherical joint (see Fig. 2.3.c). All these models allow for a simple representation of the phenomenon occurring in the shoulder girdle. However, they still do not allow for a precise understanding of the different bones in kinematics. They were mainly used as a simplification for musculoskeletal model of the humanoid robot or for ergonomic studies. The elbow is a hinge joint made up of the humerus, ulna, and radius. The unique positioning and interaction of the bones in the joint allows for a small amount of rotation. It is common to model the elbow as a 1DOF revolute joint. The forearm model is usually modeled as a one segment without considering the two forearm bones (i.e., the ulna and the radius). The simplified associated pronosupination movement between them is modeled as a supplementary DoF at the elbow or the wrist joint (Schmidt, Disselhorst-Klug, Silny, & Rau, 1999). The wrist is usually modeled as two revolute joints intersecting at one point if the pronosupination movement between ulna and radius is supplementary DoF at the elbow, or like the spherical joint (Peiper, 1968). The characteristics of the spine and torso is well analyzed by Monheit et al. (Monheit & Badler, 1990). According to them, the kinematic model of the torso consists of 17 segments (vertebrae) and 18 joints, where each joint has three degrees of rotation. They also gave calculation of the spine's joint weights and joint position.

Apart from a simplified model of the human body presented above, some research put more effort in creating detailed anatomical model. For example, Lee et al. (S. H. Lee, 2008) developed a biomimetic, musculoskeletal model which consists of 75 bones and 165 DOF, including each vertebral bone and most ribs. They incorporate 846 muscles, which are modeled as piecewise line segment simplified Hill-type force actuators (see Fig. 2.4.b). The volumetric human body model incorporates detailed skin geometry, as well as the active muscle tissues, passive soft tissues, and skeletal substructure. They introduced spline joints as a novel technique for more accurately modeling skeletal joints. Nakamura et al. (Nakamura, Yamane, Fujita, & Suzuki, 2005) constructed a detailed human musculoskeleton model. They applied simplification and grouped about 200 bones into 53 rigid links which they connected with 323 DoF. They used 366,56,91, and 34 wires to model the muscles, tendons, ligaments, and cartilages. For their musculoskeletal model, the

forward dynamics algorithm is used to simulate the whole-body motion from the even wire tensions of the muscles. Vasavada et al. (Vasavada, Li, & Delp, 1998) constructed a 3D human neck muscle model and measured the moment-generating capacity of each muscle. They visualized human neck motion in their work, but the movement is generated kinematically, with no dynamics.

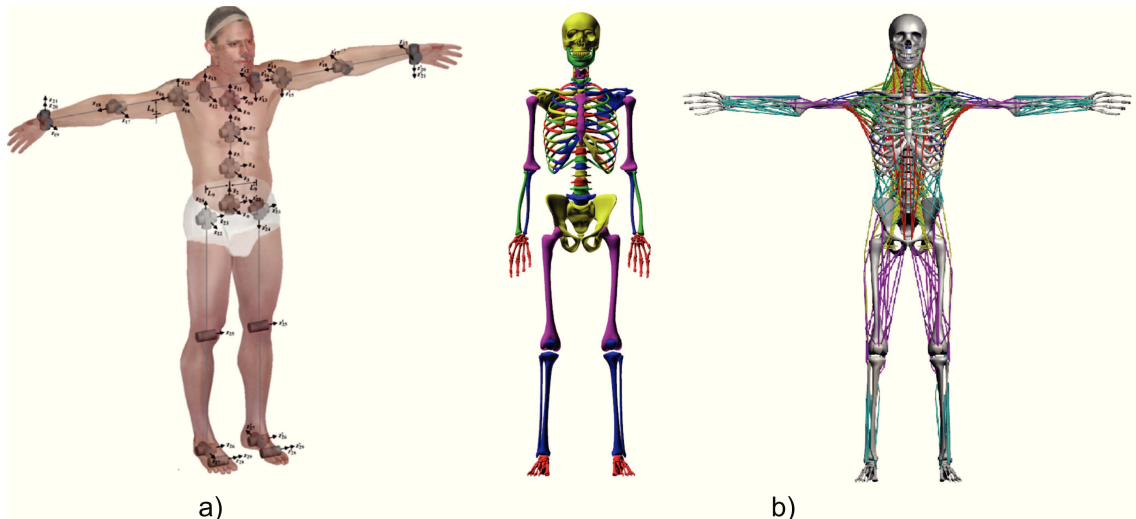


Figure 2.4: a) Santos, a Complete Virtual Human by (J. Yang et al., 2004) ; b) Skeleton model with 75 bones and 846 muscle model by (S. H. Lee, 2008).

The complex kinematic model of the human body is often used in the animation of the virtual human, such as 3DSSPP, AnyBody, Jack, and Santos (see Fig.2.4.a) (Ma, 2009; J. Yang et al., 2004). The advantage of computer animation is the possibility of simultaneous modeling of the muscles, joints, skin and segments of the human body. It can also estimate a large set of human body parameters. On the other hand, for modeling humanoids, the kinematic model of human must be simplified while basic characteristics of the human body should be contained. Standard humanoid robots mimic the human form, but the mechanisms used in such robots are very different from those in humans. Typically these robots are designed according to the same engineering techniques that are used in industrial robots, as is shown by the characteristics of their bodies: they are heavy and stiff and use precise and powerful motors to control joints with easily identifiable axes of rotation. This contrasts heavily with the human body, which is relatively light and compliant, and has a noisy and redundant actuation system controlling some complex joints (e.g. the shoulder). Current humanoids have different kinematic model depending on the purpose for which they are used. A simplified kinematic representation of each human arm and leg which is able to obtain faithful the motion like a human involves at least 6 DoFs per limbs. Table 2.1 provides an overview of the kinematics model of the humanoid robots which is able to obtain the basic human motion functionalities.

A desire to make humanoid robot that mimics as closely as possible the mechanical structures of the human body motivated researchers to make anthropomorphic musculoskeletal upper body robot ECCE (Marques et al., 2010). The skeleton of ECCE consists

Table 2.1: The kinematic model of the humanoid robots with human motion functionalities

| ROBOT | Arm | Leg | Hand | Head | Torso | Face |
|----------|-----------|-----------|-------------|------|-------|------|
| WABOT-2 | 7 per arm | 4 per leg | 14 per hand | - | - | - |
| ASIMO | 6 per arm | 6 per leg | 1 per hand | 2 | - | - |
| HRP-3 | 7 per arm | 6 per leg | 6 per hand | 2 | 2 | - |
| HRP-4C | 6 per arm | 6 per leg | 2 per hand | 3 | 3 | 8 |
| HUBO2 | 6 per arm | 6 per leg | 5 per hand | 3 | 1 | - |
| TORO | 6 per arm | 6 per leg | - | 2 | 1 | - |
| Valkyrie | 7 per arm | 5 per leg | 15 per hand | 3 | 3 | - |
| ROMEIO | 7 per arm | 6 per leg | 1 per hand | 4 | 1 | - |
| Justin | 7 per arm | - | 12 per hand | - | 3 | - |
| Robonaut | 7 per arm | - | 12 per hand | 2 | 7 | - |

of a set of rigid limb structures modeled on the corresponding human bones, which are connected by the appropriate joints, or simplifications of them. It consists of an upper torso built on top of a spine-like structure. The two shoulders of the robot are structurally different. The left shoulder has an anatomically correct joint structure with a scapula carrying a ball-and-socket joint for the humerus, and a clavicle jointed to the sternum; the right shoulder is a classically engineered joint of three orthogonal 1 DoF joints fixed to the trunk. The torso is held vertically by means of a chain of four vertebrae-like elements separated by compliant disks which allow the robot to bend in the 2 planes. The neck is similar to the spine, with three rather elongated vertebral elements allowing bending in the sagittal and coronal planes. An additional 2 DoF joints are used to rotate the head around 2 axes. The neck-head kinematic chain is held together by several longitudinally arranged shock cord segments.

The latest trends in the modeling of the human skeleton in humanoid robotics are based on the use of the caprolactone polymer that has similar characteristics as bones. This material is suitable for manual processing and making complex parts such as the vertebra and pelvis. In the future, development of modeling human skeletal will be based on new techniques such as a 3D printer. In terms of imitation of muscle and tendon activation, electric drives equipped with gearboxes as active elements are used for a long time. The geared drives are then connected in a series of inelastic thread, with an optional elastic element that functions as a muscle tendon. The human sensing system is the easiest to replicate at the current level of technology. With the development of cameras, microphones, and tactile sensors etc. we are able to realize the connection between the humanoid and the environment in the same way a human does. The main issue here is how to organize data from multiple sources. Even more so, the question is how to use these pieces of information. This question represents a control problem, which involves the human brain, but in the case of the humanoid, a central processing unit. In the future, the goal will be to increase the speed of processing data. In the end, it should be emphasized that the biggest challenge is the analysis of human intelligence. In the field of machine

learning, the way in which humans make a decision is analyzed and artificial intelligence algorithms are defined (for example, genetic algorithms, neural networks, fuzzy logic, etc). The result obtained for the artificial intelligence algorithm is used in the many fields of science and it has many applications in robotics. However, one of the problems using this algorithm is the capacity of the robot's processors and the small basis of analyzed human behaviors that we have so far.

2.2 Human motions as inspiration for the research

To begin, let's define human motion: A human movement is a coordinated gesticulation resulting from simultaneous muscle contractions generated by an electric nervous signal. The human motion may be voluntary, or a reflex, and is always motivated by a goal.

Interest in human motions goes back very far in human history, and is motivated by human curiosity (Klette & Tee, 2008). In the antique period, motion patterns of humans were usually studied in close relation to motion patterns of animals. Aristotle defined locomotion as "the parts which are useful to animals for movement in place". His text "On the Parts of Animals" is the first known document on biomechanics. It already contains very detailed observations about the motion patterns of humans when involved in some particular activity. In the period of the renaissance, Leonardo Da Vinci gave the detailed models of the human anatomy, which contain quite detailed studies about kinematics tree (today, kinematic chains), and human motion. He gave a conclusion about muscular movement, the position of the center of mass during movement, and observing and analyzing movements with the "naked eye". It is certainly impressive to see the level of detail in modeling human shape and motion for the "man going upstairs" tasks, given by da Vinci centuries ago. The scientist Giovanni Alfonso Borelli is also often called "the father of biomechanics". He applied the analytical and geometrical methods, developed by Galileo Galilei into the biological research of the human body. He defined that bones serve as levers and that muscles works according to mathematical principles. These principles became a basic principle for modeling human motion. In addition, he mathematically described the movement of blood, comparing it to a hydraulics system. He also defined the force in the muscles necessary for achieving movements. He also explained the conditions under which muscle fatigue occurs. Between Borelli and the latter half of the 19th century, there seems to not be many more important contributions to the study of human motion. This period was reserved for the development of the laws of motion proposed by Isaac Newton, analytical geometry and geometrical algebra by Rene Descartes, and investigating the myograph by Helmholtz. The 19th century was the period of producing moving pictures. A major contribution was the works of the Weber brothers. They calculated the subsequent phases of human walking using differential equations and visualized them by drawing perspective projections. They first studied the

path of the center of mass during movement. During the 19th and 20th centuries, Etienne-Jules Marey made chronophotographic gun, which was able to record several phases of motion in the same photo. Eadweard Muybridge, became known as the pioneer in motion capturing. He invented the zoopraxiscope, a device for projecting a recorded series of images of rotating glass disks in rapid succession to give the impression of motion. Muybridge's motion studies (based on multiple images) includes walking downstairs, boxing, children walking, and so forth. In the next decades, the development of the biomechanics became a worldwide discipline of science. The electromyography was developed for the purpose of measuring the electrical activity of muscles. Today, techniques for recording human movement progress rapidly because of technological developments and the needs of the military, entertainment industry, sports, medical applications, computer vision, and robotics. The research of the human gait is widely supported by marker based motion tracking systems. The camera systems used are fast and able to record the motion of the markers in real time. Computer vision already helped to produce the 3D model of the human body (avatar). Increasing the performances of the cameras, the restrictions of the marker-based system are passed and the marker-less motion capture system is developed. Parallel with recording of the markers, human movement can be characterized through the other parameters, depending on which areas are investigating human movements. All parameters for analysis of human motion are classified as kinematics quantities (information of the position, acceleration, velocity of the marker placed to the human body), dynamics quantities (ground reaction forces, muscle activities...), control parameters (EMG and EEG), and energy quantities (ECG, Oxygen consumption...).

The human motions analysis has been shown to be essential in many different types of applications. In medicine, the methods of visual observation are most commonly used for the interpretation of biomechanical parameters of human movements. However, this type of motion estimation can be very unreliable because it can only give a general impression of the human movements. Combining advanced technology measurement and biomechanical modeling, human gait can be described in quantitative and dynamic conditions of the body and limbs movement. Clinical trials and scientific studies have been conducted in order to achieve a better understanding of human movement. They seek to develop effective methods to understand how neuromuscular defects can affect movement, providing a scientific basis for treatment. Some relevant scientific work can be found in ([Audu, To, Kobetic, & Triolo, 2010](#); [Yavorskii, Sologubov, & Nemkova, 2003](#)). In sport, the biomechanical analysis of human movement is used as an effective technique for improving the performance of athletes, comparing techniques between professional athletes who carries out the same movement, as a tool for risk assessment (see ([Gittoes & Irwin, 2012](#))) since the lack of appropriate technical guidelines often leads to problems with the muscles and joints, for analyses of the influence of gender, age, and physical condition of the human performing the motion ([Fukuchi & Duarte, 2008](#)), and for simulation the dynamic and kinematic characteristics of the athlete's motion in the virtual world ([Syamsuddin &](#)

Kwon, 2011). . . Monitoring a variety of body signals, such as EMG signals, reduction of tetanic force, low frequency fatigue, and endurance time (Gini, Belluco, Mutti, Rivela, & Scannella, 2015; Vøllestad, 1997), are taken for application in the rehabilitation of the human body. In the car and design industry, the analysis of human characteristics takes place in modeling the ergonomic safe environment. Recognition gestures and pose parameters of the human are often used from gaming and entertainment (Höysniemi, Hämäläinen, Turkki, & Rouvi, 2005), sign language recognition (Chia, Licari, Guelfi, & Reid, 2013), movement assessment, senior home monitoring, device remote control, and human-robot interaction (Fong, Nourbakhsh, & Dautenhahn, 2003; Goodrich & Schultz, 2007; Trigueiros, Ribeiro, & Reis, 2013). . . In robotics, the recorded information from motion capture sensors about human motion are used for analysis of the characteristics of human motion and then transferred to the motion of the humanoid.

2.2.1 Algorithm for the human motion imitation

Once a human observes a task being carried out for the first time, he/she is usually capable of immediately performing the same action. In robotics, this process is more complex and is referred to as the motion imitation process (Do et al., 2008). The motion imitation process is based on the imitation of human movements which are pre-recorded using the motion capture system.

According to the data obtained by recording the motions of a human, the imitation process can be defined in the Cartesian space and/or joint space (A. Billard, Epars, Calinon, Schaal, & Cheng, 2004). In the Cartesian space, the motions of the hands, head, and feet are recorded and a geometric inverse model of the humanoid can be used to achieve the task. In the joint space, the objective is to enable the robot to replicate the joint motions of the human, following the human configuration. This last objective is classically used for the imitation process and allows human-like behavior especially in presence of a redundant robot. The difference in body size between a human and a humanoid has an effect on the Cartesian motion of the hands, head, and feet. For the imitation of the dual arm human motion, which requires the robot to interact with the environment using its hands and has human-like behavior of the motion, the imitation process must include the imitation process of the human motion into the joint and Cartesian spaces.

The algorithms for imitation of the human motion can be defined on the kinematic or dynamic level. In (D. Lee, Ott, & Nakamura, 2010; Ott et al., 2008), the robot imitated the human motions using dynamic equations. Based on the measurements of marker positions, they define a Cartesian control approach for the real-time imitation of the human upper body motion. Virtual springs connect the measured marker positions and the corresponding points on the humanoid robot. Since difficulties arise in the motion imitation process by humanoid robots, (such as the joints velocity and the torque limits) Suleiman et al. (Suleiman et al., 2008) also used dynamic equations to formulate a recursive optimization algorithm for imitating human motion. This permits the imitation of the upper body

of human motion within humanoid robot physical capabilities (joint, velocities, torques).

The problem of human motion imitation is solved on the kinematic level by Ude et al (Ude et al., 2004, 2000). They proposed a method to transform the recorded 3D position of the markers into high dimensional trajectories of the humanoid robot joints based on twist representation. The human body is modeled as a scaled model of the humanoid robot. They establish relationships between the motion of the robots joints and the motion of the markers using B-spline wavelets and large-scale optimization techniques. The method is applied off-line on the humanoid robot called DB. Gärtner et al. (Gärtner et al., 2010) presented an imitation algorithm which is able to map the recorded motion of the human to the motion of the robot based on the motion of the real marker by the virtual markers. The virtual markers are defined as fixed and pre-labeled points onto the surface of the voluminous anthropomorphic model. Their algorithm consists of two major constrained large-scale nonlinear optimization transfers. In the first step, they transferred a pre-captured motion of the markers to the motion of the intermediate model, Master Motor Map (MMM), using the sequential quadratic programming approach. The second optimization transfer is based on transformation motion of the MMM model to the motion of the ARMAR-III humanoid. The measure of the similarity between the motion of the humanoid and the generated movement of the MMM model is used as the criterion of the Levenberg-Marquardt approach. The humanoid motion which imitated the pre-captured human motion is obtained. Ayusawa et al. (Ayusawa, Ikegami, & Nakamura, 2014; Ayusawa, Morisawa, & Yoshida, 2015) proposed a gradient computation based Newton-Euler method for simultaneous identification of geometric parameters of a human skeletal model. They also retargeted the human motion into the motion of the humanoid using the information about the recorded position of markers. The evaluation function for human motion reproduction represents the difference between the measured position of the marker at the time and the position of the marker attached on the human model which is function of the joint angles and the dimension of the segments. In order to define the geometric parameters as segment lengths and the position of markers with respect to the robot segments, they introduced translation joints which values are time-invariant through all time of the motion.

Imitation of recorded movements in the most cases does not represent a one-to-one mapping of human movement to robot movement. The number of degrees of freedom, range of joint motions, and achievable joint velocities of today's humanoid robots are far more limited than those of the average human subject. Regarding this, Pollard in his papers presented an imitation algorithm that includes all of these robot's limitations and performs quality imitation (Pollard, Hodgins, Riley, & Atkeson, 2002; Safonova, Pollard, & Hodgins, 2003).

To sum up, the imitation process is shown as a very good and very fast method for teaching robots new motion skills without any analysis of the characteristics of the human motion. The benefits of the imitation process are realization of a natural interaction be-

tween human and robot, providing help to the elderly and the disabled in their everyday life, motivating children during physical therapy (Borovac, Gnjatović, Savić, Raković, & Nikolić, 2016), and helping humans in low-level industrial tasks by replacing them in unsafe environments (Yokoyama et al., 2003). The new trends in the imitation process are based on the more precise and on-line imitation of all types of the human motions, especially in tasks where motion is constrained by the equipment and environment.

2.2.2 Algorithm for description of human motions

With the aim of creating a robot with anatomical attributes close to a human being, the analysis of the characteristics of human motion becomes an important topic of research in the field of humanoid robotics. In order to increase a humanoid's acceptance into our human environment, researchers have been trying to create the motion of the humanoid as close as possible to human motion or inspired by human skill. Today, there are a lot of techniques for analyzing human motion, such as imitation learning and optimization approaches.

Imitation learning is based on the determination of characteristics of demonstrated motions in the task and the joint space. Looking at the state of the art on the imitation of the human motion, we can see that the Programming by Demonstration (PbD) is a core topic of research in this field. The PbD is based on encodes of motion demonstrated multiple times in either the joint space, the task space, or the torque space. Dimensionality reduction techniques (for example Principal Component Analysis and Independent Component Analysis (Calinon & Billard, 2005)) is the main tool used in the PbD. Encoding and regenerating human actions has usually been done using classical machine learning techniques, such as Hidden Markov Model (HMM) and Principal Component analysis (Asfour, Azad, Gyarfas, & Dillmann, 2008; Calinon & Billard, 2004, 2007; Calinon et al., 2005; Takano, Imagawa, & Nakamura, 2011; Tso & Liu, 1996). As an alternative to HMM and interpolation techniques, Calinon et al. (Calinon & Billard, 2007, 2008; Calinon, Guenter, & Billard, 2007) used the Gaussian Mixture Model (GMM) to encode a set of trajectories, and the Gaussian Mixture Regression (GMR) to retrieve a smooth generalized version of these trajectories and associated variabilities. Ude et al. (Ude, 1993) used spline smoothing techniques to deal with the uncertainty contained in several motion demonstrations performed in a joint space or in a task space.

In addition to the imitation learning approach, the characteristics of human motion can be analyzed using optimization approaches since the processes in humans and nature are as optimal as that of human motion (Alexander, 1984). Before starting the execution of any task, humans naturally come up with the simplest and most efficient ways in which motion can be performed. Therefore, we can say that humans, in order to create motions, are always trying to minimize some criteria that are unknown to us. The human body is a high redundant system and many different solutions exist for performing the same task. The choices of the solutions are not only influenced by biomechanical characteristics of a

human (age, gender, physical condition, restrictions on motion due to injury), but also by the strategy that a human employs when carrying out a given motion. Based on the analysis of human motions in different areas of science, we can extract some of the criteria that are often used in optimization algorithms in robotics, such as manipulability, magnitude and accuracy of the velocity and force, joint limit avoidance, joint torques and torque change, kinetics energy, muscle effort, and jerk (Chevallereau & Khalil, 1988; Chiaverini, Oriolo, & Walker, 2008; Pamanes & Zegloul, 1991; Zegloul & Pamanes-Garcia, 1993). The choice of the criterion function depends on the way in which the human motion is analyzed. Hence, analysis of human movement can be made on a kinematic or dynamic level. In our paper (see (Tomić et al., 2016)), we analyzed the influence of each kinematic criterion, including minimization of kinetic energy and velocity, minimization of deviations from the ergonomic position, and quality of imitation of the recorded human motion with and without contact. We used the Inverse Kinematic (IK) algorithm and included the criterion function using the null space of Jacobian. On the other hand, other authors based their research on human motion characterization in the dynamic level, analyzing how the dynamical criterion function describes human motion. Khatib et al (Khatib et al., 2009) defined new muscular effort minimization criterion to define optimal human postures using musculoskeletal dynamics. Their research is more based on the biomechanics of human motion. They implemented the basic concept of joint actuation on the control algorithm for the robot. Zheng et al. (Zheng & Yamane, 2013) presented the optimal criterion in order to imitate given reference motions of the human. They solved optimization problems which minimize the joint torques and associated contact forces. They considered contact between feet and floor, while contact between hands and equipment was not taken into account. Hollerbach and Suh (Hollerbach & Suh, 1987) presented the general inverse method into dynamics for minimizing the torque at the joints. They chose the joint acceleration null-space vector to minimize the joint torque in a least squares sense when the least square is weighted by allowable torque range.

Looking at the way in which humans perform a task, it is reasonable to think that the human used a combination of the different criteria functions instead of a single criterion function, which is presented in the papers above. Park et al. (I.-W. Park, Hong, Lee, & Kim, 2012) and Albrecht et al. (Albrecht et al., 2011) used dynamical parameters (such as the minimization joint's jerk and the minimization of changing the torque. . .) and made the combination of criteria functions in order to analyze human motions. For analysis of human locomotion trajectory, Mombaur et al. (Mombaur et al., 2008, 2010) defined the imitation of the human locomotion as an optimization problem. An objective function was defined as a weighted sum of the basic criterion function such as minimization of total time, the integrated squares of the three acceleration components, and the integrated squared difference of body orientation angle and direction towards the goal. The aim of their research was to produce a universal combination of the weighted coefficients for the optimization algorithm that satisfies the imitation of any type of human locomotion. Bil-

lard et al. (A. G. Billard et al., 2006) extended the pseudo-inverse optimization method for solving inverse kinematics in order to determine the optimal imitation strategy that best satisfies the constraints of a given task. They defined the objective function as a weighted sum of the basic criteria functions defined in the Cartesian and joint spaces. Their optimization algorithm minimizes the difference between the current and the desired position of the joints and the 3D Cartesian position of hands. They compute the trajectory of robot joints that imitates human motions. The constraints of the robot's body are taken into account. Unlike some previous studies, our research is based on the analysis of human motion using the inverse optimal control approach with criteria functions defined in the joint space. Given that the human body is a highly redundant system, there are different solutions for performing the same motion in the task space. Likewise, using the joint space, Yang et al. (J. Yang et al., 2004) analyzed human motion by combining basic functions such as joint displacement minimization, potential energy change, and discomfort basic functions. All of these are done in a multi-objective optimization algorithm in order to predict a static posture for the human. The virtual human Santos has been used to evaluate different performance measures and to test the applicability of their optimization algorithm for posture prediction. In each basic function, they propose a weight factor for each joint that is taken into account and defines the importance of particular joints for carrying out a given task. They applied this optimization algorithm for each basic function separately and then compared it with the results obtained for multi-objective optimization.

2.3 Humans strategies for performing tasks

The strategy used by the human during the movement is based on the experience gained. Throughout repeating the same task several times, humans find a way to do a task with minimum effort and in the most comfortable way. A large group of healthy people perform the same task in almost the same way (Lardy, Beurrier, & Wang, 2012). The difficulties in motor skills force humans to change their motion strategy and adapt it. In the same way, the motion strategy can be different due to changes in the environment in which the movement is performed. In that context, this chapter describes the basic characteristics of human movement, such as the distribution of motion through the joints and ergonomic analysis. The analysis of the influence of environment on the changes in motion strategy is also given.

2.3.1 Motion distribution through the arm joints

Distribution of motion is connected to properties of biological systems and the type of arm motion performed. The task performed by a human is largely determined by muscle activation. In humans, the high-inertia arm joints (shoulder and elbow) provide the smooth global motion, while the low-inertia hand joints (wrists) perform fast and precise local motions. The motion priority of the joints during a task is well explained in sev-

eral papers. In his paper, Potkonjak et al. (Potkonjak, Popović, Lazarević, & Sinanović, 1998) analyzed motion distribution through arm joints. According to their research on a “Handwriting” task, humans control their proximal joints while the movement of the distal joints follows them. Based on the biomechanical research, Liu et al. (Liu, Hertzmann, & Popović, 2005) analyzed the habits of humans for using some muscles more than others during motion. Using the nonlinear optimization algorithm, they minimized the energy objective functions, which compute the total amount of torque due to muscle forces, and calculated the activity of each muscle during the motion observed. Yang et al. (J. Yang et al., 2004) explains the difference of joint activation via their optimization algorithm by adding different scalar weight factors to each joint. This approach is used in our optimization algorithm via the weight matrix associated with the minimization of kinetic energies or minimization of joint velocity. The weight matrix is introduced to stress the importance of the particular joints that tend to be more active than others during the tasks. For the case of the minimization of kinetic energy, the inertial matrix is used as a weight matrix. The bigger motion priority is given to the joints with bigger inertia (trunk, shoulders, elbows). On the other hand, the minimization joint velocities criterion consists of a weight matrix, which in this case is an identity matrix and thus gives the same importance of motion to all joints during the task. According to these analyses it is expected that in the tasks where the shoulder or elbow move more, the minimization kinetic energy criterion function is dominant. However, when the task does not require the big motion of the shoulder and elbow, the minimization of the joint velocity criterion is dominant. We do an analysis of these assumptions in our research.

2.3.2 Ergonomy configuration of the human body

The introduction of comfort level is based on the motion control mechanism of the human body. In general, with the own feedback control mechanism, humans always keep their joints at a high comfort level; that is to say, humans tend to operate within a comfort region. Human bodies are loaded with sensors that feedback information to the central nervous system, regarding our internal state and the environment around us. In general, this information is utilized to affect ongoing control strategies and to suggest a role for feedback. The characteristics of human motion are largely conditioned by the equipment used during the task. If the task does not require interaction with the equipment, a human will choose the most comfortable way to perform the task as explained in (Tomić et al., 2016). In other cases, humans will adjust their motion to carry out a task and decrease discomfort as much as possible. At any moment of the human motion, when the force or torque exerted by a muscle group at a joint is close to its maximum torque, a human can feel the discomfort although he/she does not exactly know the value of the torque he/she exerts. The analysis of human comfort while performing a task is widely explored in ergonomics, biomechanics, and robotics. Yang et al. (F. Yang, Ding, Yang, & Yuan, 2005) proposed an algorithm based on the combination of inverse kinematics,

inverse dynamics, and biomechanical information for increasing the comfort level during motion. They calculated the discomfort level of each joint as a ratio between torques exerted by the joint (calculated using the inverse dynamic) and the maximum torque that can be produced by the joint (which is obtained from the ergonomics data). Discomfort minimization is the criterion that they minimized inside the inverse kinematic algorithm. Ma et al. (Ma, Chablat, Bennis, Zhang, & Guillaume, 2010) combined the conventional posture analysis techniques (proposed in ergonomic analysis) and the fatigue index in the muscles to calculate comfort during manual handling operations. Yang et al. (J. Yang et al., 2004) proposed a discomfort index as an objective way to estimate the most comfortable position of the human body during a task. They defined the ergonomic configuration of the joints, for which the values of the joints are in the middle of their ranges, as the most comfortable position for the human. In our research, we analyzed the level of human comfort during the motion analysis. We defined the criterion in our optimization algorithm as the minimized difference between the current configuration of joints and the ergonomic configuration proposed by Yang et al. (J. Yang et al., 2004).

2.3.3 Feasibility measure of the task

The characteristics of the body and the type of the motion greatly affects the feasibility of the task. The ability of the robot to move its end-effectors in any direction is presented via the manipulability index (Angeles & Gosselin, 1991; Yoshikawa, 1984, 1985). The manipulability index is defined as a ratio between norm of the motion in the joint space and Cartesian space. The feasibility of the task is additionally explained with the manipulability ellipsoid (Kurazume & Hasegawa, 2006). The axes of the manipulability ellipsoid give the capacity of motion in an appropriate direction. The direction of the minor axis represents the direction of developing speed with worse capacity while the direction of the major axis gives the motion in that direction more feasibility. The feasibility of the hands motion for the dual-arm manipulation tasks performed by a robot is extensively analyzed in various pieces of literature. Lee et al. (S. Lee, 1989) defined dual-arm manipulability as the measure of geometrical similarity between the desired manipulability ellipsoid and the dual-arm manipulability ellipsoid. Dual-arm manipulability is represented by the volume of intersection between the two manipulability ellipsoids from individual arms. The desired manipulability ellipsoid is defined along the Cartesian position trajectory based upon the velocity and force requirements for a given task. Vahrenkamp et al. (Vahrenkamp, Asfour, Metta, Sandini, & Dillmann, 2012) presented an approach for analyzing the workspace capabilities of the robot using reachability information. They extended classical measurements, which are mostly based on analyzing the manipulability ellipsoid, in order to consider constraints coming from joint limitations, workspace obstacles, or self-distance. A large set of predefined grasps for a given object is filtered in order to select the reachable subset for which the inverse kinematics problem has to be solved. In analyses of human motion, the manipulability index de-

scribes the quality measure between human configuration and the singular configuration. A joint configuration of the human body close to a singularity is characterized by a small value of manipulability. Conversely, the ergonomic configuration of the human body is characterized by large manipulability because the human is able to perform the motion in any direction in the joint and Cartesian spaces. Following the same principle, we analyze the characteristics of the human motion defining one of the criteria in our optimization algorithm which maximized the index of manipulability.

Human to humanoid motion conversion for dual–arm manipulation tasks

The objective of this chapter is to present a conversion process for imitation of human dual arm motion with a humanoid robot. The conversion from human to humanoid motion is represented in four steps: the first step corresponds to the analysis and record of the human motion; in the second a kinematic model of the humanoid with human size is defined; the third step uses the imitation algorithm to obtain motion in joint and Cartesian space for the humanoid; the fourth step concerns the generation the motions (with and without contact) of the robot ROMEO using the results obtained from the imitation algorithm. The overview of the conversion from human to humanoid motion is given in Fig. 3.1. Each of the conversion steps is analyzed in detail below.

3.1 Dual-arm manipulation

Human motion can be defined as a needed action which humans apply in order to acquire the task. Humans use one arm or both arms for manipulation, depending on the characteristics of the task and equipment. In comparison with one arm manipulation, dual arm manipulation is a very complex operation which humans learn while growing up. The better way for a good understanding of dual-arm motion characteristics is to represent it as a set of elementary motions.

The classification of bimanual tasks has been given by Zöllner et al. (Zöllner et al., 2004). They developed a segmentation algorithm for each type of two hand actions. They classified elementary motions into uncoordinated and coordinated groups, with the coordinated groups either being symmetric or asymmetric. The other classifications of

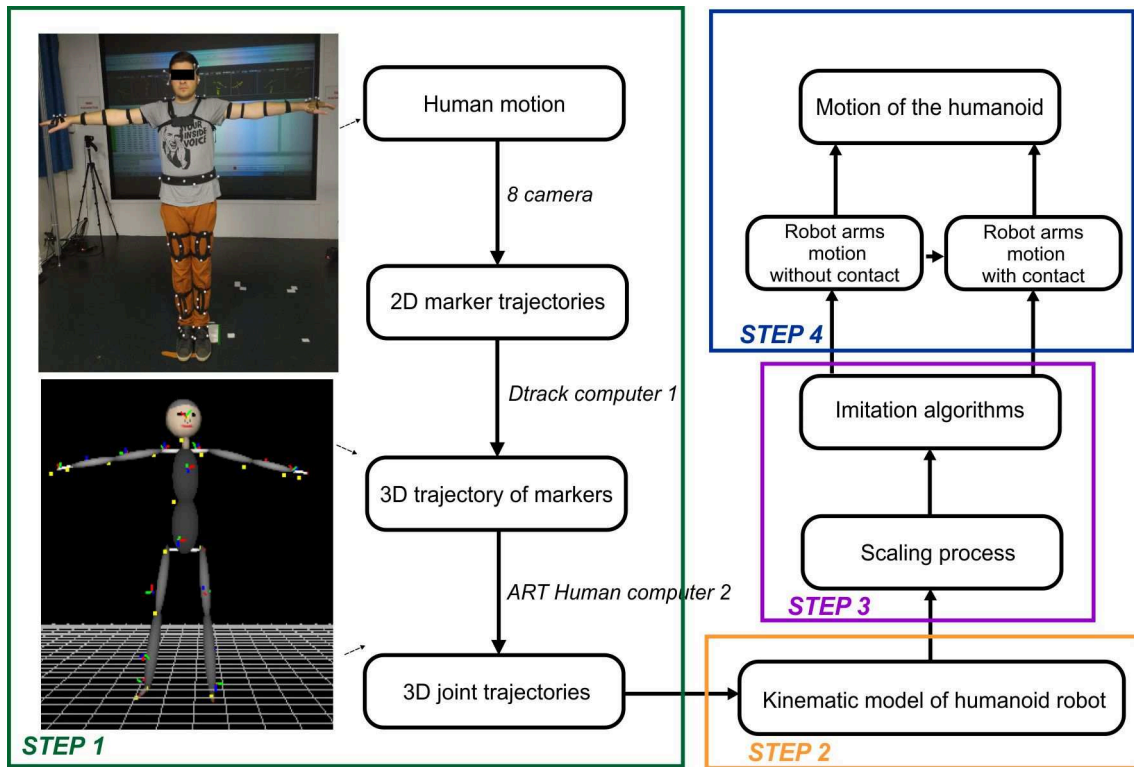


Figure 3.1: Overview of the conversion from human to humanoid motions.

coordinated dual-arm motion were given by Krüger et al. (Krüger et al., 2011). The classification of motion is done according to the characteristics of the motion in the task space. According to them, the coordinated motion can be subdivided into goal-coordinated and pure bimanual motions. Goal-oriented motions are the most complicated manual activities where hands manipulate different objects in order to achieve the task. Arms are in contact with equipment but interaction between arms does not exist. In bimanual motions, both hands are manipulating with the same object, creating a close kinematic chain. The cooperation between arms and interaction with equipment are required for the task. The bimanual motion can be subdivided symmetrically or asymmetrically, congruent or non-congruent. On Fig. 3.2, classification of simple dual-arm motions based to on the classification above is given. In the symmetric motion, both arms do the same translation/rotation motion in the same direction with the aim to achieve the task with tools (see Fig. 3.2 motions 4, 5, 6). In asymmetric motion, the direction of translation/rotation is different (see Fig. 3.2 motions 7, 8, 9). According to this, movements can be divided into translational and rotational movements (e.g. the in the Fig. 3.2 motion 1 is defined as a rotation around vertical axis while motion 2 is defined as rotation around horizontal axis). For one arm support motion, one arm is used to hold the equipment while the other hand performs the task (see Fig. 3.2 motions 10, 11, 12).

Each motion, inside of the same group of motions, has different characteristics which are related to the different fashion of a human performing the task. Various constraints have influence on the way in which the task will be performed. All constraints may be divided into:

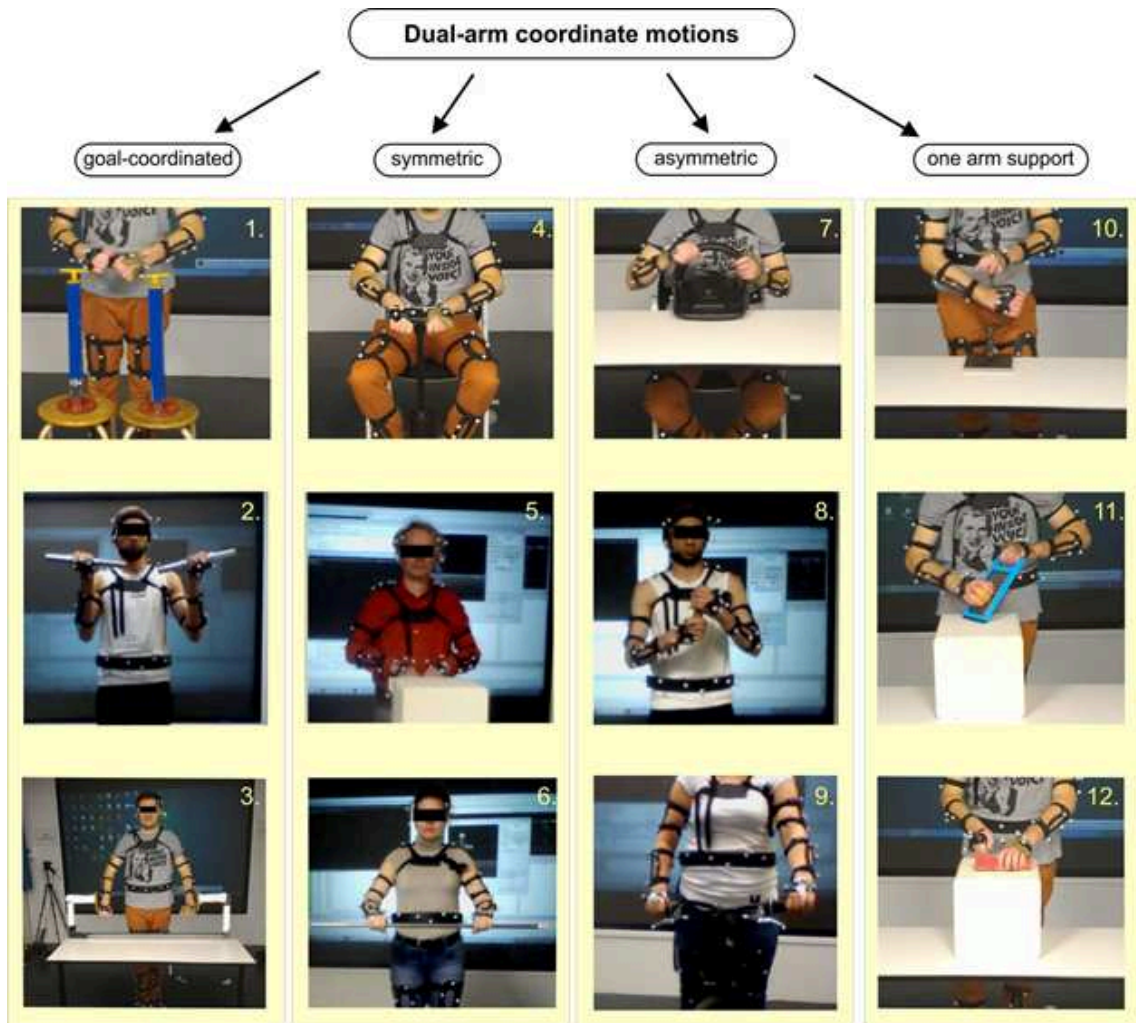


Figure 3.2: Classification of dual-arm coordinates motions.

1. Constrains dictated by the characteristics of the equipment
2. Control constraints for achieving a task
3. Uncontrolled constraints

On the example of the “Opening/Closing a drawer” motion, the position and orientation of hands are fixed and dictated by the equipment (the fingers of both hands are placed inside the drawer with the palms down). In order to perform the “Opening/closing a drawer” motion, only horizontal translation of hands is allowed, which represents the control constraint. The uncontrolled constraints are related with the characteristics of the human (size of body segments, joint angle range...) and cannot be controlled. All of these constraints have influence on the group of the muscles which are activated during the task. The characteristics of human motion are more evident in motion that is more limited. It is expected that there is a predefined way humans perform a task when the human motion is constrained by equipment characteristics and control constraints. In our research we analyze the characteristics of the motions that are more limited by constraints. We do this with the aim to obtain the pure characteristics of the motions.

In order to define the characteristics of human motion for elementary dual arm tasks, we analyzed seven dual arm motions from the recorded motions in Fig. 3.2. We have chosen the different types of the motions according to the classification above and the axis of the rotation/translation. Motions are classified as rotational motions (“Rotation of the steering wheel”, “Rotation of the valves”, “Rotation of the canoe paddles”) and translational motions (“Cutting food with the knife”, “Inflating a mattress using a pump”, “Grating the food”, “Opening/closing a drawer”). These motions are grouped as:

- task oriented motions- “Rotation of the valves” (Fig. 3.2 motion 1) and “Rotation of the canoe paddles” (Fig. 3.2 motion 3)
- symmetric motions- “Inflating a mattress using a pump” (Fig. 3.2 motion 4) and “Opening/closing the drawer” (Fig. 3.2 motion 5)
- asymmetric motions- “Rotation of steering wheel” (Fig. 3.2 motion 7)
- one arm support motions- “Cutting food with the knife” (Fig. 3.2 motion 12) and “Grating the food” (Fig. 3.2 motion 11)

We have chosen these motions because they are more limited with the characteristics of the equipment. We believe that the characteristics of these motions will be more evident compared to other motions.

Each recorded task consists of a dual-arm motion that is repeated five times. Before recording, all actors practiced each motion for approximately 5 minutes. Each actor carried out the required motions under the same conditions and using the same equipment. Thirteen male and six female individuals (with age 32 ± 11 years; and with the height 1.7 ± 0.1 cm) participated in the experiments. Each recorded task consists of three phases: The Initial Configuration Phase (ICP), The Transition and Grasping Phase (TGP) and The Periodic Motion Phase (PMP). Tasks start with the ICP where the actor stands/sits in the center of the working space and maintains the Initial configuration for one second. The

initial configuration consists of both arms being fully extended in front of the actor with the palms facing towards the floor. The motion speed is equal to zero during the ICP. Once the actor has assumed the required position, he will start the second and third phases of the motion. In TGP the actor moves the arms in order to grasp the equipment. The way in which the actor will grasp the equipment is up to him/her. The grasping is constrained by the characteristics of the equipment. In PMP the actor performs dual-arm motions. The PMP is considered as the most important of the three phases because it is the only phase that undergoes any form of analysis.

Task 1. Consider the task of “Rotation of the valves” (see Fig. 3.2 motion 1). The “Rotation of the valves” is a goal-oriented rotational motion around the vertical axis. The task presents the simultaneous unwinding of two valves that are positioned vertically at the same height (1.15m). The valves are placed in front of the actor parallel to the actor’s sagittal axis on either side. In order to turn the valves, the actor rotates the handles in the horizontal plane around the vertical axis of the valves. The distance between the vertical axes of the valves is 0.32m. The radius of the valves is 0.1m. The actor stands during the task.

Actor starts motion from the initial position. At the transition phases of the motion, palms are placed perpendicularly to the room’s floor and he/she grasps the handles vertically placed on the valves. The height of hands is determined by the characteristics of the valves. During the PMP phase both arms work independently while performing this task. Arms rotate the valve’s handles five times continuously during the motion.

Task 2. Consider the task of “Opening/closing a drawer” (see Fig. 3.2 motion 5). The “Opening/closing a drawer” task represents a symmetric horizontal-translation motion. The table (height of 0.75m) with a drawer (height of 0.3m) is placed in front of the actor at a distance that is comfortable for the actor to perform the task. The actor should open the drawer with both hands simultaneously. The actor stands during the task.

Actor starts motion from the initial position. At the transition phase of the motion the actor puts their hands inside of the drawer. The orientation of their hands is fixed and prescribed by the equipment (the fingers of both hands are placed inside the drawer with the palms down). In the PMP phase, the motion of the hands is constrained by the equipment and only horizontal translation of the hands is allowed.

Task 3. Consider the task of “Rotation of the canoe paddles” (see Fig. 3.2 motion 3). The “Rotation of the canoe paddles” task represents a goal-coordinated rotational motion around one horizontal axis. The handles are connected to the U-shaped platform which is fixed on the horizontal table. The design of this prop simulates paddling a canoe. The actor rotates the handles in the vertical planes around the horizontal axis. The actor stands during the task.

Actor starts motion from the initial position. At the transition phase the actor grasps the handles. Palms of the hands are kept parallel to the room floor. The relative position between the arms is constant and determined by the characteristics of the equipment. In

the PMP phase the actor rotates the handles with both hands simultaneously around the common horizontal axis.

Task 4. Consider the task of “Rotation of steering wheel” (see Fig. 3.2 motion 7). The “Rotation of a steering wheel” task is an asymmetric dual-arm rotational motion. The Logitech steering wheel is used for simulation of driving a car task. The wheel is fixed on the horizontal table and tilted relative to it at an angle of 30 degrees. The diameter of the steering wheel is 0.14m. The actor is sitting while they carry out the tasks and the steering wheel is placed in front of him/her.

The actor starts the motion with his/her hands extended horizontally as in the initial configuration. The PMP phase starts when the arms are symmetrically placed on the wheel. The hands are able to rotate the steering wheel in both directions (in the experiments the motion was ± 90 degrees starting from the grasped position of the hands). The motion of the hands is circular in accordance with the form of a steering wheel. During the motion, the relative position between both hands is unchangeable.

Task 5. Consider the task of “Inflating a mattress using a pump” (see Fig. 3.2 motion 4). The “Inflating a mattress using a pump” task is a symmetric dual-arm translation motion. The actors are sitting while they carry out the tasks with hands horizontally placed as in initial position. The hands grasp the pump’s handle horizontally and their relative position does not change during the motion. The motion is obtained when the actor pulls up and down the pump’s handle.

Task 6. Consider the task of “Cutting with a knife” (see Fig. 3.2 motion 12). The “Cutting with a knife” task is a one-arm support translation motion. The right/left hand does the translational motion in order to perform the task. The left/right (opposite) hand is used as a support hand and holding a box that does not move. The motion of the hand which performs the task is not strongly defined by the type of equipment used. The hand which performs a task can rotate around the handle of the knife. The amplitudes of the hand’s motion are limited by the size of the knife. During the PMP phase the actor simulates the cutting motion. The actor stands during the task.

Task 7. Consider the task of “Grating of food” (see Fig. 3.2 motion 11). The “Grating of food” task is also one-arm support translation motion. The right/left hand does the translational motion slipping the ball over the grater’s surface. The opposite hand holds the grater so that it does not move. The orientation of the hand which performs the task is restricted and the palm should be in line with the plane surface of the grater. The trajectory of the hand which performs the task is connected with the angle between the grater and the table surface, which is not predefined. The actor used the grater in a way they considered most comfortable. The motion’s amplitudes of the hand which performs the task are limited by the size of the grater. The actor stands during the task. During the PMP phase the actor simulated the grating motion.

3.1.1 Segmentation of the human motion in the motion primitives

Since recorded human motion is represented as a complex motion with several actions, it can be segmented to the sequence of predefined actions (motion primitives). These motion primitives are the elementary actions of motion which accomplish a complete goal-directed behavior (A. Billard, Calinon, Dillmann, & Schaal, 2008; Nakazawa, Nakaoka, Ikeuchi, & Yokoi, 2002). The segmentation of the recording motion in motion primitives is done using different techniques, such as Dynamic Time Warping, k-means (Albrecht et al., 2011), and on-line segmentation presented by Kulic ((Kulic & Nakamura, 2008; Kulić, Ott, Lee, Ishikawa, & Nakamura, 2012; Kulic, Takano, & Nakamura, 2008, 2009). The motion primitives of the signal can be analyzed in the joint space by looking at specific points of the joint trajectories. Encoded human motion from the motion primitives can be obtained by different algorithms such as the hierarchical Bayesian models (Rueckert, Mundo, Paraschos, Peters, & Neumann, 2015) and statistical HMM algorithm (Kulić, Takano, & Nakamura, 2008; Kulic et al., 2009; D. Lee & Nakamura, 2014). In their research, Kulic and Nakamura (Kulić et al., 2012) gave a detailed review of techniques for segmentation of human motion to motion primitives and an analysis of the characteristics of motion.

3.1.2 Our approach-phases of motion and normalized circle motion

The periodic motion phases consist of a five time repetition of a dual-arm motion primitive. In order to reach the starting and ending point of one primitive motion, we paid attention to the samples in which the minimum values of the joint velocity are detected and hands are currently stopped. One execution of a primitive motion is represented as a part of the joint trajectories between the samples of two minimum values, which are repeated during the motion. We normalized temporarily each primitive motion in order to have the common phase for performing the same motion for all actors. The primitive motion is used for analysis on the characteristics of the motions invariants.

3.1.3 Conclusion

This chapter presents the dual-arm manipulation tasks which can be used for the analysis of human motion behavior. According to the state of the art in the field of the dual-arm manipulation, the different types of dual-arm motion are considered for analysis. We assume that the more constrained tasks will give us more precise analysis of human motion. Thus, we have chosen seven dual-arm motions which will be analyzed in the Cartesian space in this chapter. Since our task is to define human motion behaviors, we should analyze human motion in the Cartesian and joint spaces. In addition to the analysis presented in this chapter, in the next chapters we represent human motion in the joint space, analyzing the activation of each upper body joints. This knowledge will help us to define

the strategies that humans use during dual-arm motions, as well as to obtain the control algorithm for a robot to imitate human motion.

3.2 Motion capture systems and recording human motions

The understanding and modeling of the human motion is based on observation. Motion observation evolves with the evolution of the available technologies. Some of the first systems of recording human motion are presented in [section 2.2](#). Today, there are a lot of techniques for recording and analyzing human motions such as inertial, optical, magnetic, acoustic or mechanical systems. The type of motion capture system used depends on the volume of measurements taken, the required resolution, the characteristics of the motion recorded and the environment in which the motion is performed. Acoustic ([Vlasic et al., 2007](#)), inertial ([Miller, Jenkins, Kallmann, & Mataric, 2004](#)) and magnetic ([Aloui, Villien, & Leseq, 2015](#)) motion capture systems, are able to record outdoor and indoor human motions. Optical and mechanical motion capture systems require predefined position of the cameras and sensors. The sensors can be placed on actor for recording human motion or on the robots for making as feedback information for control loop. The most commonly used technique for recording human movement is marker based and marker-less motion capture systems. In order to increase accuracy and obtain online imitation of the human motion Do et al. ([Do et al., 2008](#)) used a combination of the marker-based Vicon and stereo-based marker less motion capture systems. Compared with other techniques, the marker based techniques do not accumulate errors during the recording, provide better accuracy and resolution, have a bigger volume of measurements and are not sensitive to the electromagnetic fields and external noises. Some of the disadvantages of this type of marker based system are longer actor's preparation times, inability to directly set markers on the human skeleton for better acquisition of data, inflexibility in motion capture location, off-line processing of the data. Comparative analyses of different motion capture systems are given in references ([Ceseracciu, Sawacha, & Cobelli, 2014](#); [Zhou & Hu, 2008](#)).

Recorded data from motion capture system should be further processed. The motion capture systems have the functionalities to analyze and process data from sensors. The primary functionalities of motion capture processing are initialization, tracking, pose estimation and recognition. In accordance with the aforementioned, Moeslund and Granum ([Moeslund & Granum, 2001](#)) gave a comprehensive review of relevant works in a field of motion capture system.

3.2.1 ART motion capture system

Our research is based on analysis of the human motion in Cartesian and joint space. Since the all characteristics of the human motions cannot be obtain with one motion capture system we choice the motion capture system which is suitable to record the human motion with big precision and which will give us enough information to estimate human motion. Advanced Realtime Tracking (ART) motion capture system produced by ART Company is used for the purpose of our research.

The ART system consists of a hybrid suit of 17 sets of markers relative to the feet, shins, thighs, shoulders, upper-arms, forearms, hands, head, hip, back and torso (see Fig. 3.1 step 1). A set of 8 infra-red (IR) cameras is used for recording the motion of the markers. Motion capture hardware is supported with DTrack and ART Human software for tracking and reproducing the motion of the actor in a virtual environment. The DTrack software acquires the 2D information of each IR camera and provides the transformation matrices relative to the different marker frames attached to the body parts with respect to the global reference frame. The positions of the joint frames are estimated using the intersections of the marker frames defined with respect to the reference frame. Joint orientations are given with respect to unknown local frames and cannot be used. Referent frame is defined during the room calibration process and connected on the surface of the floor. ART Human uses the information provided by DTrack and estimates location of the human joint frames (ARTCompany, 2018). The flowchart diagram of the work motion capture system is given in Fig. 3.1. step 1. The sampling frequency for the acquisition data is set to 100Hz.

The motion capture system is able to recognize and find correspondences between the segments of the actor body in consecutive frames, and give a graphical representation of the actor (avatar) within a virtual environment (see Fig. 3.1. step 1). The kinematic model of the avatar realistically represents the human body and includes 60 DoFs (20 joints with 3DoFs per joint). Avatar body segments are modeled as three-dimensional ellipsoids and have dimension of the human body segments estimated by ART Human software. Since the kinematic model of the humanoid, which is used in the imitation process, has less DoF than the avatar and has only few rotational joints, the motions of the avatar cannot be used directly and reduced model that enables human to humanoid motion replication has to be adopted.

3.3 Kinematic model of the humanoid as a human model

The information obtained from the motion capture system is used to define the characteristics of the human body and his motions. There exist numerous human motion capture systems that produce output in terms of different model of avatars that are stored in different formats making it more difficult to exchange avatar modules in an overall infrastructure for humanoid robots. The avatar model can be directly used in the conversion

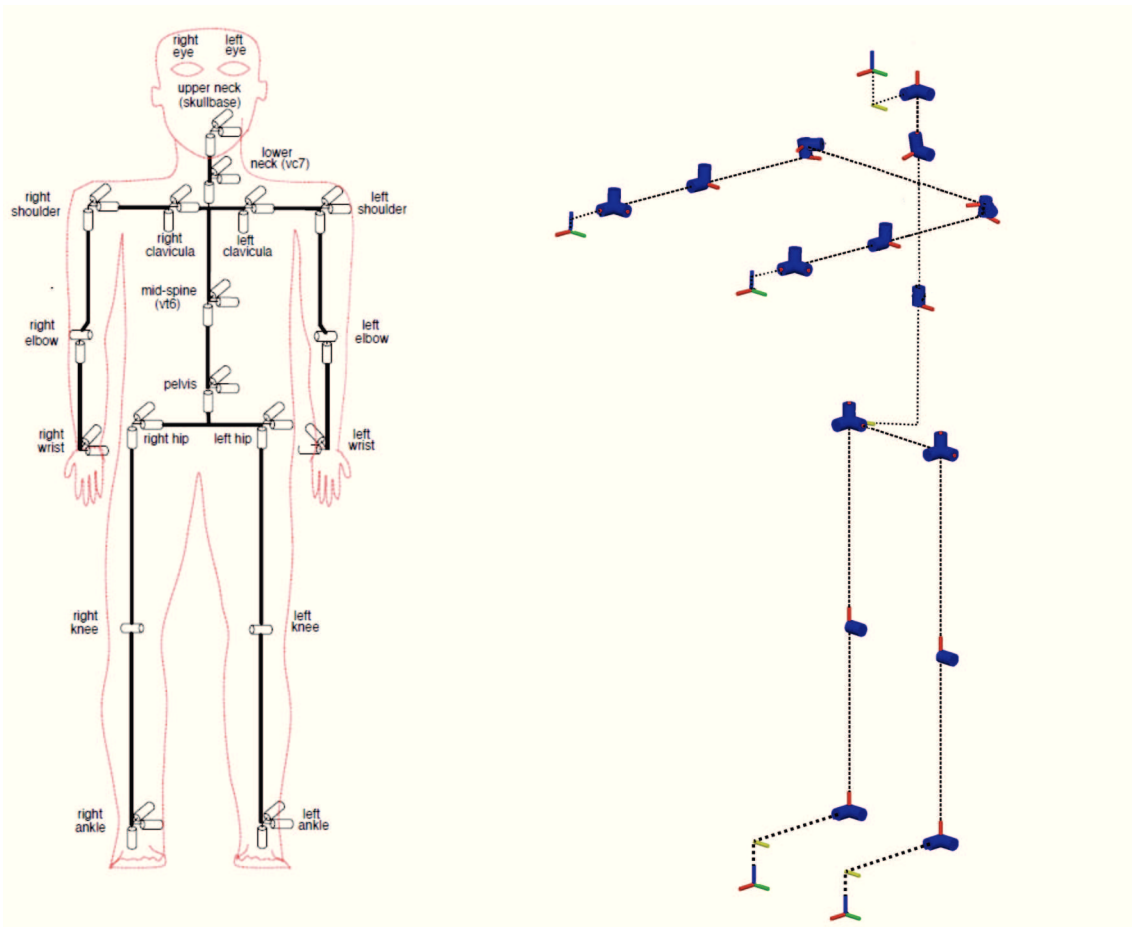


Figure 3.3: a) Kinematic model of Master Motor Map (Azad et al., 2007); b) Kinematic model of the robot ROMEO.

process if it is near the kinematic model of the robot. Since the avatar model can have more or less DoFs compared to the model of the robot, the intermediate model of the human body should be defined. To overcome the deficiencies mentioned above in papers (Azad et al., 2007; Terlemez et al., 2014) are proposed an intermediate kinematic model, which they call the Master Motor Map (MMM) (see Fig. 3.3 a). Their strategy is to define the maximum number of DoF that might be used by any visualization, recognition, or reproduction module, but not more than that. The MMM model consists of the 52 DoF. The MMM model allows the simplification to the model of the humanoid robot or on the simplified model of the human. The intermediate model can be scaled in terms of body weight and height. Since the effort is very high to create a model for each subject individually, we also define the intermediate model. According to the characteristics of the humanoid robot presented in the subsection 2.1.1 and Table 2.1, we have chosen kinematic model of the robot ROMEO to represent the intermediate model of the human body.

3.3.1 Robot ROMEO

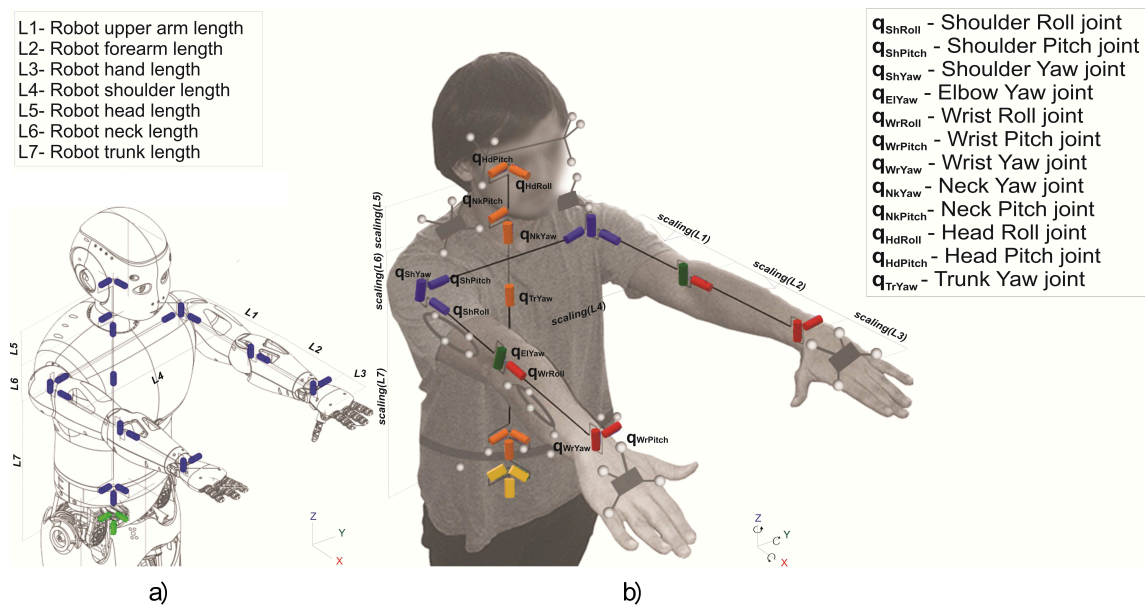


Figure 3.4: Scaling process: a) extended kinematic model of robot ROMEO in a basic configuration; b) Intermediate model - scaled extended kinematic model of the robot ROMEO to the dimensions of the human in the initial configuration with markers and marker frames.

The humanoid robot ROMEO has been developed by Aldebaran Robotics (see Fig. 2.1.). Romeo is a 1.4 meters-tall and 36kg weight humanoid robot, designed to explore and further research into assisting elderly people and those who are losing their autonomy. Taller than the Pepper and Nao robots, ROMEO really has been designed with assisting people in their daily lives in mind, and would in the long term be able to carry out actions such as opening a door or picking up objects from a table. Fitted with two cameras in its

eyebrows allowing it to measure distances. ROMEO is equipped with four computers to manage its sight, hearing, movements and artificial intelligence. The characteristics of the actuators implemented into the robot are given in the appendix A. ROMEO incorporates a mass of innovations required for its future role as a personal assistant. Robot ROMEO has 37 DoF including, 7 DoF per arm, 6 DoF per leg, 2 DoF for each eye, 1 DoF for each foot, 2 DoF for the neck, 2DoF for the head and 1 DoF for the backbone. The spinal column, design, battery and solidity are improved in the second version of the robot. The upper body model of the robot ROMEO is used for the purposes of our research. We additionally include 6 DoF in the trunk, which are not included in the kinematic model of the ROMEO, and emulate the leg and spine motions (3 prismatic and 3 rotation joints (see Fig. 3.4 a)). The modified Denavit and Hartenberg (DH) convention is used in the process of defining the kinematic model (Khalil & Kleinfinger, 1986). The principles of the modified DH convention are explained in appendix D. In this way, we made an intermediate model, as kinematic model of the human, which is extended kinematic model of the robot ROMEO.

3.3.2 Scaling process

The transformation the kinematic model of the avatar to the model of the robot ROMEO represents scaling process and in our research is given in two levels. At the first level, we take into account the simplification of the kinematic model and reduced the kinematic model of the avatar (60 DoFs) to the model of the robot ROMEO (37 DoFs). This kinematic model which has the size of the segments as the avatar model and numbers of DoFs as kinematic model of the robot ROMEO represent intermediate model. In our research intermediate model is called a scaled model of the robot ROMEO. The scaled model of the robot ROMEO is used in the imitation algorithm in order to take all information about human motion in joint and Cartesian spaces. Human motion in joint space is used for analysis the human motion behaviors and human motion characteristics while the representation of the human motion in Cartesian space defines the task which robot should obtain. At the second level, the difference of the body segments between human and robot ROMEO is taken into account and the intermediate model is transformed to the model of the robot ROMEO. Acquired information about human motion calculated for the scaled model of the robot ROMEO has been applied to imitate the human motion with the real model of the robot ROMEO.

Since the kinematic model of the robot ROMEO is taken as intermediate model, size of the robot segment should be scaled to the size of the actor limbs. For the purpose of the scaling process the initial configuration is defined. The basic configuration of the humanoid robot q_{basic} (see Fig. 3.4 a)), with the values of the all joints equal 0, is proposed as initial configuration of the actors. In the initial configuration arms are horizontally extended forwards with palms facing towards the floor (see Fig. 3.4 b)). This configuration is well defined and can be easily achieved. In order to make relevant scaling process and transformation the kinematic model of the human to the scaled model

of the robot ROMEO, the scaled model of the robot ROMEO is defined with respect to the global referent system.

Positions of the joint frames estimated by the motion capture system can be used to estimate the size of the human segment required for the scaling process. The dimensions of the human segments are calculated by taking the mean Euclidean distance between two adjacent joints, and using several data samples taken from the recorded data, when the actor keep the initial configuration. The dimensions of paired segments located on left and right sides of the body are assumed to be identical and are calculated by taking the mean value of the estimated segment dimensions on right and left side from each actor.

The frames' position and orientation of the markers physically attached to the actor body (Real Markers) are known and calculated by the ART Human software. In order to attach frames of the Real Markers to the intermediate model, we must place the intermediate model in the 3D position (with respect to the global referent system) and body configuration same as the human model. The initial configuration which keeps actors at the beginning of the motion is used for this purpose. Calculation the configuration of the intermediate model which aligned the human initial configuration and the position of the human body with respect to the global referent system is done by the initialization algorithm which is explained in detailed in the Algorithm 1. Since the intermediate model is posed on the initial configuration of the human, the frames of the Real Markers are easily replicated to the intermediate model. These frames are hereinafter called as Virtual Markers. Virtual Markers frames are defined as fixed and pre-labeled frames onto the surface of the voluminous intermediate model which are set up in advance. Virtual Marker frames are defined according to Real Marker frames at the initial configuration during the initialization process and in the imitation algorithms will be used for matching motions of the Real Markers frames.

3.3.3 Un-modeled kinematics of the human body

The conversion from human to humanoid motion is based on the effective kinematic model of the humanoid robot according to his joint mobility and size. The closer is the kinematic model of the humanoid to the model of human in size, joint limits and kinematic model, the better can be the imitation. Since we used extended kinematic model of the robot ROMEO as kinematic model of the human, we can expect the inconsistencies in the motion imitation will appear. A lot of humanoid robots do not have complex structure of the shoulder girdle as the human. The dimensions of the segments are assumed constant in the model of the humanoid. In reality these quantity vary during the motion of the human due to the un-modeled joints of the human and the motion of the skin. The un-modeled joint in the shoulders are responsible for the vertical displacement of the shoulders (see Fig. 3.5). Error will appear and a perfect imitation of the human motion with kinematic model of the humanoid is not possible. The relative position of the Real Marker with respect to the corresponding proximal frame of the actor joint and

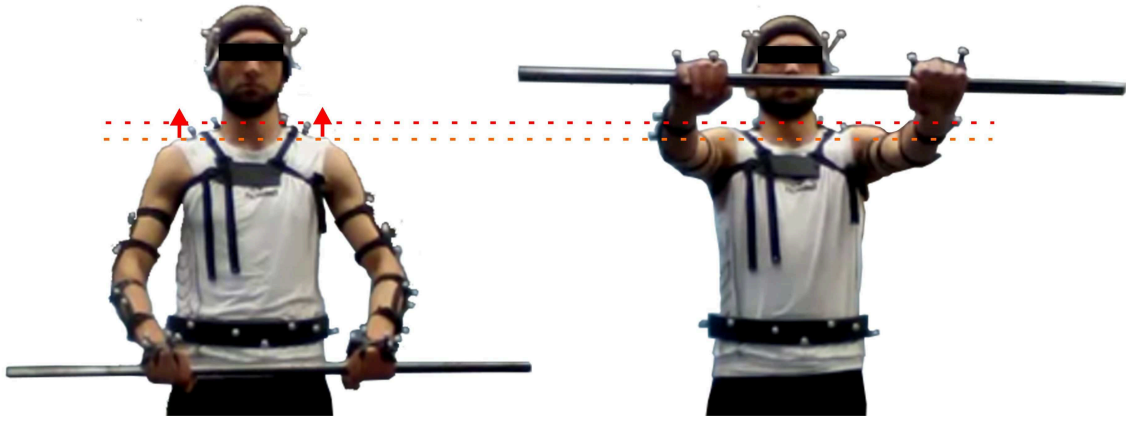


Figure 3.5: The displacement of the shoulder joints and Real Markers attached to the shoulders during the motion.

dimensions of the segments are calculated and assumed constant in the scaled model of the ROMEO robot. In reality, this quantity varies during the motion of the actor due to the un-modeled joints of the human and motion of the skin. The un-modeled joints in the shoulders are responsible for the vertical displacement of the shoulders and the Real Markers attached on the shoulders (see Fig. 3.5). Although the markers are strongly attached to the body segments, distance between the Real Marker and its proximal joint is not constant due to the motion of the skin. This phenomenon is the most obvious in the case of hand and shoulder markers. An error appears and a perfect imitation of the human motion by the scaled kinematic model of robot ROMEO is not possible. More details about calculation frame of Virtual Markers are given in 1.

3.3.4 Estimation of the human body segments parameters

The essential part of the conversion framework is based on a three-dimensional whole-body, kinematic model enriched with proper body segment properties (BSP), such as mass distribution, segment length, moment of inertia, etc. In the following, it is shown how BSP can be calculated in order to determine various dynamic properties of a body segment.

Many different methods exist for estimation BSP such as cadaver-based method, mass scanning-based method and geometrical methods. Most of them are based on statistics. Each of the method leads to different results of BSP which depend on the chosen segmentation. The first Hanavan model of the human body has 15 segments which are define with 25 anthropometric parameters. In 1974 he gave the more precise model of the human body with 16 segments but defined with 41 anthropometric parameters. The complex segmentation is done by Yeadon who represents human body with 40 solids and 95 anthropometric parameters. Jensen (Jensen, 1978) proposed Elliptical zone method and segmented human body with elliptical disks of about 20mm width. Each of the method are not adapted to variety of human body such as difference made between a young healthy sportsman and an obese woman or an old person in terms of mass distribution and mass density.

For the purpose of our research we choice geometric method named modified Hanavan

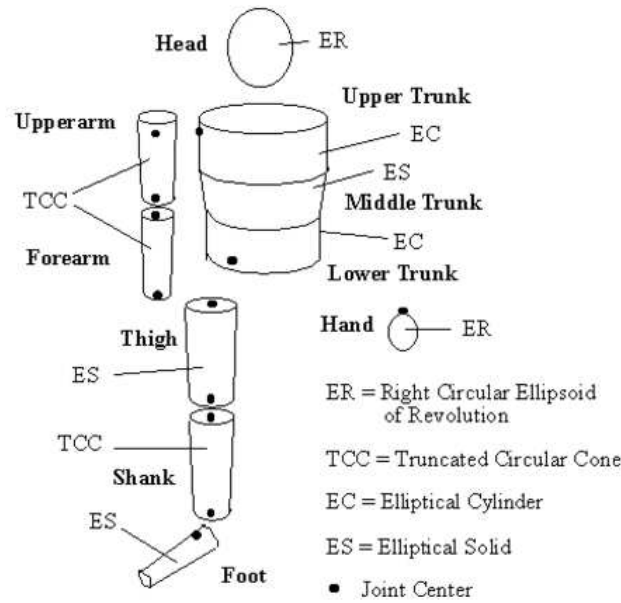


Figure 3.6: Human body segmentation according to the modified Hanavan notation.

method. The Hanavan model represents the human body as a set of the solids which have anthropometric dimensions. An anthropomorphic, voluminous model is useful in terms of motion synthesis, adaption, and analysis. To determine a sufficient voluminous model from the applied anthropometric data, appropriate geometric primitives such as cylinders, cones and spheres are used. These geometrical primitives fit the human shape well. According to the modified Hanavan notation the trunk was divided into the three segments at the amphalon and xyphion level. The upper and lower trunk is represent as elliptical cylinder while middle trunk is represents as elliptical solid. The hand is defined as an ellipsoid of revolution. The upper arm, forearm and shank are defined as circular cones. The foot is defined as an elliptical solid with the base (proximal end) being circular. The thigh is defined as an elliptical solid with the top (distal end) being circular. The human body segmentation according to the modified Hanavan model is shown in Fig. 3.6. In total, 42 anthropometric parameters are needed for make model of the human body using these geometrical representations. Since the each body segment is geometrical represented, BSP parameters for the human body can be calculated according to the mathematical equations of segment mass, center of mass and moment of inertia. The list of the modified Hanavan anthropometric body parameters, segments mass prediction equations and the description of the geometrical shapes which represent body segment and calculation of the inertia matrix and center of masses position are given in appendix B.

3.4 Initialization process

The aim of Initialization process is to define the initial configuration of the scaled model of the ROMEO robot, according to the initial configuration of the actor at the

beginning of the motion, and to attach the Virtual Markers frames on the scaled model of the ROMEO robot. Starting with the basic configuration of the robot q_{basic} , the joint positions of the scaled model of the ROMEO robot should correspond to the positions found on the actor. The joint positions of the robot are calculated by initial configuration algorithm taking the joint positions of the actor from $t_{i=1}$ to $t_{i=n_{init}}$ time instances during its initial configuration shown in Fig. 8 when the actor did not move. The orientation of the robot hands (taken from the basic configuration of the robot), are transferred onto the scaled model and remain unchanged. The initial configuration algorithm is represented as a nonlinear optimization problem for the minimization of the objective function:

$$\min_{q_{init}} \left(\left\| \begin{bmatrix} \bar{P}_{ajLeftSc} - P_{rjLeftSc}(q_{init}) \\ \bar{P}_{ajRightSc} - P_{rjRightSc}(q_{init}) \\ \bar{P}_{ajLeftEl} - P_{rjLeftEl}(q_{init}) \\ \bar{P}_{ajRightEl} - P_{rjRightEl}(q_{init}) \\ \bar{P}_{ajLeftWr} - P_{rjLeftWr}(q_{init}) \\ \bar{P}_{ajRightWr} - P_{rjRightWr}(q_{init}) \\ \Delta \vec{e}_{rjLeftWr}(q_{init}) \\ \Delta \vec{e}_{rjRightWr}(q_{init}) \end{bmatrix} \right\|^2 \right) \quad (3.1)$$

where \bar{P}_{aj_n} is the mean value of the actor $n \in \{LeftSh, RightSc, LeftEl, RightEl, LeftWr, RightWr\}$ joint position $P_{aj_n}(t_{i=1..n_{init}})$ in n_{init} time instances during the initial configuration, $P_{rj_n}(q_{init})$ is the current position of the robot joint, $\Delta \vec{e}_{rj_h}$ is the orientation error of the $h \in \{LeftWr, RightWr\}$ robot joint between the basic and the current configuration. The rotation matrices, $R_{rj_h}(q)$ is rewritten in terms of quaternions as

$$Q_{rj_h}(q) = \begin{bmatrix} Q^1_{rj_h}(q) & Q^2_{rj_h}(q) & Q^3_{rj_h}(q) & Q^4_{rj_h}(q) \end{bmatrix} \quad (3.2)$$

where $\eta_{rj_h} = Q^1_{rj_h}(q)$, $\vec{e}_{rj_h} = \begin{bmatrix} Q^2_{rj_h}(q) & Q^3_{rj_h}(q) & Q^4_{rj_h}(q) \end{bmatrix}^T$. The transformation process from the rotation matrix to the quaternions is explained in appendix C in details. The orientation error $\Delta \vec{e}_{rj_h}(q_{init})$ is calculated by using equation (Siciliano, Sciavicco, Villani, & Oriolo, 2010):

$$\Delta \vec{e}_{rj_h}(q_{init}) = \eta_{rj_h}(q_{init}) \cdot \vec{e}_{rj_h}(q_{basic}) - \eta_{rj_h}(q_{basic}) \cdot \vec{e}_{rj_h}(q_{init}) - S(\vec{e}_{rj_h}(q_{basic})) \cdot \vec{e}_{vm_{rj_h}}(q_{init}) \quad (3.3)$$

where $S(\cdot)$ is the skew-symmetric operator of the vector.

The initial guess for the optimization function is q_{basic} . The trunk, shoulder, elbow and wrist joints are used in the algorithm. The neck and head joints are fixed.

The initial configuration q_{init} is important for the initialization the positions of the Virtual Markers on the scale model of the ROMEO robot. The Virtual Markers are placed on the scale model of the robot and connected with the robot joints in the initial configuration. The Virtual Marker frame (with transformation matrix T_{vm_l}), is attached to the

body where it is fixed and connected with the closest proximal frame attached to the joint $T_{rj_n}(q_{init})$ via transformation matrix ${}^{rj_n}T_{vm_l}$.

The Virtual Marker with correspond proximal joint frames are paired as

$$\begin{aligned} & \left\{ T_{rj_{LeftSh}, T_{vm_{LeftUArm}}} \right\}, \left\{ T_{rj_{RightSh}, T_{vm_{RightUArm}}} \right\}, \left\{ T_{rj_{LeftEl}, T_{vm_{LeftFArm}}} \right\} \\ & \left\{ T_{rj_{RightEl}, T_{vm_{RightFArm}}} \right\}, \left\{ T_{rj_{LeftWr}, T_{vm_{LeftHd}}} \right\}, \left\{ T_{rj_{RightWr}, T_{vm_{RightHd}}} \right\} \end{aligned} \quad (3.4)$$

The Virtual Marker holds the mean values of the Real Marker transformation matrices $T_{rm_l}(t_{i=1..n_{init}})$ in n_{init} time instances of the actor initial configuration. A transformation matrix ${}^{rj_n}T_{vm_l}$ is calculated for each pair joint-marker and remains unchanged within the imitation algorithm.

The initialization process is described by the following nine-step scheme:

Algorithm 1 Initialization process

- 1: Initialization: $q_{basic}, n_{init}, P_{aj}(t_i), T_{rm}(t_i)$, scaling kinematic model of upper part of the ROMEO robot
 - 2: Scaling process: segments lengths, scaled model of upper part of robot $\leftarrow P_{aj}(t_{i=1:n_{init}})$
 - 3: $T_{rj}(q_{basic}) \leftarrow DirectKinematics(q_{basic})$
 - 4: $P_{rj}(q_{basic}), R_{rj}(q_{basic}) \leftarrow T_{rj}(q_{basic})$
 - 5: $\bar{P}_{aj} \leftarrow mean(P_{aj}(t_{i=1:n_{init}}))$
 - 6: Optimization algorithm: $fmincon q_{init} \leftarrow fmincon(\text{objective function (see Eq.(1)), } q_{basic})$
 - 7: $\bar{T}_{rm} \leftarrow mean(T_{rm}(t_{i=1..n_{init}}))$
 - 8: $T_{vm} = \bar{T}_{rm}$
 - 9: ${}^{rj_n}T_{vm_l} = inv(T_{rj_n}(q_{init}))T_{vm_l}$
 where $l \in \{LeftUArm, RightUArm, LeftFArm, RightFArm, LeftHd, RightHd\}$ and $n \in \{LeftSh, RightSh, LeftEl, RightEl, LeftWr, RightWr\}$
-

3.5 Imitation algorithms as optimization approach

In this section, the numerical and analytical imitation algorithms for extraction of the human Cartesian motions and joint motions from the data obtained with motion capture system are introduced. Ude et al. (Ude et al., 2004, 2000) proposed an approach to the formulation and optimization of the joint trajectories for humanoid robots. Their imitation algorithm is based on following the 3D position of the marker physically attached on the human body with the marker placed on the scaled robot model. The imitation algorithm propose by Ude is developed for imitating free human motion (motion without the contact). The same approach is used in our imitation algorithms. Our imitation algorithms are upgrade of algorithm proposed by Ude for the tasks which required precise imitation of the human motion by humanoids.

The imitation algorithms are formulated as an optimization algorithm which calculate the generalized coordinates of the joints $q_{imitation}(t_i)$ for the scaled model of the ROMEO

robot, for each time sample t_i , with $i \in [1 \dots N]$, where N represents the number of time samples of the recorded motion. The criterion function which should be minimize is given as the error between the position of the frames attached to the joint of the actor and those of the scaled model of the ROMEO robot and the error between the position and orientation of the frames attached to the marker of the human (Real Marker) and Virtual Marker of the scaled ROMEO robot model. Since the precision of orientation measurement is lower compared to that of position measurement, and orientations of the proximal segment are implicitly taken into account via their effect on distal joint positions and markers. The orientations of the proximal frames are not taken into account in the criterion of minimization. Only the orientation of the distal segment is included.

The optimization criterion is:

$$\zeta = \|\varepsilon(t_i, q)\|^2 \quad (3.5)$$

where

$$\varepsilon(t_i, q) = \begin{bmatrix} \alpha \left(\vec{P}_{rm}(t_i) - \vec{P}_{vm}(q) \right) \\ \beta \left(\vec{P}_{aj}(t_i) - \vec{P}_{rj}(q) \right) \\ \gamma \left(\Delta \vec{e}_{rvmLeftHd}(t_i, q) \right) \\ \gamma \left(\Delta \vec{e}_{rvmRightHd}(t_i, q) \right) \\ \delta \left(P_{ajLeftHd}(t_i) - P_{rjLeftHd}(q) \right) \\ \delta \left(P_{ajRightHd}(t_i) - P_{rjRightHd}(q) \right) \end{bmatrix} \quad (3.6)$$

and the generalized joint configuration is:

$$q_{imitation}(t_i) = \min_q (\zeta) \quad (3.7)$$

where α, β, γ and δ are the weighted factors, $\vec{P}_{rm}(t_i)$ and $\vec{P}_{aj}(t_i)$ are vectors of the recorded positions of the Real Markers and proximal actor joints at the time sample t_i , respectively, $\vec{P}_{vm}(q)$ and $\vec{P}_{rj}(q)$ are vectors of the positions of the Virtual Markers and proximal robot joints at in the current joints configuration q :

$$\vec{P}_{rm}(t_i) = \begin{bmatrix} P_{rmLeftUArm}(t_i) \\ P_{rmRightUArm}(t_i) \\ P_{rmLeftFArm}(t_i) \\ P_{rmRightFArm}(t_i) \\ P_{rmLeftHd}(t_i) \\ P_{rmRightHd}(t_i) \end{bmatrix}; \vec{P}_{vm}(q) = \begin{bmatrix} P_{vmLeftUArm}(q) \\ P_{vmRightUArm}(q) \\ P_{vmLeftFArm}(q) \\ P_{vmRightFArm}(q) \\ P_{vmLeftHd}(q) \\ P_{vmRightHd}(q) \end{bmatrix}$$

$$\vec{P}_{aj}(t_i) = \begin{bmatrix} P_{ajLeftSh}(t_i) \\ P_{ajRightSh}(t_i) \\ P_{ajLeftEl}(t_i) \\ P_{ajRightEl}(t_i) \end{bmatrix}; \vec{P}_{rj}(q) = \begin{bmatrix} P_{rjLeftSh}(q) \\ P_{rjRightSh}(q) \\ P_{rjLeftEl}(q) \\ P_{rjRightEl}(q) \end{bmatrix}$$

$P_{ajLeftHd}(t_i)$ and $P_{ajRightHd}(t_i)$ are positions of the left and right actor hand joints at the time sample t_i , respectively, $P_{rjLeftHd}(q)$ and $P_{rjRightHd}(q)$ are positions of the left and right robot hand joints at the current joints configuration q ; $\Delta\vec{e}_{rvmLeftHd}$ and $\Delta\vec{e}_{rvmRightHd}$ are the orientation errors between the Real and Virtual Markers attached to the left and right hands (distal markers) at the time sample t_i and joint configuration q , respectively. The orientation errors are represented in terms of quaternions. The rotation matrices, $R_{rmLeftHd}(t_i)$ and $R_{vmLeftHd}(q)$ (which express the orientations of the Real and Virtual Markers of the left hand, respectively), can be rewritten in terms of quaternions as:

$$Q_{rmLeftHd} = \begin{bmatrix} Q^1_{rmLeftHd}(t_i) & Q^2_{rmLeftHd}(t_i) & Q^3_{rmLeftHd}(t_i) & Q^4_{rmLeftHd}(t_i) \end{bmatrix} \quad (3.8)$$

$$Q_{vmL} = \begin{bmatrix} Q^1_{vmLeftHd}(t_i) & Q^2_{vmLeftHd}(t_i) & Q^3_{vmLeftHd}(t_i) & Q^4_{vmLeftHd}(t_i) \end{bmatrix}$$

respectively, where

$$\eta_{rmLeftHd} = Q^1_{rmLeftHd}(t_i), \vec{e}_{rmLeftHd} = \begin{bmatrix} Q^2_{rmLeftHd}(t_i) & Q^3_{rmLeftHd}(t_i) & Q^4_{rmLeftHd}(t_i) \end{bmatrix}^T, \eta_{vmLeftHd} = Q^1_{vmLeftHd}(q), \text{ and } \vec{e}_{vmLeftHd} = \begin{bmatrix} Q^2_{vmLeftHd}(q) & Q^3_{vmLeftHd}(q) & Q^4_{vmLeftHd}(q) \end{bmatrix}^T.$$

The orientation error $\Delta\vec{e}_{rvmLeftHd}$ is calculated by using equation (Siciliano et al., 2010):

$$\Delta\vec{e}_{rvmLeftHd}(t_i, q) = \eta_{vmLeftHd}(q) \cdot \vec{e}_{rmLeftHd}(t_i) - \eta_{rmLeftHd}(t_i) \cdot \vec{e}_{vmLeftHd}(q) - S(\vec{e}_{rmLeftHd}(t_i)) \cdot \vec{e}_{vmLeftHd}(q) \quad (3.9)$$

where $S(\cdot)$ is the skew-symmetric operator of the vector.

The orientation error of the right hand $\Delta\vec{e}_{rvmRightHd}$ is calculated in the same way.

3.5.1 Numerical approach for solving inverse optimal imitation problem

In the subsection 2.2.1 we gave the extensive review of the existing imitation algorithms. Numerous algorithms are used for solving imitation problems. For example, Ude et al. (Ude et al., 2000) proposed an approach to the formulation and optimization of the joint trajectories for humanoid robots using B-spline wavelets. Since the imitation algorithm is represented as an optimization approach, in this section we give the numerical solution. Standard optimization toolbox solvers propose a lot of nonlinear optimization algorithms such as trust-region approach (Moré & Sorensen, 1983), nonlinear and linear least-squares method, quasi-Newton updating method, sequential quadratic programming method (SQP) (Powell, 1978a, 1978b). We choose standard numerical optimization algo-

rithm SQP which is able to minimize the criterion function given with equation 3.5 on the best way.

For the purpose of our study we defined numerical imitation algorithm using the MATLAB *fmincon* solver with an active-set function, which is based on SQP method (Powell, 1978b). The joint configuration is found based to the search the local minimum of the criterion function 3.5. In order to obtain the global minimum of the criterion function 3.5 the initial guess for the optimization algorithm must be well defined. The initial guess for the imitation algorithm in the first sample is taken to be the initial configuration q_{init} , which is calculated from the Initial configuration algorithm. In future samples of the imitation algorithm, q_{init} is replaced with the optimal solution from the previous sample and then used as the initial guess for the current optimization algorithm. The values of objective function cannot be zero due to the large differences in the kinematic model between the human and humanoid. For the case studied, the neck and head joints are kept fixed.

According to the criterion function 3.5, in our numerical imitation algorithm, the factors α , β , γ and δ assign different priority levels with regards to following the marker or joint positions, respectively. With the aim of reducing the effect of the skin motion (which has a direct influence on the motion of the markers) and increasing the accuracy of the imitation we adjusted the factors α , β , γ and δ to give a larger priority on following the joint position with respect to the marker. All of the arms' Real Markers and arms' joint positions are used in the criterion function, with the aim of improving how well the orientation of the proximal joints are followed, since this is not handled by the criterion function. In our numerical imitation algorithm we chose: $\alpha = 1$, $\beta = 2$, $\gamma = 10$ and $\delta = 20$.

Our numerical imitation algorithm is the extension of the imitation algorithm proposed by Ude et. al (Ude et al., 2000). Therefore, Ude et. al (Ude et al., 2000) imitation approach corresponds to our numerical imitation algorithm with $\alpha = 1$, $\beta = 0$, $\gamma = 0$ and $\delta = 0$.

The obtained results from the imitation algorithms must be further processed. In order to eliminate the effects of the noise from the motion capture system and make smoother the joint trajectories from the imitation algorithm, we applied a Savitzky–Golay filter which is based on the fitting successive sub-sets of adjacent data points with a low-degree polynomial by the method of linear least squares (Orfanidis, 1995). For generation these filters we used the *sgolayfilt* MATLAB function and defined the 5th order polynomial for the sub-sets of the 31 adjust points. In this way, we obtained smoother joint trajectories $Q_{imitation}$ which are further used.

Our numerical imitation algorithm is described by the following fifteen-step scheme:

3.5.2 Analytical approach for solving inverse optimal imitation problem based on the Jacobian matrix

The second imitation algorithm corresponds to an optimization problem which has an analytical solution for the value $q_{imitation}(t_i)$ at each time sample t_i , minimizing the

Algorithm 2 Numerical imitation algorithm

- 1: **Initialization:** $q_{init}, n_{init}, P_{aj}(t_i), T_{rm}(t_i)$, extended kinematic model of upper part of the ROMEO robot
 - 2: Scaling process: segments lengths, scaled model of upper part of robot using $P_{aj}(t_{i=1:n_{init}})$
 - 3: Define $\alpha, \beta, \gamma, \delta$
 - 4: **Initialization process**
 - 5: **for** $t_i = 1$ to N **do**
 $q = q_{init}$
 $T_{rj(q)} \leftarrow DirectKinematics(q);$
 $P_{rj(q)} \leftarrow T_{rj(q)}$
 $T_{vm}(q) = T_{rj(q)}^{rj} T_{vm}$
 $P_{vm}(q), R_{vm}(q) \leftarrow T_{vm}(q)$
 $P_{rm(t_i)}, R_{rm(t_i)} \leftarrow T_{rm(t_i)}$
Optimization algorithm: $fmincon$ $q_{imitation}(t_i) \leftarrow fmincon(\text{objective function (see Eq. 3.5.)}, q_{init})$
 - 6: **end for**
 - 7: $Q_{imitation}(t_i) \leftarrow sgolayfilt(q_{imitation}(t_i))$
-

criterion function given by Eq. 3.5. Since the initial configuration of the robot, q_{init} , is calculated in the initialization process and the initial position of the robot joint and Virtual Markers are known, the current value $q_{imitation}(t_i)$ can be calculated incrementally by using $q_{imitation}(t_{i-1})$ calculated in the previous iteration $q_{imitation}(t_i) = q_{imitation}(t_{i-1}) + \Delta q$. Therefore, the criterion function, $\varepsilon(q(t_i))$, can be expressed as a function of Δq :

$$\begin{aligned}
 \varepsilon(t_i, q(t_i)) &= \varepsilon(t_i, q_{imitation}(t_{i-1}) + \Delta q) = \\
 \varepsilon_\alpha(t_i, q_{imitation}(t_{i-1})) &+ \varepsilon_\beta(t_i, q_{imitation}(t_{i-1})) \Delta q = \\
 &\left[\begin{array}{l}
 \alpha \left(\vec{P}_{rm}(t_i) - \vec{P}_{vm}(q_{imitation}(t_{i-1}) + \Delta q) \right) \\
 \beta \left(\vec{P}_{aj}(t_i) - \vec{P}_{rj}(q_{imitation}(t_{i-1}) + \Delta q) \right) \\
 \gamma \left(\Delta \vec{e}_{rvmLeftHd}(t_i, q_{imitation}(t_{i-1}) + \Delta q) \right) \\
 \gamma \left(\Delta \vec{e}_{rvmRightHd}(t_i, q_{imitation}(t_{i-1}) + \Delta q) \right) \\
 \delta \left(P_{ajLeftHd}(t_i) - P_{rjLeftHd}(q_{imitation}(t_{i-1}) + \Delta q) \right) \\
 \delta \left(P_{ajRightHd}(t_i) - P_{rjRightHd}(q_{imitation}(t_{i-1}) + \Delta q) \right)
 \end{array} \right] \quad (3.10)
 \end{aligned}$$

where vector $\varepsilon_\alpha(t_i, q_{imitation}(t_{i-1}))$ can be evaluated based on equation 3.6, and matrix $\varepsilon_\beta(t_i, q_{imitation}(t_{i-1}))$ based on its derivative. The current position of k^{th} robot joint is represented by relation:

$$P_{rjk}(q(t_i)) = P_{rjk}(q_{imitation}(t_{i-1})) + J_{rjk}(q_{imitation}(t_{i-1})) \Delta q \quad (3.11)$$

where $k \in \{LeftSh, RightSh, LeftEl, RightEl\}$. $J_{rjk}(q)$ represents the Jacobian matrix of the k^{th} proximal robot joint calculated analytically by using the software SYMORO+

(Khalil & Creusot, 1997). The current position of the l^{th} Virtual Marker is calculated by using the equation:

$$P_{vm_l}(q(t_i)) = P_{vm_l}(q_{imitation}(t_{i-1})) + J_{vm_l}(q_{imitation}(t_{i-1}))\Delta q. \quad (3.12)$$

$J_{vm_l}(q)$ represents the Jacobian matrix of the l^{th} Virtual Marker

$l \in \{LeftU Arm, RightU Arm, LeftF Arm, RightF Arm, LeftHd, RightHd\}$ calcu-

lated by equation $J_{vm_l}(q) = \begin{bmatrix} A_{rj_n} & -A_{rj_n} {}^{rj_n}\widehat{P}_{vm_l} \\ O_3 & A_{rj_n} \end{bmatrix} \cdot \begin{bmatrix} A_{rj_n} & O_3 \\ O_3 & A_{rj_n} \end{bmatrix}^{-1} J_{rj_n}(q)$, where

A_{rj_n} is the orientation matrix of the closest proximal frame attached to the joint T_{rj_n} ,

and ${}^{rj_n}\widehat{P}_{vm_l}$ is a skew-symmetric matrix defined by a component of the vector ${}^{rj_n}P_{vm_l}$.

The matrix ${}^{rj_n}P_{vm_l}$ is part of the matrix ${}^{rj_n}T_{vm_l}$. The current orientation of the Virtual

Markers on the left hand is calculated in the same way as the position $Q_{vm_{LeftHd}}(q(t_i)) =$

$Q_{vm_{LeftHd}}(q_{imitation}(t_{i-1})) + J_{Q_{vm_{LeftHd}}}(4 : 7, q_{imitation}(t_{i-1}))\Delta q$. $J_{Q_{vm_{LeftHd}}}(q)$ is the

Jacobian matrix of the left hand Virtual Marker represented in terms of quaternion and

calculated by equation $J_{Q_{vm_{LeftHd}}}(q) = \begin{bmatrix} I_{3x3} & O_{3x3} \\ O_{4x3} & \Omega(q) \end{bmatrix} J_{vm_{LeftHd}}(q)$, where

$$\Omega(q) = \begin{bmatrix} -Q^2_{vm_{LeftHd}}(q) & -Q^3_{vm_{LeftHd}}(q) & -Q^4_{vm_{LeftHd}}(q) \\ Q^1_{vm_{LeftHand}}(q) & Q^4_{vm_{LeftHand}}(q) & -Q^3_{vm_{LeftHd}}(q) \\ -Q^4_{vm_{LeftHd}}(q) & Q^1_{vm_{LeftHd}}(q) & Q^2_{vm_{LeftHd}}(q) \\ Q^3_{vm_{LeftHd}}(q) & -Q^2_{vm_{LeftHd}}(q) & Q^1_{vm_{LeftHand}}(q) \end{bmatrix} \text{ and } Q_{vm_{LeftHd}} = \begin{bmatrix} Q^1_{vm_{LeftHd}}(q) & Q^2_{vm_{LeftHd}}(q) & Q^3_{vm_{LeftHd}}(q) & Q^4_{vm_{LeftHd}}(q) \end{bmatrix}^T. \text{ The current orientation of the Virtual Marker on the right hand is calculated in the same way.}$$

The analytical expression for Δq is deduced for the optimality condition

$$\frac{\partial \zeta}{\partial \Delta q} = \frac{\partial (\|\varepsilon(t_i, q_{imitation}(t_{i-1})) + \Delta q\|^2)}{\partial \Delta q} = 0 \text{ and gives:}$$

$$\Delta q = -\varepsilon_\beta(t_i, q_{imitation}(t_{i-1}))^+ \varepsilon_\alpha(t_i, q_{imitation}(t_{i-1})) \quad (3.13)$$

where $\varepsilon_\beta(t_i, q_{imitation}(t_{i-1}))^+$ represents the pseudo inverse of the matrix $\varepsilon_\beta(t_i, q_{imitation}(t_{i-1}))$.

According to the previous equations, vector $\varepsilon_\alpha(t_i, q_{imitation}(t_{i-1}))$ and matrix $\varepsilon_\beta(t_i, q_{imitation}(t_{i-1}))$

from equation (3.10) take the form:

$$\varepsilon_\alpha(t_i, q_{imitation}(t_{i-1})) = \begin{bmatrix} \alpha \left(\vec{P}_{rm}(t_i) - \vec{P}_{vm}(q_{imitation}(t_{i-1})) \right) \\ \beta \left(\vec{P}_{aj}(t_i) - \vec{P}_{rj}(q_{imitation}(t_{i-1})) \right) \\ \gamma \cdot \varepsilon_{\alpha_{LeftHand}}^R \\ \gamma \cdot \varepsilon_{\alpha_{RightHand}}^R \\ \delta \left(P_{aj_{LeftHand}}(t_i) - P_{rj_{LeftHand}}(q_{imitation}(t_{i-1})) \right) \\ \delta \left(P_{aj_{RightHand}}(t_i) - P_{rj_{RightHand}}(q_{imitation}(t_{i-1})) \right) \end{bmatrix} \quad (3.14)$$

$$\varepsilon_{\beta}(t_i, q_{imitation}(t_{i-1})) = \begin{bmatrix} -\alpha \cdot \vec{J}_{vm}(q_{imitation}(t_{i-1})) \\ -\beta \cdot \vec{J}_{rj}(q_{imitation}(t_{i-1})) \\ \gamma \cdot \varepsilon_{\beta_{LeftHand}}^R \\ \gamma \cdot \varepsilon_{\beta_{RightHand}}^R \\ -\delta \cdot J_{rj_{LeftHand}}(q_{imitation}(t_{i-1})) \\ -\delta \cdot J_{rj_{RightHand}}(q_{imitation}(t_{i-1})) \end{bmatrix} \quad (3.15)$$

where

$$\varepsilon_{\alpha_{LeftHand}}^R = \begin{pmatrix} \eta_{vm_{LeftHand}}(q_{imitation}(t_{i-1})) \cdot \vec{e}_{rm_{LeftHand}}(t_i) - \\ \eta_{rm_{LeftHand}}(t_i) \cdot \vec{e}_{vm_{LeftHand}}(q_{imitation}(t_{i-1})) - \\ S(\vec{e}_{rm_{LeftHand}}(t_i)) \cdot \vec{e}_{vm_{LeftHand}}(q_{imitation}(t_{i-1})) \end{pmatrix}$$

$$\varepsilon_{\alpha_{RightHand}}^R = \begin{pmatrix} \eta_{vm_{RightHand}}(q_{imitation}(t_{i-1})) \cdot \vec{e}_{rm_{RightHand}}(t_i) - \\ \eta_{rm_{RightHand}}(t_i) \cdot \vec{e}_{vm_{RightHand}}(q_{imitation}(t_{i-1})) - \\ S(\vec{e}_{rm_{RightHand}}(t_i)) \cdot \vec{e}_{vm_{RightHand}}(q_{imitation}(t_{i-1})) \end{pmatrix}$$

$$\varepsilon_{\beta_{LeftHand}}^R = \begin{pmatrix} \vec{e}_{rm_{LeftHand}}(t_i) \cdot J_{Qvm_{LeftHand}}(4, q_{imitation}(t_{i-1})) - \\ \eta_{rm_{LeftHand}}(t_i) \cdot J_{Qvm_{LeftHand}}(5 : 7, q_{imitation}(t_{i-1})) - \\ S(\vec{e}_{rm_{LeftHand}}(t_i)) \cdot J_{Qvm_{LeftHand}}(5 : 7, q_{imitation}(t_{i-1})) \end{pmatrix}$$

$$\varepsilon_{\beta_{RightHand}}^R = \begin{pmatrix} \vec{e}_{rm_{RightHand}}(t_i) \cdot J_{Qvm_{RightHand}}(4, q_{imitation}(t_{i-1})) - \\ \eta_{rm_{RightHand}}(t_i) \cdot J_{Qvm_{RightHand}}(5 : 7, q_{imitation}(t_{i-1})) - \\ S(\vec{e}_{rm_{RightHand}}(t_i)) \cdot J_{Qvm_{RightHand}}(5 : 7, q_{imitation}(t_{i-1})) \end{pmatrix}$$

\vec{J}_{vm} is the vector of the Jacobian matrices for all Virtual Markers and \vec{J}_{rj} is a vector of the Jacobian matrices for the all proximal robot joints. Δq is calculated according to equations (3.13), (3.14) and (3.15). The initial guess for the imitation algorithm at the first sample is taken to be the initial configuration, q_{init} , of the scaled model of the robot. In future samples of the imitation algorithm, the solution from the previous sample $q_{imitation}(t_{i-1})$ is used as the initial guess for the current iteration in the optimization algorithm. Values of the objective function cannot be zero due to large differences between the kinematic model of human and humanoid.

Factors α , β , γ and δ are defined on the same way as in the numerical imitation algorithm and take same values.

The actor motion in the Cartesian space is re-calculated using the $q_{imitation}(t_i)$ and direct geometric model of the scaled model of the ROMEO robot.

3.6 The simulation results of the imitation algorithms

In this section, we will analyze the results of our imitation algorithms. In order to show the general characteristics of our imitation algorithms we tested them on the set

of 7 different and complex dual arm tasks (explained in the [chapter 3](#)). Each task is performed by 19 actors. Results obtained by our imitation algorithms are compared with result obtained with numerical algorithm proposed by Ude ([Ude et al., 2004, 2000](#)).

The imitation algorithm starts when the scaled model of the ROMEO robot is set to the actor initial configuration. The Initial configuration algorithm should perfectly match the initial joint configuration of the scaled model of the ROMEO robot with the recorded initial actor joint configuration. Some differences between the actors skeletal structure and the robots structure can cause significant error in the initial configuration algorithm, especially in the shoulder joints. Quality of the matching actor's initial position for one motion is represented as $E_{P_{aj}, P_{rj}}$, the Euclidian distance between positions of the recorded actor joint P_{aj} and the joint of the scaled model of the ROMEO robot P_{rj} . In order to present the general performance of the Initial configuration algorithm for each actor, we calculated $\mu(E_j)$, as the mean value of E_j of j^{th} joint for all the motions performed by each actor. On the same way the normed hand orientation error between the basic and the current configuration of the scaled model of the robot is calculated. The general characteristics of Initial configuration algorithm for each actor and each joint are shown in [Fig. 3.7](#). According to the results obtained from each actor for all experiments, the highest position error of the shoulder joints is around 12mm. The reason for this is the approximated kinematic model of a human which has more DoF in the shoulder and spine, compared with the robots kinematic model. The results from the other actors show that the average Euclidian distance between actor and scaled model of the ROMEO robot joints are less than 2mm. The scaled model of the ROMEO robot has enough DoF in its hands to achieve the orientation of the hands as shown in the robot basic configuration which confirms results in [Fig. 3.7 d](#)).

Starting from the calculated q_{init} , the generalized coordinates of the scaled model of the ROMEO robot motion are calculated using our imitation algorithms. Our imitation algorithms are defined to give the highest priority to the hand position and orientation following in order to ensure the task is done properly. According to the results for the "Open/close drawer" task presented here (see [Fig. 3.8](#), blue color), one can conclude that the our imitation algorithms produced the same motion of the actor hands as the scaled model of the ROMEO robot. The highest normed errors in following the actor hands trajectories are around 5mm which is obtained our numerical imitation algorithm (see [Fig. 3.8](#), blue solid line). Since the robot model has enough DoFs, the imitation algorithm gives good performance in following hands orientations. Bigger errors in following the shoulder and elbow joints motions (the biggest amplitude around 30mm) are the results of simplifying the kinematic model of human by using the model of robot ROMEO. In order to point out performances of the proposed imitation algorithms, results are compared with the numerical algorithm proposed by Ude et al. ([Ude et al., 2004, 2000](#)) and shown in the [Fig. 3.8](#) red scale. Since the numerical algorithm proposed by Ude is based on following the 3D markers positions, errors in following the joint position and orientation

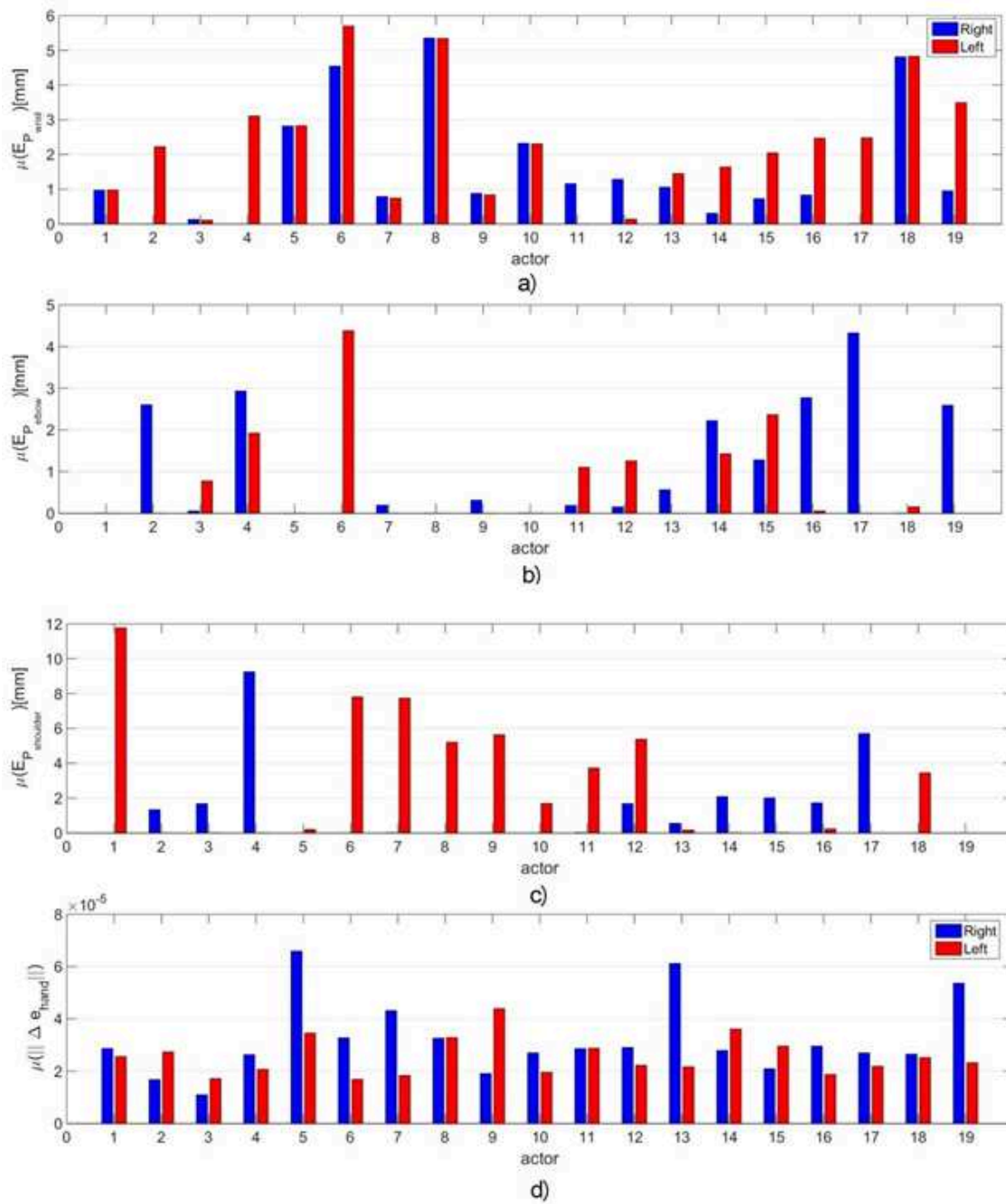


Figure 3.7: The position and orientation errors in matching actor's initial configuration with the scaled model of the ROMEO robot generated by our Initial configuration algorithm: (a), (b) and (c) represent average position errors of the arm joints $\mu(E_j)$ for the 19 actors in millimetres; (d) represents average normed orientation errors $\mu(\|\Delta \vec{e}_{hand}\|)$ of the hand joints in quaternion.

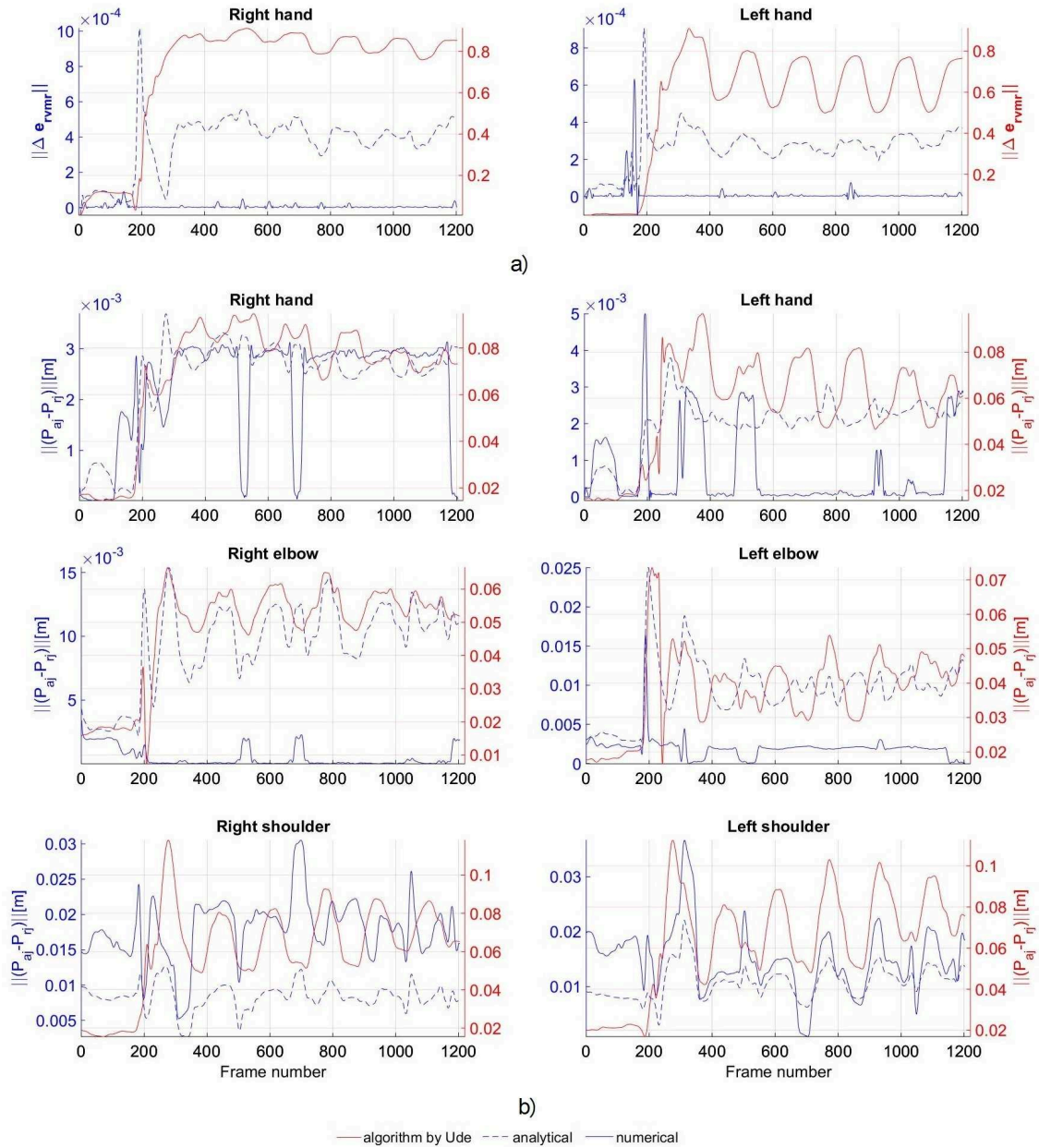


Figure 3.8: The orientation and position errors between the recorded and obtained motion generated by our analytical (blue scale, dashed line) and numerical (blue scale, solid line) imitation algorithms and the numerical imitation algorithm proposed by Ude (Ude et al., 2004) (red scale): a) the normed orientation errors $\Delta \vec{e}_{rvmRightHd}$ and $\Delta \vec{e}_{rvmLeftHd}$ of the right and left hand markers in quaternion; b) represents the normed position errors $P_{aj}(t_i) - P_{rj}(t_i)$ of the arm joints in meters.

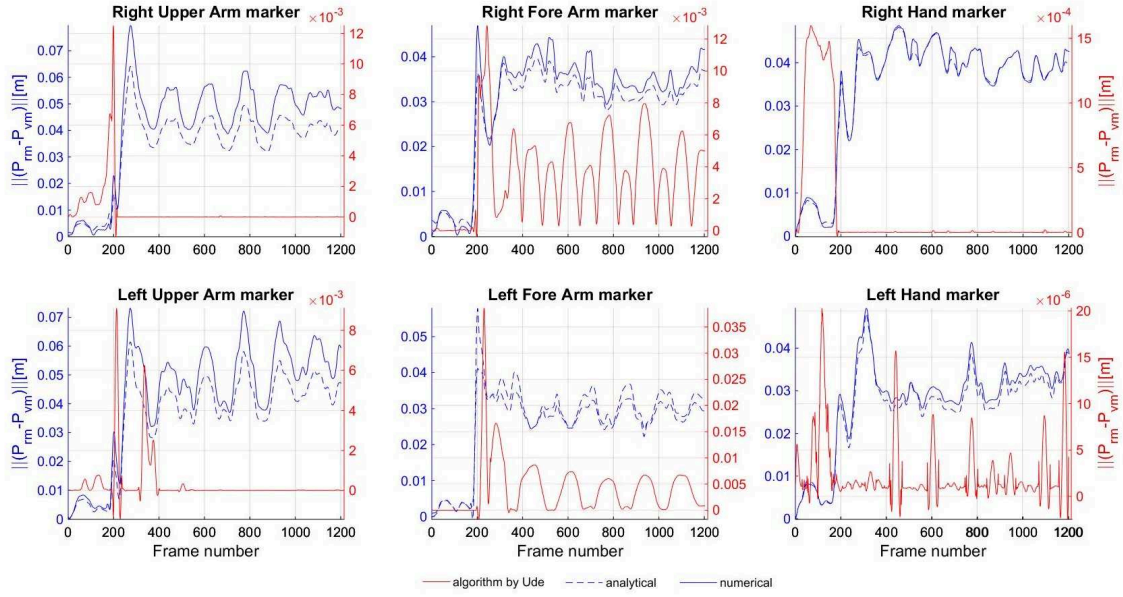


Figure 3.9: The normed position errors in following Real Marker P_{rm} with Virtual Marker P_{vm} obtained with our analytical (blue scale, dashed line) and numerical (blue scale, solid line) imitation algorithms and the numerical imitation algorithm proposed by Ude (Ude et al., 2000) (red scale) in meters.

are bigger comparing with our imitation algorithms (see Fig. 3.8). In (Ude et al., 2000), big errors in following hand joints position and orientation will disable robot ROMEO to achieve contact between hands and equipment and the task will not be obtained. Imitation algorithm proposed by Ude is developed for imitating free human motion (motion without the contact). On the other hand, errors in following the position of the Real Marker with Virtual Marker obtained with algorithm proposed by Ude are smaller compare with results from our imitation algorithms since hand position tracking is of the highest priority in our algorithms (see Fig. 3.9). Although the algorithm proposed by Ude gives small error in following 3D position of the markers, the precise following position and orientation of hands joints is not guaranteed. The reasons are the calculation of the transformation matrix between Real Markers and closest proximal joint which is not so precise and the fact that this transformation matrix may be changed due to the skin motion. It can be noticed that our imitation algorithms allow a better tracking of the hand motion compared with algorithm proposed by Ude one and also permit a correct tracking to the pose of the shoulder and elbow that characterize the shape of the arm, i.e. its configuration.

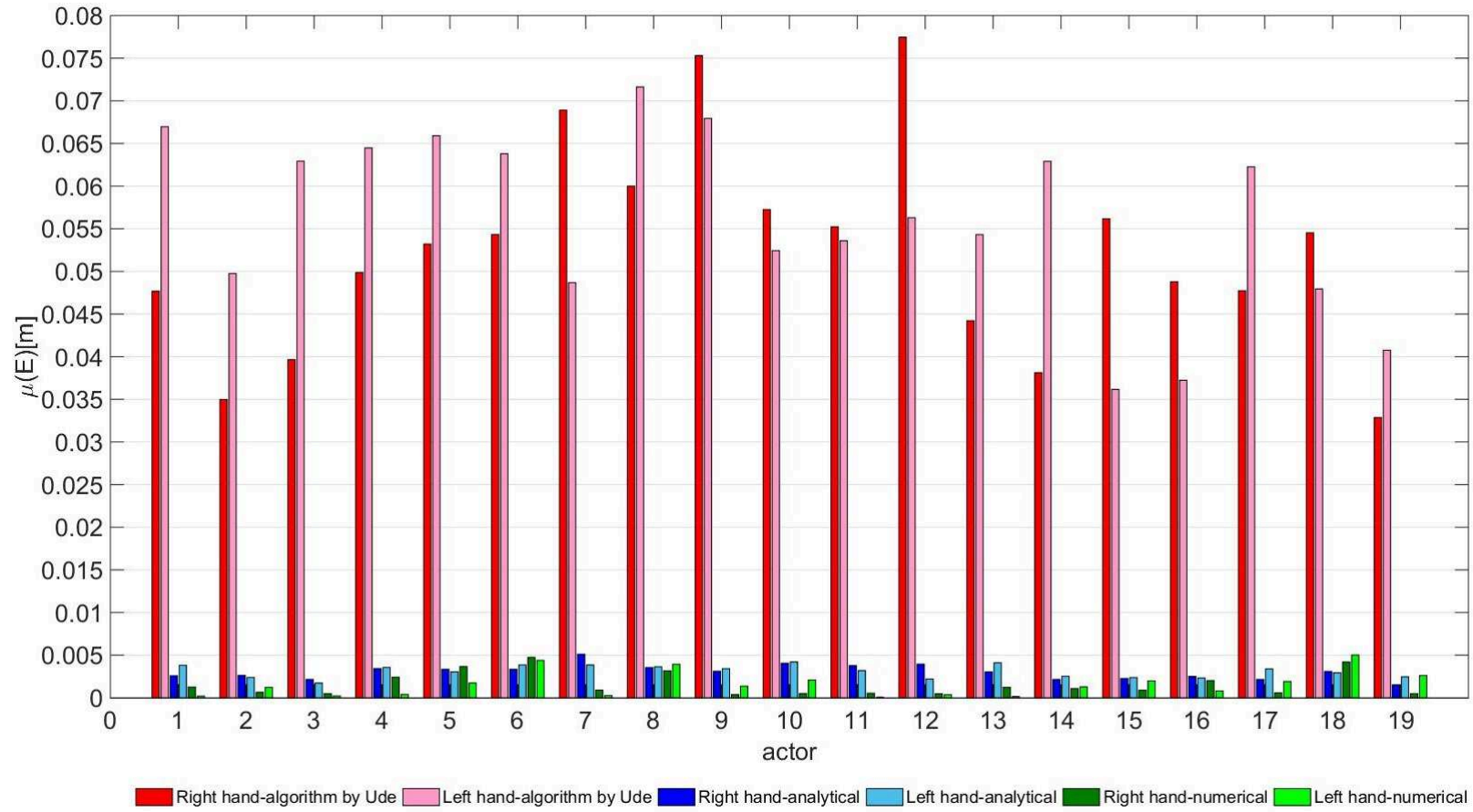


Figure 3.10: Quality of the imitations of the right and left hand motions, expressed by $\mu(E)$, for the 19 actors obtained by our analytical (blue color) and numerical (green color) algorithms and the numerical algorithm proposed by Ude (red color).

The imitation algorithms are also tested on a set of different dual arms motions each performed by 19 actors, as well. Quality of the imitation for one motion is represented as $E = \mu(d_{P_{hand}(t_{i...N}), P_{rhand}(t_{i...N})})$, the mean value of the Euclidian distance between positions of the recorded hands joints P_{hand} and the hands joints obtained with the our imitation algorithm P_{rhand} during all samples of the motion. In order to present the general performance of our imitation algorithms for each actor, we calculated $\mu(E)$, and the mean value of E for all the motions performed by each actor. The general characteristics of our imitation algorithms for each actor expressed by $\mu(E)$ and imitation algorithm proposed by Ude are shown in Fig. 3.10.

The results show that our imitation algorithms give average errors in following the desired hand positions of around 3mm for most actors. For some actors, these errors are somewhat bigger, around 5mm. The reason is a big disparity of the estimated and real actor kinematic model (confidence in the distance between joints).

Summing up, the obtained hand trajectories generated through our imitation algorithms can be used as a desired robot motion in the conversion process in the inverse kinematic algorithm for the task with and without contact between hands and equipment. According to the results shown in the Fig. 3.8 the numerical imitation algorithm gives better performance in following desired position of some joints compare with analytical imitation algorithm. This is not crucial to define a numerical algorithm as better than analytical algorithm since the errors in following the position of the hands' joints are about the same. The additional advantage of our analytical imitation algorithm is that it can be used to imitate the movement in real-time. That is way we used the results from our analytical algorithm in the algorithm for humanoid motion generation presented in next section.

3.7 From the Imitation Results to the Motion of Robot ROMEO

The motion obtained with the imitation algorithm described previously cannot be directly used by humanoid robot ROMEO, because neither size of the humanoid robot nor joint limitations have been taken into account. If joint motion $q_{imitation}(t)$ is used, the motion in Cartesian space will not be preserved, thus contact with the environment will not be achieved. If Cartesian motion is used, human skill will not be preserved. In what follows we will propose different strategies depending of the existence of contact with the environment or not. A contact with environment is assumed to exist via the hands of the robot. The case of contact with another part of the body may be considered in a similar way. The transition strategy will also be proposed between the contact and no contact phases.

During a motion with contact, motion of the actor hands is constrained with the characteristics of the equipment. In (Jovanovic, Potkonjak, & Holland, 2014), we thoroughly

elaborated types of contact constraints and therefore corresponding mathematical representations. We study the case where the robot should do the task in the same environment of the human with the same type of contact. The moment when robot hands establish contact with the equipment is calculated using the hands positions of the scaled model of the robot and the known position of the equipment. To that end, hands coordinates of the scaled model of the robot and equipment coordinates are represented in the same referent frame. For the phase of contact, the robot hands should be able to follow the same motion in the Cartesian space as the actor hands. A necessary condition for performing the task by the robot is that the trajectories of actor hands (for the phase of contact) are within the workspace of the robot. The workspace of robot ROMEO is defined according to the robot segments size and the joint limits on the ways proposed in the papers (Bagheri, Ajoudani, Lee, Caldwell, & Tsagarakis, 2015; Wenger, 2010). If this condition is satisfied when the robot is initially at the same place as the actor, then the motion will be achieved in this way. Otherwise, a new initial position and orientation of the robot can be calculated in order that the task becomes feasible. In this last case, the transformation matrix describing the displacement of the robot will be taken into account in order to modify the desired motion of the hands of the robot accordingly.

3.7.1 The inverse kinematic algorithm as a tool for generation of human like motion

The process of imitation of the human motion requires the possibility for the robot to perform the task like a human. Since robot ROMEO is of a redundant structure, the same motion as that of the human hands can be obtained for different configurations of the arms. By using the inverse kinematic algorithm, the recorded human joint motion can be imitated by robot ROMEO. The minimized difference between the current joint trajectories $q_{robot}(t)$ and joint trajectories $q_{imitation}(t)$ obtained with imitation algorithm of the scaled model of the robot $|q_{robot}(t) - q_{imitation}(t)|^2$ are included in the inverse kinematic algorithm as an secondary criterion:

$$\begin{aligned} dq_{robot}(t_i) &= J^{+\lambda} dX(t_i) - (I - J^+ J)(q_{robot}(t_{i-1}) - q_{imitation}(t_i)) \\ q_{robot}(t_i) &= q_{robot}(t_{i-1}) + dq_{robot}(t_i) \end{aligned} \quad (3.16)$$

where $J^{+\lambda}$ is the damped least-square inverse of the Jacobian matrix J and damping factor (Wampler, 1986) $\lambda = 0.003$ which is introduced with aim of solving the problem of discontinuity of the pseudoinverse solution at a singular configuration, J^+ is pseudo-inverse of the Jacobian matrix J of robot ROMEO calculated for the robot size, I is Identity matrix, $dX(t_i)$ is the positional and the orientation variation between the desired trajectories of the robot hands $X_{hands}^d(t_i)$ and the current position of the robot hands $X_{hands}^c(q_{robot}(t_{i-1}))$ calculated by the direct geometric model and using the real size of

the robot:

$$dX(t_i) = X_{hands}^d(t_i) - X_{hands}^c(q_{robot}(t_{i-1})) \quad (3.17)$$

The joint limits are included in the inverse kinematic algorithm by using the internal clamping loop that checks and removes the joints that reach their upper or lower joint limits q_{robot}^{\min} and q_{robot}^{\max} , respectively. In the case that a joint has passed through the limit, the joint value will be clamped to the limit value. The elements of the Jacobian matrix J and Identity matrix I related with the clamped joint will be set to zero. In this way, we prevent the motion of the clamped joint. The inverse kinematic algorithm continues to initiate other joints in order to reach desired values of the hands. The inverse kinematic algorithm with the clamping loop is in detailed explained in Baerlocher et al. (Baerlocher & Boulic, 2004).

The primary task of the inverse kinematic algorithm is to follow the desired trajectories of the hands $X_{hands}^d(t_i)$. In the case of a motion when the contact between hands and equipment is required and robot should use the same equipment as a human, the desired motions of the robot hands are defined in the imitation of algorithm. However it is important to remark that $q_{imitation}(t)$ has been defined for a scaled model of the robot and that Jacobian matrix J used here is calculated for the real size of robot ROMEO. The $q_{imitation}(t)$ and $X_{hands}^d(t_i)$ are not consistent, thus the secondary task will not be achieved and $q_{robot}(t)$ will differ from $q_{imitation}(t)$.

3.7.2 Motion of the robot hands without a contact

A robot will not be able to follow simultaneously the hands and joints motions recorded from imitation, since the size and the joint limits of the robot and a human are not the same. When there is no contact with the environment, it may be preferable to follow the joints motions of the human rather than his Cartesian motion in order to express human skill.

However, in order to keep the same control approach in the cases with and without contact with the environment, and to take into account the joint limits, we propose the use of equation (3.16) but with:

$$dX(t_i) = X_{hands}^c(q_{imitation_Modif}(t_i)) - X_{hands}^c(q_{robot}(t_{i-1})) \quad (3.18)$$

where $q_{imitation_Modif}(t_i)$ is the modified value of $q_{imitation}(t)$, when the value of $q_{imitation}(t)$ can be outside the robot joint limits. The modification is done by using the algorithm proposed by Safonova et al. (Safonova et al., 2003). In this way, $X_{hands}^c(q_{imitation_Modif}(t_i))$ is inside the workspace of the robot.

In this way the desired motion in the joint and Cartesian spaces is coherent and consistent with the dimension of the humanoid robot. The joint limits are also taken into account.

3.7.3 The transition strategy connecting the motions without and with contact

For a motion with or without contact of the hands with the environment, we have proposed to use the algorithm given by equation (3.16). The difference between the two cases is in the way used to define the desired Cartesian motion of the hands. As a consequence, we propose a transition strategy based on rescaling the size of the robot to the size of the actor. The transition strategy starts if the relative position between robot hands, during the motion without contact, and the object to be contacted reaches prescribed vicinity. Here we assume the prescribed vicinity is the sphere of 0.1m radius. During the transition strategy, the size of the robot segments in the model are linearly modified to reach the size of the actor. The trajectories of the hands are calculated for the incrementally rescaled model of the robot by using the value of $q_{imitationModif}(t_i)$ which corresponds to this part of the motion. The transition strategy is finished when the size of the rescaled model of the robot is the same as the actor size and value of $q_{imitationModif}(t_i)$ is the same as the one corresponding to the sample when the contact between actor hands and equipment is achieved. In this way, the connection between hands and the equipment is made.

The desired trajectories of the robot hands can be further processed. In order to smooth trajectories of the robot hands, we applied a Savitzky–Golay filter which is based on fitting successive sub-sets of adjacent data points with a low-degree polynomial by the method of linear least squares (Orfanidis, 1995).

3.7.4 Handling collision

In our investigations, we analyzed dual arm motions performed by actors. Any actor naturally avoids collision with equipment and self-collision. Since we used data generated from the imitation algorithm, which characterize human skills, to generate the motion of the robot, it is expected that the robot, similarly to the actor, will avoid self-collision. Also, trajectories of the hands during the contact phase of the motion are the same as those of a human, thus collision with the equipment is eliminated. For the tested motion collisions do not occur. In other cases, collision avoidance could be included in the generation of the humanoid motion by using the technics developed in (Dariush et al., 2009; Mühlig, Gienger, & Steil, 2012; Ruchanurucks, 2015).

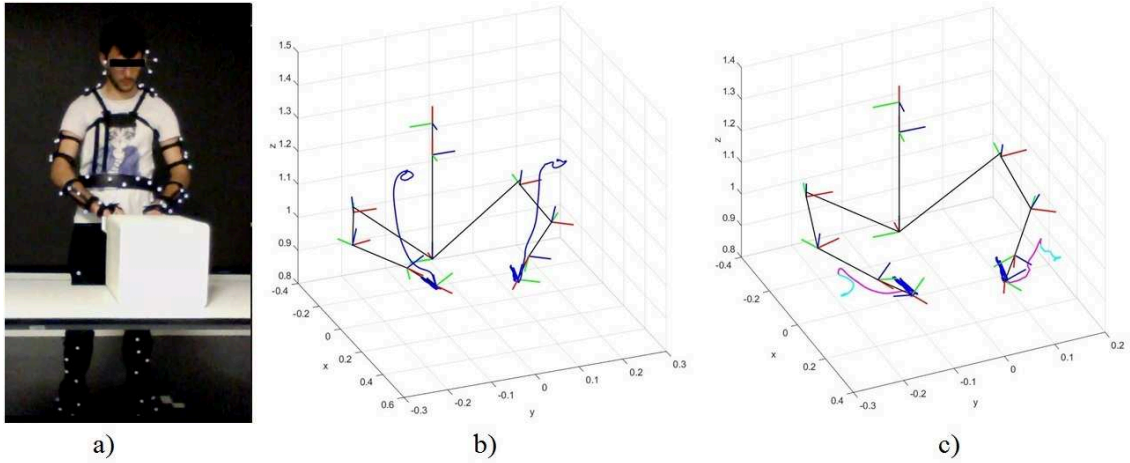


Figure 3.11: The motion "Open/close drawer" performed by the actor and robot: a) Actor during the task. Simulation model of the robot and the calculated trajectories of the robot hands, b) in the imitation algorithm, c) in the algorithm for generation of humanoid motion.

3.8 The simulation and experimental results of the motion of robot ROMEO

The conversion process is based on the results obtained from the imitation algorithm, which are applied in the algorithm for generation of humanoid motion. Trajectories of the motion of hands obtained for the scaled model of the robot by using the imitation algorithm are shown in Fig. 3.11 b). Since the size of the robot is not the same as the size of the actor, the desired trajectories of the hands during the motion without contact are outside the robot workspace and the robot is not able to perform the motion. Therefore, the motion of the hands, generated with the imitation algorithm should be additionally modified according to the characteristics of the robot, in the way proposed in our algorithm for generation of humanoid motion. The generated trajectories of the robot hands during the motion without and with contact, as well as the transition strategy, are presented in Fig. 3.11 c).

The cyan color of the trajectories is the motion without contact with equipment obtained in the way proposed in subsection 3.7.2; magenta color of the trajectories represents the motion obtained with transition strategy when the contact between hands and equipment is calculated by using the proposed algorithm in subsection 3.7.3; and dark blue color represents the actor hands trajectories during the motion with the contact. The desired trajectories of the robot hands are obtained according to the results of the actor motion from the imitation algorithm and/or the motion of the robot arms imitating human motion. According to this, motion of the robot hands is free of collision with equipment and self-collision like the recorded human motion. The experimental results of the actor "open/close drawer" motion and the same motion performed with robot ROMEO are given in Fig. 3.12. Robot and actor perform the task using the same environment. The height of the robot is less than the height of the actor.

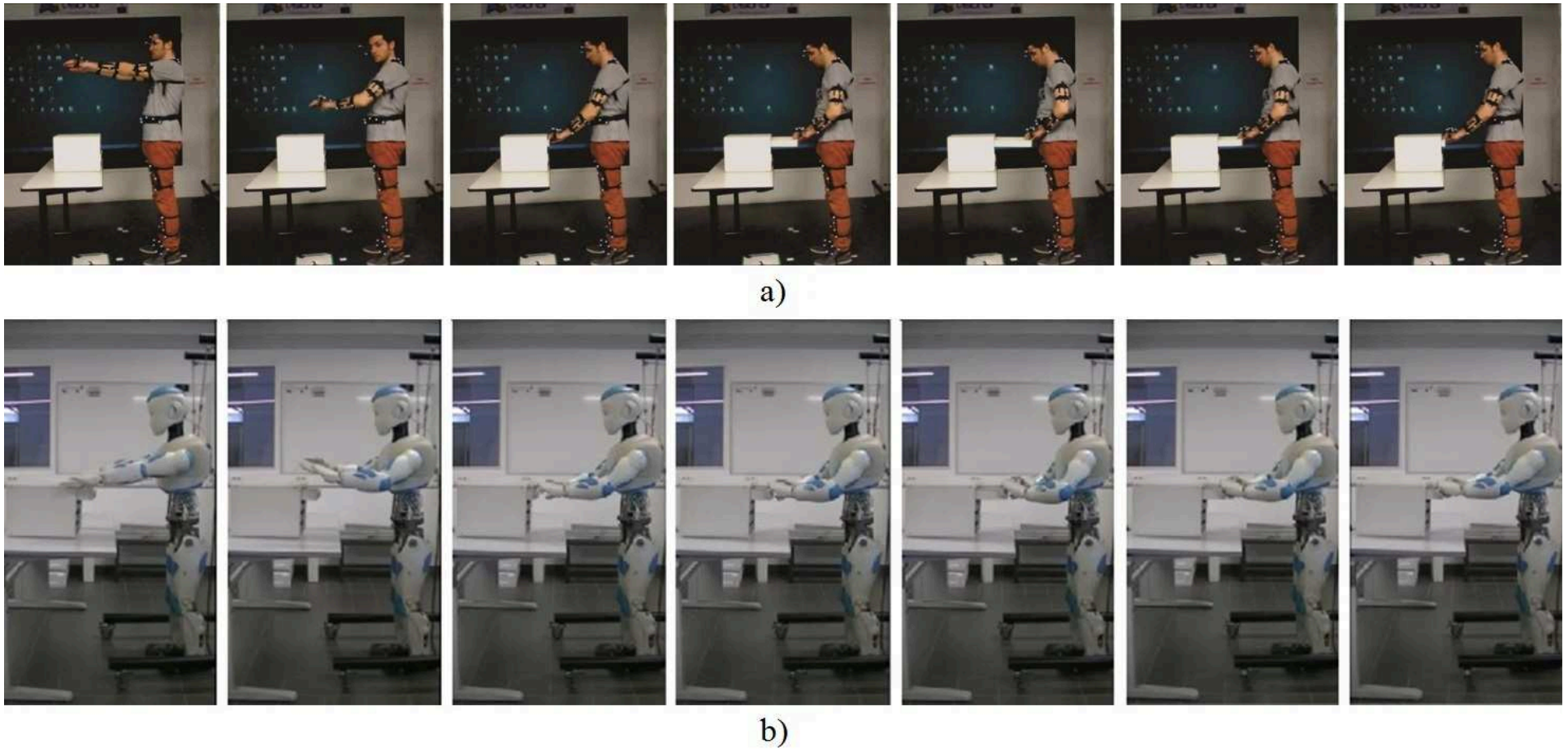


Figure 3.12: Snapshot of the "Open/close drawer" motion performed by: (a) the actor; (b) and robot ROMEO. The robot is able to perform the same task under the same conditions as the actor.

Consequently, the robot performs the task at the level of its chest, while the actor performs the task at the level of his waist. Robot ROMEO has simple hands with flexible fingers which are not actuated and robot is required just to open and close hands. This is the reason why the drawer was a little open at the beginning of the experiment. With the robot which has complex hands with actuated joints, the contact between hands and drawer will be possible with a closed drawer exactly in the way the actor does.

3.9 Conclusion

The conversion process for imitation of dual arm human motion, utilizing the upper body has been presented in this chapter. The conversion process consists of the imitation algorithms and the algorithm for humanoid motion generation. Imitation algorithms, defined for the scaled model of robot ROMEO, are based on Virtual Markers which follow the Real Markers motions and incorporates additionally recorded joint motions. The analytical imitation algorithm is based on the analytical expression of the Jacobian matrices and is able to define the expected motion of the scaled robot in the real time. On the other hands, numerical algorithm is based on the well known nonlinear optimization approach and obtains imitation of the human motion with the same performance as analytical algorithm. Since the numerical algorithm used the MATLAB `fmincon` solver, the imitation cannot be done in real time. Comparing to existing algorithm, our imitation algorithms provide a better accuracy of the motion imitation in Cartesian space. Precise imitation of hands' motions in Cartesian space is essential for the task where the hands come into the contact with the environment. The algorithm for humanoid motion generation is based on the inverse kinematic algorithm aiming to follow the desired robot hands motions and, at same time, resemble human motion behavior to the motion of the humanoid. Since our task consists of the with and without contact motion phases, we additionally defined the algorithm for the transition between such phases. Therefore, as the important contribution of this work, the proposed conversion algorithm is suitable for the human motion imitation with humanoid for the task with and without contact, as well as the complex tasks which consists both type of the motions which is not case of the other imitation algorithms. The results obtained from our conversion process are experimentally tested on the real ROMEO robot. Eventually, one can say that the proposed conversion methodology can be used as a universal and robust algorithm for the human to humanoid motion conversion, regardless of the dual arm motions type and the actor characteristics.

Dual-arm manipulation inspired by human skills

In the nature of every human being is to perform motion in the simplest way and with minimum effort. Therefore, we can assume that humans are always minimizing some unknown criteria in order to create motions. In this chapter we describe the ways in which human motion skills can be mathematically represented. We began with the assumption that human motion represents an optimization process. The aim of this research is to define the inverse optimal control algorithm which is able to generate the same human motion by the humanoid robot including human motion behavior. Unlike some previous studies presented in the [chapter 2](#), our research is based on the analysis of human motion characteristics at the kinematic level. According to this, we defined the set of the criteria functions such as minimization of kinetic energy, velocity, minimization of deviations from the ergonomic position and maximization manipulability which are suitable for analysis of human motions. The inverse optimal control approaches are used as a mathematical representation of the human motion. At the beginning of our research, we try to explain human motion behavior with the well-known control algorithm in robotics such as IK algorithm. We included each of the criterion function into the IK algorithm. The ability of the IK algorithm to generate a recorded human motion with each of the criterion function is compared. We have come to the conclusion about which criterion function makes the best imitation of the recorded human movement. Accordingly, the conclusion about the characteristics of the human movement can be made. In order to precisely analyze the human motions, we decided to combine all of these criteria functions. We defined the inverse optimal control algorithm which minimized the weighted combinations of the all criteria functions. According to the values of each weighted factors we are able to describe the characteristics of the human motion behaviors and to

define the strategy which human used during the tasks.

4.1 Mathematical representation of the human motion behaviors using criteria functions

The criteria functions used in our algorithms are chosen on the way to represent the characteristics of the human body (such as the muscle activation, distribution of the energy. . .) during the motion and to explain them by mathematical equations. According to the human motions analysis presented on [section 2.3](#) relations between criteria functions and the characteristics of the human motion which they interpret is explained on this chapter.

4.1.1 Criterion minimization of joint velocities

This criterion function is proposed by Whitney ([Whitney, 1969](#)) in order to define the control algorithm which is able to automatically avoid singularities position of redundant robots. The criterion is based on minimization norm of the joint velocities $\|\dot{q}\|^2$. In order to avoid numerical difficulties and non-differentiability, the criterion function is described with equations:

$$\phi_v(\dot{q}_t) = \frac{1}{2} \dot{q}_t^T I \dot{q}_t \quad (4.1)$$

where \dot{q}_t is joint velocities vector, I is identity matrix. The inverse kinematic algorithm based on Jacobian pseudoinverse is formulated using this criterion function.

In the analysis of the human motion behavior the criterion minimization of joint velocities gives the same motion importance of all joints during the task since the identity matrix is used as a weight matrix. It is expected that this criterion will described motions on which the all joints are equally active during the task.

4.1.2 Criterion minimization of the kinetic energy

The criterion minimization of the kinetic energy is formulated using the basic equations of the kinetic energy and takes a form:

$$\phi_{en}(\dot{q}_t) = \frac{1}{2} \dot{q}_t^T A \dot{q}_t \quad (4.2)$$

The criterion function is a quadratic function of joint velocities \dot{q}_t (as a criterion minimization velocity) where the weighted matrix is the inertia matrix of the dynamic model of the actor. The inertial matrix is calculated based on the scaled kinematic model of the ROMEO robot and BSP of actor, using the robotics software SYMORO ([Khalil & Creusot, 1997](#)). The calculation of the inertia matrix gives the high inertia for the joints with big mass such as trunk, shoulder, and elbow joints. Wrist joints have significant

smaller values of the inertia compare with other joints. In the analysis of the human motion behavior the criterion minimization kinetic energy gives bigger motion priorities to the joints with bigger inertia. It is expected that this criterion will described motions on which trunk or shoulders or elbows are more active during the task.

4.1.3 Criterion minimization of distance between the current position and the ergonomic configuration of human

This criterion function is given by equation:

$$\phi_{ergonomiy}(q_t) = \frac{1}{2}(q_t - q_{ergonomiy})^T A (q_t - q_{ergonomiy}) \quad (4.3)$$

where $q_{ergonomiy}$ is the ergonomic configuration of the human proposed by Yang et al. (J. Yang et al., 2004). The resulting vector $q_{ergonomiy}$ is defines as:

$$\begin{aligned} q_{ergonomiy}[i] &= 0; i = 1, \dots, 11 \\ q_{ergonomiy}[12] &= 20^0, q_{ergonomiy}[13] = 5^0, q_{ergonomiy}[14] = 10^0, q_{ergonomiy}[15] = -80^0 \\ q_{ergonomiy}[16] &= 30^0, q_{ergonomiy}[17] = 0^0, q_{ergonomiy}[18] = 15^0, q_{ergonomiy}[19] = 20^0 \\ q_{ergonomiy}[20] &= -5^0, q_{ergonomiy}[21] = -10^0, q_{ergonomiy}[22] = 80^0, q_{ergonomiy}[23] = -30^0 \\ q_{ergonomiy}[24] &= -80^0, q_{ergonomiy}[25] = 15^0 \end{aligned} \quad (4.4)$$

according to the kinematic model given in appendix D (see Fig. D.2 in appendix D).

The inertia matrix A is chosen in order to include the motion priority of each joint (Tomić et al., 2016). The criterion $\phi_{ergonomiy}(q_t)$ can be adapted as a function of the \dot{q}_t , using the relation between q_t and \dot{q}_t :

$$\phi_{ergonomiy}(\dot{q}_t) = \frac{1}{2}(q_{t-\Delta t} + \Delta t \dot{q}_t - q_{ergonomiy})^T A (q_{t-\Delta t} + \Delta t \dot{q}_t - q_{ergonomiy}) \quad (4.5)$$

where $q_{t-\Delta t}$ is the previous value of the joints generalized coordinate and Δt is the increment of the time calculated according to the frequency for data acquisition.

4.1.4 Criterion maximization of the manipulability

In the field of robotics criterion manipulability is used as a measure of the ability of the mechanism to move its end-effector. The criterion maximization of the manipulability is given with equation:

$$\phi_4(\dot{q}_t) = \det(J \cdot J^T) \quad (4.6)$$

where $J = J(q_t)$. Since we define the criterion function which should be minimized, the criterion $\phi_4(\dot{q}_t)$ is written in the form:

$$\phi_4(\dot{q}_t) = \frac{1}{2}(\dot{q}_t - p\omega)^T (\dot{q}_t - p\omega) \quad (4.7)$$

proposed by Zhang (Zhang, Li, & Zhang, 2013). The $\omega = \frac{\partial \det(JJ^T)}{\partial q_t}$ is a vector of manipulability gradient $\det(JJ^T)$, and $p \in \mathbb{R}^+$ is a constant coefficient. The i_{th} element of is calculated using the equation:

$$\omega_i = \frac{\partial \det(JJ^T)}{\partial q_t^i} = \det(JJ^T) \text{trace} \left((JJ^T)^{-1} \left(\frac{\partial J}{\partial q_t^i} J^T + J \left(\frac{\partial J}{\partial q_t^i} \right)^T \right) \right) \quad (4.8)$$

Here, $\text{trace}(\cdot)$ denotes the trace of a matrix argument and q_t^i is the i_{th} element of the vector q_t . This criterion allows that the joint motion tends toward the motion that maximizes manipulability. The value p ($p = 10^6$) is selected to minimize the coefficient of manipulability calculated with $\det(JJ^T)$. In the analysis of the human motion behavior, the manipulability criterion will describe motions which are near the singular position of the human body. According to this, we will be able to analyze the influence of the relative position between actor and environment during the task.

4.2 Inverse Kinematic algorithm as a tool for identification of human motion skills

Looking the motion imitation process, the task of each arm of the scaled model of the robot is to follow a desired position and orientation of the recorded arms' motions. Based on the results from the imitation algorithm and the intermediate model of the humanoid robot we are able to formulate the control algorithm which will obtained recorded human motion. This task can be solved using the simplest IK algorithm. The primary task of the IK algorithm is following the desired trajectories of the end-effector (for the case of the dual-arm manipulation that are the trajectories of the hands). As an optimization algorithm, the IK algorithm can additionally include a criterion function to optimize which can give characteristics of the human motion. The purpose of our research is to analyze the criterion function which will be minimizing with the IK algorithm in order to transfer human skills to humanoid on the best way. Since the scaled model of the ROMEO robot has more degrees of the freedom compared with the task, the IK algorithm should make a deal with redundancy. In robot control, the redundancy is generally solved at the kinematic level using IK algorithm by minimization of criterion or by definition of several tasks with different priority level (Mansard & Chaumette, 2007). The numerical approach for solving IK algorithm of redundant robots gives one solution from the set of infinite solutions. There are several methods for solving numerical IK problems of redundant robots.

4.2.1 Moore-Penrose pseudoinverse algorithm

In his previous work Whitney (Whitney, 1969) proposed to use the Moore-Penrose pseudoinverse of the no square Jacobean matrix in order to control redundant of the robot.

The pseudoinverse has a least squares property that generates the minimum norm joint velocities $\|\dot{q}\|^2$. The IK algorithm with pseudoinverse of the Jacobean matrix can be considered as optimal problem and derivate using the Lagrange multiplier mathematical method. The optimal problem is given by:

$$\begin{bmatrix} \min_{\dot{q}} & \frac{1}{2}\dot{q}^T\dot{q} \\ s.t. & \dot{X} = J(q)\dot{q} \end{bmatrix} \quad (4.9)$$

where $J(q)$ is the Jacobean matrix and the velocity vector of the robot end-effector. The theorem states that the optimal solution is obtained where the gradients of the Lagrange equation:

$$\Lambda(\dot{q}, \lambda) = \frac{1}{2}\dot{q}^T\dot{q} + \lambda(-J(q)\dot{q} + \dot{X}) \quad (4.10)$$

with respect to the $\dot{q} \in \mathbb{R}^n$ and Lagrange multiplier $\lambda \in \mathbb{R}^n$ becomes all zero. Therefore one gets:

$$\frac{\partial \Lambda(\dot{q}, \lambda)}{\partial \dot{q}} = \dot{q}^T - \lambda J(q) = 0 \rightarrow \dot{q} = J(q)^T \lambda^T \quad (4.11)$$

$$\frac{\partial \Lambda(\dot{q}, \lambda)}{\partial \lambda} = (-J(q)\dot{q} + \dot{X}) \rightarrow \dot{X} = J(q)\dot{q} \quad (4.12)$$

According to the equations 4.11 and 4.12, the solution for the IK algorithm with pseudoinverse of the Jacobean matrix is given on the form:

$$\dot{q} = \underbrace{J(q)^T (J(q)J(q)^T)^{-1}}_{J^+(q)} \dot{X} \rightarrow \dot{q} = J^+(q)\dot{X} \quad (4.13)$$

The main disadvantage of this method is that it produces discontinuity in joint velocities near the singularities (Buss, 2004).

4.2.2 Weighted pseudoinverse algorithm

Park (J. Park, Choi, Chung, & Youm, 2001) proposed the weighted pseudoinverse algorithm. This algorithm is based on the minimization criterion function

$$\begin{bmatrix} \min_{\dot{q}} & \frac{1}{2}\dot{q}^T A \dot{q} \\ s.t. & \dot{X} = J(q)\dot{q} \end{bmatrix} \quad (4.14)$$

where matrix A is arbitrary matrix depending on the criterion which we minimize. The equation of the IK weighted pseudoinverse algorithm is calculated using the Lagrange multiplier mathematical method on the same way as previous:

$$\dot{q}(t) = A^{-1}(q)J^T(JA^{-1}(q)J^T)^{-1}\dot{X}(t) \quad (4.15)$$

If we consider A as an inertial matrix of the human body, the weighted pseudoinverse algorithm will minimize the kinetic energy. The optimization criterion can also be the joint limit avoidance, obstacle avoidance, mathematical singularity avoidance, dexterity, energy minimizing and other criteria (Baillieul, 1985; Chiaverini et al., 2008; Nenchev, Tsumaki, & Uchiyama, 2000).

4.2.3 Inverse Kinematic algorithm with optimization term

Apart from the pseudoinverse algorithms, the criterion function can be including into the IK algorithm using the null space of Jacobian. On this way, the IK algorithm finds a joint configuration which satisfies the end-effectors' task and minimizes the chosen criterion. The general solution of the IK with optimization term is given as:

$$\dot{q} = J^+ \dot{X} + (I - J^+ J)Z \quad (4.16)$$

where J^+ is the pseudo inverse of J matrix. The second term belongs to the null space of Jacobian matrix J and represents optimization term. This term can be used to optimize a desired function $\phi(q)$. Taking $Z = \beta \nabla \phi$ where $\nabla \phi$ is the gradient of function $\phi(q)$ with respect to the q , permits to minimize the function $\phi(q)$ when $\beta < 0$ and to maximize $\phi(q)$ when $\beta > 0$ (Khalil & Dombre, 2004). In this case, the equation 4.16 can be rewritten as:

$$\dot{q} = J^+ \dot{X} + \beta(I - J^+ J)\nabla \phi \quad (4.17)$$

where:

$$\nabla \phi = \left[\frac{\partial \phi}{\partial q_1} \quad \cdot \quad \cdot \quad \cdot \quad \frac{\partial \phi}{\partial q_n} \right]^T \quad (4.18)$$

4.2.4 Inverse Kinematic algorithm and the criteria functions

The set of the criteria functions which can be including into the analysis of the human motion is proposed. According to the previous derivations of the IK algorithm, the each criterion function is included into the IK algorithm at the appropriate way.

- IK algorithm with criterion minimization of joint velocities $\frac{1}{2} \dot{q}^T I \dot{q}$ (IK with velocity criterion): This solution is directly given by the pseudoinverse algorithm:

$$\dot{q}(t) = J^+ \dot{X}(t)$$

- IK algorithm with criterion minimization of the kinetic energy $\frac{1}{2} \dot{q}^T A \dot{q}$ (IK with energy criterion): This solution is obtained using weighed pseudo inverse algorithm:

$$\dot{q}(t) = A^{-1}(q) J^T (J A^{-1}(q) J^T)^{-1} \dot{X}(t)$$

- IK algorithm with criterion minimization of the weighted distance between current and the ergonomic configuration $\frac{1}{2} (q_t - q_{ergonomy})^T A (q_t - q_{ergonomy})$ (IK with er-

gonomic criterion) This solution is obtained using weighed pseudo inverse algorithm and optimization term:

$$\dot{q}(t) = J_A^+ \dot{X} - (\Delta t)^{-1} (I - J_A^+ J) (q(t - \Delta t) - q_{ergonomy})$$

where $J_A^+ = A^{-1}(q)J^T(JA^{-1}(q)J^T)^{-1}$.

- IK algorithm with criterion maximization of the manipulability $\det(J \cdot J^T)$ (IK with manipulability criterion) This solution is obtained using the optimization term:

$$\dot{q} = J^+ \dot{X} + \beta(I - J^+ J) \frac{\partial(\det(J \cdot J^T))}{\partial q}$$

4.2.5 Results

In this chapter the general characteristics of IK algorithms with different criterion, previously defined, for the generation the human like motion are analyzed. The each IK algorithm is tested on the set of the seven dual arm motion performed by 15 actors. The PMP phase of the each motion is analyzed since it is the only phase that undergoes any form of analysis.

In order to calculate the measure of similarity of generated motion by IK algorithm and desired motion, an integral error between the desired and obtained position of two shoulders and two elbows joints in Cartesian space is calculated using the trapezoidal numerical integration. A small value of the integral error indicates a good match between the desired and the obtained motion. The values of the integral error per sample calculated according to the results of each IK algorithms for different experiments in the case of the all actor are given on the Fig. 4.1.

At the Fig. 4.1 we can see that the IK algorithm with ergonomic criterion gives the worst imitation of the human motion (the biggest value of the integral error). The reason may be the activation of each joint during movement. Since defined motions are far from the ergonomic configuration of a human the IK algorithm with ergonomic criterion are not able to generate human like motion.

On the other side, the IK algorithm with energy criterion or velocity criterion gives good performance in generation of the human like motion for the most of the tasks. According to the results we can note that the IK algorithm with velocity criterion gives the best imitation for tasks which require activation of shoulder and elbow joints, such as “Cutting with knife” (see Fig. 4.1 b)) and “Opening/closing a drawer” (see Fig. 4.1 d)). The IK algorithm with energy criterion gives the smaller value of the integral error in the case when the motion of one joint is dominant during the task, such as elbow joint in the task “Grating of food” (see Fig. 4.1 e)) or shoulder joint in the task “Inflating mattress using a pump” (see Fig. 4.1 c)). Exceptions to this rule can be observed at each of these movements. The same movement can be done in different ways, depending on the characteristics of the actors and the relative distance between the actor and the equipment. The

actor height determines which of the joints is active during the movement in many cases. Therefore, it is expected that different IK algorithms can be used for better imitate of the same motion with different actors.

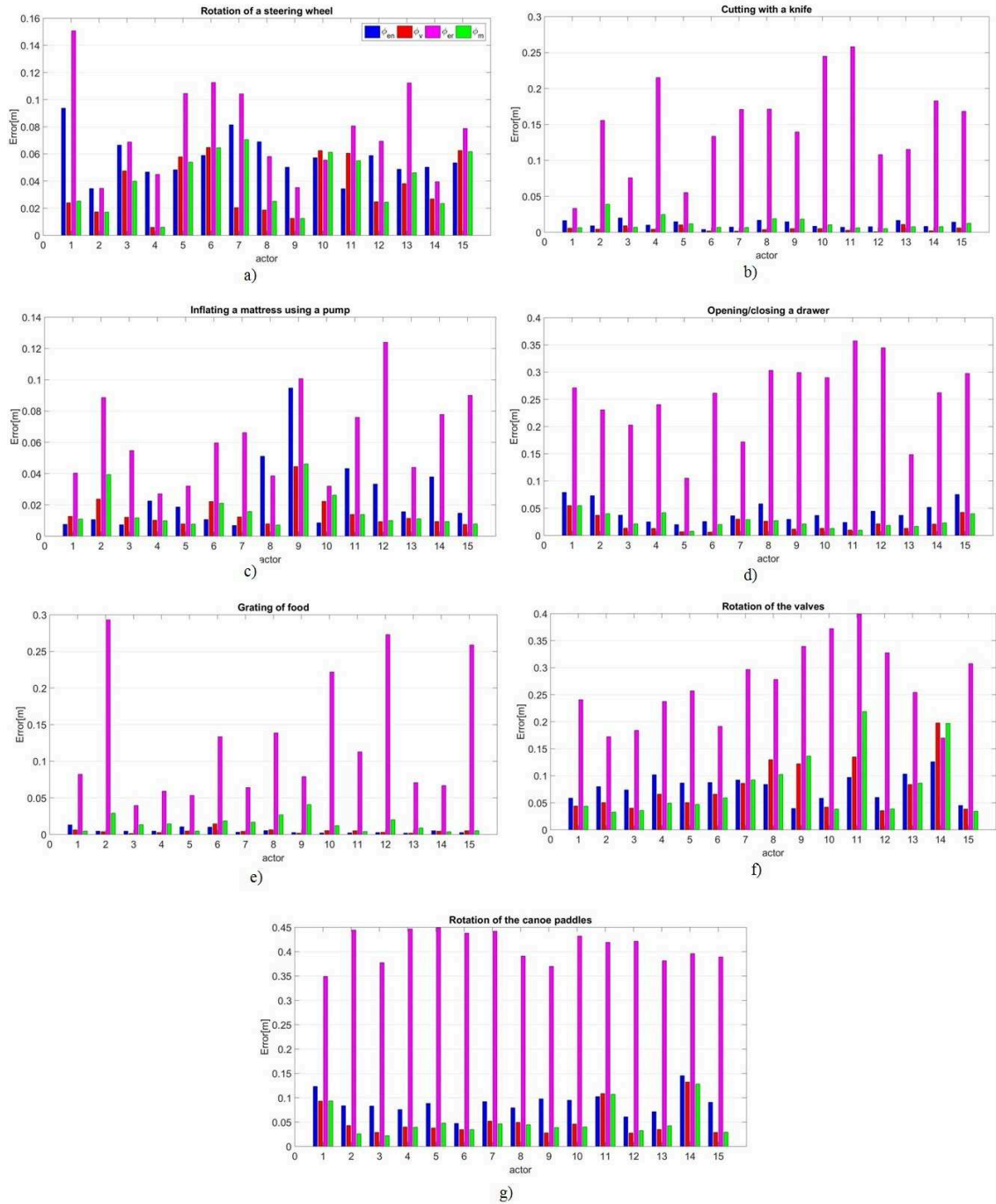


Figure 4.1: The integral errors per sample calculated according to the results of each IK algorithms for different experiments in the case of all actors.

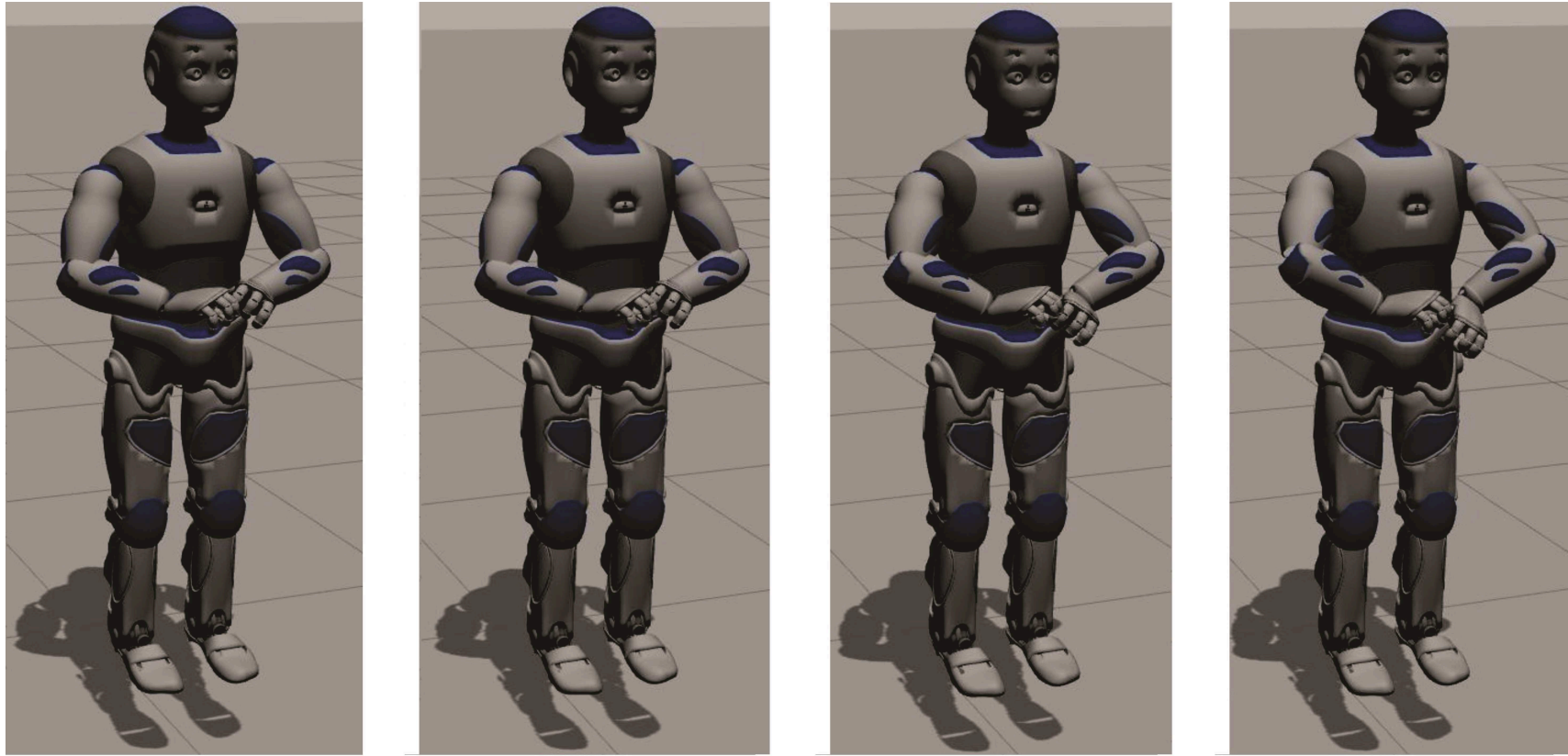


Figure 4.2: The “Opening/closing a drawer” task performed by the robot ROMEO. The pose obtained with a) IK algorithm with velocity criterion; b) IK algorithm with manipulability criterion; c) IK algorithm with energy criterion; d) IK algorithm with ergonomic criterion.

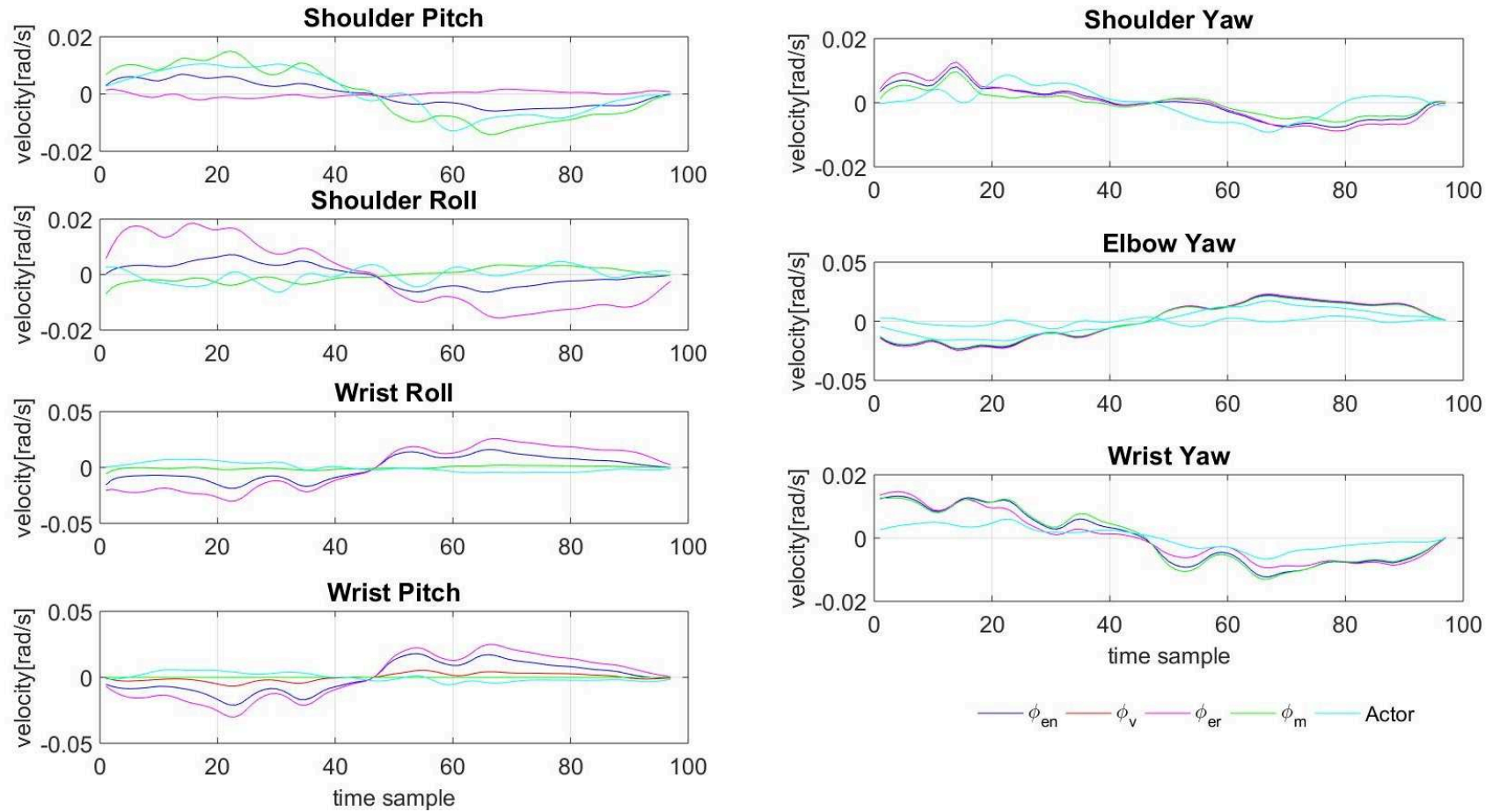


Figure 4.3: The actor and the robot ROMEO joint velocities during the “Opening/closing a drawer” task. The robot ROMEO joint velocities obtained by IK algorithm with velocity criterion and IK algorithm with manipulability criterion are similar and near the actor joint velocities.

The relative distance between the actor and the equipment can be responsible for the generation the motion near singular configuration which can be detected with the help of IK with manipulability criterion. In the “Rotation of the valves” (see Fig. 4.1 f) and “Rotation of the canoe paddles” (see Fig. 4.1 g)) tasks, This IK algorithm imitates the human motion on the best way for the actor who is not well positioned to perform the task. If the actors are well posed to perform the task IK algorithm with velocity criterion or IK algorithm with energy criterion will gives the best imitation of these motions depending of the which joints are active. The same conclusion can be used for the any types of the motion. The defined IK algorithms can be used for generation the motion with robot ROMEO. Since the robot ROMEO and the actor has the different body characteristics, such as the size of the segments, the trajectory of the human hands should inside of the robot ROMEO workspace. Therefore, the “Opening/closing a drawer” motion is selected to analyze the results since the trajectories of the human hands are in the robot ROMEO work space. In the Fig. 4.2 we are shown the robot ROMEO pose at the middle of the motion generated by Gazebo simulator. According to the results on the Fig. 4.2 we can see that the motion pose obtained by IK algorithm with velocity criterion (see Fig. 4.2 a)) and IK algorithm with manipulability criterion (see Fig. 18 b)) are the similar. This conclusion is logical and is associated with results illustrated in Fig.4.1 d). Both algorithms generate the same motion with the same values of the integral errors in the most of the cases. On the other hands, the robot motion pose generated by the IK algorithm with energy criterion is different. The elbow positions in the Fig. 4.2 c) are more different compare with in the Figs. 4.2 a) and b). The robot performs the motion using the elbow joints. At the end, in the Fig. 4.2 d) the robot motion pose obtained by the IK algorithm with ergonomic criterion is presented. The motion obtained with this algorithm is quite different than other motions since the algorithm tries to keep robot configuration near human ergonomic configuration. The motion generated on this way is far from the human like motion which is proven with the big values of the integral error (see Fig. 4.1 d)). The trajectories of the left arm joint velocities obtained for the case of the one human and the robot with different IK algorithm are presented in the Fig. 4.3. The results presented in the Fig. 19 shows that the IK algorithm with velocity criterion and IK algorithm with manipulability criterion generate the same joint motions which are the more human-like motion compare with other IK algorithms. The difference in the robot ROMEO pose shown in the Fig. 4.2 is confirmed with the joint velocities trajectories shown in the Fig. 4.3.

4.2.6 Conclusion

In this section we analyzed the performance of the IK algorithm with different criterion function in the imitation of the human motion. According to the results we can say that each of the motion is connected with the some IK algorithm which imitates them on the best way. The activation of the joints can define which IK algorithm does imitation of the human motion in the best way. The human characteristics and the relative position

between actor and equipment also take influence in choice of the IK algorithm. Hence, the motion near singularity or ergonomic motion can be detected by these IK algorithms.

In the next step we are mention that the each human motion can be perfectly imitated by the scaled model of the robot if best combination of criteria functions is selected. Those, we combine these 4 criteria functions into inverse optimal control algorithm using the weight coefficients for each criterion. We are expected that the motion which is more similar with human motion will be obtained. Also we expected that we will obtain combination of the criteria functions for each task which will be universal for that type of the motions.

4.3 The inverse optimal control algorithm

At the previous chapter we analyzed abilities of the IK algorithm to generate the recorded human motion using different criterion function. We mention that the batter imitation can be obtained if we include more criteria functions into the objective function which will be minimized. Our assumption is that the inverse optimal control algorithm with the appropriate combination of the criteria functions will be able to generate the same motion as a human.

Unlike some previous studies, our research is based on the analysis of human motion using the inverse optimal control approach with criteria functions defined in the joint space. The objective function of the inverse optimal control algorithm is defined as a weighted combination of the criteria functions given in [section 4.1](#). Each criterion function is multiplied with weight coefficient which defines its influence into the inverse optimal control algorithm. We seek the combination of the values of the weight coefficients that generates the humanoid motion that is closest to the recorded human motion. This weight will define the criterion optimized by human behavior. Compare with previous studies, we calculate the values of weight coefficients separately for the different types of the dual-arm motions. On this way we are able to make relation between characteristics of the human motion in the joint space and the criterion function which describe them.

Our objective is to find an objective function that optimized by human produces the motion recorded experimentally. Since the studied motion involves at least partially contact with the environment, the criterion is optimized with the constraint that human hands follow a given motion defined by the task. We consider an optimal control problem of the form:

$$\begin{aligned} \min \quad & \Phi(q_t, \dot{q}_t) \\ \text{s.t.} \quad & \dot{X} = J(q)\dot{q}_t \end{aligned} \tag{4.19}$$

where $J(q)$ is the Jacobian matrix of the scaled model of the robot ROMEO that maps joint motion to hand motion, t is a time sample, $q_t, \dot{q}_t \in \mathbb{R}^n$ are joint position and velocities as a function of t , respectively, \dot{X} velocity vector of the actor's hands obtained by the

imitation algorithm and the $\Phi(\cdot)$ is the objective function that should be minimized. For the objective function $\Phi(\cdot)$ we make the assumption that it is expressed as a weighted sum of the n basic criterion function $\phi_i(\cdot)$ with the corresponding weight factor $k_i \in \mathfrak{R}^+$:

$$\Phi(q_t, \dot{q}_t, k) = \sum_{i=1}^n k_i \phi_i(q_t, \dot{q}_t) \quad (4.20)$$

Consequently, the task of determining the best objective function $\Phi(\cdot)$ is reduced to determining the best weight factors k_{energy} , $k_{velocity}$, $k_{ergonomiy}$ and $k_{manipulability}$ ¹ .

The final equation for objective function $\Phi(\dot{q}_t)$ which includes basic criteria functions analyzed in [section 4.1](#) and with weight coefficients is:

$$\begin{aligned} \Phi(\dot{q}_t) = & k_{energy} \frac{1}{2} \dot{q}_t^T A \dot{q}_t + k_{velocity} \frac{1}{2} \dot{q}_t^T I \dot{q}_t + \\ & k_{ergonomiy} \frac{1}{2} (q_{t-\Delta t} + \Delta t \dot{q}_t - q_{ergonomiy})^T A (q_{t-\Delta t} + \Delta t \dot{q}_t - q_{ergonomiy}) + \\ & k_{manipulability} \frac{1}{2} (\dot{q}_t - p\omega)^T (\dot{q}_t - p\omega) \end{aligned} \quad (4.21)$$

where k_{energy} , $k_{velocity}$, $k_{ergonomiy}$, $k_{manipulability}$ are the weight factors which correspond to criteria minimization of kinetic energy, minimization of joint velocities, minimization of the distance between the current position and the ergonomic configuration of human and maximization of manipulability, respectively. The weights represent the contribution in percentage of each criterion to the optimal function ($k_{energy} + k_{velocity} + k_{ergonomiy} + k_{manipulability} = 1$).

The optimal problem is solved under the constraint $\dot{X} = J(q)\dot{q}_t$ given in the equation [4.19](#) that describes the task to be achieved by the human hand with or without contact with the environment. The task can be integrated in the optimal problem using the Lagrange multiplier mathematical method with selected set of optimization criteria and constraints:

$$\Lambda(\dot{q}_t, \lambda) = \Phi(\dot{q}_t) + \lambda(-J(q)\dot{q}_t + \dot{X}) \quad (4.22)$$

The theorem states that the optimal solution is obtained where the gradient of the equation [4.22](#) with respect to the \dot{q}_t and Lagrange multiplier $\lambda \in \mathfrak{R}^n$ becomes all zero. Therefore, the joint velocity for the criterion defined by k_{energy} , $k_{velocity}$, $k_{ergonomiy}$, $k_{manipulability}$ is:

1. $k_1 = k_{energy}$, $k_2 = k_{velocity}$, $k_3 = k_{ergonomiy}$, $k_4 = k_{manipulability}$. This notation is used to be explicit and easy to read.

$$\dot{q}_t = K \begin{pmatrix} J(q)^T \left(J(q)KJ(q)^T \right)^{-1} \dot{X} + \\ k_{ergonomy} \Delta t J(q)^T \left(J(q)KJ(q)^T \right)^{-1} J(q)KA^T (q_{t-\Delta t} - q_{ergonomy}) - \\ k_{manipulability} p J(q)^T \left(J(q)KJ(q)^T \right)^{-1} J(q)K\omega - \\ k_{ergonomy} \Delta t A^T (q_{t-\Delta t} - q_{ergonomy}) + k_{manipulability} p \omega \end{pmatrix} \quad (4.23)$$

where $K = (k_{energy}A^T + k_{velocity}I + k_{ergonomy}\Delta t^2 A^T + k_{manipulability}I)^{-1}$.

4.3.1 Genetic algorithm for calculation of the weight coefficients

The observed dual arm model is a redundant system and enables performing the same task differently. By using varied combinations of weight coefficients, we are able to generate different types of motion in the joint space within the same task of the hands in Cartesian space. In such context, it is necessary to define the fitness function, which represents a measure of similarity of generated motion by our inverse optimal control algorithm and the desired movement. Since wrist position error is eliminated by introducing the constraint in the optimization function 4.22, the fitness function $F(\cdot)$ is calculated as an integral of the error between the desired and obtained position of shoulder and elbow in Cartesian space using the trapezoidal numerical integration:

$$F(C) = \int_0^{t_{end}} E(t) dt \approx \frac{t_{end}}{2N} \sum_{n=1}^N (E(t_n, C) - E(t_{n+1}, C)) \quad (4.24)$$

$$E(t, C) = \left\| \vec{P}_j^d(t) - \vec{P}_j^o(t, C) \right\|$$

where $C = \{k_{energy}, k_{velocity}, k_{ergonomy}, k_{manipulability}\}$ is a combination of the weight coefficients, t_{end} is the motion duration, N is the number of samples during the motion, $E(t, C)$ is the square norm of the error between the vectors of the desired value of the arm joints obtained via the imitation process $\vec{P}_j^d(t_i) = [P_{RightSh}^d(t_i) \ P_{LeftSh}^d(t_i) \ P_{RightEl}^d(t_i) \ P_{LeftEl}^d(t_i)]$ and the position of the arm joints calculated by 4.23 for the C combination of the weight coefficients $P_j^o(t_i, C) = [P_{RightSh}^o(t_i, C) \ P_{LeftSh}^o(t_i, C) \ P_{RightEl}^o(t_i, C) \ P_{LeftEl}^o(t_i, C)]$. A small value of the fitness function indicates a good match between the desired and the obtained motion.

Since the fitness function admits many local minimum, the algorithm based on the gradient calculation would not always give global solution. This is why a genetic algorithm, suitable for such context, has been used (Goldberg & Holland, 1988). A set of 40 individuals defined the population, where each individual is a combination of the weight coefficients. A uniform distribution is used to generate the initial population. The imposed condition for stopping the genetic algorithm is that the change of the best value of the fitness function $F(\cdot)$ is not greater than 10^{-6} for the previous 50 generations.

| Task | Rotation of the valves | Rotation of the canoe paddles | Rotation of a steering wheel | Inflating a mattress using a pump | Cutting with a knife | Grating of food | Opening /closing a drawer |
|------------|------------------------|-------------------------------|------------------------------|-----------------------------------|----------------------|-----------------|---------------------------|
| Fitness[m] | 0.0466 | 0.0413 | 0.0127 | 0.0096 | 0.0043 | 0.0029 | 0.0206 |

Table 4.1: The average values of the fitness function in one time sample of all actors for the all tasks.

The convergence rate of a genetic algorithm depends on the initial population. The properties of genetic algorithms, such as mutations, may bring individuals out of the local minimum and move towards the global one. This accelerated the convergence of the genetic algorithm towards optimal solutions.

4.3.2 Human motion strategy as a result of the inverse optimal control algorithm

In this section, the characteristics of the human motion strategy will be analyzed using two approaches: the results of the inverse optimal control algorithm and the characteristics of the motion define in the joint space. A qualitative motion evaluation in joint space will give the influence of the each joint on generation the motion. On the other hands, the inverse optimal control algorithm will defined the influence of the each basic criterion function in generation the human motion. In this chapter we will try to make connection between results of the human motion obtained in joint space and using inverse optimal control algorithm. The final part of this section will provide a general conclusion on motion characteristics and association with basic criteria functions. For the purpose of our research the PMP of the each task is analyzed in order to obtain the pure characteristics of each motion. The each motion is test on the sets of 15 actors which perform motion on the same virtual environment using the same equipment. Since the characteristics of the human motion (criterion optimized) are obtained by imitating the recorded human motion using our inverse optimal control algorithm and the criteria functions, the quality of imitation is defined through the value of the fitness function (see the equation 4.24). The fitness function, calculated for the best combination of the weight coefficients, represents the minimum deviation between the obtained and recorded motion. According to the results of the genetic algorithm, the best combination of the basic criteria functions with same value of the fitness function is obtained if more than 80% individuals in a generation converge to the same solution. The average values of the fitness function are calculated per sample for all actors. Table 4.1 presents the fitness function for all experiments.

The fitness function given in Table 4.1 represents integral sum of the errors between the achieved and the recorded position of all observed joints (right elbow, right shoulder, left elbow, and left shoulder). Therefore, the average error in the following motion of each

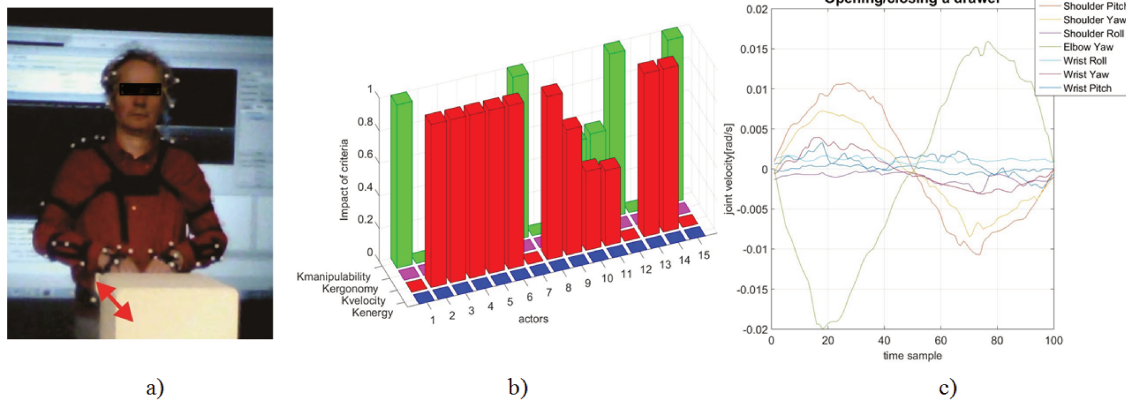


Figure 4.4: a) “Opening/closing drawer” task b) Resulting weight factors defining the objective function - criterion minimization of joint velocity prevail c) Joint motions - shoulder and elbow motions dominate.

joint per sample in “Opening/closing a drawer” task is about 0.0052m, since the fitness function sums displacement of four joints - two elbows and two shoulders. Hence, the conclusion is that each recorded human motion can be reproduced with great accuracy by the appropriate combination of criteria functions.

In comparison with the results obtained by the IK algorithms and presented on the Fig. 4.1 we can say that the inverse optimal control algorithm with combination of the criteria functions generates the motion which is more human-like motion. Hence, the conclusion is that each recorded human motion can be reproduced with great accuracy by the appropriate combination of criteria functions.

4.3.3 “Opening/closing a drawer”

In this subsection, the characteristics of the “Opening/closing a drawer” task is presented. The “Opening/closing a drawer” task represents a symmetric horizontal-translation motion (see Fig. 4.4(a)). The motion is constrained by the equipment and only horizontal translation of hands is allowed. The orientation of hands is fixed and prescribed by the equipment (the fingers of both hands are placed inside the drawer with the palms down). The height of hands is determined by the characteristics of the drawer.

Upon observing the trajectories of hand motion for the task, recorded by the motion capture system, it is obvious that the motions of all actors for the given task are close, mainly because it is highly conditioned by the characteristics of the equipment. The analysis of motion in joint space is performed using the results from the imitation algorithm, which give us trajectories of each DoF. The results show that during this motion the shoulder (Shoulder Pitch and Shoulder Yaw) and elbow joints move more than other joints (see Fig. 4.4(c)). Furthermore, the motion of the elbow yaw joints is larger than motion of shoulder joints. The trajectories of the joints given in Fig. 4.4(c) represent the mean values obtained for all actors during the same motion. We also noticed that the size of an actor affects the motion of arm joints during the task because the position of the equip-

ment was fixed and was not determined by the size of the actor. In the case when the actor is taller, the actor's arms are bended down. On the other hand, smaller actors did not bend down their arms and had to rely more on their elbows and trunk joints to perform the task.

The combination of the weight coefficients obtained by the genetic algorithm while solving the inverse optimal problem for the task "Opening/closing a drawer" are given in Fig. 4.4(b). The results of the genetic algorithm, obtained for all actors in the same motion, are depicted in three-dimensional graph where horizontal axes shows number of the actor and particular criterion, while vertical axis show the impact of particular criterion per each actor. For descriptive and consistent illustration impact of each criterion is highlighted in same color:

- green- maximization of manipulability criterion
- magenta- ergonomy criterion (minimization of distance between the current and ergonomic configuration criterion).
- red- minimization of joint velocity criterion
- blue- minimization of kinetic energy criterion

The results show that 9 out of 15 actors use the velocity minimization criterion with the value $k_{velocity}$ takes values near 1. Since the shoulder and elbow joints have far greater motion than other joints, the velocity minimization criterion is dominant for such type of motion. The criterion of manipulability is dominant in the case of 6 actors when an actor has some restrictions on motion caused by its dimensions and/ or distance from the drawer (indicated in green color in Fig. 4.4(b)). Some problems appear when an actor is not well positioned for performing the task. Since the "Opening/closing a drawer" task is horizontal-translation motion the distance between actor and equipment has influence on the way on which motion will be performed. If the actor is far from the drawer, he/she will keep the arms straight and try to perform the task. This arm configuration is near singularities and reduces the possibilities of arm manipulation. The actor tries to move hands away from the singularity and maximizes manipulability. The problem of manipulation also appears in the case when the actor is near the drawer. That is why the actor moves all joints more in order to increase manipulability and perform the task.

Eventually, one can conclude that for "Opening/closing a drawer" task human motion is planned so to minimize joint velocities and maximize manipulability, while their relative ratio depends on actor and equipment characteristics.

4.3.4 "Rotation of the valves"

In this subsection, the characteristics of the task "Rotation of the valves" will be presented. The "Rotation of the valves" is a goal-oriented rotational motion around the vertical axis (see Fig. 4.5(a)). Both arms work independently while performing this task. Palms are placed perpendicularly to the room floor and grasp the handles vertically placed on the valves. The height of hands is determined by the characteristics of the valves.

According to the analysis of the motion in the joint space, it is obvious that some com-

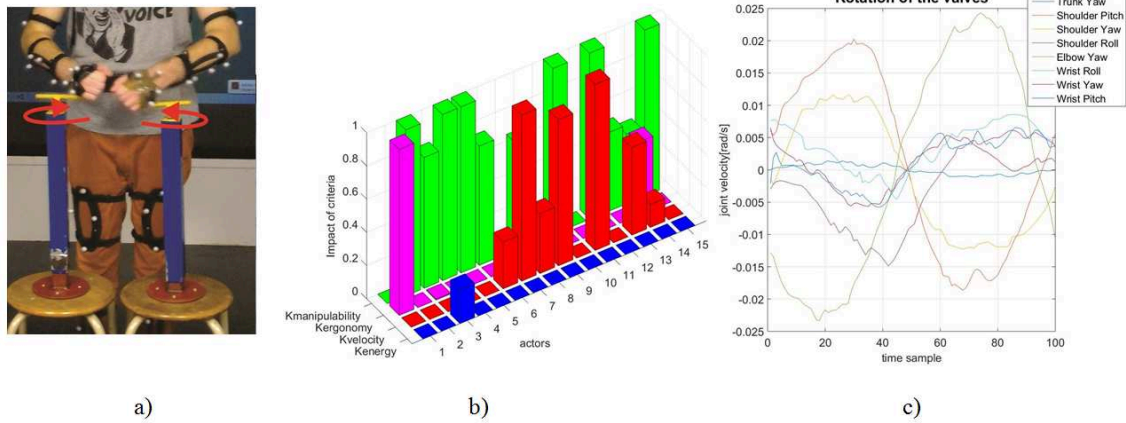


Figure 4.5: a) “Rotation of the valves” task b) Resulting weight factors defining the objective function - criterion maximization of manipulability prevail c) Joint motions - shoulder and elbow motions dominate.

mon characteristics could be observed for “Rotation of the valves” and “Opening/closing a drawer” tasks. The results obtained into the joint space (see Fig. 4.5(c)) show that during these motions the shoulder (Shoulder Pitch and Shoulder Yaw) and elbow joints move more than other joints. Those, it is also expected that minimization of joint velocity criterion is dominant for the “Rotation of the valves” motion.

Although one can intuitively expect that minimization of joint velocity dominates due to intensive joint movements, obtained results could be well justified and explained. The combination of the weight coefficients obtained by the genetic algorithm shows that for this motion the criterion maximization manipulability is dominant in the case of the 9 actors, the minimization of joint velocity criterion is dominant in the case of the 4 actors, and the minimization of distance between the current position and the ergonomic configuration in the case of 2 actors (see Fig. 4.5(b)). The criterion maximization of manipulability is dominant when the position between actor and equipment or actor current pose are not suitable for performing the motion in a common way. The actor is forced to take a certain pose in order to accomplish the task easier. In the example of “Rotation of the valves” motion several cases appear:

- the actor is tall and far from the equipment- the actor bends the trunk (increase amplitude of the Trunk Pitch joint) and perform the task moving shoulder and elbow joints
- the actor is small (or tall) and near the equipment- the actor keeps trunk vertically and moves shoulder and elbow joints more in order to perform the task

Since the actor is far or near equipment these body poses require additional movements to avoid singularities.

Human tendency to perform the task in the most comfortable manner is evident in the case of the 2 actors, for whom ergonomics criterion prevails. The comparison between average configuration of the actor through the motion and the comfortable configuration shows that in the case of the 2 actors these configurations are similar.

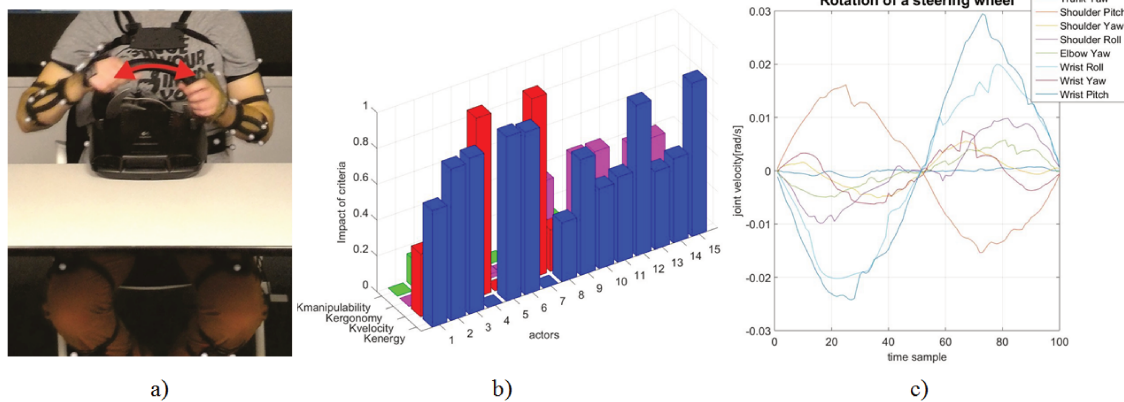


Figure 4.6: a) “Rotation of a steering wheel” task b) Resulting weight factors defining the objective function - criterion minimization of kinetic energy prevail c) Joint motions - shoulder and wrist motions dominate.

According to the results we can conclude that in the “Rotation of the valves” motion the position between actor and equipment, and actor characteristics have strong influence on criterion contribution. In a line with analysis of the motion in the joint space, it is evident that the minimization of joint velocity criterion describes this motion best if the actor is well posed with the respect to the equipment and he/she is of medium height. In the cases when these conditions are not satisfied the criteria minimization of distance between the current and ergonomic configuration and maximization of manipulability are dominant.

4.3.5 “Rotation of a steering wheel” and “Inflating a mattress using a pump”

The “Rotation of a steering wheel” task is an asymmetric dual-arm rotational motion (see Fig. 4.6(a)). The motion of the hands is circular in accordance with the form of a steering wheel. The rotation starts from the initial position where the arms are symmetrically placed on the wheel. The hands are able to rotate the steering wheel (diameter 0.3m) in both directions (in the experiments the motion was ± 90 degrees starting from the initial position). During the motion, the relative position between both hands is unchangeable. The “Inflating a mattress using a pump” task a symmetric dual-arm translation motion (see Fig. 4.7(a)). The hands grasp the equipment horizontally and their relative position does not change during the motion. In both motions, the actors are sitting while they carry out the tasks.

During the “Rotation of a steering wheel” task, the hands have a large motion in the Cartesian space and the task requires greater activation of shoulder and wrist joints compared to the motion of other joints (see Fig. 4.6(c)). The wrist joints (Wrist Pitch and Wrist Roll) are active during the motion because the actors should change the hand orientation with respect to the referent coordinate system in order to perform the motion. As for this motion, the actors use their hands only and sit comfortable while using the

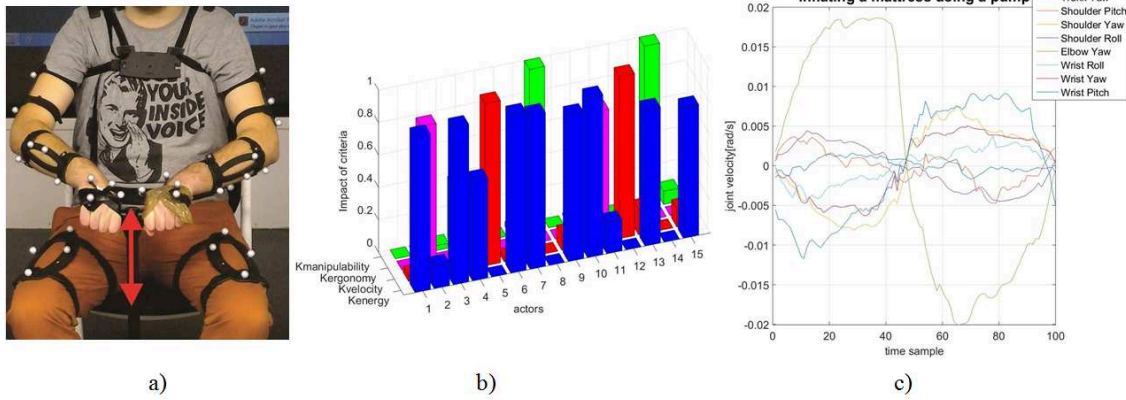


Figure 4.7: a) “Inflating a mattress using a pump” task b) Resulting weight factors defining the objective function - criterion minimization of kinetic energy prevail c) Joint motions - elbow and wrist motions dominate .

equipment. The trunk motion is limited.

The results show that the criterion of kinetic energy minimization is dominant for this type of the motion (see in the Fig. 4.6(b)). The influence of the inertia is evident in these results. The criterion of kinetic energy minimization is dominant in the case of the 8 actors since the motion of the joints with big effective inertia is greater compared with other joints. The motion of the wrist joint does not have big influence on choice of the criteria functions because its inertia is significantly smaller compared with the inertia of the other joints.

During the “Rotation of a steering wheel” motion, the actor’s body position is near the human ergonomic position. This is evident in results whereas in the case of 5 actors the criterion of kinetic energy minimization shares its domination with ergonomomy criterion (values of the weight coefficients are near 0.5). Two of the actors adapted the position of joints in order to decrease the motion of shoulders. In this case, the velocity minimization criterion is dominant, which is also supported by the results of our inverse optimal control algorithm.

The angle of rotation of a steering wheel is not limited and it happened that some actors made a bigger angle of rotation compared to others. This fact confirms that the choice of criterion function is related to the activation of joints during the motion.

In the case of “Inflating a mattress using a pump” task, elbows are the most active joints compared with other joints and the criterion of kinetic energy minimization is dominant in the case of 9 actors as confirmed by the results presented in Fig. 4.7(b). The pump produces great resistance during the motion of the handle and additional effort was needed to perform the task. Beside the elbow, 2 actors used shoulder more intensively to perform the task and the criterion of the velocity minimization is dominant in their cases. As well, the motions of some actors passed through the human ergonomic configuration and the criterion which minimizes of distance between the current and the ergonomic configuration is dominant in 2 cases. The criterion of manipulability appeared as dominant in the case of 2 actors when the actors kept the arm straight and carried out the task moving

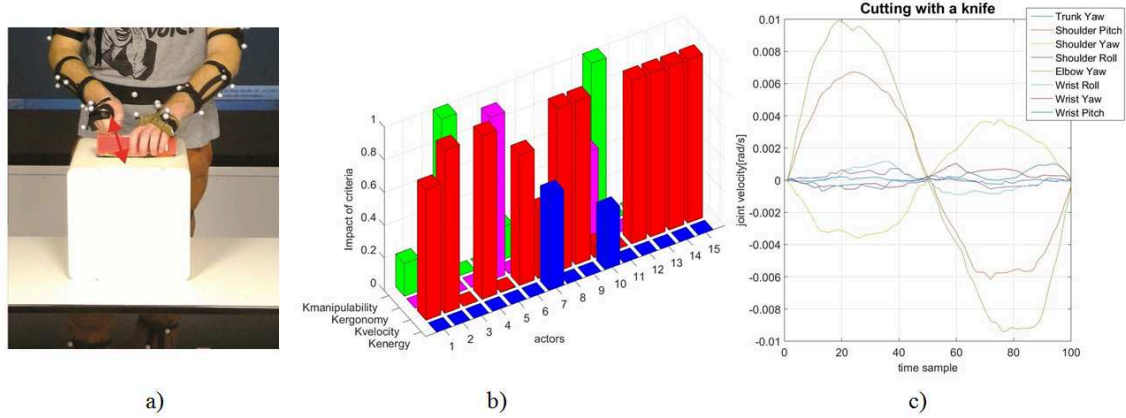


Figure 4.8: a) “Cutting with a knife” task b) Resulting weight factors defining the objective function - criterion minimization of joint velocity prevail c) Joint motions - shoulder and elbow motions dominate .

the trunk.

Conclusion is that “Rotation of a steering wheel” and “Inflating a mattress using a pump” point out minimization of kinetic energy as a dominant criterion because the motion of a particular joints, especially the shoulder joint (for “Rotation of a steering wheel”) and the elbow joints (for “Inflating a mattress using a pump”), which have big effective inertia move more than other joints.

4.3.6 “Cutting with a knife” and “Grating of food”

In this sections we analyzed “Cutting with a knife” and “Grating of food” together in order to compare same type of the motion. During the motion, the left hand is used as a hand support while the right hand performs the task.

The “Cutting with a knife” task is one-arm support translation motion (see Fig. 4.8(a)). The right hand does the translational motion in order to perform the task. The motion of the right hand is not strongly defined by the type of the equipment used. The right hand can rotate around the handle of the knife. The amplitudes of the right hand’s motion are limited by the size of the knife.

The “Grating of food” task is also one-arm support translation motion (see Fig. 4.9(a)). The orientation of the right hand is restricted and the palm should be in line with the plane surface of the grater. The trajectory of the right hand is related to the angle between the grater and the table surface, which is not predefined. Actors used grater in a way they considered the most comfortable. The right hand’s motion is limited by the size of the grater.

The “Cutting with a knife” task is performed by the activation of the shoulder (Shoulder Pitch and Shoulder Yaw) and the elbow joints during the motion. The criterion of velocity minimization gives the same priorities to motions of these joints. The weight coefficient $k_{velocity}$ takes values near 1 in the case of 10 actors.

The influence of the relative positions between actors and equipment and actor char-

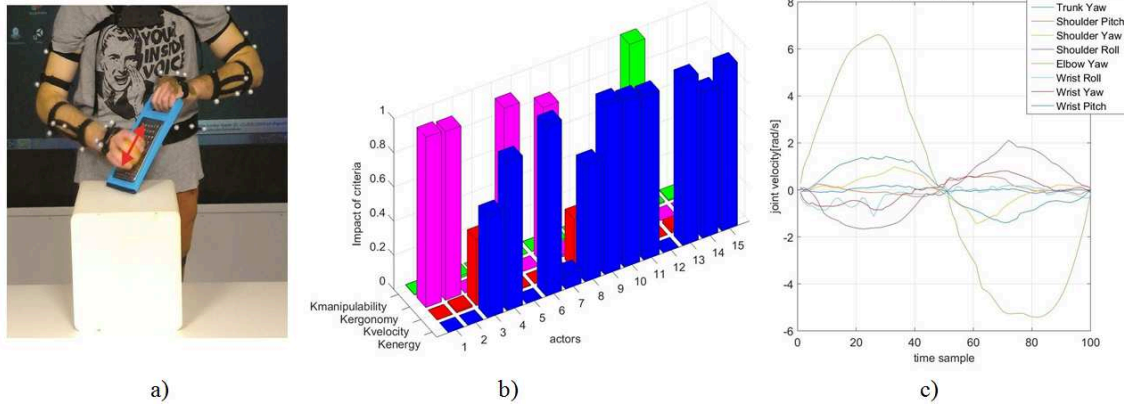


Figure 4.9: a) “Grating of food” task b) Resulting weight factors defining the objective function - criterion minimization of kinetic energy prevail c) Joint motions - elbow motions dominate .

acteristics are showed up in this motion. The criterion of maximization manipulability is dominant in 2 cases when the actor is small and near the equipment and in the case when the actor is tall and far from the equipment. Therefore, the same motion planning pattern from the “Rotation of the valves” tasks appeared in these motions. Since the actors were free to perform the task on the most comfortable way for them, in the cases of the 2 actors the ergonomy criterion is dominant. For these actors, further analysis showed that the average position of the actors’ right hands joints during the motion is near the human ergonomic configuration.

In the “Grating of food” task, the motion of the elbow joint is dominant compared to other joints, which is shown in Fig. 4.9(c). The criterion of kinetic energy minimization is dominant in this motion, which is supported by greater values of the weight coefficient k_{energy} in the case of 10 actors. This results is expected since the motion of the elbow joint is greater than the movements of others joints (such as the case of the “Inflating a mattress using a pump” task too). The other criteria are dominant in the particular cases (the criterion of maximization manipulability is dominant in 1 case while criterion of minimization of distance between the current and the ergonomic configuration is dominant in 4 cases). Since the “Grating of food” and “Cutting with a knife” tasks are the one arm support motions the same conclusion for these exceptions stands.

4.3.7 “Rotation of the canoe paddles”

The “Rotation of the canoe paddles” task represents a goal-coordinated rotational motion around one horizontal axis (see Fig. 4.10(a)). The relative position between the arms is constant and determined by the characteristics of the equipment. Palms of the hands are kept parallel to the room floor. According to the motion analysis for each joint, we can see that for this task the shoulder (Shoulder Pitch) and elbow joints have the biggest motion amplitude.

This motion requires motion of many joints to perform the rotational hand motion

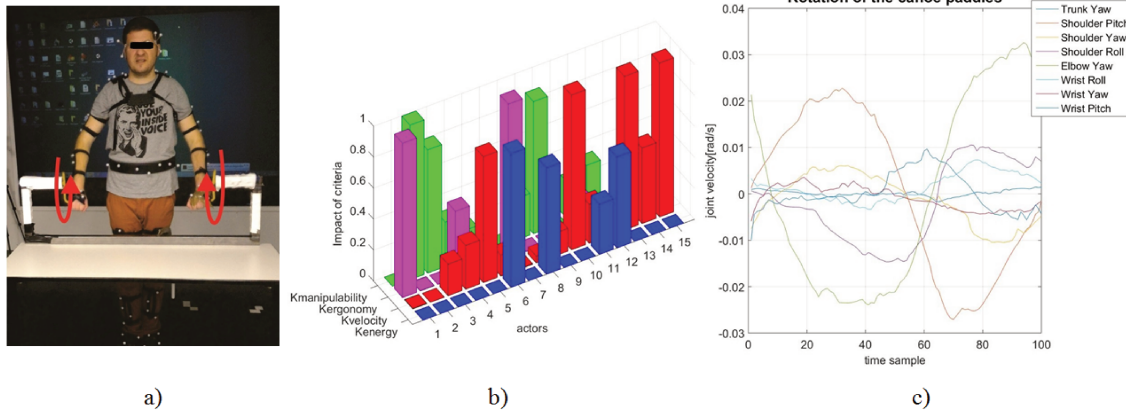


Figure 4.10: a) “Rotation of the canoe paddles” task b) Resulting weight factors defining the objective function - criterion minimization of joint velocity prevail although all other criteria is present depending of the actors characteristic c) Joint motions - shoulder and elbow motions dominate.

in the sagittal plane at the same distance independent of the actor in frontal plane. Consequently domination of different criteria depends a lot of actors body characteristics. Intensive joint motions lead to domination of velocity minimization criterion in the case of 5 actors. On the other hand, the other criteria also describe this motion. The criterion of maximization manipulability appeared as a dominate in the case of the 3 actors, the criterion of minimization of kinetic energy is dominant in the case of the 3 actors, the criterion the minimization of distance between the current and the ergonomic configuration is dominant in the case of 2 actor while the combination of all criteria is evident in the cases of the 2 actors. It is very difficult to conclude which of the criterion function represented this motion best but, the relative position between actor and equipment as well as the human characteristics definitively has significant influence to the criteria which will be selected.

4.3.8 Discussion

The results reveal that the amplitude of each particular joint and a combination of joint activations during the motion influences domination of the corresponding criterion function. In the case where the joints with big effective inertia are moved more compared to other joints, the human body needs more effort and energy to perform the motion. Thus minimization of kinetic energy criterion dominates and the value of the weight coefficient k_{energy} is the largest compared to the values of other weight coefficients. In the tasks where the motions of all joints are with small amplitudes, the human does not waste a lot of energy during the task and consequently minimization of velocity criterion is dominant while the weight coefficient $k_{velocity}$ has the biggest value.

The influence of inertia matrices is well presented in the task “Rotation of a steering wheel”. The motion is obtained by moving the shoulder and wrist joints and the minimization of velocity criterion could be expected to be dominant because the amplitude of

the motion of both joints for performing the task is similar. However, this is not the case because the effective inertia of the wrist joint is negligible compared to the inertia of the shoulder and the criterion of kinetic energy minimization is dominant. We can conclude that the choice of the criterion function and the motion strategy are highly related to the type of motion.

Moreover, the environmental characteristics, such as the size of the human body and the distance between the human and the environment also affect the choice of criteria. Accordingly, it is expected that the same motion in the task space, performed by several people, can show different characteristics in the joint space. The criterion of manipulability appears as dominant for each task where the positions of the hands are close to a singular position or when joint motions are near the joint limits. The actor should adapt his/her motion in order to perform the task. The criterion of maximization of manipulability is the most expressed in the task “Rotation of the valves”. The fact that human performs a task in the comfortable (ergonomic) manner is proven in the cases of the several motions. The ergonomy criterion (minimization of the distance between the current and the ergonomic configuration) dominates in majority of motions where average joint positions are near the human ergonomic configuration. The influence of this criterion is evident for the task “Rotation of a steering wheel” since the equipment size and position are defined to be comfortable for the human. To sum up, a human will use a specific strategy (combination of the criteria functions) to perform the same task in different environment provided that he/she is positioned well while performing the task. In some tasks, the choice of the criterion will be additionally defined by the characteristics of the actor.

The results obtained by the genetic algorithm show that the best imitation of the human motion (minimal value of the fitness function) is not obtained in the case when only the dominant criterion is included in the inverse kinematics algorithm but weighted combination of the criteria functions. The influence of each criterion separately and the combination of the criteria in the inverse kinematics algorithm without using the weight coefficients were earlier presented in our paper (Tomić, Chevallereau, et al., 2018). The best imitation is obtained with the combination of all criteria functions with different values of the weight coefficients. However, changes in the value of some weight coefficients, even those are not dominant, can greatly affect the quality of imitation and increase the value of the fitness function.

4.4 Human like dual-arm motion of the robot ROMEO

In the previous section we defined the optimization algorithm for characterization of human motion. The algorithm is based on the inverse optimal control approach and criteria functions, which are able to describe human-like motions. The obtained results from the inverse optimal control algorithm are included in the inverse kinematics algorithm given by the equation 4.23.

| Task/criteria functions | Rotation of the valves | Rotation of the canoe paddles | Rotation of a steering wheel | Inflating a mattress using a pump | Cutting with a knife | Grating of food | Opening /closing a drawer |
|-------------------------|------------------------|-------------------------------|------------------------------|-----------------------------------|----------------------|-----------------|---------------------------|
| k_{energy} | 0 | 0.2862 | 0.4448 | 0.7987 | 0 | 0.4384 | 0 |
| $k_{velocity}$ | 0.3916 | 0.2223 | 0.0683 | 0.1942 | 1 | 0.0942 | 0.9989 |
| $k_{ergonomy}$ | 0 | 0.2833 | 0.4869 | 0 | 0 | 0.4673 | 0.0007 |
| $k_{manipulability}$ | 0.6084 | 0.2082 | 0 | 0.0070 | 0 | 0.0001 | 0.0003 |

Table 4.2: The generalized combination of criteria functions calculated for each experiment.

The following paragraphs show that our inverses kinematics approach with the optimal combination of the criteria functions is able to generate the human-like motions for the real humanoid robot ROMEO. The experimental validation is presented in this section.

The kinematic structure of robot hands is similar to a human and allows the robot to faithfully imitate all human motions. Furthermore, the distribution of segments masses of the robot ROMEO coincides with the human and it can be expected that the criteria functions which describe the motions of human arms will be the same for the motion of the robot. An additional condition that occurs is that the motion of the robot must be defined according to the characteristics of the robot (the length of segments and restrictions in the joints). In order to obtain human-like dual-arm manipulation task performed by the robot, the original motion of human hands should still be evident in the robot motion, although it has been modified according to the characteristics of the robot.

The knowledge on the weights of each criterion for the task will help us to define the generalized combination of criteria functions for each motion, which will eliminate the exceptions based on the position between the actor and the equipment and the characteristics of the actor. We additionally defined the genetic algorithm which calculates the combination of weight coefficients and minimizes the sum of the fitness function of all actors while performing the same task. The results are presented in Table 4.2.

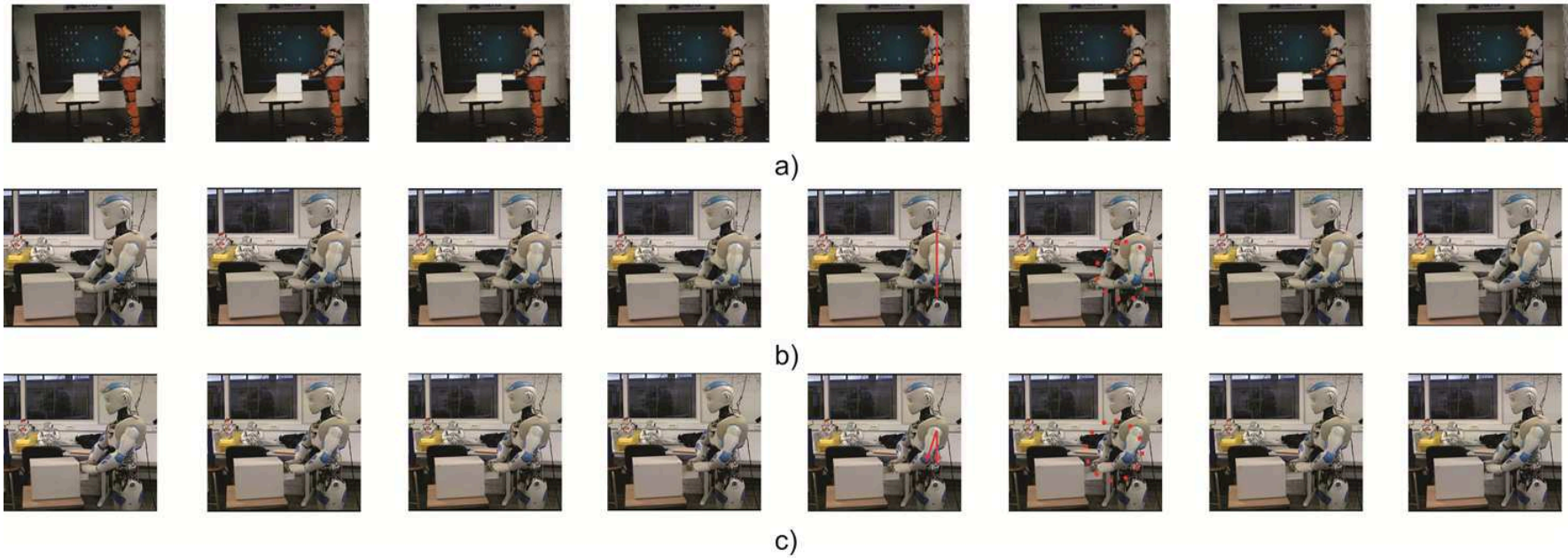


Figure 4.11: “Opening/closing a drawer” task performed by the actor and the robot ROMEO. The motion of the robot obtained for the generalized combination of the weight coefficients (b) tends to be more similar to the actor motion (a), compared to the motion of the robot obtained with the criterion minimization of the kinetic energy (c).

Inverse kinematics algorithm proposed by equation 4.23 with a calculated combination of the weight coefficients will produce the human-like motion of the robot ROMEO. Fig. 4.11 shows the snapshots of the motion in “Opening/closing a drawer” task performed by the actor and the robot ROMEO. The motion of the robot shown in the Fig. 4.11(b) is obtained by our inverse kinematics algorithm with the generalized combination of the weight coefficients (presented in Table 4.2) while the motion of the robot shown in the Fig. 4.11(c) is obtained for the combination of the weight coefficients $k_{energy} = 1, k_{velocity} = k_{manipulability} = k_{ergonomiy} = 0$. The joint limits are included in the inverse kinematics algorithm using the approach explained in detail in Baerlocher and Boulic (2004). The motion of the robot hands is free of the collision with the equipment. The self-collision is avoided since the robot imitates the recorded human motion which is out of the self-collision. Images show that the motion of the robot obtained for the generalized combination of the weight coefficient tends to be more similar to the actor motion, compared to the motion of the robot obtained with the criterion minimization of the kinetic energy.

The robot motion generated with the generalized combination of the weight coefficient produced motions in shoulder and elbow joints, as can be seen in the Fig. 4.11(b). The obtained motion of the robot is similar to the actor motion (see Fig. 4.11(a)) and fully resembles the human motion. On the other side, the robot motion obtained by minimization of the kinetic energy is characterized by a large movement of the elbow joints while the motion of shoulders is insignificant. The robot performs the task by moving the elbows to the side, away from the trunk. Moreover, we can see that upper arm in scenario (b) is aligned with vertical axis as it is case with the actor’s motion while in scenario (c) it is not the case. Therefore, the obtained motion in (c) is not like the actor’s motion. These results are confirmed by the similarity measure. The similarity measure between the recorded actor’s motion (expressed as the motion of the scaled model of the robot ROMEO using imitation process $\dot{q}_{imitation}$) and the obtained motion of the robot ROMEO using the inverse kinematics algorithm and weight coefficients \dot{q}_{ROBOT}) is calculated as a sum squared error over all joints velocities.

$$S = \sum_{n=1}^N (\dot{q}_{imitation}(t_n) - \dot{q}_{ROBOT}(t_n))^2 \quad (4.25)$$

The similarity measure of the robot’s motion obtained for the generalized combination of the weight coefficient is 0.0269 while the similarity measure for the robot motion obtained by minimization of kinetic energy criterion is 0.0762. The conclusion is that inverse kinematics algorithm given by 4.23 with the combination of the weight coefficients, obtained from our inverse optimal control algorithm, can generate the same human-like motion with a humanoid robot with the kinematic structure close to or resembling that of the human body.

4.5 Conclusion

The present study presents the inverse optimal control algorithm as the optimization tool for the analysis of the characteristics of the basic dual arm human motion using the combination of the basic criteria functions. The study is performed on the set of seven basic human motions performed by 15 actors. The obtained results provide general conclusions on human motion, as follows:

- The characteristics of dual-arm motions performed by a healthy human are directly connected with the activation of the particular arm joints and a combination of joint activations since these humans try to do motions in the way they consider most comfortable (optimal).
- The criterion of kinetic energy minimization is a dominant criterion for the tasks that require greater mobility of the shoulder, elbow or trunk joints (the joints with bigger values of the inertial matrix) but not wrist joint.
- Tasks that are not characterized by a large motion of the joints or evenly activation of the joints have a dominant criterion of minimization of velocity.
- In tasks where the human performs motion near the singular configuration or near his joint limits, the criterion of manipulability minimization is dominant.
- In each of the analyzed motions which pass near human ergonomic configuration the criterion minimization of the distance between the current and the ergonomic configuration is dominant since humans will perform the motion on the most comfortable way if it is according to the characteristics of the task.
- The optimal function (using weights of basic criterion function) exists. Changes in the value of some weight coefficients even those which are not dominant, significantly affect the quality of the imitation and increase the value of fitness function.
- The strategy of performing the same motion by different actors is the same, but may change due to the influence of the environment and human body characteristics.
- Our inverse kinematics algorithm with the optimal combination of criteria functions, (calculated by the inverse optimal control algorithm for each motion separately) is able to generate the same motion with a redundant humanoid robot with the kinematic characteristics close to or resembling those of humans.

The results of the research can be applied to several areas. The characteristics of the basic motion of healthy people acquired in this work can be used for the analysis of human motion with the disability in motor skills. Furthermore, our inverse kinematics algorithm can be used for generation of a complex motion, which represents a set of the analyzed basic motions, changing the combination of the weight coefficients from one basic motion to another. Implementation of the explored characteristics of human motion on the humanoid robot will enable the most natural cooperation between humanoids and humans, help the elderly persons in their everyday life, and allow better integration of humanoid robots into the human environment.

Our future research should be directed towards enlarging the set of the analyzed basic human motions and inclusion of basic criterion functions which consider dynamics. The soft computing methods, such as fuzzy logic, will be implemented to calculate the characteristics of new human motion (the weights), which will be used in the inverse kinematic model to generate human-like humanoid motion.

Fuzzy logic algorithms for the analysis of human motion behaviors

The aim of the research in this chapter is to link the presented conclusions about the characteristics of human motion behavior and define the method for their analysis using the artificial intelligence algorithms. Considering that in the previous research we analyzed the characteristics of the basic dual-arm manipulation motions, in this chapter we will define the fuzzy logic algorithm based on acquired knowledge. The obtained conclusions from the movement analysis in the previous chapter will be used as expert knowledge to define the fuzzy rules. Our fuzzy logic algorithm should represent a tool for defining the characteristic of human movements (i.e. a combination of criterion functions) for movements that have not been previously analyzed. Therefore, in this chapter we will present the general characteristics of the fuzzy logic and the fuzzy system and its implementation for the analysis of human movements. Evaluation of the resulting fuzzy system will be performed on different manipulation movement that has not been analyzed previously.

5.1 Fuzzy logic and fuzzy logic system

The Fuzzy sets and fuzzy logic were developed as a means for representing, manipulating, and utilizing uncertain information and to provide a framework for handling uncertainties and imprecision in real-world applications. Fuzzy logic (FL) is based on the way the brain deals with inexact information. Fuzzy system is structured numerical estimators which is suitable for solving many problems and achieving some degree of machine intelligence.

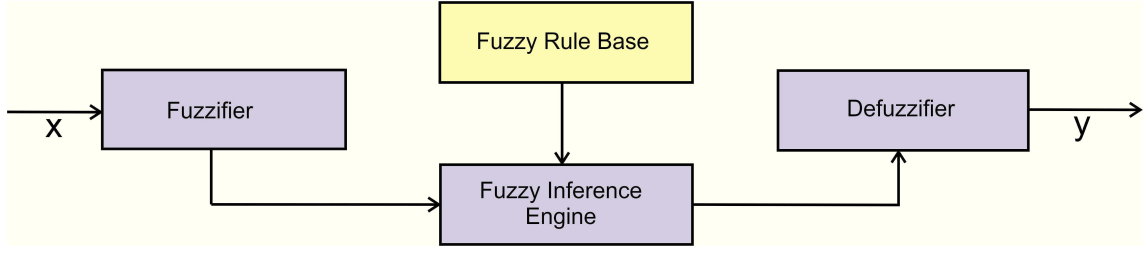


Figure 5.1: Basic configuration of fuzzy logic system.

A classical (crisp) set is a collection of distinct objects. It is defined in such a way as to dichotomize the elements of a given universe into two groups: members and nonmembers. A fuzzy set, on the other hand, introduces vagueness by eliminating the sharp boundary that divides members from nonmembers in the group. Thus, the transition between full membership and non membership is gradual rather than abrupt. A fuzzy set A in the universe of discourse U can be defined as a set of ordered pairs:

$$A = \{(x, \mu_A(x)) | x \in U\} \quad (5.1)$$

where $\mu_A(x)$ is the grade of membership of x in A . In a one universe, a different number of phases sets with its grade of membership function can be defined. The membership functions may be linear, triangular or trapezoidal, or may have Gaussian or sinusoidal forms.

The typical architecture of a fuzzy logic decision system is shown in Fig. 5.1, which is comprised of four principal components: a fuzzifier, a fuzzy rule base, an inference engine (decision-making logic), and a defuzzifier. The fuzzifier has the effect of transforming measured data into suitable linguistic values using fuzzication approach. The fuzzification approach is widely applicable because it greatly simplifies the creation of the fuzzy rules. The fuzzy rule base stores the empirical knowledge of the operation of the process of the domain experts. The inference engine is the kernel of a fuzzy logic decision system, and it has the capability of simulating human decision making by performing approximate reasoning to achieve a desired control strategy. The defuzzifier is utilized to yield a nonfuzzy decision or control action from an inferred fuzzy control action by the inference engine.

Example:

Let define input x and output variables of the fuzzy systems as:

$$\begin{aligned} x &= \{(x_i, U_i, \{A_{x_i}^1, A_{x_i}^2, \dots, A_{x_i}^{k_i}\}, \{\mu_{x_i}^1, \mu_{x_i}^2, \dots, \mu_{x_i}^{k_i}\}) | i=1,2,\dots,n\} \\ z &= \{(z_i, V_i, \{B_{z_i}^1, B_{z_i}^2, \dots, B_{z_i}^{k_i}\}, \{\mu_{z_i}^1, \mu_{z_i}^2, \dots, \mu_{z_i}^{k_i}\}) | i=1,2,\dots,n\} \end{aligned} \quad (5.2)$$

where $U = U_1 \times U_2 \times \dots \times U_n$ and $V = V_1 \times V_2 \times \dots \times V_n$ represents fuzzy input and output spaces, $A(x_i) = \{A_{x_i}^1, A_{x_i}^2, \dots, A_{x_i}^{k_i}\}$ and $B(z_i) = \{B_{z_i}^1, B_{z_i}^2, \dots, B_{z_i}^{k_i}\}$ are the term sets (set of names of linguistic variables of x_i and z_i) with membership function $\mu_{x_i}^{k_i}$ and $\mu_{z_i}^{k_i}$, respectively. The membership function as well as term sets of the fuzzy system are chosen

base of our subjective impressions of the process.

In the first step, a fuzzifier performs the function of fuzzification where the set of input variables are mapped into the fuzzy sets. The specific value x_i is mapped to the fuzzy set $A_{x_i}^1$ with the membership function $\mu_{x_i}^1$ and to the fuzzy set $A_{x_i}^2$ with the membership function $\mu_{x_i}^2$, and so on.

With the completion of the fuzzification of the input parameters, the fuzzy rules can be defined. For second step, it is necessary to collect all the expert knowledge about the system in order to make a more efficient system of reasoning. The fuzzy rules are defined by the *IF-THEN* relations that delineate the relations between input and output variables. In generally, fuzzy system is a system with multiple inputs and multiple or one outputs. In this example we will present a typical layout for the fuzzy rules of the system with multiple inputs and one output. The one fuzzy rule is defined as:

$$R_i : \text{if } x_1 \text{ is } A_{x_1}^i \text{ and } x_2 \text{ is } A_{x_2}^i \text{ then } z \text{ is } B^i, \quad i = 1, 2, \dots, n$$

where x and z are linguistic variables which represents the input and output state variables, respectively, and $A_{x_j}^i$ and B^i are their linguistic values in the universes U and V , respectively. The linguistic term are characterized by fuzzy membership functions $\mu_{A_{x_1}^i}(x_1)$ and $\mu_{B^i}(z)$, respectively. Each R_i can be viewed as a fuzzy implication $A_{x_1}^i \times A_{x_2}^i \dots \times A_{x_n}^i \rightarrow B^i$ with $\mu_{A_{x_1}^i \times A_{x_2}^i \dots \times A_{x_n}^i \rightarrow B^i}(x, z) = \mu_{A_{x_1}^i}(x_1) * \mu_{A_{x_2}^i}(x_2) * \dots * \mu_{A_{x_n}^i}(x_n) * \mu_{B^i}(z)$. The most used operator for “*” is called Mamdani operator which is represents as $\mu_{A_{x_1}^i \times A_{x_2}^i \dots \times A_{x_n}^i \rightarrow B^i}(x, z) = \mu_{A_{x_1}^i}(x_1) \wedge \mu_{A_{x_2}^i}(x_2) \wedge \dots \wedge \mu_{A_{x_n}^i}(x_n) \wedge \mu_{B^i}(z)$, where \wedge denotes a conjunction of intersection operator.

The fuzzy inference engine employs fuzzy rules from the fuzzy rule base, to determine a mapping from the fuzzy sets in the input space U to the fuzzy sets in the output space V . Let A_x be an arbitrary fuzzy set in U , and then each rule R_i determines a fuzzy set $A_x \circ R_i$ in V based on the sup-star composition (C.-C. Lee, 1990):

$$\begin{aligned} \mu_{A_x \circ R_i}(z) &= \sup_{x \in U} \left[\mu_{A_x}(x) * \mu_{A_{x_1}^i \times A_{x_2}^i \dots \times A_{x_n}^i \rightarrow B^i}(x, z) \right] = \\ & \sup_{x \in U} \left[\mu_{A_x}(x) * \mu_{A_{x_1}^i}(x_1) * \mu_{A_{x_2}^i}(x_2) * \dots * \mu_{A_{x_n}^i}(x_n) * \mu_{B^i}(z) \right] \end{aligned} \quad (5.3)$$

The defuzzifier performs a mapping from the fuzzy sets $A_x \circ R_i$ in V to a crisp point in $z \in V$. This mapping may be chosen as weighted average centroid defuzzifier (Wang & Mendel, 1992):

$$z = \frac{\sum_{i=1}^N \omega_i \mu_{A_x \circ R_i}(\omega_i)}{\sum_{i=1}^N \mu_{A_x \circ R_i}(\omega_i)} \quad (5.4)$$

where ω_i is the point in V at which $\mu_{B^i}(z)$ achieves its maximum value (usually we assume that $\mu_{B^i}(\omega_i) = 1$).

5.2 Fuzzy system as the tool for modeling human motion strategy

Designing of each fuzzy system goes through several basic steps:

1. Defining the input and output variables
2. Selecting the fuzzy sets over the input and output universes, as well as selecting the membership functions these sets
3. Specifies the type of fuzzy rules
4. Specifies the method of the combination the fuzzy rules
5. Choosing defuzzification mode

Fulfilling the first two steps largely depend on the type of process, the universe of variables, and its exploitation in the process. The choice of fuzzy sets over the universe should be a compromise between the possibility of a detailed analysis of the variables and the computational complexity.

Fuzzy system gives the possibility of choosing a different membership functions. Depending on the type of process, the different membership functions can affect the quality differently on the decision-making. The choice of a criterion is quite subjective. Therefore, at the very beginning, it is recommended to define a set of 3 simplest fuzzy sets that encompass the whole universe. In order to get a more detailed and better analysis of the given process, the form of membership functions can be modified, and new membership functions can be added (Klir & Yuan, 1995).

The linguistic statements of the fuzzy rules are the heart of the fuzzy system and should give the essential characteristics of the analyzed process. The fuzzy rules usually come from two sources: human experts and training data.

In the next subsection we define the fuzzy system for analysis human motion strategy following the previous definition of the fuzzy systems and the method of it design.

5.2.1 Human motion parameters as a fuzzy inputs and output variables

In this subsection we used the fuzzy logic system to analyze the characteristics of the human movement of dual-arm manipulation inspired by the idea to present the process of human deduction using the artificial intelligence algorithms based on human reasoning. The deciding process of the weight coefficients values, presented in the previous chapter, was transmitted in the fuzzy logic system, emulating the thinking and perceptions of the human brain. Based on a detailed analysis of the movement presented in [chapter 4](#) and [chapter 2](#), the domination of a criterion function has been determined by the activity of the joints, the characteristic of the human body and the position of the human relative to the equipment. Therefore, input parameters are chosen so that maximize decision-making

influence, reduce the complexity of the system, and facilitate the decision-making process and definition of the membership functions. If we take the assumption that during the motion actors are well posed with respect to the equipment and they perform motions on the most comfortable way for them, we will be able to analyze pure motions without taking into account position of the human relative to the equipment. At this stage of our research, we decided to simplify our analysis and took into account the cases where criteria minimization of the kinetic energy (energy criterion), minimization of joint velocities (velocity criterion), and minimization distance between current and the ergonomic configuration (ergonomics criterion) are dominant. We wanted to avoid cases in which the actors modified their motions due to the additional influence of an environment that is not related to the limitations defined by the movement itself. According to the analysis presented in [chapter 4](#), the next variables represent the set of the fuzzy input parameters:

- average value of the shoulder, elbow, and trunk joints velocity ($vShoulderPitch$, $vShoulderYaw$, $vShoulderRoll$, $vElbowYaw$, and $vTrunkPitch$) are defined as input variables which are used to describe the energy and velocity criteria.
- average distance between the human ergonomic and current configuration of the arm joints ($ergonomicsShoulderPitch$, $ergonomicsShoulderYaw$ and $ergonomicsElbowYaw$) joints in Cartesian space are defined as a input variable which are used to describe the ergonomics criterion.

The average value of the fuzzy inputs are normalized in the range from 0 to 1 in order to make the easier comparison of the input variable values. Average joint velocities are normalized according to the values of the joint velocities, where the values 0 or 1 correspond to the joints which average velocity is minimal or maximal, respectively, with respect to the rest of the actor joints. The difference between current and ergonomic Cartesian position of the shoulder pitch, shoulder yaw and elbow yaw joints are normed in the range from 0 to 1. The value 0 corresponds to the joint position which is same as ergonomic configuration while value 1 corresponds to the joint position far from the ergonomic configuration.

According to the results obtained with inverse optimal control algorithm, the values of the weighted coefficients are usually near 0 or 1 and the fuzzy output variables are mostly defined by linguistic values *ExtraSmall* or *ExtraBig* (see [Fig. 5.3](#)).

Our fuzzy system for human motion analysis has 4 output variables which correspond to the one weight coefficient: $Kenergy$, $Kvelocity$, $Kergonomics$. Each output variable is in the range from 0 to 1. The output variables of the fuzzy system are defined in the relative form. The sum of these four coefficients is equal 1 how is defined in [chapter 4](#). As a reference set of output variables for defining the fuzzy system we used the results obtained by inverse optimal control algorithm (referred to [chapter 4](#)).

Fuzzy inputs and outputs are represented as a combination of linguistic values: extra small, small, medium, big and extra big. Linguistic variables of the fuzzy inputs $vShoulderPitch$, $vShoulderYaw$, $vShoulderRoll$, $vElbowYaw$, and $vTrunkPitch$ have Gaussian

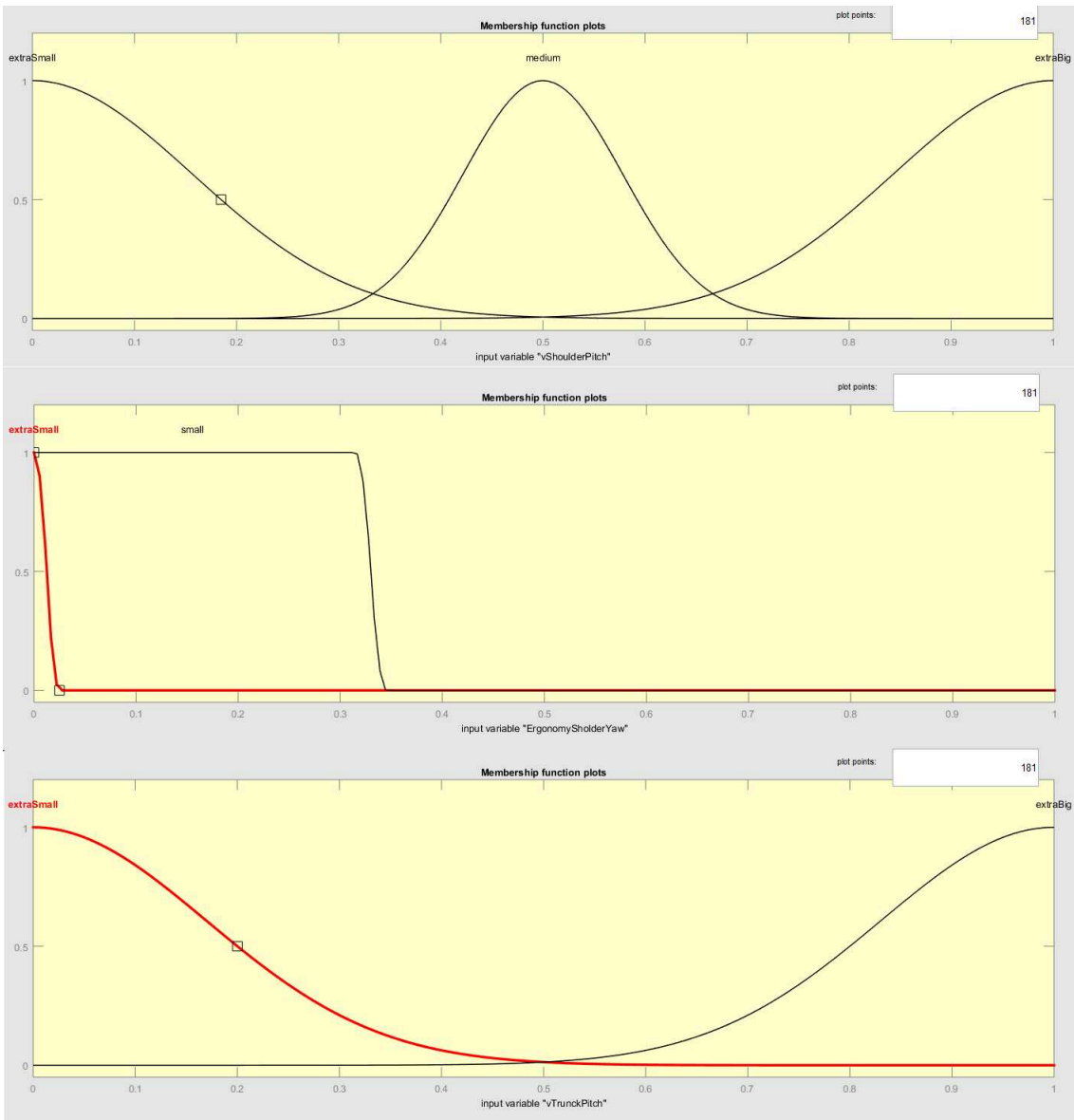


Figure 5.2: The linguistic variables and membership functions of the fuzzy input: a) *vShoulderPitch*; b) *ergonomyShoulderYaw*; and c) *vTrunckPitch*.

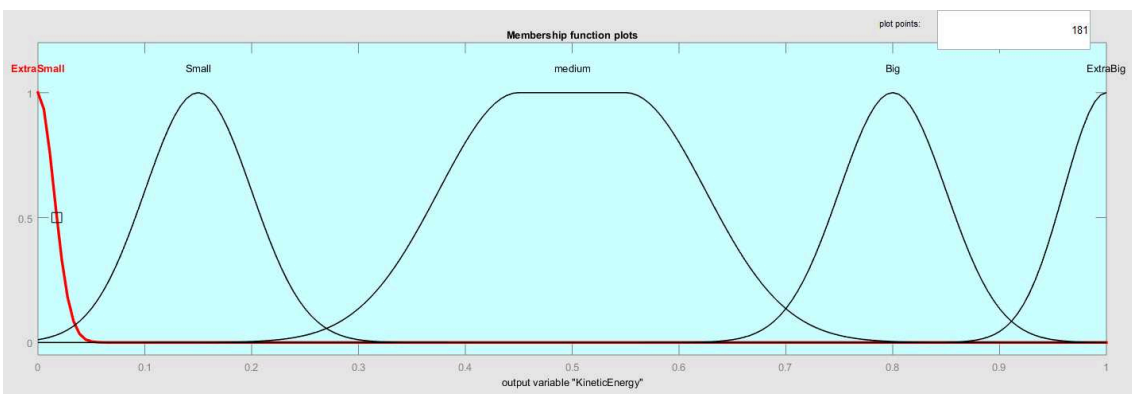


Figure 5.3: The linguistic variables and membership functions of the fuzzy output *Ken-ergy*.

shape of the membership function, while linguistic variables of the fuzzy inputs *ergonomyShoulderPitch*, *ergonomyShoulderYaw* and *ergonomyElbowYaw* have Z-shaped membership function. The parameters of Gaussian and Z-shaped membership functions depend of the linguistic variables and the type of the fuzzy input which represent. During the initialization process of the fuzzy algorithm, the membership function parameters are tuned by hands, while for final calculation of these parameters *fmincon* optimization function is used. The way on which the fuzzy universes and linguistic variables are defined are directly connected with the expert experience about the process:

- The universes of fuzzy inputs *vShoulderPitch*, *vShoulderYaw*, *vShoulderRoll*, and *vElbowYaw* are defined with linguistic values: *ExtraSmall*, *Medium*, *ExtraBig*.
- The universe of fuzzy input *vTrunckPitch* is defined with linguistic variables: *ExtraSmall* and *ExtraBig*.
- The universes of fuzzy inputs *ergonomyShoulderPitch*, *ergonomyShoulderYaw*, *ergonomyElbowYaw* are defined with linguistic variables: *ExtraSmall* and *Small*.
- The universe of each fuzzy output *Kenergy*, *Kvelocity*, *Kmanipulability*, *Kergonomy* consists of 5 linguistic variables: *ExtraSmall*, *Small*, *Medium*, *Big*, *ExtraBig*.

Linguistic variables and their membership functions for some fuzzy inputs and outputs are shown in Figs. 5.2 and 5.3.

5.2.2 Human motion strategy presented through the fuzzy rules

Our fuzzy system represents a system with multiple inputs and multiple outputs. According to knowledge obtained through analyzes of the human motion behavior (we can say that is expert knowledge) we are able to represent it in the form of the fuzzy rules. In fact, the relation that exists between activation of the joints and characteristics of actors and equipment, from the one side, and the domination of the criterion function, from the other side, allowed us to write *IF-THEN* relations.

The fuzzy rules which describe the energy or velocity criterion as dominant include the joint velocities as fuzzy inputs. Fuzzy inputs (*vShoulderPitch* and *vShoulderYaw* and *vShoulderRoll*) or *vElbowYaw* which have big membership value of the linguistic variables *Big* or *ExtraBig* define fuzzy output K_{energy} (big membership value of the linguistic variables *Big* or *ExtraBig*). The *IF-THEN* fuzzy rules which describe the criterion minimization of kinetic energy are presented in Table 5.1.

The fuzzy rules which describe the velocity criterion include arm joints with big value of the inertia as the fuzzy inputs. Therefore, in the cases where fuzzy inputs (*vShoulderPitch* or *vShoulderYaw* or *vShoulderRoll*), and *vElbowYaw* have big membership value of linguistic variables *Big* or *ExtraBig*, the fuzzy output $K_{velocity}$ has big membership value of the linguistic variables big or extra big. The *IF-THEN* fuzzy rules which describe the criterion minimization of velocity as dominant are present in Table 5.2.

Table 5.1: Fuzzy rules which describe the energy criterion as dominant

| | <i>vShoulderPitch</i> | | <i>vShoulderYaw</i> | | <i>vElbowYaw</i> | | <i>vTrunkPitch</i> | | <i>vShoulderRoll</i> | | <i>Kenergy</i> | | <i>Kvelocity</i> | | <i>Kergonomy</i> |
|--------------|-----------------------|------------|---------------------|------------|------------------|------------|--------------------|------------|----------------------|-------------|----------------|------------|------------------|------------|------------------|
| 1.If | ExtraSmall | and | ExtraSmall | and | ExtraBig | and | - | and | - | Then | ExtraBig | and | ExtraSmall | and | ExtraSmall |
| 2.If | ExtraSmall | and | - | and | ExtraSmall | and | - | and | - | Then | ExtraBig | and | ExtraSmall | and | ExtraSmall |
| 3.If | ExtraBig | and | - | and | ExtraSmall | and | - | and | - | Then | ExtraBig | and | ExtraSmall | and | ExtraSmall |
| 4.If | ExtraBig | and | ExtraSmall | and | ExtraSmall | and | - | and | - | Then | ExtraBig | and | ExtraSmall | and | ExtraSmall |
| 5.If | ExtraBig | and | Medium | and | ExtraSmall | and | - | and | - | Then | ExtraBig | and | ExtraSmall | and | ExtraSmall |
| 6.If | Medium | and | ExtraSmall | and | ExtraBig | and | - | and | - | Then | ExtraBig | and | ExtraSmall | and | ExtraSmall |
| 7.If | Medium | and | ExtraBig | and | Medium | and | - | and | - | Then | ExtraBig | and | Small | and | ExtraSmall |
| 8.If | ExtraSmall | and | - | and | ExtraBig | and | - | and | - | Then | ExtraBig | and | ExtraSmall | and | ExtraSmall |
| 9.If | Medium | and | Medium | and | ExtraBig | and | - | and | Medium | Then | ExtraBig | and | ExtraSmall | and | ExtraSmall |
| 10.If | - | and | - | and | - | and | ExtraBig | and | - | Then | ExtraBig | and | ExtraSmall | and | ExtraSmall |

Table 5.2: Fuzzy rules which define the velocity criterion as dominant

| | <i>vShoulderPitch</i> | | <i>vShoulderYaw</i> | | <i>vElbowYaw</i> | | <i>Kenergy</i> | | <i>Kvelocity</i> | | <i>Kergonomy</i> |
|--------------|-----------------------|------------|---------------------|------------|------------------|-------------|----------------|------------|------------------|------------|------------------|
| 11.If | - | and | ExtraBig | and | ExtraBig | Then | ExtraSmall | and | ExtraBig | and | ExtraSmall |
| 12.If | ExtraBig | and | - | and | ExtraBig | Then | ExtraSmall | and | ExtraBig | and | ExtraSmall |
| 13.If | ExtraBig | and | ExtraBig | and | ExtraBig | Then | ExtraSmall | and | ExtraBig | and | ExtraSmall |
| 14.If | Medium | and | Medium | and | ExtraBig | Then | ExtraSmall | and | ExtraBig | and | ExtraSmall |

Table 5.3: Fuzzy rules which define the ergonomy as dominant

| | <i>ErgonomyShPitch</i> | | <i>ErgonomyShoulderYaw</i> | | <i>ErgonomyElbowYaw</i> | | <i>Kenergy</i> | | <i>Kvelocity</i> | | <i>Kergonomy</i> |
|--------------|------------------------|------------|----------------------------|------------|-------------------------|-------------|----------------|------------|------------------|------------|------------------|
| 15.If | Small | and | Small | and | Small | Then | ExtraSmall | and | ExtraSmall | and | ExtraBig |
| 16.If | ExtraSmall | and | ExtraSmall | and | ExtraSmall | Then | ExtraSmall | and | ExtraSmall | and | ExtraBig |

Table 5.4: Fuzzy rule which provides equal domination of energy and ergonomy criteria

| | <i>vShoulderPitch</i> | | <i>vShoulderYaw</i> | | <i>vElbowYaw</i> | | <i>ErgonomyElbowYaw</i> | | <i>Kenergy</i> | | <i>Kvelocity</i> | | <i>Kergonomy</i> |
|--------------|-----------------------|------------|---------------------|------------|------------------|------------|-------------------------|-------------|----------------|------------|------------------|------------|------------------|
| 17.If | ExtraSmall | and | ExtraSmall | and | ExtraBig | and | ExtraSmall | Then | ExtraBig | and | ExtraSmall | and | ExtraBig |

The fuzzy rules which describe ergonomy criterion as dominant is based on analysis the difference between current and ergonomic position of the shoulder and elbow joints.

These fuzzy inputs of our fuzzy rules are *ergonomyShoulderPitch*, *ergonomyShoulderYaw*, *ergonomyElbowYaw*. The analysis presented in [chapter 4](#) shows that the value of these fuzzy inputs are close to 0. Therefore, these fuzzy inputs are described with linguistic variables (*ExtraSmall* and *Small*) in order to increase precision of making decision with our fuzzy system. In the fuzzy rules which define the ergonomy criterion as dominant, the fuzzy output $K_{ergonomy}$ is describe with linguistic variables big and extra big. The IF-THEN fuzzy rules which describe the ergonomy criterion as dominant are present in [Table 5.3](#).

Since in some cases the domination of criteria was not strictly defined and more criteria could take the *ExtraBig* values like in the case of rule shown in [Table 5.4](#).

The all described fuzzy rules are combined using the Mamdani operator. The combination of the several fuzzy rules can obtain the fuzzy output which is not in correlation with our human motion behavior analysis. Consequently, additional relationships should be defined. During our analysis of the human motion behavior we concluded that the human perform the motion on the way suitable for them if they are well posed with respect to the equipment. On the other hands, the human modify their motion and the criterion of maximization manipulability will be dominant. According to this, we defined the hierarchy in combining fuzzy rules. The fuzzy rules which defined the ergonomy criterion have priority 0.7 while the fuzzy rules which describe energy and velocity criteria have the same priority 0.1 because they represent relations between activation of the joints in the task.

5.3 Optimization algorithm vs. fuzzy algorithm

The quality of the results obtained by the fuzzy algorithm on the test set is quantified in this subsection. The fuzzy rules are made on the way to take into account the characteristics of the human motion in the joint space according to recorded and analyzed actors' motions during the all tasks. The general characteristics of each motion are included in the fuzzy rules. Therefore, it is expected that the results obtained by fuzzy algorithm deviate from results obtained by optimization in exceptional cases which is analyzed in [chapter 4](#). The results obtained by fuzzy logic system are presented for each tasks separately.

5.3.1 “Grating of food” task

The analysis of this task proposed that the energy criterion is dominant in the most of cases. The analysis in the joint space shows that actors usually used elbow joints in order to perform the task. Accordingly, the $vElbowYaw$ has the big value and is defined with the linguistic variable *Big*.

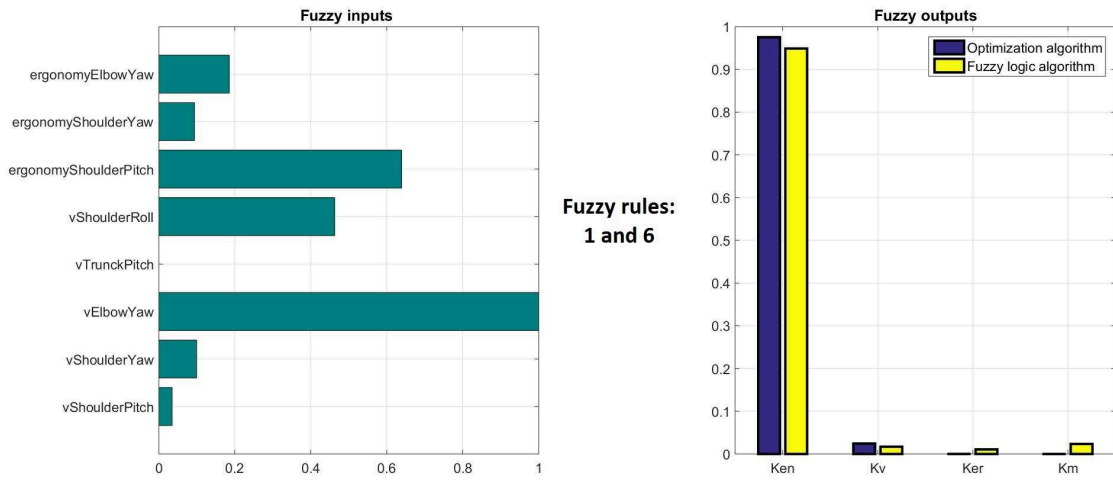


Figure 5.4: "Grating of food" task: Fuzzy inputs, fuzzy rule and fuzzy outputs.

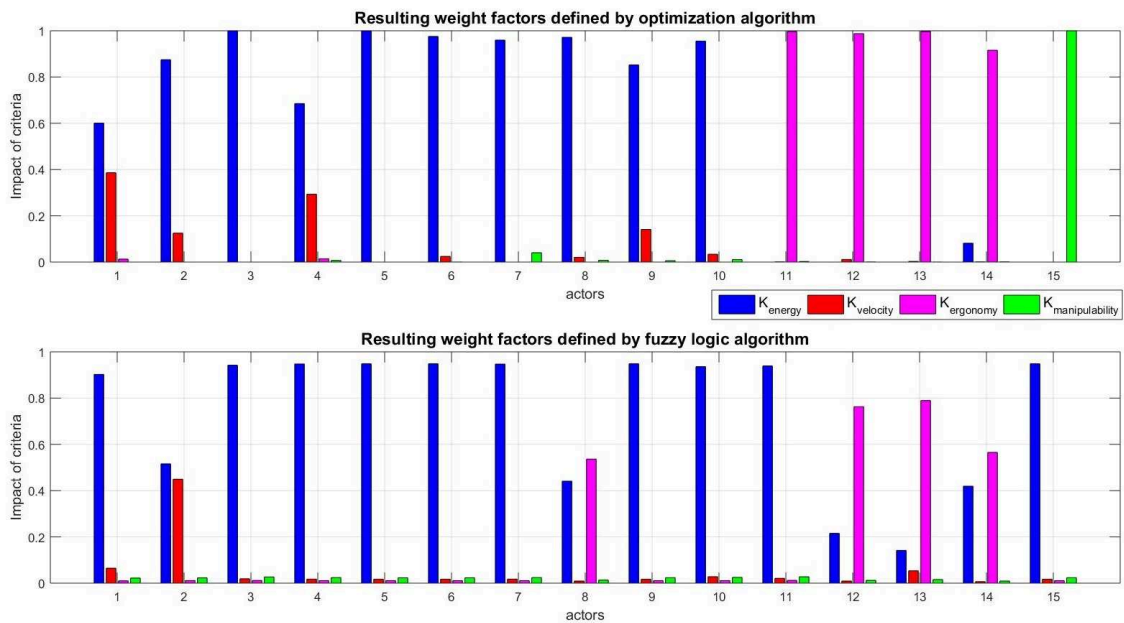


Figure 5.5: "Grating of food" task: Comparative analysis of weight coefficients obtained by optimization and fuzzy algorithms.

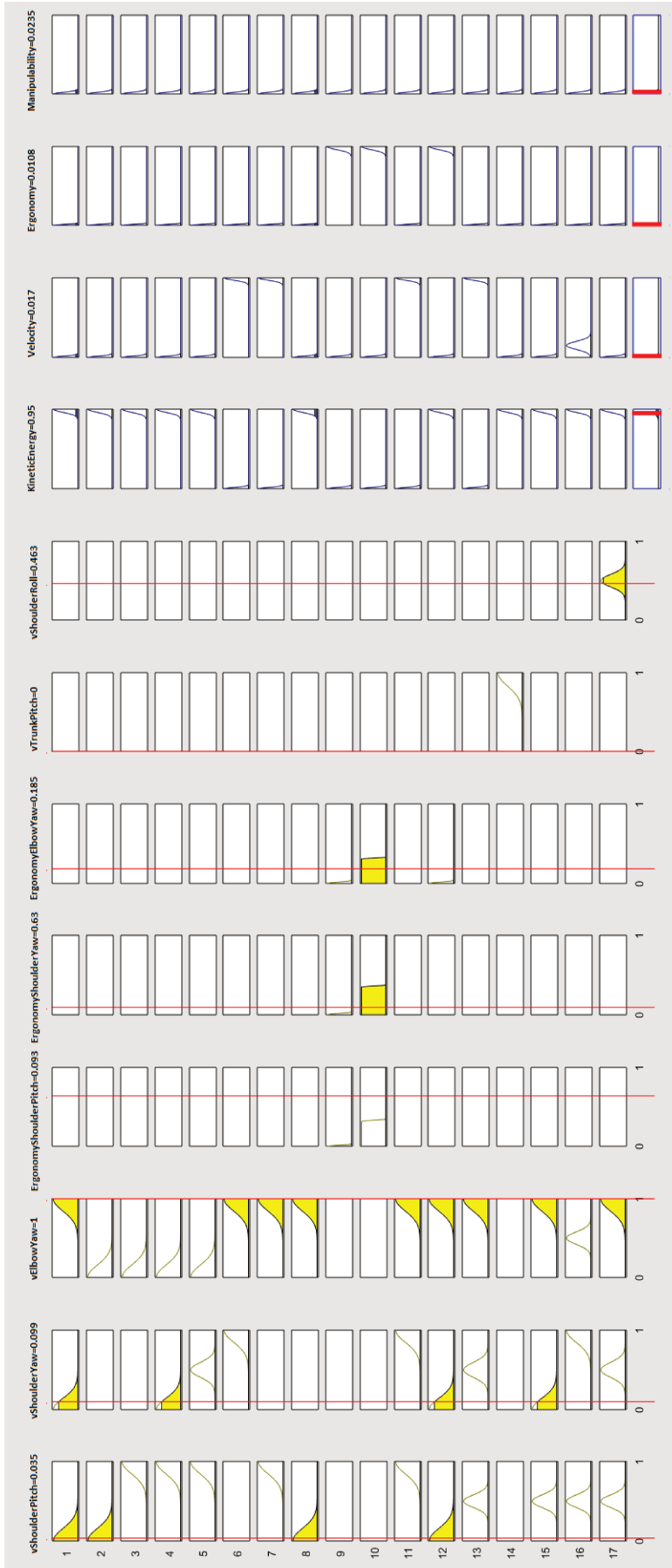


Figure 5.6: "Grating of food" task: Fuzzy rules, linguistic variables and membership functions.

The relation between fuzzy inputs, fuzzy rules and fuzzy outputs for the one case (actor No. 10 in Fig. 5.5) is given in Fig. 5.4. The value of the fuzzy input $vElbowYaw$ is equal 1 and is mapped to linguistic variables *Big*. Values of fuzzy inputs $vShoulderPitch$ and $vShoulderYaw$ are less than 0.1 and are mapped to linguistic variables *ExtraSmall*. The value of fuzzy input $vShoulderRoll$ is above 0.46 and is mapped to linguistic variables *Medium*. Fuzzy inputs $ergonomyShoulderYaw$ and $ergonomyElbowYaw$ have values 0.09384 and 0.1856, respectively, and are mapped to linguistic variables *ExtraSmall*. Fuzzy input $ergonomyShoulderPitch$ has value 0.6392 and is mapped to linguistic variables *Small*. The values of the fuzzy inputs, linguistic variables and the values of the membership function are presented in Fig. 5.6. The linguistic variables which describe fuzzy inputs are represented with yellow color. The all fuzzy inputs except $ergonomyShoulderPitch$ have membership function equal 1 or 1. The fuzzy rules which is satisfied with these values of the fuzzy inputs are 1 and 8 (see Table 5.1). For this fuzzy rules the fuzzy output $Kenergy$ is defined with the linguistic variable *ExtraBig* and takes value equal 0.95, while the other fuzzy outputs are defined with the linguistic variable *ExtraSmall* and take small values.

The analysis of results obtained by fuzzy algorithm shows that:

- Fuzzy algorithm confirm result obtained by optimization algorithm in cases: Nos. 3, 5, 6, 7, 9, 10, 12, and 13;
- Fuzzy algorithm increase influence of dominant criterion in cases: Nos. 1 and 4;
- Fuzzy algorithm decrease influence of dominant criterion (criterion is still dominant) in cases: Nos. 2 and 14
- Fuzzy algorithm gives different results from the optimization algorithm in cases: Nos. 8 and 11.

In the 85% of the cases fuzzy and optimization algorithms determined the same criterion as a dominant (see Fig. 5.5). In the cases Nos. 2, 8 and 14 criteria shares its domination. The case No. 15 where domination of the manipulability criterion is replaced with energy criterion, according to the characteristics of the task in the joint space. The analysis of the fitness functions (see Fig. 5.7) shows that change the impact of criteria K_{energy} and $K_{velocity}$ has drastical influence on the fitness function values (see cases Nos. 1, 2 and 4). It is expected since those actors performed motions using the shoulder, elbow and trunk joints. In the case No. 1 the trunk joint was most active. In the case No. 2 the motion is performed using the elbow and shoulder joint (elbow joint is more active) and the fuzzy results share domination between energy and velocity criteria. Motions obtained in the cases Nos. 8 and 14 have same characteristics in joint space. The fuzzy algorithm shared domination between energy and ergonomy criteria since just elbow joint is active and the motion is near ergonomy configuration. In these cases fitness functions are differ.

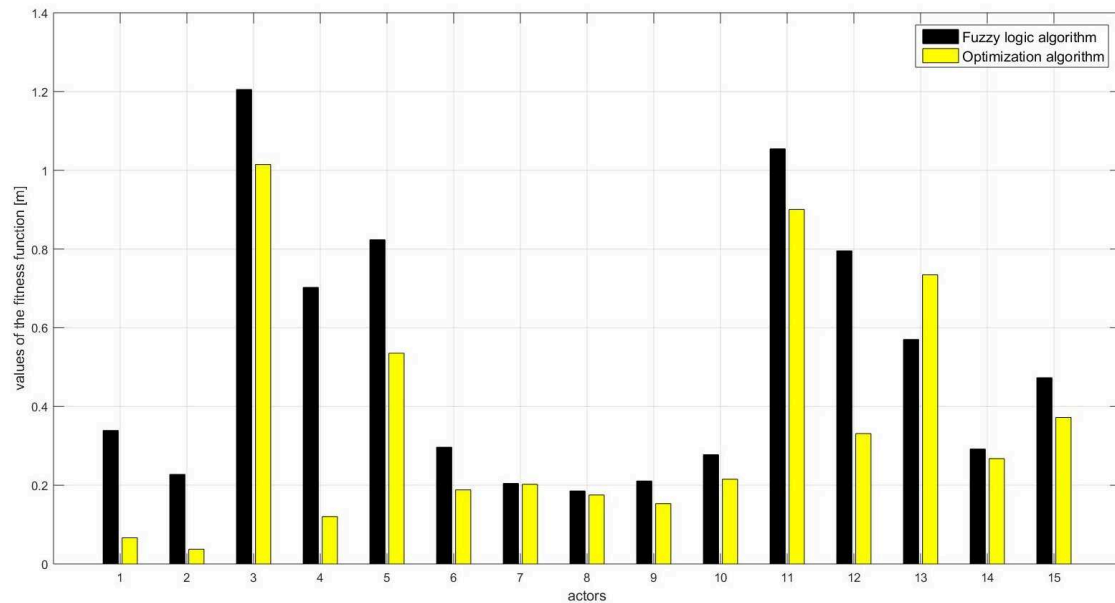


Figure 5.7: "Grating of food" task: Comparative analysis of fitness functions obtained by optimization and fuzzy algorithms.

5.3.2 "Rotation of a steering wheel" task

According to the results obtained by optimization algorithm the energy criterion is dominant or shared its domination with ergonomy criterion in this task. The analysis of the actors' motions in the joint space shows that shoulders are the most active during this task. Since task is characterized with the motion near ergonomy configuration, the values of the fuzzy inputs *ergonomyShoulderPitch* or *ergonomyShoulderYaw* or *ergonomyElbowYaw* is near 0 and is defined with linguistic variable *Small* or *ExtraSmall*. The results obtained by optimization and fuzzy algorithms are presented in Fig. 5.8. The analysis of the results obtained by fuzzy algorithm shows that:

- Fuzzy algorithm confirm result obtained by optimization algorithm in cases: Nos. 4, 5, 7, 9, and 11;
- Fuzzy algorithm increase influence of dominant criterion in cases: Nos. 12, 13, 14 and 15;
- Fuzzy algorithm gives different results from the optimization algorithm in cases: Nos. 1, 2, 3, 6, 8 and 10.

The results show that the same criterion function is dominant in the 60% of the cases. In cases Nos. 1 and 2 the fuzzy algorithm chosen the ergonomy criterion as dominant while an energy criterion can be. The reason is priority factors which is bigger for the fuzzy rules which define ergonomy criterion. Since the fuzzy and optimization algorithm used the different approaches to obtained results the inconsistency in results between two algorithms can occur such as in the cases Nos. 1, 2, 3, 6, 8 and 10. The fuzzy algorithm applies the general characteristics of the human motions analyzed in the joint space while the optimization algorithm searches for the minimal value of the fitness function. Change of criteria dominations take influence on the fitness function values. The results presented

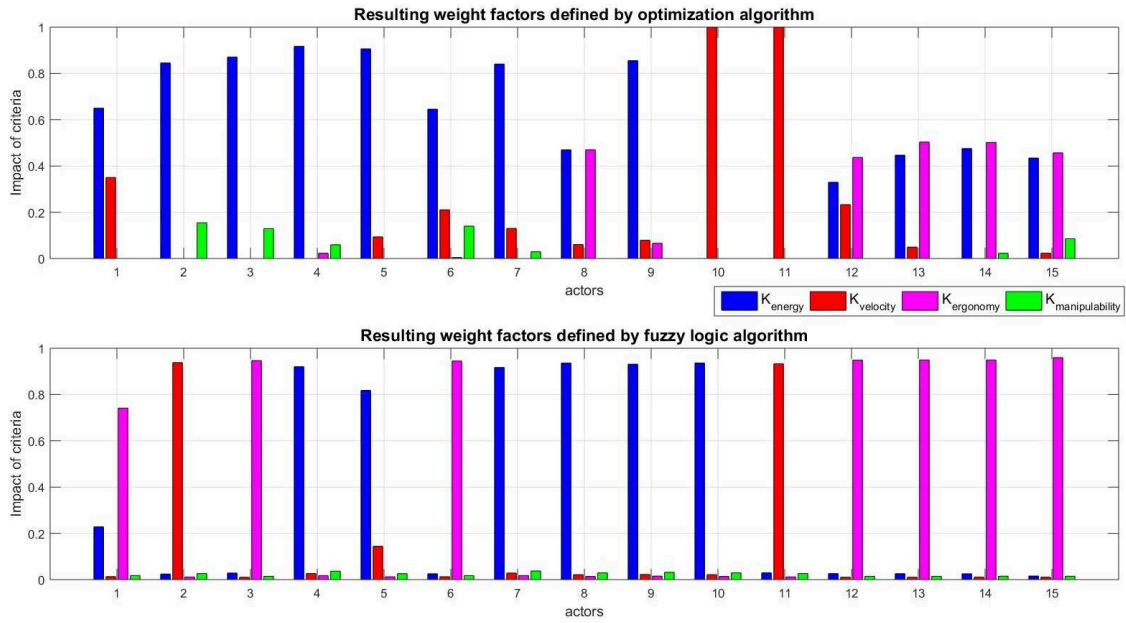


Figure 5.8: "Rotation of a steering wheel" task: Comparative analysis of weight coefficients obtained by optimization and fuzzy algorithms.

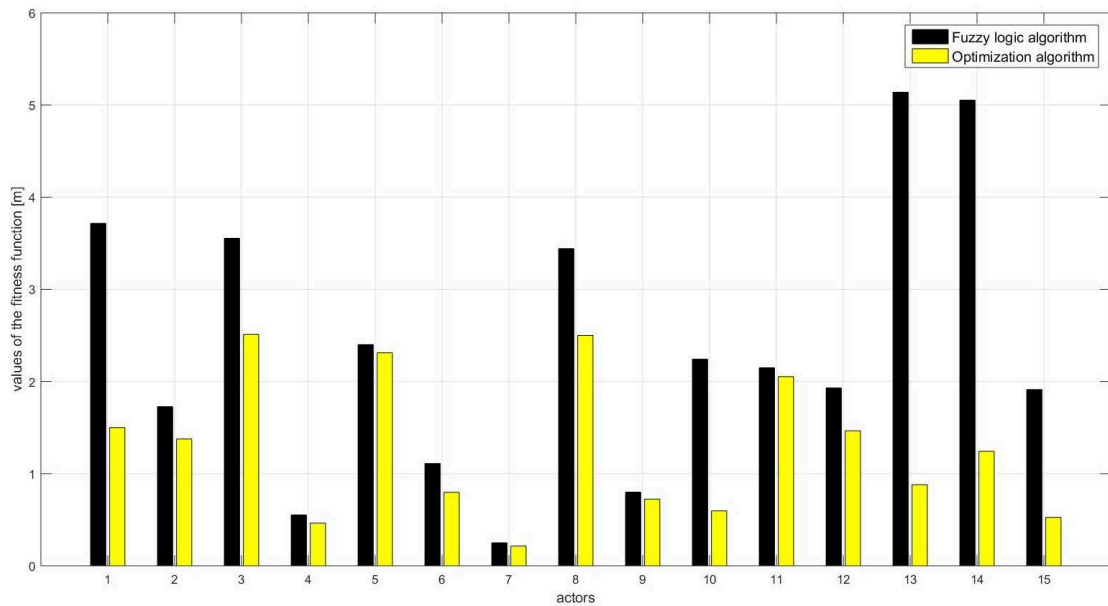


Figure 5.9: "Rotation of a steering wheel" task: Comparative analysis of fitness functions obtained by optimization and fuzzy algorithms.

on the Fig. 5.9 shows that in the cases Nos. 1, 2, 3, 6, 8, and 10 (fuzzy algorithm gave different results from the optimization algorithm) the fitness function is increased. Also, in the cases where the dominant criterion increase their impact (Nos. 12, 13, 14 and 15), the fitness function increased.

5.3.3 “Rotation of the canoe paddles” task

The analysis of this motion in [chapter 4](#) did not propose any criterion as a dominant. The activation of the joints during the motion is associated with an actor who performs the motion, not with the motion itself. The analysis of the results obtained by fuzzy algorithm

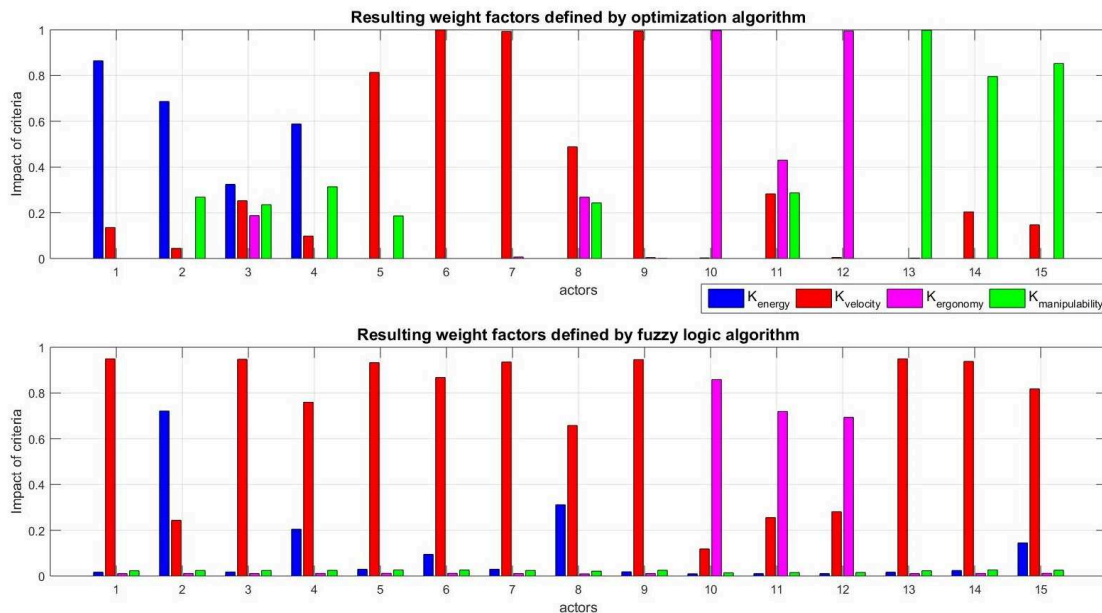


Figure 5.10: "Rotation of the canoe paddles" task: Comparative analysis of weight coefficients obtained by optimization and fuzzy algorithms.

shows that:

- Fuzzy algorithm confirm result obtained by optimization algorithm in cases: Nos. 2, 5, 6, 7, 9, 10 and 12;
- Fuzzy algorithm increase influence of dominant criterion in cases: Nos. 11 and 8;
- Fuzzy algorithm gives different results from the optimization algorithm in cases: Nos. 1, 3, and 4.

The comparison of results of the optimization algorithm and the fuzzy algorithm (see [Fig. 5.10](#)) defines that the same criterion function is dominant in the 75% of the cases. In the cases where the manipulability criterion is dominant the fuzzy algorithm provided the velocity criterion as a dominant since the shoulder and elbow were the most active during the task.

The comparative analysis of the fitness functions presented in [Fig. 5.11](#) shows that in the cases of the Nos. 1, 3, and 4 the values of the fitness function increases since values of weighted coefficients are different. We can also note that the decrease of the value of the dominant criterion affect to the values of the fitness function and decrease it, which is evident in the case No. 12.

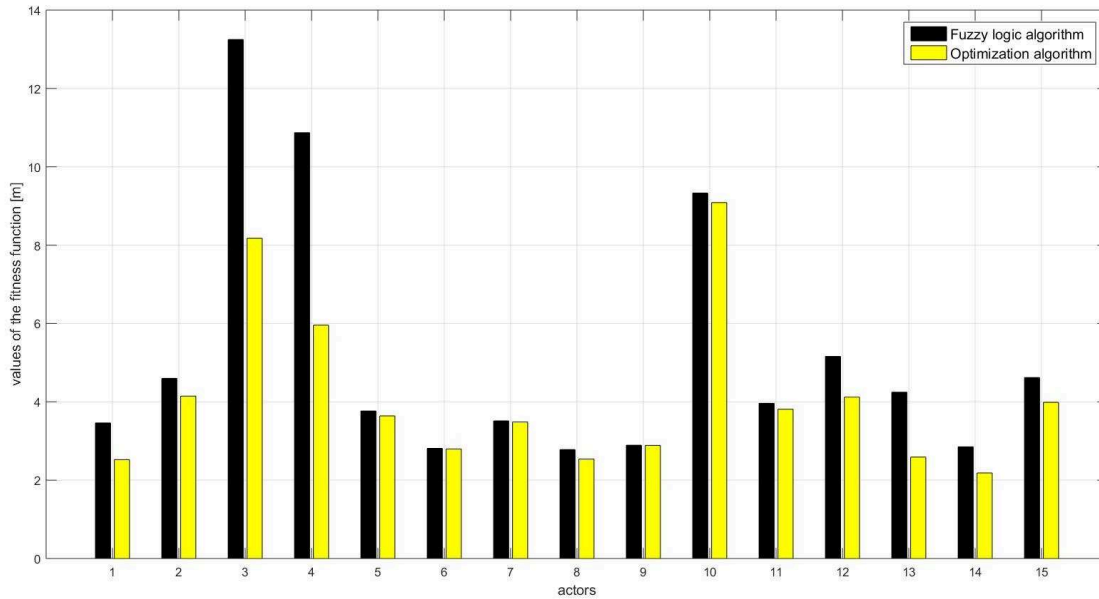


Figure 5.11: "Rotation of the canoe paddles" task: Comparative analysis of fitness functions obtained by optimization and fuzzy algorithms.

5.3.4 "Rotation of the valves" task

The previous analysis of this task proposed that the velocity criterion is dominant in the cases when the actors' position were suitable for performing the motion in a common way (in the case of the 8 actors). During the execution of the task the big motions of shoulders and elbows are evident (*Big* and *Medium* values of the fuzzy input variables $vShoulderPitch$, $vShoulderYaw$, $vShoulderRoll$, and $vElbowYaw$). The analysis of the results obtained by fuzzy algorithm shows that

- Fuzzy algorithm confirm result obtained by optimization algorithm in cases: Nos. 2, 3,4, and 6;
- Fuzzy algorithm increase influence of dominant criterion in cases: Nos. 5 and 7;
- Fuzzy algorithm gives different results from the optimization algorithm in case: No. 1.

According to the results shown in Fig. 5.12, in the 85% fuzzy and optimization algorithms proposed the same criterion as a dominant. In cases Nos. 5 and 7 the fuzzy algorithm increased the impact of the dominant criterion. The domination of the manipulability criterion (obtained by optimization algorithm) is replaced by domination of the velocity criterion, since this task is characterized with the big motions of shoulders and elbows. The analysis of the fitness function values (see Fig. 5.13) shows that the fitness functions are not drastically different. In the cases Nos.1 and 6 the fuzzy algorithm decrease influence of the dominant criterion and the value of the fitness function significantly increased. On the other side, the increased influence of the dominant criterion (case Nos. 5 and 7) is do not have big influence on the value of fitness functions.

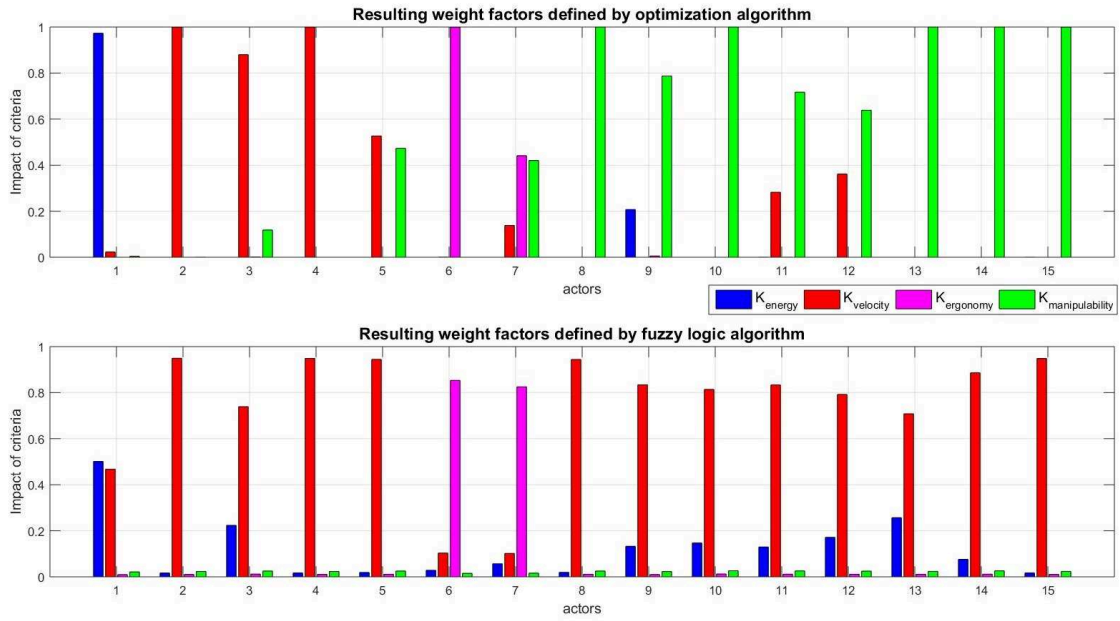


Figure 5.12: "Rotation of the valves" task: Comparative analysis of weight coefficients obtained by optimization and fuzzy algorithms.

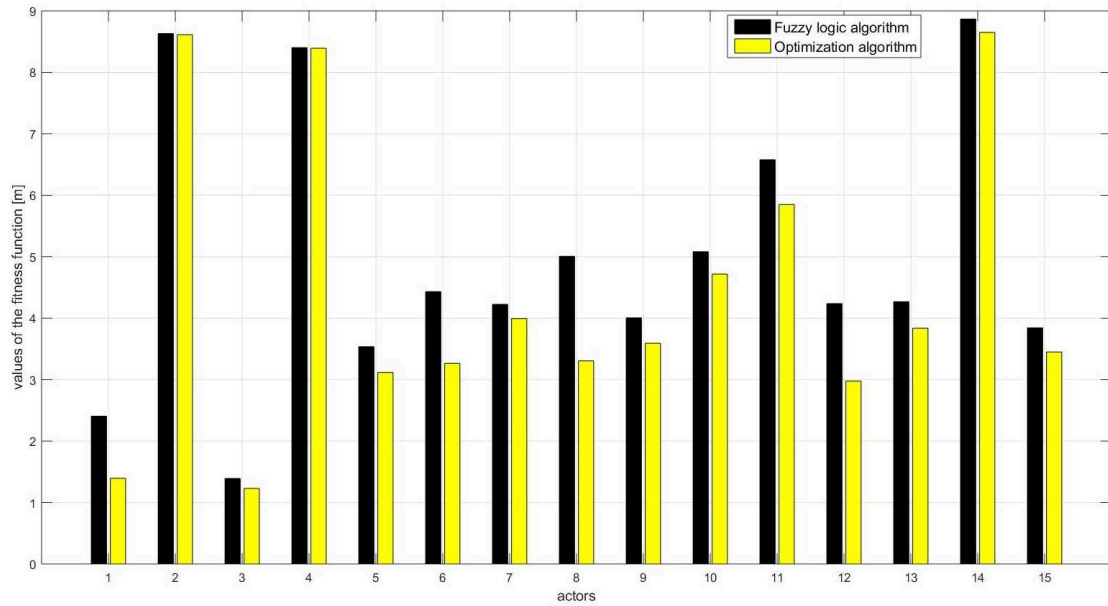


Figure 5.13: "Rotation of the valves" task: Comparative analysis of fitness functions obtained by optimization and fuzzy algorithms.

5.3.5 "Opening/closing drawer" task

The analysis of this task in [chapter 4](#) shows that the shoulders and elbows are the most active during the task and the velocity criterion is dominant. The fuzzy inputs $vShoulderPitch$, $vShoulderYaw$, is defined with linguistic values *Big* or *Medium* while the $vElbowYaw$ with *Big*. Looking at results obtained by fuzzy algorithm in Fig.5.14 we can see that:

- Fuzzy algorithm confirm result obtained by optimization algorithm in cases:Nos. 1, 3, 5, 6, and 8;

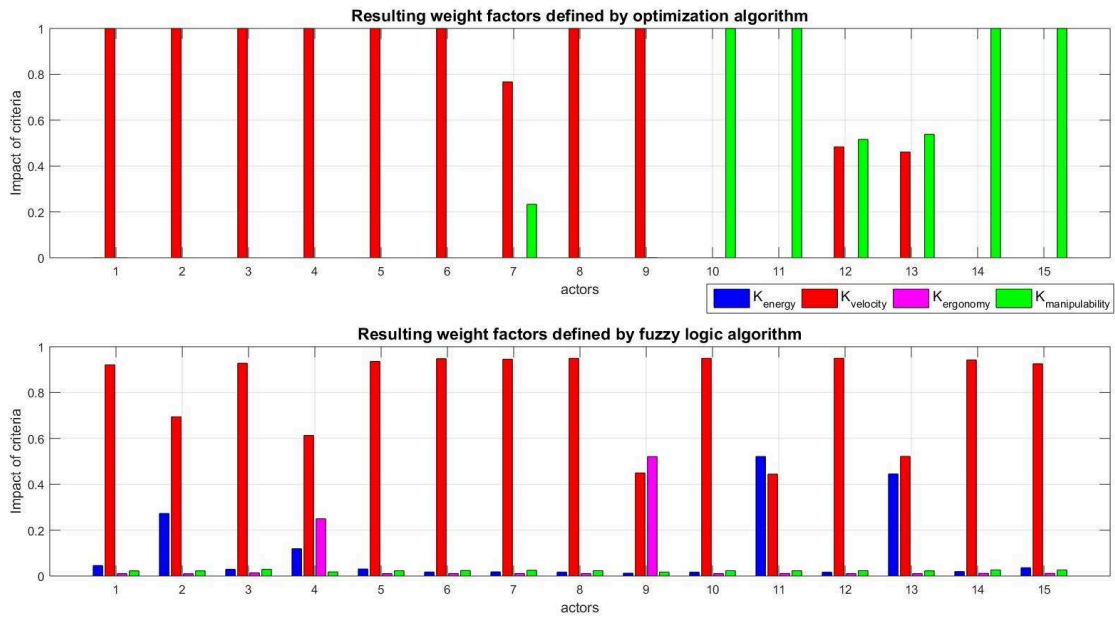


Figure 5.14: "Opening/closing drawer" task: Comparative analysis of weight coefficients obtained by optimization and fuzzy algorithms.

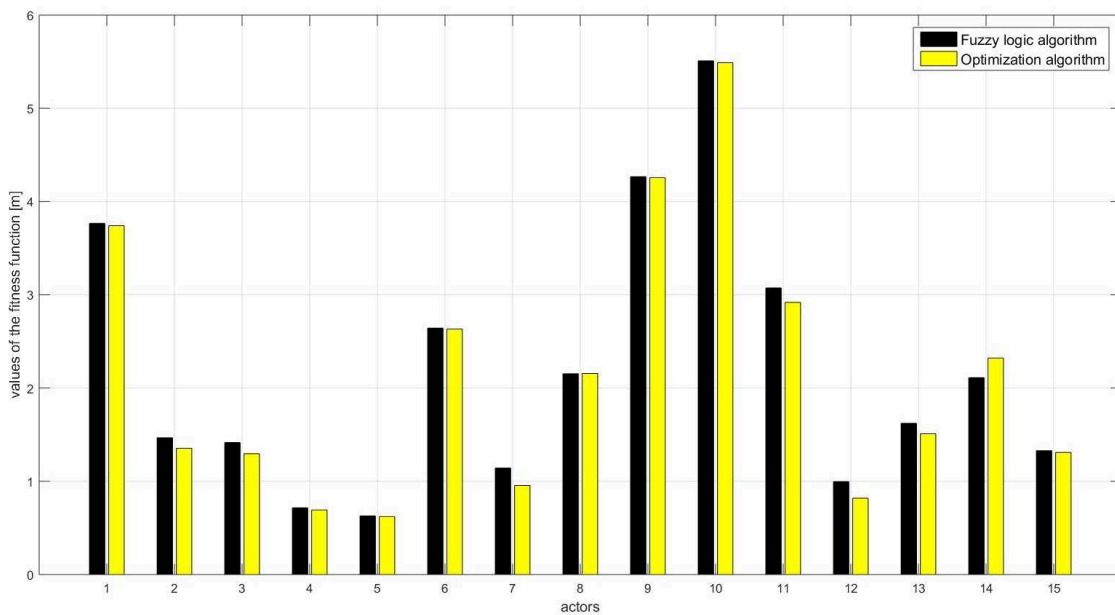


Figure 5.15: "Opening/closing drawer" task: Comparative analysis of fitness functions obtained by optimization and fuzzy algorithms.

- Fuzzy algorithm increase influence of dominant criterion in case: No. 7;
- Fuzzy algorithm decrease influence of dominant criterion (criterion is still dominant) in cases: Nos. 2 and 4
- Fuzzy algorithm gives different results from the optimization algorithm in case: No. 9.

In the 88% of the cases fuzzy and optimization algorithms determined the same criterion as a dominant. In the 5 cases the fuzzy and optimization algorithms obtained the same results, while in the 3 cases the results are slightly different, but the same criterion is

dominant. Since the velocity criterion is dominant in the most of the cases, the fuzzy logic system defined it as a dominated even when manipulability is dominant since this criterion is not considered with the fuzzy algorithm. The result presented in the Fig. 5.15 shows that fuzzy logic and optimization algorithms obtained motion with very similar value of the fitness functions. In the case No. 9 where the criteria function is different the fitness functions are near which means that the combination of the criteria functions obtained by fuzzy algorithm is able to imitate motion with the same accuracy.

5.3.6 “Inflating a mattress using a pump” task

The analysis of results in chapter 4 shown that during this task the elbow joint is the most active and the energy criterion as a dominant in the most of the cases. Results obtained by fuzzy algorithm given in Fig. 5.16 shows that:

- Fuzzy algorithm confirm result obtained by optimization algorithm in cases:Nos. 1, 2, 4, 5, 6, 7, 8, 9,11 and 13;
- Fuzzy algorithm decrease influence of dominant criterion (criterion is still dominant) in case:No. 10
- Fuzzy algorithm gives different results from the optimization algorithm in cases: Nos. 3 and 12.

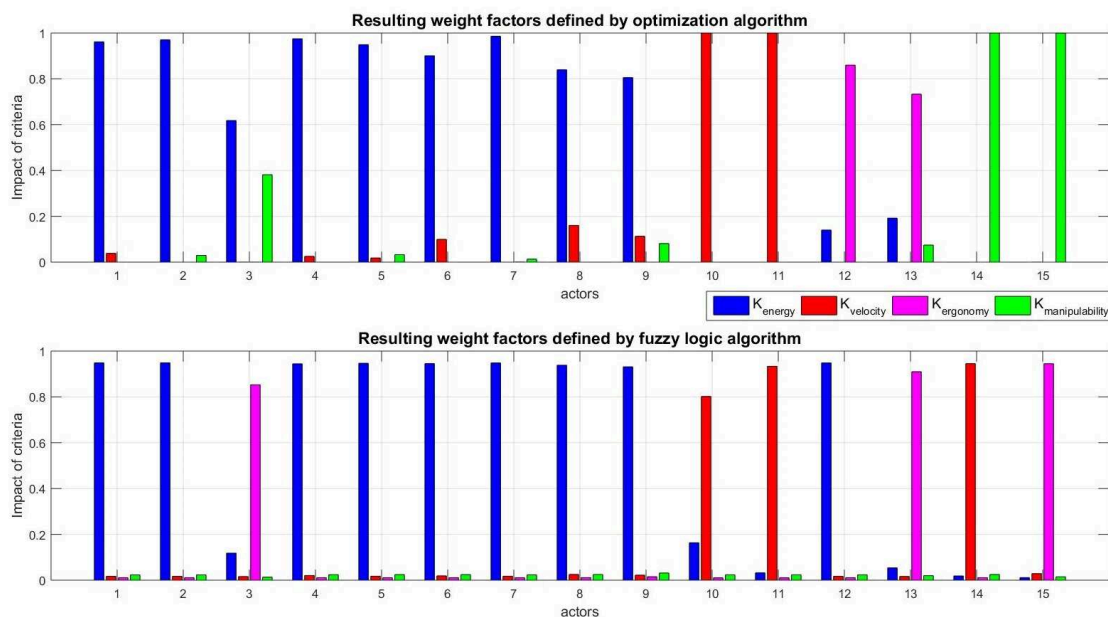


Figure 5.16: "Inflating a mattress using a pump" task: Comparative analysis of weight coefficients obtained by optimization and fuzzy algorithms.

In the 85% of the cases fuzzy and optimization algorithms determined the same criterion as a dominant. Since in this task the motion of the elbow joint is the biggest, the fuzzy and optimization algorithm gave the impact of the K_{energy} near the 1. In the cases Nos. 10 and 11, the shoulders are moved during the task and the both algorithm are proposed the velocity criterion as a dominant.

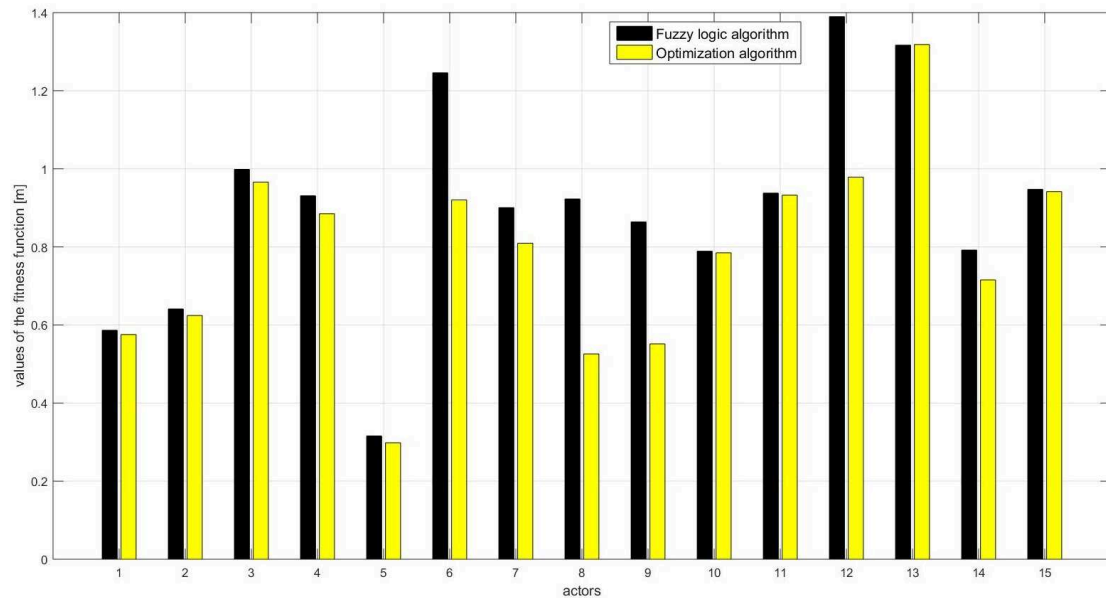


Figure 5.17: "Inflating a mattress using a pump" task: Comparative analysis of fitness functions obtained by optimization and fuzzy algorithms.

The comparison of fitness functions obtained by fuzzy and optimization algorithms is proposed in the Fig. 5.17. In the cases Nos. 6, 8 and 9 the influence of the velocity criterion is lost and fitness functions obtained by fuzzy algorithm increased their values. We can conclude that the small influence of the velocity criterion (small motions of the other joints) is also characteristics of this task. In the case No. 12, the domination of the criterion is changed and the fitness function is increased.

5.3.7 "Cutting with a knife" task

The analysis of results obtained by optimization algorithm and the activation of the joint during the task shows that in this task shoulder and elbow are the most active and the velocity criterion is dominant. Results obtained by fuzzy algorithm shows that:

- Fuzzy algorithm confirm result obtained by optimization algorithm in cases:Nos. 5, 8, 9, 12 and 13;
- Fuzzy algorithm decrease influence of dominant criterion (criterion is still dominant) in cases:Nos. 6, 7, and 10
- Fuzzy algorithm gives different results from the optimization algorithm in cases: Nos. 1, 2, 3, 4, and 11.

In the 61% of the cases fuzzy and optimization algorithms determined the same criterion as a dominant, while in the 38% the fuzzy algorithm gave the same result as optimization algorithm (see Fig. 5.18). According to the comparative analysis of the fitness functions given in Fig. 5.19 it is evident that the values of the fitness functions is sensitive on the small changes of the weight coefficients which is evident in the cases Nos. 5, 7, 12 and 13. In other cases, the change of the dominant criterion significantly influences the value of the fitness function in cases Nos.2, 3, 4 and 11.

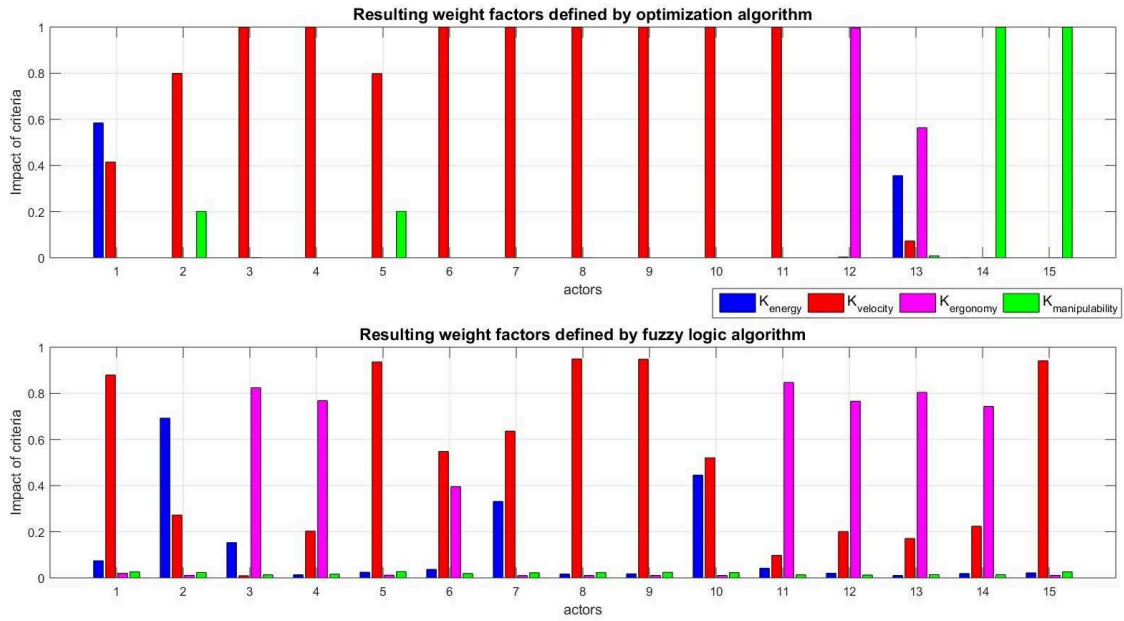


Figure 5.18: "Cutting with a knife" task: Comparative analysis of weight coefficients obtained by optimization and fuzzy logic algorithms.

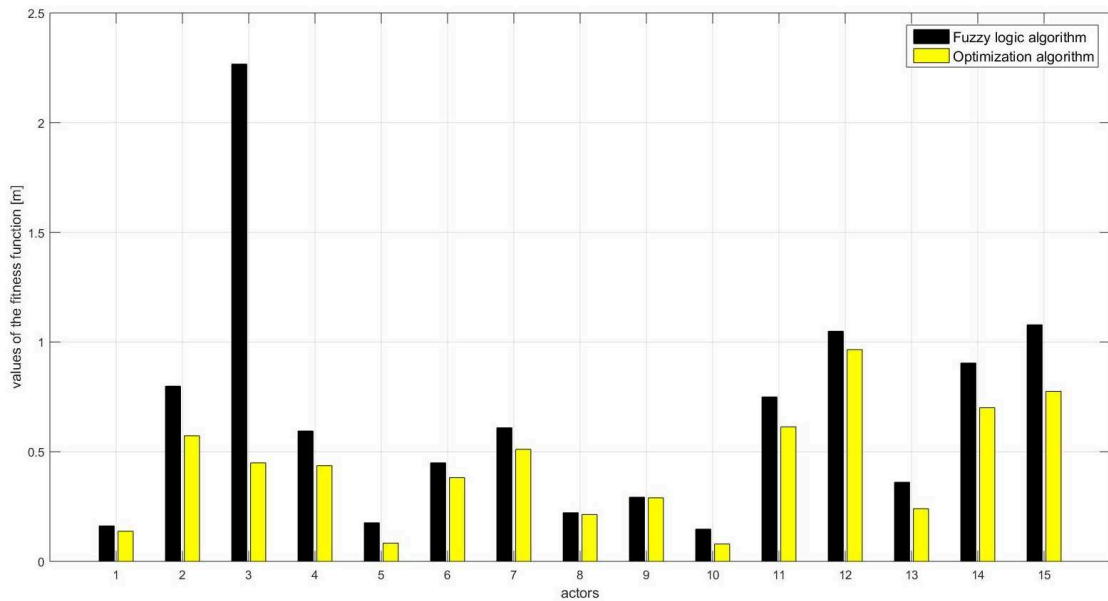


Figure 5.19: "Cutting with a knife" task: Comparative analysis of fitness functions obtained by optimization and fuzzy logic algorithms.

5.4 Implementation fuzzy algorithm for a new motion

In this subsection we implemented our fuzzy algorithm for detection values of weight coefficients in task which is not previous analyzed. In Fig. 5.20 (a) is shown testing task "Turning a hand drill" which is one-arm support rotation motion. The task is performed by 6 actors on the way which was comfortable for them. The "Turning a hand drill" task is characterized by the motion of the shoulder and elbow joints. The elbow yaw joints were most active during tasks, while shoulder joints has medium activity. During the task

the actors' right hand configuration was near human ergonomics configuration. The results obtained by optimization algorithm showed the ergonomics criterion was dominant in 5 cases while in the one case energy criterion was dominated.

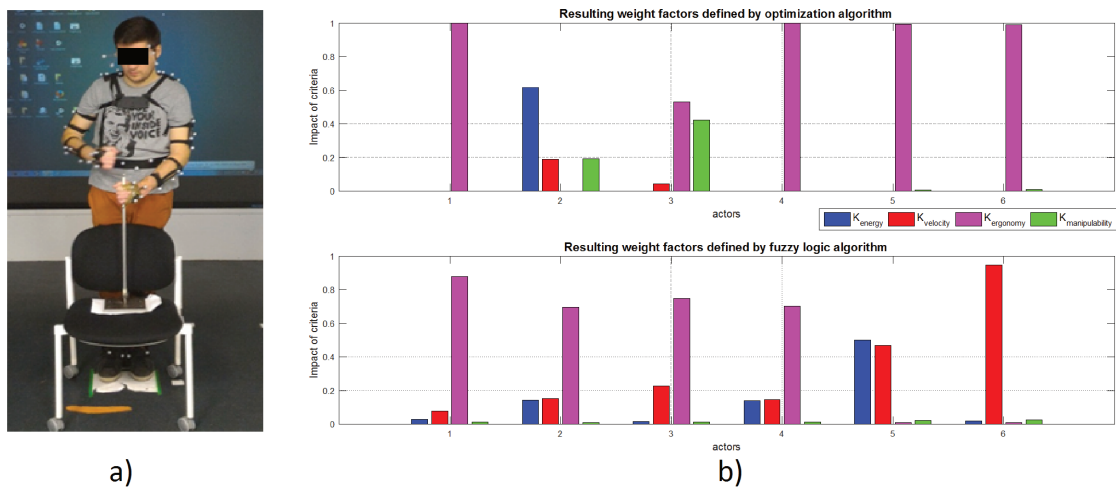


Figure 5.20: a) "Turning a hand drill" test task, b) Comparative analysis of weight coefficients obtained by optimization and fuzzy algorithms.

In order to analyze universality of our fuzzy algorithm we applied our fuzzy algorithm on "Turning a hand drill" task and calculated values of the weight coefficients. The comparative analysis of the results obtained by optimization and fuzzy algorithm for these tasks is shown in Fig. 5.20 (b). The results presented in the Fig. 5.20 (b) show that the fuzzy algorithm provides the same criterion as a dominant in the 50% cases. In these cases the ergonomics criterion is dominant. The value of the fuzzy input *ergonomicsShoulderPitch* or *ergonomicsShoulderYaw* or *ergonomicsElbowYaw* is near 0 and the priority factor of the fuzzy rules which defines ergonomics criterion is higher than other rules. In the other cases the velocity criterion was dominant or shared impact with energy criterion since the shoulder and elbow moved during the task.

5.5 Conclusion

In this section we proposed fuzzy logic system as a way evaluate the criterion optimized by human during its motion. The main parameters which explained human motion presented in chapter 4, such as velocity of the actor's joints and the relative position between actor's and ergonomics configurations were used as the fuzzy input variables. Since the task of our research was to calculate the optimal combination of the weight coefficients, these parameters represented fuzzy output. The general conclusion about human motion behavior defined in chapter 4 were used for making fuzzy rules. The parameters of the fuzzy algorithm, such as linguistic variables and membership functions, were adjusted according to the values of actor joint velocities and positions calculate for all analyzed tasks in chapter 4. Performance of the fuzzy algorithm was shown through comparative

analysis of the results obtained by fuzzy and optimization algorithms. The results shows that in the tasks “Rotation of the valves”, “Grating of food”, “Opening/closing drawer”, and “Inflating a mattress using a pump” fuzzy and optimization algorithms provided in about 85% of the cases the same criterion as a dominant. In the tasks “Rotation of a steering wheel “, “Rotation of the canoe paddles”, and “Cutting with a knife” the same criterion was dominant between 60% and 75% of the cases. The “Turning a hand drill” task was a test motion which had not been previously analyzed. The results obtained by fuzzy and optimization algorithms showed the same criterion as a dominant in 50% of cases. There are several reasons why the results obtained by fuzzy algorithm and optimization algorithm are different. Fuzzy algorithm did not include all human motion behavior which was appeared in the tested motion. Another reason was setting the parameters of the membership functions. The values of the fuzzy inputs which were between two linguistic variables gave the small value of the membership functions for both linguistic variables and the defined fuzzy rule had small influence on the final results. Because of that the value of the weight coefficients obtained by fuzzy algorithm and optimization algorithm were different. Based on the results we can say that the fuzzy algorithm can be used for prediction of the criterion minimized, for a type a motion that has been previously studied. The new test motion “Turning a hand drill” showed that fuzzy algorithm did not covered all characteristics of the human motion behavior and in this form cannot be used as universal logic for representation human motion. In the future, the characteristics of other dual-arm manipulation motions should be included in the process of the fuzzy algorithm setting. The set of the fuzzy inputs and fuzzy rules should be increased in order to take into account the new human motion behaviors. At the end, more powerful artificial intelligence algorithm can be proposed for analysis human motion behavior.

Conclusion

The aim of this thesis is to propose a new approach for generating dual arm robot manipulation inspired by human motion skills. In the thesis, we analyse all steps of the human to the humanoid motion conversion. First, we have chosen to analyze the dual arm manipulation since they are not sufficiently explored in the literature. We have recorded 12 different dual arm motions which are classified according to the characteristics of the motion in the task space (goal-coordinated, symmetric, asymmetric and one arm support) and the axis of the rotation/translation. For the purpose of the research in this thesis we have chosen the 7 recorded dual arm manipulation tasks:

- rotational motions (“Rotation of the steering wheel”, “Rotation of the valves”, “Rotation of the canoe paddles”)
- translational motions (“Cutting food with the knife”, “Inflating a mattress using a pump”, “Grating the food”, “Opening/closing a drawer”).

We have chosen these motions because they are more limited with the characteristics of the equipment. The characteristics of these motions are more evident compared to the other motions and give us more precise analysis of the human motion. Since our task is to define human motion behaviors, we have analyzed these motions in the Cartesian and joint spaces.

Second, we defined the conversion process for imitation of dual arm human motion, utilizing the upper body. The conversion process consists of the imitation algorithm and the algorithm for humanoid motion generation. The imitation algorithm is based on the Virtual Markers which follow the Real Markers motions and incorporates additionally recorded joint motions. The imitation algorithm uses data about human motion acquired by a motion capture system (Cartesian position of the Real Markers and Cartesian position and orientation of the human joints) and the scaled model of robot ROMEO as the human kinematic model. The imitation algorithm used an analytical expression based

on the Jacobian matrix. In comparison to existing algorithms, our imitation algorithm provides a better accuracy of the motion imitation in the Cartesian space and enable real time imitation of the human motion by humanoid robot. The results from the imitation algorithm is the recorded human motion represents in the joint space for the studied humanoid robot. These results are further used in the conversion process. The algorithm for humanoid motion generation is based on the inverse kinematics algorithm. This algorithm generates humanoid motion by following the recorded human hand motions in Cartesian space and, at the same time, resemble human motion behavior to the motion of the humanoid using the human motion represented in the joint space. Since our task consists of the motion phases with and without contact, we additionally have defined an algorithm for the transition between such phases. Therefore, as the important contribution of this work, the proposed conversion algorithm is suitable for the human motion imitation with humanoid for the task with and without contact, as well as the complex tasks which consists both types of the motions which is not the case of the other imitation algorithms. The algorithm for humanoid motion generation generates the robot motion for phases with and without contact and enable the robot to obtain contact between hands and equipment in a transition phase. The results obtained from our conversion process are experimentally tested on the real ROMEO robot. The ROMEO robot performs tasks in the same way as a human.

Third, we have investigated the inverse optimal control algorithm as the optimization tool for the analysis of the characteristics of the basic dual arm human motion. At the beginning of our research, we explained human motion behavior using IK algorithm and the basic criterion functions such as minimization of kinetic energy, minimization of joint velocities, minimization of the distance between the current and ergonomic positions, and maximization of manipulability. We included each of the criterion function into the IK algorithm. We have come to the conclusion about which criterion function does the best imitation of the recorded human movement. Accordingly, the conclusion about the characteristics of the human movement is made. In order to precisely analyze the human motions we decided to combine all of these criterion functions. We defined the inverse optimal control algorithm which minimized the weighted combinations of the four criteria functions. According to the values of each weight coefficient, calculated using genetic algorithm, we are able to describe the characteristics of the human motion behaviors and to define the strategy which human used during the tasks. We are able to make some conclusions about human motion characteristics and strategy of generation the motion:

- the characteristics of dual-arm motions performed by a healthy human are directly connected with the activation of the particular arm joints and a combination of joint activations. The criterion of kinetic energy minimization is a dominant criterion for the tasks that require greater mobility of the joints with big inertia. The criterion of minimization of velocity is dominant in the tasks that are not characterized by a large motion of the joints

- the dual arm motions on which hands perform task near their joint limits or near singularity configuration is defined with the maximization of manipulability as a dominant criterion
- since the humans try to do motions in the way they consider most comfortable, in each of the analyzed motions which pass near human ergonomic configuration the criterion minimization of the distance between the current and the ergonomic configuration is dominant
- the optimal combination of criterion functions most often generates the best imitation of the human motion and is able to describe the strategy of generating a human movement in more detail.

Since in our research the each task is performed by 15 actors, we compared the same motion performed by different actors. The conclusion is that the strategy of performing the same motion by different actors is the same, but may change due to the influence of the environment and human body characteristics. At the end, our inverse kinematics algorithm is able to generate the human-like motions with a redundant humanoid robot with the kinematic characteristics close to or resembling those of humans. The inverse kinematics algorithm with different combination of weight coefficients will produce the different robot's motion in joint space for the same motion of the robot's hands in the task space. Our inverse kinematics algorithm with a generalized combination of weight coefficients (calculated for each task separately) will produce the robot's motions which are closest to recorded human motions.

Finally, we presented fuzzy logic system as a way for finding the criterion minimized by human motion. The results obtained by analysis 7 different dual-arm motion each performed by 15 actors is used as expert knowledge for making fuzzy logic rules. Since the task of our research is to calculate the optimal combination of the weighted coefficients, our fuzzy system calculates them as fuzzy output variables using the velocities of shoulder, elbow and trunk joints, and distance between current and ergonomics human configurations as fuzzy input variables. In order to evaluate the performance of our fuzzy system, we tested it on the dual-arm task which was not analysed before. The results show that fuzzy logic system gives the combination of weight coefficients for the new task which is in correlation with the our analysis of the human motion behavior.

The results of the research can be applied to several areas. The characteristics of the basic motion of healthy people acquired in this thesis can be used for the analysis of human motion with the disability in motor skills. Furthermore, our inverse kinematics algorithm can be used for generation of a complex motion, which represents a set of the analyzed basic motions, changing the combination of the weight coefficients from one basic motion to another. Implementation of the explored characteristics of human motion on the humanoid robot will enable the most natural cooperation between humanoids and humans, help the elderly persons in their everyday life, and allow better integration of humanoid robots into the human environment. Our future research should be directed

towards enlarging the set of the analyzed basic human motions and inclusion of basic criterion functions which consider dynamics. The different leaning techniques, as neurols network or deep learning can be used to calculate the characteristics of human motion.

References

- Adorno, B. V. (2011). *Two-arm manipulation: from manipulators to enhanced human-robot collaboration* (Unpublished doctoral dissertation). Université Montpellier II-Sciences et Techniques du Languedoc.
xv, 139
- Albrecht, S., Ramirez-Amaro, K., Ruiz-Ugalde, F., Weikersdorfer, D., Leibold, M., Ulrich, M., & Beetz, M. (2011). Imitating human reaching motions using physically inspired optimization principles. In *Humanoid robots (humanoids), 2011 11th IEEE International Conference on* (pp. 602–607).
20, 31
- Aldebaran. (2013). *Project romeo*. Website. Retrieved 2013, from <http://projetromeo.com>
9
- Alexander, R. M. (1984). Walking and running: Legs and leg movements are subtly adapted to minimize the energy costs of locomotion. *American Scientist*, 72(4), 348–354.
19
- Aloui, S., Villien, C., & Lesecq, S. (2015). A new approach for motion capture using magnetic field: models, algorithms and first results. *International Journal of Adaptive Control and Signal Processing*, 29(4), 407–426.
32
- Angeles, J., & Gosselin, C. (1991). A global performance index for the kinematic optimization of robotic manipulators. *Journal of Mechanical Design*, 113(3), 220–226.
23
- ARTCompany. (2018). *Advanced realtime tracking system*. Website. Retrieved 2018, from <https://ar-tracking.com/products/tracking-systems/>
33
- Asfour, T., Azad, P., Gyarfas, F., & Dillmann, R. (2008). Imitation learning of dual-arm manipulation tasks in humanoid robots. *International Journal of Humanoid Robotics*, 5(02), 183–202.
19
- Audu, M. L., To, C. S., Kobetic, R., & Triolo, R. J. (2010). Gait evaluation of a novel hip constraint orthosis with implication for walking in paraplegia. *IEEE Transactions*

on Neural Systems and Rehabilitation Engineering, 18(6), 610–618.

16

Ayusawa, K., Ikegami, Y., & Nakamura, Y. (2014). Simultaneous global inverse kinematics and geometric parameter identification of human skeletal model from motion capture data. *Mechanism and Machine Theory*, 74, 274–284.

18

Ayusawa, K., Morisawa, M., & Yoshida, E. (2015). Motion retargeting for humanoid robots based on identification to preserve and reproduce human motion features. In *Intelligent robots and systems (iros), 2015 ieee/rsj international conference on* (pp. 2774–2779).

18

Azad, P., Asfour, T., & Dillmann, R. (2007). Toward an unified representation for imitation of human motion on humanoids. In *Robotics and automation, 2007 ieee international conference on* (pp. 2558–2563).

xii, 34, 35

Baerlocher, P., & Boulic, R. (2004). An inverse kinematics architecture enforcing an arbitrary number of strict priority levels. *The visual computer*, 20(6), 402–417.

55, 86

Bagheri, M., Ajoudani, A., Lee, J., Caldwell, D. G., & Tsagarakis, N. G. (2015). Kinematic analysis and design considerations for optimal base frame arrangement of humanoid shoulders. In *Robotics and automation (icra), 2015 ieee international conference on* (pp. 2710–2715).

54

Baillieul, J. (1985). Kinematic programming alternatives for redundant manipulators. In *Robotics and automation. proceedings. 1985 ieee international conference on* (Vol. 2, pp. 722–728).

65

Billard, A., Calinon, S., Dillmann, R., & Schaal, S. (2008). *Survey: Robot programming by demonstration* (Tech. Rep.). MIT Press.

31

Billard, A., Epars, Y., Calinon, S., Schaal, S., & Cheng, G. (2004). Discovering optimal imitation strategies. *Robotics and autonomous systems*, 47(2), 69–77.

17

Billard, A. G., Calinon, S., & Guenter, F. (2006). Discriminative and adaptive imitation in uni-manual and bi-manual tasks. *Robotics and Autonomous Systems*, 54(5), 370–384.

2, 21

Bluethmann, W., Ambrose, R., Diftler, M., Askew, S., Huber, E., Goza, M., . . . Magruder, D. (2003). Robonaut: A robot designed to work with humans in space. *Autonomous robots*, 14(2), 179–197.

10

Borovac, B., Gnjatović, M., Savić, S., Raković, M., & Nikolić, M. (2016). Human-like robot marko in the rehabilitation of children with cerebral palsy. In *New trends in medical and service robots* (pp. 191–203). Springer.

19

BostonDynamics. (2013). *Robot atlas*. Website. Retrieved 2013, from http://www.bostondynamics.com/robot_Atlas.html

9

Buchholz, B., Armstrong, T. J., & Goldstein, S. A. (1992). Anthropometric data for describing the kinematics of the human hand. *Ergonomics*, 35(3), 261–273.

11

Buss, S. R. (2004). Introduction to inverse kinematics with jacobian transpose, pseudoinverse and damped least squares methods. *IEEE Journal of Robotics and Automation*, 17(1-19), 16.

64

Calinon, S., & Billard, A. (2004). Stochastic gesture production and recognition model for a humanoid robot. In *Intelligent robots and systems, 2004.(iros 2004). proceedings. 2004 ieee/rsj international conference on* (Vol. 3, pp. 2769–2774).

1, 19

Calinon, S., & Billard, A. (2005). Recognition and reproduction of gestures using a probabilistic framework combining pca, ica and hmm. In *Proceedings of the 22nd international conference on machine learning* (pp. 105–112).

19

Calinon, S., & Billard, A. (2007). Incremental learning of gestures by imitation in a humanoid robot. In *Proceedings of the acm/ieee international conference on human-robot interaction* (pp. 255–262).

1, 19

Calinon, S., & Billard, A. (2008). A probabilistic programming by demonstration framework handling constraints in joint space and task space. In *Intelligent robots and systems, 2008. iros 2008. ieee/rsj international conference on* (pp. 367–372).

19

Calinon, S., Guenter, F., & Billard, A. (2005). Goal-directed imitation in a humanoid robot. In *Robotics and automation, 2005. icra 2005. proceedings of the 2005 ieee international conference on* (pp. 299–304).

1, 19

Calinon, S., Guenter, F., & Billard, A. (2007). On learning, representing, and generalizing a task in a humanoid robot. *IEEE Transactions on Systems, Man, and Cybernetics, Part B (Cybernetics)*, 37(2), 286–298.

19

Ceseracciu, E., Sawacha, Z., & Cobelli, C. (2014). Comparison of markerless and

marker-based motion capture technologies through simultaneous data collection during gait: proof of concept. *PloS one*, 9(3), e87640.

[32](#)

Chevallereau, C., & Khalil, W. (1988). A new method for the solution of the inverse kinematics of redundant robots. In *Robotics and automation, 1988. proceedings, 1988 ieee international conference on* (pp. 37–42).

[20](#)

Chia, L., Licari, M., Guelfi, K., & Reid, S. (2013). A comparison of running kinematics and kinetics in children with and without developmental coordination disorder. *Gait & posture*, 38(2), 264–269.

[17](#)

Chiaverini, S., Oriolo, G., & Walker, I. D. (2008). Kinematically redundant manipulators. In *Springer handbook of robotics* (pp. 245–268). Springer.

[20, 65](#)

Cho, B.-K., Park, S.-S., & Oh, J.-h. (2009). Controllers for running in the humanoid robot, hubo. In *Humanoid robots, 2009. humanoids 2009. 9th ieee-ras international conference on* (pp. 385–390).

[9](#)

Dariush, B., Gienger, M., Arumbakkam, A., Zhu, Y., Jian, B., Fujimura, K., & Goerick, C. (2009). Online transfer of human motion to humanoids. *International Journal of Humanoid Robotics*, 6(02), 265–289.

[56](#)

Do, M., Azad, P., Asfour, T., & Dillmann, R. (2008). Imitation of human motion on a humanoid robot using non-linear optimization. In *Humanoid robots, 2008. humanoids 2008. 8th ieee-ras international conference on* (pp. 545–552).

[1, 17, 32](#)

Englsberger, J., Werner, A., Ott, C., Henze, B., Roa, M. A., Garofalo, G., ... others (2014). Overview of the torque-controlled humanoid robot toro. In *Humanoid robots (humanoids), 2014 14th ieee-ras international conference on* (pp. 916–923).

[9](#)

Fong, T., Nourbakhsh, I., & Dautenhahn, K. (2003). A survey of socially interactive robots. *Robotics and autonomous systems*, 42(3), 143–166.

[17](#)

Fukuchi, R. K., & Duarte, M. (2008). Comparison of three-dimensional lower extremity running kinematics of young adult and elderly runners. *Journal of sports sciences*, 26(13), 1447–1454.

[16](#)

Gärtner, S., Do, M., Asfour, T., Dillmann, R., Simonidis, C., & Seemann, W. (2010). Generation of human-like motion for humanoid robots based on marker-based motion capture data. In *Robotics (isr), 2010 41st international symposium on and 2010*

6th german conference on robotics (robotik) (pp. 1–8).

18

Gini, G., Belluco, P., Mutti, F., Rivela, D., & Scannella, A. (2015). Towards a natural interface for the control of a whole arm prosthesis. *New Trends in Medical and Service Robots: Assistive, Surgical and Educational Robotics*, 38, 47.

17

Gittoes, M. J., & Irwin, G. (2012). Biomechanical approaches to understanding the potentially injurious demands of gymnastic-style impact landings. *Sports Medicine, Arthroscopy, Rehabilitation, Therapy & Technology*, 4(1), 4.

16

Goldberg, D. E., & Holland, J. H. (1988). Genetic algorithms and machine learning. *Machine learning*, 3(2), 95–99.

73

Goodrich, M. A., & Schultz, A. C. (2007). Human-robot interaction: a survey. *Foundations and trends in human-computer interaction*, 1(3), 203–275.

17

Hartenberg, R. S., & Denavit, J. (1955). A kinematic notation for lower pair mechanisms based on matrices. *Journal of applied mechanics*, 77(2), 215–221.

139

Hollerbach, J. M., & Suh, K. C. (1987). Redundancy resolution of manipulators through torque optimization. *Robotics and Automation, IEEE Journal of*, 3(4), 308–316.

20

Höysniemi, J., Hämäläinen, P., Turkki, L., & Rouvi, T. (2005). Children’s intuitive gestures in vision-based action games. *Communications of the ACM*, 48(1), 44–50.

17

IEEE Spectrum. (2016). *Nasa’s valkyrie humanoid upgraded, delivered to robotics labs in u.s. and europe*. Website. Retrieved 2016, from <http://spectrum.ieee.org/autotom/robotics/humanoids/new-r5-valkyrie-robots>

10

Jensen, R. K. (1978). Estimation of the biomechanical properties of three body types using a photogrammetric method. *Journal of biomechanics*, 11(8-9), 349–358.

38

Jovanovic, K., Potkonjak, V., & Holland, O. (2014). Dynamic modeling of an anthropomorphic robot in contact tasks. *Advanced Robotics*, 28(11), 793–806.

53

Kaneko, K., Harada, K., Kanehiro, F., Miyamori, G., & Akachi, K. (2008). Humanoid robot hrp-3. In *Intelligent robots and systems, 2008. iros 2008. ieee/rsj international conference on* (pp. 2471–2478).

9

Kaneko, K., Kanehiro, F., & Kajita, S. (2004). Humanoid robot hrp-2. In *International conference on robotics and automation* (pp. 1083–1090).

9

Kaneko, K., Kanehiro, F., Morisawa, M., Miura, K., Nakaoka, S., & Kajita, S. (2009). Cybernetic human hrp-4c. In *Humanoid robots, 2009. humanoids 2009. 9th ieee-ras international conference on* (pp. 7–14).

9

Khalil, W., & Creusot, D. (1997). Symoro+: a system for the symbolic modelling of robots. *Robotica*, *15*, 153–161.

46, 61

Khalil, W., & Dombre, E. (2004). *Modeling, identification and control of robots*. Butterworth-Heinemann.

65, 137

Khalil, W., & Dombre, E. (2007). Robot manipulators: modeling, performance analysis and control. *London, UK, ISTE Ltd*.

140

Khalil, W., & Kleinfinger, J. (1986). A new geometric notation for open and closed-loop robots. In *Robotics and automation. proceedings. 1986 ieee international conference on* (Vol. 3, pp. 1174–1179).

3, 36

Khatib, O., Demircan, E., De Sapiro, V., Sentis, L., Besier, T., & Delp, S. (2009). Robotics-based synthesis of human motion. *Journal of Physiology-Paris*, *103*(3), 211–219.

2, 20

Kirk, A. G., O'Brien, J. F., & Forsyth, D. A. (2005). Skeletal parameter estimation from optical motion capture data. In *Computer vision and pattern recognition, 2005. cvpr 2005. ieee computer society conference on* (Vol. 2, pp. 782–788).

11

Klette, R., & Tee, G. (2008). Understanding human motion: A historic review. In *Human motion* (pp. 1–22). Springer.

15

Klir, G., & Yuan, B. (1995). *Fuzzy sets and fuzzy logic* (Vol. 4). Prentice hall New Jersey.

92

Klopčar, N., & Lenarčič, J. (2006). Bilateral and unilateral shoulder girdle kinematics during humeral elevation. *Clinical Biomechanics*, *21*, S20–S26.

12

Koehler, T., Pruzinec, M., Feldmann, T., & Wörner, A. (2008). Automatic human model parametrization from 3d marker data for motion recognition. In *Proceedings of wscg*.

11

- Koganezawa, K., Takanishi, A., & Sugano, S. (1991). Development of waseda robot: The study of biomechanisms and kato laboratory. *Ichiro Kato Laboratory*, 8
- Krüger, J., Schreck, G., & Surdilovic, D. (2011). Dual arm robot for flexible and cooperative assembly. *CIRP Annals-Manufacturing Technology*, 60(1), 5–8.
3, 26
- Kulic, D., & Nakamura, Y. (2008). Scaffolding on-line segmentation of full body human motion patterns. In *Intelligent robots and systems, 2008. iros 2008. ieee/rsj international conference on* (pp. 2860–2866).
31
- Kulić, D., Ott, C., Lee, D., Ishikawa, J., & Nakamura, Y. (2012). Incremental learning of full body motion primitives and their sequencing through human motion observation. *The International Journal of Robotics Research*, 31(3), 330–345.
31
- Kulic, D., Takano, W., & Nakamura, Y. (2008). Combining automated on-line segmentation and incremental clustering for whole body motions. In *Robotics and automation, 2008. icra 2008. ieee international conference on* (pp. 2591–2598).
31
- Kulić, D., Takano, W., & Nakamura, Y. (2008). Incremental learning, clustering and hierarchy formation of whole body motion patterns using adaptive hidden markov chains. *The International Journal of Robotics Research*, 27(7), 761–784.
31
- Kulic, D., Takano, W., & Nakamura, Y. (2009). Online segmentation and clustering from continuous observation of whole body motions. *IEEE Transactions on Robotics*, 25(5), 1158–1166.
31
- Kurazume, R., & Hasegawa, T. (2006). A new index of serial-link manipulator performance combining dynamic manipulability and manipulating force ellipsoids. *IEEE transactions on robotics*, 22(5), 1022–1028.
23
- Lahr, D., & Hong, D. (2008). Development of charli: a linear actuator powered full size humanoid robot. In *International conference on ubiquitous robots and ambient intelligence, seoul, s. korea*.
9
- Lardy, J., Beurier, G., & Wang, X. (2012). Effects of rotation amplitude on arm movement when rotating a spherical object. *Ergonomics*, 55(12), 1524–1534.
21
- Lee, C.-C. (1990). Fuzzy logic in control systems: fuzzy logic controller. i. *IEEE Transactions on systems, man, and cybernetics*, 20(2), 404–418.
91

- Lee, D., & Nakamura, Y. (2014). Motion recognition and recovery from occluded monocular observations. *Robotics and Autonomous Systems*, 62(6), 818–832.
31
- Lee, D., Ott, C., & Nakamura, Y. (2010). Mimetic communication model with compliant physical contact in human—humanoid interaction. *The International Journal of Robotics Research*, 29(13), 1684–1704.
17
- Lee, S. (1989). Dual redundant arm configuration optimization with task-oriented dual arm manipulability. *IEEE Transactions on Robotics and Automation*, 5(1), 78–97.
23
- Lee, S. H. (2008). *Biomechanical modeling and control of the human body for computer animation*. ProQuest.
xii, 12, 13
- Lenarcic, J., & Stanisic, M. (2003). A humanoid shoulder complex and the humeral pointing kinematics. *IEEE Transactions on Robotics and Automation*, 19(3), 499–506.
12
- Lenarcic, J., & Umek, A. (1994). Simple model of human arm reachable workspace. *IEEE Transactions on Systems, Man, and Cybernetics*, 24(8), 1239–1246.
12
- Liu, C. K., Hertzmann, A., & Popović, Z. (2005). Learning physics-based motion style with nonlinear inverse optimization. *ACM Transactions on Graphics (TOG)*, 24(3), 1071–1081.
22
- Lohmeier, S., Buschmann, T., & Ulbrich, H. (2009). Humanoid robot lola. In *Robotics and automation, 2009. icra'09. ieee international conference on* (pp. 775–780).
9
- Ma, L. (2009). *Contributions pour l'analyse ergonomique de mannequins virtuels* (Unpublished doctoral dissertation). Nantes.
13
- Ma, L., Chablat, D., Bennis, F., Zhang, W., & Guillaume, F. (2010). A new muscle fatigue and recovery model and its ergonomics application in human simulation. *Virtual and Physical Prototyping*, 5(3), 123–137.
23
- Mansard, N., & Chaumette, F. (2007). Task sequencing for high-level sensor-based control. *IEEE Transactions on Robotics*, 23(1), 60–72.
63
- Marques, H. G., Jäntschi, M., Wittmeier, S., Holland, O., Alessandro, C., Diamond, A., . . . Knight, R. (2010). Ecce1: The first of a series of anthropomorphic musculoskeletal upper torsos. In *Humanoid robots (humanoids), 2010 10th ieee-ras international*

conference on (pp. 391–396).

13

Metta, G., Sandini, G., Vernon, D., Natale, L., & Nori, F. (2008). The icub humanoid robot: an open platform for research in embodied cognition. In *Proceedings of the 8th workshop on performance metrics for intelligent systems* (pp. 50–56).

9

Miller, N., Jenkins, O. C., Kallmann, M., & Mataric, M. J. (2004). Motion capture from inertial sensing for untethered humanoid teleoperation. In *Humanoid robots, 2004 4th IEEE/RAS International Conference on* (Vol. 2, pp. 547–565).

32

Moeslund, T. B., & Granum, E. (2001). A survey of computer vision-based human motion capture. *Computer vision and image understanding*, 81(3), 231–268.

32

Mombaur, K., Laumond, J.-P., & Yoshida, E. (2008). An optimal control model unifying holonomic and nonholonomic walking. In *Humanoid robots, 2008. humanoids 2008. 8th IEEE-RAS International Conference on* (pp. 646–653).

2, 4, 20

Mombaur, K., Truong, A., & Laumond, J.-P. (2010). From human to humanoid locomotion—an inverse optimal control approach. *Autonomous robots*, 28(3), 369–383.

2, 4, 20

Monheit, G., & Badler, N. I. (1990). A kinematic model of the human spine and torso. *Technical Reports (CIS)*, 746.

12

Moré, J. J., & Sorensen, D. C. (1983). Computing a trust region step. *SIAM Journal on Scientific and Statistical Computing*, 4(3), 553–572.

43

Mühlig, M., Gienger, M., & Steil, J. J. (2012). Interactive imitation learning of object movement skills. *Autonomous Robots*, 32(2), 97–114.

56

Naaim, A. (2016). *Advanced kinematics and dynamics of the upper limb for clinical evaluation* (Unpublished doctoral dissertation). Université de Lyon.

12

Nakamura, Y., Yamane, K., Fujita, Y., & Suzuki, I. (2005). Somatosensory computation for man-machine interface from motion-capture data and musculoskeletal human model. *IEEE Transactions on Robotics*, 21(1), 58–66.

12

Nakazawa, A., Nakaoka, S., Ikeuchi, K., & Yokoi, K. (2002). Imitating human dance motions through motion structure analysis. In *Intelligent robots and systems, 2002. IEEE/RSJ International Conference on* (Vol. 3, pp. 2539–2544).

31

- Nelson, G., Saunders, A., Neville, N., Swilling, B., Bondaryk, J., Billings, D., . . . Raibert, M. (2012). Petman: A humanoid robot for testing chemical protective clothing. *Journal of the Robotics Society of Japan*, 30(4), 372–377.
9
- Nenchev, D. N., Tsumaki, Y., & Uchiyama, M. (2000). Singularity-consistent parameterization of robot motion and control. *The International Journal of Robotics Research*, 19(2), 159–182.
65
- Orfanidis, S. J. (1995). *Introduction to signal processing*. Prentice-Hall, Inc.
44, 56
- Ott, C., Lee, D., & Nakamura, Y. (2008). Motion capture based human motion recognition and imitation by direct marker control. In *Humanoid robots, 2008. humanoids 2008. 8th IEEE-RAS International Conference on* (pp. 399–405).
2, 17
- Pamanes, G., & Zegloul, S. (1991). Optimal placement of robotic manipulators using multiple kinematic criteria. In *Robotics and automation, 1991. proceedings., 1991 IEEE International Conference on* (pp. 933–938).
20
- Park, I.-W., Hong, Y.-D., Lee, B.-J., & Kim, J.-H. (2012). Generating optimal trajectory of humanoid arm that minimizes torque variation using differential dynamic programming. In *Robotics and automation (ICRA), 2012 IEEE International Conference on* (pp. 1316–1321).
20
- Park, J., Choi, Y., Chung, W. K., & Youm, Y. (2001). Multiple tasks kinematics using weighted pseudo-inverse for kinematically redundant manipulators. In *Robotics and automation, 2001. proceedings 2001 ICRA. IEEE International Conference on* (Vol. 4, pp. 4041–4047).
64
- Pearsall, D. J., & Reid, G. (1994). The study of human body segment parameters in biomechanics. *Sports Medicine*, 18(2), 126–140.
10
- Peiper, D. L. (1968). *The kinematics of manipulators under computer control* (Tech. Rep.). DTIC Document.
12
- Pollard, N. S., Hodgins, J. K., Riley, M. J., & Atkeson, C. G. (2002). Adapting human motion for the control of a humanoid robot. In *Robotics and automation, 2002. proceedings. ICRA'02. IEEE International Conference on* (Vol. 2, pp. 1390–1397).
18
- Potkonjak, V., Popović, M., Lazarević, M., & Sinanović, J. (1998). Redundancy problem in writing: from human to anthropomorphic robot arm. *Systems, Man, and*

Cybernetics, Part B: Cybernetics, IEEE Transactions on, 28(6), 790–805.

22

Powell, M. J. (1978a). The convergence of variable metric methods for non-linearly constrained optimization calculations. *Nonlinear programming*, 3.

43

Powell, M. J. (1978b). A fast algorithm for nonlinearly constrained optimization calculations. In *Numerical analysis* (pp. 144–157). Springer.

43, 44

Ruchanurucks, M. (2015). Humanoid robot upper body motion generation using b-spline-based functions. *Robotica*, 33(04), 705–720.

56

Rueckert, E., Mundo, J., Paraschos, A., Peters, J., & Neumann, G. (2015). Extracting low-dimensional control variables for movement primitives. In *Robotics and automation (icra), 2015 IEEE international conference on* (pp. 1511–1518).

31

Safonova, A., Pollard, N., & Hodgins, J. K. (2003). Optimizing human motion for the control of a humanoid robot. *Proc. Applied Mathematics and Applications of Mathematics*, 78.

18, 55

Schmidt, R., Disselhorst-Klug, C., Silny, J., & Rau, G. (1999). A marker-based measurement procedure for unconstrained wrist and elbow motions. *Journal of Biomechanics*, 32(6), 615–621.

12

Siciliano, B., Sciavicco, L., Villani, L., & Oriolo, G. (2010). *Robotics: modelling, planning and control*. Springer Science & Business Media.

40, 43, 137

Spong, M. W., Hutchinson, S., & Vidyasagar, M. (2006). *Robot modeling and control* (Vol. 3). Wiley New York.

140

Suleiman, W., Yoshida, E., Kanehiro, F., Laumond, J.-P., & Monin, A. (2008). On human motion imitation by humanoid robot. In *Robotics and automation, 2008. icra 2008. IEEE international conference on* (pp. 2697–2704).

2, 17

Syamsuddin, M. R., & Kwon, Y.-M. (2011). Simulation of baseball pitching and hitting on virtual world. In *Complex, intelligent and software intensive systems (cisis), 2011 international conference on* (pp. 663–667).

16

Takano, W., Imagawa, H., & Nakamura, Y. (2011). Prediction of human behaviors in the future through symbolic inference. In *Robotics and automation (icra), 2011 IEEE international conference on* (pp. 1970–1975).

- Terlemez, Ö., Ulbrich, S., Mandery, C., Do, M., Vahrenkamp, N., & Asfour, T. (2014). Master motor map (mmm)—framework and toolkit for capturing, representing, and reproducing human motion on humanoid robots. In *Humanoid robots (humanoids), 2014 14th ieee-ras international conference on* (pp. 894–901).
- 35
- Tomić, M., Chevallereau, C., Potkonjak, V., Jovanović, K., & Rodić, A. (2018). Human to humanoid motion conversion for dual arm manipulation tasks. *Robotica*.
- 5, 83
- Tomić, M., Jovanović, K., Chevallereau, C., Potkonjak, V., & Rodić, A. (2018). Toward optimal mapping of human dual-arm motion to humanoid motion for tasks involving contact with the environment. *International Journal of Advanced Robotic Systems*, 15(1), 1729881418757377.
- 5
- Tomić, M., Vassallo, C., Chevallereau, C., Rodić, A., & Potkonjak, V. (2016). Arm motions of a humanoid inspired by human motion. In *New trends in medical and service robots* (pp. 227–238). Springer.
- 2, 5, 20, 22, 62
- Trigueiros, P., Ribeiro, A., & Reis, L. P. (2013). Vision-based gesture recognition system for humancomputer interaction. *Computational Vision and Medical Image Processing IV: VIPIMAGE, 2013*, 137–142.
- 17
- Tso, S., & Liu, K. (1996). Hidden markov model for intelligent extraction of robot trajectory command from demonstrated trajectories. In *Industrial technology, 1996.(icit'96), proceedings of the ieee international conference on* (pp. 294–298).
- 19
- Ude, A. (1993). Trajectory generation from noisy positions of object features for teaching robot paths. *Robotics and Autonomous Systems*, 11(2), 113–127.
- 19
- Ude, A., Atkeson, C. G., & Riley, M. (2004). Programming full-body movements for humanoid robots by observation. *Robotics and autonomous systems*, 47(2), 93–108.
- xii, 2, 3, 18, 41, 48, 50
- Ude, A., Man, C., Riley, M., & Atkeson, C. G. (2000). *Automatic generation of kinematic models for the conversion of human motion capture data into humanoid robot motion* (Tech. Rep.). Georgia Institute of Technology.
- xiii, 2, 18, 41, 43, 44, 48, 51
- Vahrenkamp, N., Asfour, T., Metta, G., Sandini, G., & Dillmann, R. (2012). Manipulability analysis. In *2012 12th ieee-ras international conference on humanoid robots (humanoids 2012)* (pp. 568–573).

23

Vasavada, A. N., Li, S., & Delp, S. L. (1998). Influence of muscle morphometry and moment arms on the moment-generating capacity of human neck muscles. *Spine*, 23(4), 412–422.

13

Vlasic, D., Adelsberger, R., Vannucci, G., Barnwell, J., Gross, M., Matusik, W., & Popović, J. (2007). Practical motion capture in everyday surroundings. In *Acm transactions on graphics (tog)* (Vol. 26, p. 35).

32

Vøllestad, N. K. (1997). Measurement of human muscle fatigue. *Journal of neuroscience methods*, 74(2), 219–227.

17

Wampler, C. W. (1986). Manipulator inverse kinematic solutions based on vector formulations and damped least-squares methods. *IEEE Transactions on Systems, Man, and Cybernetics*, 16(1), 93–101.

54

Wang, L.-X., & Mendel, J. M. (1992). Fuzzy basis functions, universal approximation, and orthogonal least-squares learning. *IEEE transactions on Neural Networks*, 3(5), 807–814.

91

Wenger, P. (2010). Performance analysis of robots. In *Modeling, performance analysis and control of robots manipulators* (pp. 141–183). Iste.

54

Whitney, D. E. (1969). Resolved motion rate control of manipulators and human prostheses. *IEEE Transactions on man-machine systems*, 10(2), 47–53.

61, 63

Wimböck, T., Nenchev, D., Albu-Schäffer, A., & Hirzinger, G. (2009). Experimental study on dynamic reactionless motions with dlr's humanoid robot justin. In *Intelligent robots and systems, 2009. iros 2009. ieee/rsj international conference on* (pp. 5481–5486).

10

Wu, G., Siegler, S., Allard, P., Kirtley, C., Leardini, A., Rosenbaum, D., ... others (2002). Isb recommendation on definitions of joint coordinate system of various joints for the reporting of human joint motion—part i: ankle, hip, and spine. *Journal of biomechanics*, 35(4), 543–548.

11

Wu, G., Van der Helm, F. C., Veeger, H. D., Makhsous, M., Van Roy, P., Anglin, C., ... others (2005). Isb recommendation on definitions of joint coordinate systems of various joints for the reporting of human joint motion—part ii: shoulder, elbow, wrist and hand. *Journal of biomechanics*, 38(5), 981–992.

- 11
- Yang, F., Ding, L., Yang, C., & Yuan, X. (2005). An algorithm for simulating human arm movement considering the comfort level. *Simulation Modelling Practice and Theory*, 13(5), 437–449.
- 22
- Yang, J., Abdel-Malek, K., & Nebel, K. (2003). *The reach envelope of a 9 degree-of-freedom model of the upper extremity* (Tech. Rep.). DTIC Document.
- 12
- Yang, J., Marler, R. T., Kim, H., Arora, J., & Abdel-Malek, K. (2004). Multi-objective optimization for upper body posture prediction. In *10th aiaa/issmo multidisciplinary analysis and optimization conference* (Vol. 30).
xii, 3, 13, 21, 22, 23, 62
- Yavorskii, A., Sologubov, E., & Nemkova, S. (2003). Analysis of gait in patients with different forms of infantile cerebral paralysis. *Biomedical Engineering*, 37(6), 322–327.
- 16
- Yokoyama, K., Handa, H., Isozumi, T., Fukase, Y., Kaneko, K., Kanehiro, F., ... Hirukawa, H. (2003). Cooperative works by a human and a humanoid robot. In *Robotics and automation, 2003. proceedings. icra'03. ieee international conference on* (Vol. 3, pp. 2985–2991).
- 19
- Yoshikawa, T. (1984). Analysis and control of robot manipulators with redundancy. In *Robotics research: the first international symposium* (pp. 735–747).
- 23
- Yoshikawa, T. (1985). Dynamic manipulability of robot manipulators. In *Robotics and automation. proceedings. 1985 ieee international conference on* (Vol. 2, pp. 1033–1038).
- 23
- Zanchettin, A. M., Rocco, P., Bascetta, L., Symeonidis, I., & Peldschus, S. (2011). Kinematic analysis and synthesis of the human arm motion during a manipulation task. In *Robotics and automation (icra), 2011 ieee international conference on* (pp. 2692–2697).
xii, 11
- Zeghloul, S., & Pamanes-Garcia, J.-A. (1993). Multi-criteria optimal placement of robots in constrained environments. *Robotica*, 11(02), 105–110.
- 20
- Zhang, Y., Li, J., & Zhang, Z. (2013). A time-varying coefficient-based manipulability-maximizing scheme for motion control of redundant robots subject to varying joint-velocity limits. *Optimal Control Applications and Methods*, 34(2), 202–215. doi: 10.1002/oca.2017

Zheng, Y., & Yamane, K. (2013). Human motion tracking control with strict contact force constraints for floating-base humanoid robots. In *Humanoid robots (humanoids), 2013 13th IEEE-RAS International Conference on* (pp. 34–41).

2, 20

Zhou, H., & Hu, H. (2008). Human motion tracking for rehabilitation—a survey. *Biomedical Signal Processing and Control*, 3(1), 1–18.

32

Zöllner, R., Asfour, T., & Dillmann, R. (2004). Programming by demonstration: dual-arm manipulation tasks for humanoid robots. In *Iros* (pp. 479–484).

3, 25



ROMEO robot motor information

Table A.1: The information of robot ROMEO motors

| Joint name | Motor | Reduction | Robot Inertia [gcm^2] |
|---------------|--------------------------|-----------|----------------------------------|
| NeckYaw | RE25_339156 | 150.2680 | 13.9 |
| NeckPitch | RE25_339156 | 143.2200 | 13.9 |
| HeadPitch | RE-max24_222055 | 130.8480 | 4.11 |
| HeadRoll | RE-max24_222055 | 201.3050 | 4.11 |
| ShoulderPitch | RE25_339156 | 135.5800 | 13.9 |
| ShoulderYaw | RE25_339156 | 85.6300 | 13.9 |
| ElbowRoll | RE25_339156 | 85.6300 | 13.9 |
| ElbowYaw | RE25_339156 | 85.2400 | 13.9 |
| WristRoll | | | |
| WristYaw | RE25_339156 | 50.6100 | 13.9 |
| WristPitch | RE25_339156 | 36.2500 | 13.9 |
| BaseX | Joints are underactuated | | |
| BaseY | | | |
| BaseZ | | | |
| BaseYaw | | | |
| BaseRoll | | | |
| BasePitch | | | |
| TrunkYaw | | | |
| TrunkYaw | | | |



Hanavan model of the human body

B.1 Modified Hanavan parameters

Table B.1: Anthropometric parameters used in the Modified Hanavan model

| No | Parameter | No | Parameter |
|----|--|----|---|
| 1 | Length, Hand | 21 | Circumference, Toe |
| 2 | Length, Wrist to Knuckle | 22 | Circumference, Ankle |
| 3 | Length, Forearm | 23 | Circumference, Shank |
| 4 | Length, Upperarm | 24 | Circumference, Knee |
| 5 | Length, Elbow to Acromion | 25 | Circumference, Upper Thigh |
| 6 | Length, Foot | 26 | Circumference, Head |
| 7 | Length, Shank | 27 | Circumference, Chest |
| 8 | Length, Thigh | 28 | Circumference, Xyphion Level |
| 9 | Length, Head | 29 | Circumference, Omphalion Level |
| 10 | Length, Upper Trunk | 30 | Circumference, Buttock |
| 11 | Length, Xyphion to Acromion Level | 31 | Width, Hand |
| 12 | Length, Middle Trunk | 32 | Width, Wrist |
| 13 | Length, Lower Trunk | 33 | Width, Foot |
| 14 | Circumference, Fist | 34 | Width, Toe |
| 15 | Circumference, Wrist | 35 | Depth, Hip |
| 16 | Circumference, Forearm | 36 | Width, Chest |
| 17 | Circumference, Elbow | 37 | Width, Xyphion Level |
| 18 | Circumference, Axillary Arm | 38 | Width, Omphalion Level |
| 19 | Circumference, Foot | 38 | Width, Coxae |
| 20 | Circumference, Ball of Foot | 40 | Length, Xyphion Level to Chin/Neck Intersection |
| 41 | Length, Hip to Chin/Neck Intersection = $P_{12} + P_{13} + P_{40}$ | | |

Table B.2: Mass prediction equations

| Segment | Prediction Equation |
|----------|---|
| Hand | $m = 0.038 \cdot P_{15} + 0.080 \cdot P_{32} - 0.660$ |
| Forearm | $m = 0.081 \cdot M + 0.052 \cdot P_{16} - 1.650$ |
| Upperarm | $m = 0.007 \cdot M + 0.092 \cdot P_{18} + 0.050 \cdot P_5 - 3.101$ |
| Foot | $m = 0.003 \cdot M + 0.048 \cdot P_{22} + 0.027 \cdot P_6 - 0.869$ |
| Shank | $m = 0.135 \cdot P_{23} - 1.318$ |
| Thigh | $m = 0.074 \cdot M + 0.138 \cdot P_{25} - 4.641$ |
| Head | $m = 0.104 \cdot P_{26} + 0.015 \cdot M - 2.189$ |
| Trunk | $m_{WT} = 0.349 \cdot M + 0.423 \cdot P_{41} + 0.229 \cdot P_{27} - 35.460$ |

M= whole-body mass P_i =anthropometric parameters shown in Table B.1

The whole trunk mass m_{WT} is calculated from the prediction equation while those of the individual segments are calculated based on the volumes and the density factors (0.92 for the upper trunk and 1.01 for both middle and lower trunks) of the trunk segments:

$$sf = \frac{m_{WT}}{0.92 \cdot V_{UT} + 1.01 \cdot (V_{MT} + V_{LT})} \quad (B.1)$$

$$m_{UT} = 0.92 \cdot V_{UT} \cdot sf \quad (B.2)$$

$$m_{MT} = 1.01 \cdot V_{MT} \cdot sf \quad (B.3)$$

$$m_{LT} = 1.01 \cdot V_{LT} \cdot sf \quad (B.4)$$

$$(B.5)$$

where UT, MT, LT = upper, middle and lower trunk, respectively, m = mass, V = volume, and sf = scaling factor.

Table B.3: Geometric Shapes and Arguments of the BSP Functions

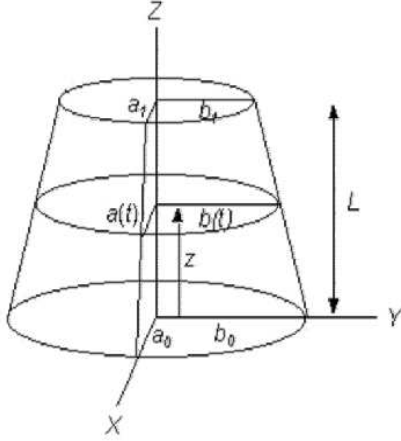
| Segment | Geometric Shape | Group | Arguments of the BSP Functions |
|----------|-----------------------|-------|--|
| Hand | ER | SE | $a_0 = b_0 = \frac{P_{14}}{2\pi}, c_0 = \frac{P_2}{2}$ |
| Forearm | TCC | ES | $a_0 = b_0 = \frac{P_{17}}{2\pi}, a_1 = b_1 = \frac{P_{15}}{2\pi}, L = P_3$ |
| Upperarm | TCC | ES | $a_0 = b_0 = \frac{P_{18}}{2\pi}, a_1 = b_1 = \frac{P_{17}}{2\pi}, L = P_5$ |
| Foot | ES with Circular Base | ES | $a_0 = b_0 = \frac{P_{19}}{2\pi}, a_1 = \frac{P_{33}+P_{34}}{4}, b_1 = \frac{P_{20}+P_{21}}{2\pi}, L = P_6$ |
| Shank | TCC | ES | $a_0 = b_0 = \frac{P_{24}}{2\pi}, a_1 = b_1 = \frac{P_{22}}{2\pi}, L = P_7$ |
| Thigh | ES with Circular Top | ES | $b_0 = \frac{P_{35}}{2}, a_0 = \frac{P_{25}}{\pi} - b_0, a_1 = b_1 = \frac{P_{24}}{2\pi}, L = P_8$ |
| Head | ER | SE | $a_0 = b_0 = \frac{P_{26}}{2\pi}, c_0 = \frac{P_9}{2}$ |
| U Trunk | EC | ES | $a_0 = a_1 = \frac{P_{36}+P_{37}}{4}, b_0 = b_1 = \frac{P_{27}+P_{28}}{2\pi} - a_0, L = P_{11}$ |
| M Trunk | ES | ES | $a_0 = \frac{P_{37}}{2}, a_1 = \frac{P_{38}}{2}, L = P_{12}, b_0 = \frac{P_{28}}{\pi} - a_0, b_1 = \frac{P_{29}}{\pi} - a_1$ |
| L Trunk | EC | ES | $a_0 = a_1 = \frac{P_{38}+P_{39}}{4}, L = P_{13}, b_0 = b_1 = \frac{P_{29}+P_{30}}{2\pi} - a_0$ |

EC = Elliptical Column, ER = Ellipsoid of Revolution, ES = Elliptical Solid, SE = Semi-Ellipsoid,

TCC = Truncated Circular Cone, P_i = anthropometric parameter shown in Table B.1, $a_0, a_1, b_0, b_1, c_0, L$ = symbols used in the BSP equations

B.2 Geometrical shape

Elliptical solid (ES):



$$\text{CoM position} = L \frac{A_2^{ab}}{A_1^{ab}}$$

$$I_{XX} = \frac{1}{4} m \frac{A_4^{abbb}}{A_1^{ab}} + mL^2 \frac{A_3^{ab}}{A_1^{ab}} - m \left(L \frac{A_2^{ab}}{A_1^{ab}} \right)^2$$

$$I_{YY} = \frac{1}{4} m \frac{A_4^{aaab}}{A_1^{ab}} + mL^2 \frac{A_3^{ab}}{A_1^{ab}} - m \left(L \frac{A_2^{ab}}{A_1^{ab}} \right)^2$$

$$I_{ZZ} = \frac{1}{4} m \frac{A_4^{aaab} + A_4^{abbb}}{A_1^{ab}}$$

Notations:

$$\begin{aligned} A_1^{ab} &= \frac{B_1^{ab}}{3} + \frac{B_2^{ab}}{2} + B_3^{ab} \\ A_2^{ab} &= \frac{B_1^{ab}}{4} + \frac{B_2^{ab}}{5} + \frac{B_3^{ab}}{2} \\ A_3^{ab} &= \frac{B_1^{ab}}{5} + \frac{B_2^{ab}}{4} + \frac{B_3^{ab}}{3} \\ A_4^{abcd} &= \frac{B_4^{abcd}}{5} + \frac{B_5^{abcd}}{4} + \frac{B_6^{abcd}}{3} + \frac{B_7^{abcd}}{2} + B_8^{abcd} \end{aligned} \quad (\text{B.6})$$

$$B_1^{ab} = (a_1 - a_0)(b_1 - b_0)$$

$$B_2^{ab} = a_0(b_1 - b_0) + b_0(a_1 - a_0)$$

$$B_3^{ab} = a_0 b_0$$

$$B_4^{abcd} = (a_1 - a_0)(b_1 - b_0)(c_1 - c_0)(d_1 - d_0)$$

$$B_5^{abcd} = a_0(b_1 - b_0)(c_1 - c_0)(d_1 - d_0) + b_0(a_1 - a_0)(c_1 - c_0)(d_1 - d_0)$$

$$+ c_0(b_1 - b_0)(a_1 - a_0)(d_1 - d_0) + d_0(a_1 - a_0)(b_1 - b_0)(c_1 - c_0)$$

$$B_6^{abcd} = a_0 b_0 (c_1 - c_0)(d_1 - d_0) + a_0 c_0 (b_1 - b_0)(d_1 - d_0) + a_0 d_0 (b_1 - b_0)(c_1 - c_0)$$

$$+ b_0 c_0 (a_1 - a_0)(d_1 - d_0) + b_0 d_0 (a_1 - a_0)(c_1 - c_0) + c_0 d_0 (a_1 - a_0)(b_1 - b_0)$$

$$B_7^{abcd} = b_0 c_0 d_0 (a_1 - a_0) + a_0 c_0 d_0 (b_1 - b_0) + a_0 b_0 d_0 (c_1 - c_0) + a_0 b_0 c_0 (d_1 - d_0)$$

$$B_8^{abcd} = a_0 b_0 c_0 d_0$$

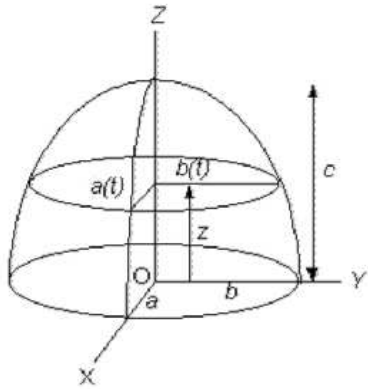
(B.7)

$A_4^{abbb}, B_4^{abbb}, B_5^{abbb}, B_6^{abbb}, B_7^{abbb}, B_8^{abbb}$ are calculated for the equations for $A_4^{abcd}, B_4^{abcd}, B_5^{abcd}, B_6^{abcd}, B_7^{abcd}, B_8^{abcd}$, respectively, where $c = b$ and $d = b$.

On the same way $A_4^{aaab}, B_4^{aaab}, B_5^{aaab}, B_6^{aaab}, B_7^{aaab}, B_8^{aaab}$ are calculated for the equations for

$A_4^{abcd}, B_4^{abcd}, B_5^{abcd}, B_6^{abcd}, B_7^{abcd}, B_8^{abcd}$, respectively, where $b = a, c = a$ and $d = b$.

Semi ellipsoid (SE)



CoM position = $\frac{3}{8}c$

$$I_{XX} = \frac{1}{5}m \left[(b^2 + c^2) - \left(\frac{3}{8}c\right)^2 \right]$$

$$I_{YY} = \frac{1}{5}m \left[(a^2 + c^2) - \left(\frac{3}{8}c\right)^2 \right]$$

$$I_{ZZ} = \frac{1}{5}m(a^2 + b^2)$$

The values a, b, c are equal $a = a_0, b = b_0, c = c_0$ and are taken from the Table B.3.



Quaternions

The unit quaternion is representation of Euler parameters which used four parameters to express the orientation. The quaternion is useful tools for calculation the orientation with avoiding the singularity. The calculation of quaternion from the cosine transformation matrix and algebraic properties of quaternion are proposed in (Khalil & Dombre, 2004) and (Siciliano et al., 2010).

Quaternions describe the orientation by a rotation of an angle θ ($0 \leq \theta \leq \pi$) above an axis of unit vector $u = [u_x \ u_y \ u_z]^T$ (Khalil & Dombre, 2004). The quaternion is defined as:

$$\begin{aligned} Q_1 &= \cos\left(\frac{\theta}{2}\right) \\ Q_2 &= u_x \sin\left(\frac{\theta}{2}\right) \\ Q_3 &= u_y \sin\left(\frac{\theta}{2}\right) \\ Q_4 &= u_z \sin\left(\frac{\theta}{2}\right) \end{aligned} \tag{C.1}$$

The condition which must be obtained is:

$$Q_1^2 + Q_2^2 + Q_3^2 + Q_4^2 = 1 \tag{C.2}$$

The angle θ and unit vector u are calculate using the angle/axis representation of rotation matrix. If the R is rotation matrix represent as:

$$R = \begin{bmatrix} s_x & n_x & a_x \\ s_y & n_y & a_y \\ s_z & n_z & a_z \end{bmatrix} \tag{C.3}$$

Then the

$$\begin{aligned}\cos(\theta) &= \frac{1}{2}(s_x + n_y + a_z - 1) \\ \sin(\theta) &= \frac{1}{2}\sqrt{(n_z - a_y)^2 + (a_x - s_z)^2 + (s_y - n_x)^2}\end{aligned}\tag{C.4}$$

From the equations (C.4) it is easy to calculate angle θ as:

$$\theta = a \tan 2(\sin(\theta), \cos(\theta))\tag{C.5}$$

with $0 \leq \theta \leq \pi$

u_x, u_y, u_z are calculated using equation:

$$\begin{aligned}u_x &= (n_z - a_y)/(2 \sin(\theta)) \\ u_y &= (a_x - s_z)/(2 \sin(\theta)) \\ u_z &= (s_y - n_x)/(2 \sin(\theta))\end{aligned}\tag{C.6}$$

if $\sin(\theta) \neq 0$

When $\sin(\theta)$ is small, the element u_x, u_y, u_z cannot be determined with good accuracy by this equation. In a case where $\cos(\theta) < 0$, we obtain u_x, u_y, u_z more accurately using the equation:

$$\begin{aligned}u_x &= \text{sign}(n_z - a_y)/\sqrt{(s_x - \cos(\theta))/(1 - \cos(\theta))} \\ u_y &= \text{sign}(a_x - s_z)/\sqrt{(n_y - \cos(\theta))/(1 - \cos(\theta))} \\ u_z &= \text{sign}(s_y - n_x)/\sqrt{(a_z - \cos(\theta))/(1 - \cos(\theta))}\end{aligned}\tag{C.7}$$

The same quaternion with different sing of all elements gives same transformation matrix.

D

Modified DH parameters of the ROMEO robot

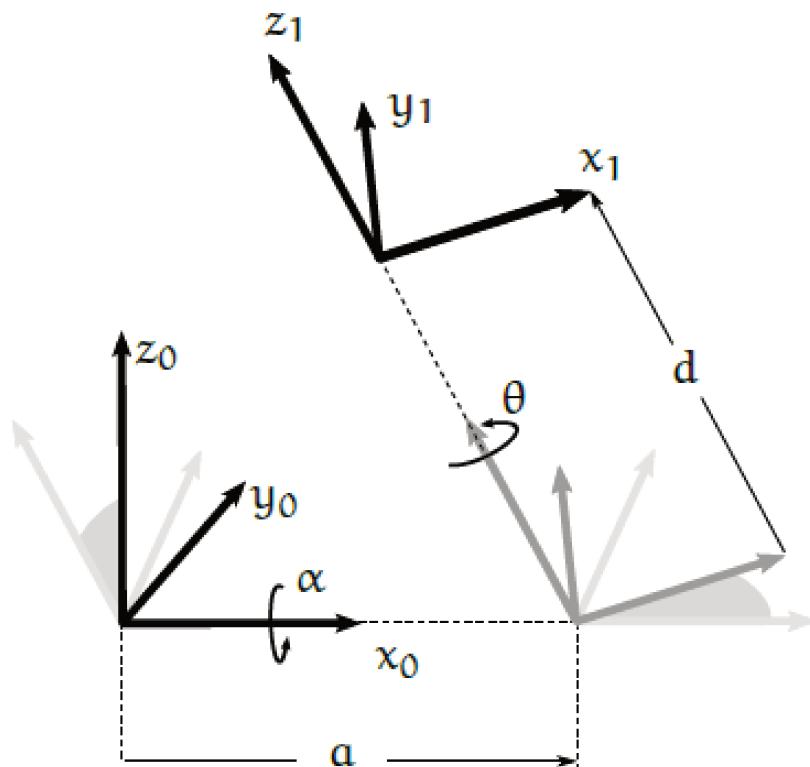


Figure D.1: The transformations described by the modified DH parameters between two joints. First a rotation α is performed around the x axis, followed by a translation a along the x axis; then, a rotation θ is done around the z axis, followed by a translation d along the z (Adorno, 2011).

The DH-method (Hartenberg & Denavit, 1955) provides a matrix notation and ap-

proach for relating the position of a point in one coordinate system to another coordinate system, by using a unique transformation matrix. Such an approach is useful with kinematic systems in which a series of components are connected by joints. A local coordinate system and a local transformation matrix are associated with each joint, describing its configuration with respect to the previous joint and coordinate system. Multiple transformation matrices can be combined to determine the position of any point on the kinematic system with respect to any local coordinate system or with respect to a global coordinate system, based on all of the joint displacements.

Typically, a serial robot is modeled by using the DH convention (Khalil & Dombre, 2007; Spong, Hutchinson, & Vidyasagar, 2006) or modified DH convention (Khalil & Dombre, 2007). Both methods use four parameters to describe the pose of the joint with respect to the previous one in the kinematic chain. The modified DH conversion is used for the purpose of our studies.

In order to define the relationship between the location of joints, we assign a frame T_j attached to each joint j , such that:

- The z_j axis is along the axis of joint j .
- The x_j axis is aligned with the common normal between z_j and z_{j+1} . If z_j and z_{j+1} are parallel or collinear, the choice of x_j is not unique. The intersection of x_j and z_j defined the origin O_j . In the case of the intersecting joints axes, the origin is at the point of intersection of the joint axes.
- The y_j axis is formed by the right-hand rule to complete the coordinate system (x_j, y_j, z_j) .

The transformation matrix from frame T_{j-1} to frame T_j is expressed as a function of the following parameters:

- α_j : the angle between z_{j-1} and z_j about x_{j-1}
- a_j : the distance between z_{j-1} and z_j along x_{j-1}
- θ_j : the angle between x_{j-1} and x_j about z_j
- d_j : the distance between x_{j-1} and x_j along z_j

In Fig. 1 is shown the transformations described by the modified DH parameters between two joints. The variable of joint j , defining the relative orientation or position between joints $j - 1$ and j , is either θ_j or d_j depending on whether the joint is revolute or prismatic, respectively. It is defined by the relation: $q_j = \bar{\sigma}_j \theta_j + \sigma_j d_j$ With:

- $\sigma_j = 0$ if joint is revolute
- $\sigma_j = 1$ if joint is prismatic
- $\bar{\sigma}_j = \sigma_j - 1$

The transformation matrix ${}^{j-1}T_j$ is obtained as:

$${}^{j-1}T_j = \text{rot}(x, \alpha_j) \text{trans}(x, a_j) \text{rot}(z, \theta_j) \text{trans}(z, d_j) \quad (\text{D.1})$$

The humanoid robot is a tree structured robot. Thus, a tree structure has as many main branches as the number of terminal joints. The humanoid robots usually have 5 terminal

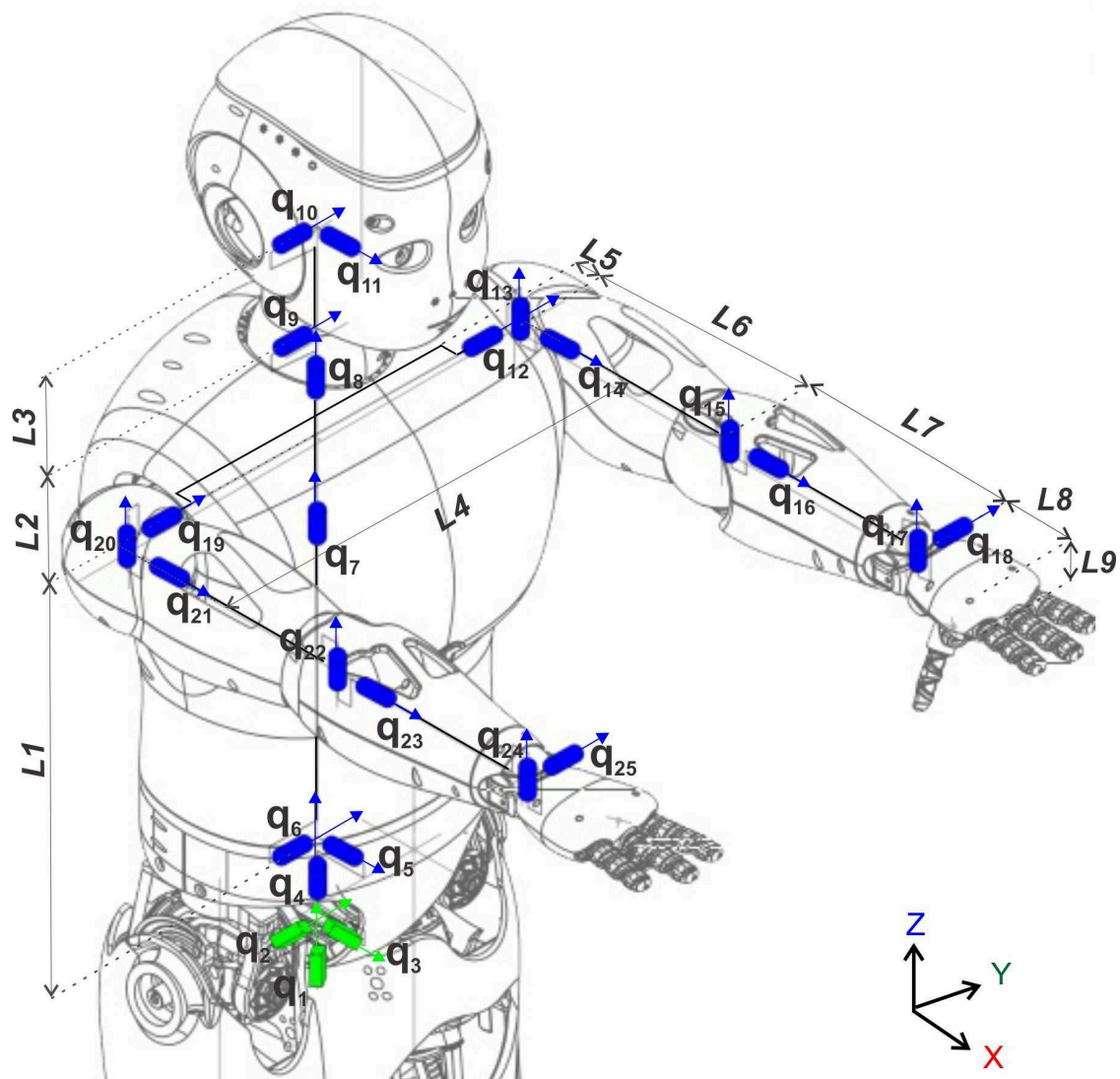


Figure D.2: Kinematic model of for the extended upper body model of the robot ROMEO. 3 translation and 3 rotation joints into the trunk are included in order to estimate motions of legs.

joints (2 feet, 2 hands an head). In the case of the upper body humanoid robot, which is used in our research, kinematic model has 3 terminal joints (2 hands and head) and 3 branches (see Fig. D.2.). Since to the same segments is connected more than one joint the 2 cases are considered for computing the transformation matrix ${}^i T_j$, which defines the location of the frame j relative to antecedent frame $i = ant(j)$:

1. If x_i is along the common normal between z_i and z_j the transformation matrix ${}^i T_j$ is same as the transformation matrix between two consecutive frames of serial structure. It is obtained as a function of the four geometrical parameters $(\alpha_j, a_j, \theta_j, d_j)$.
2. If x_i is not along the common normal between z_i and z_j then the transformation matrix ${}^i T_j$ must be defined using six geometrical parameters. To obtain the six parameters defining frame j relative to frame i , we defined u_j as the common normal between z_i and z_j . The transformation from frame j to frame i can be obtained as a function of the six geometric parameters $(\gamma_j, b_j, \alpha_j, a_j, \theta_j, d_j)$ where:
 - γ_j is the angle between x_i and u_j about z_i
 - b_j is the distance between x_i and u_j along z_i

The transformation matrix ${}^i T_j$ is obtained as:

$${}^{j-1} T_j = rot(z, \gamma_j) trans(z, b_j) rot(x, \alpha_j) trans(x, a_j) rot(z, \theta_j) trans(z, d_j) \quad (D.2)$$

We set $\sigma_j = 2$ to define a frame j with constant position and orientation with respect to their antecedent frame $ant(j)$. The parameter μ gives information about joint activation. If the joint j is activated then $\mu_j = 1$ otherwise $\mu_j = 0$.

The modified DH parameter for the extended upper body model of the robot ROMEO is given in Table D.1.

Table D.1: Modified DH parameters for the extended upper body model of the robot ROME0

| j | ant | μ | σ | γ | b | α | a | θ | d |
|-----|-------|-------|----------|----------|-------|----------|-------|-------------------|-----------|
| 1 | 0 | 1 | 1 | 0 | 0 | 0 | 0 | 0 | q_1 |
| 2 | 1 | 1 | 1 | 0 | 0 | $-\pi/2$ | 0 | $-\pi/2$ | q_2 |
| 3 | 2 | 1 | 1 | 0 | 0 | $-\pi/2$ | 0 | $-\pi/2$ | q_3 |
| 4 | 3 | 1 | 0 | 0 | 0 | $-\pi/2$ | 0 | q_4 | 0 |
| 5 | 4 | 1 | 0 | 0 | 0 | $\pi/2$ | 0 | $\pi/2 + q_5$ | 0 |
| 6 | 5 | 1 | 0 | 0 | 0 | $\pi/2$ | 0 | $\pi/2 + q_5$ | 0 |
| 7 | 6 | 1 | 0 | 0 | 0 | $\pi/2$ | 0 | q_7 | 0 |
| 8 | 7 | 1 | 0 | 0 | 0 | 0 | 0 | q_8 | L_1+L_2 |
| 9 | 8 | 1 | 0 | 0 | 0 | $-\pi/2$ | 0 | $-\pi/2 + q_9$ | 0 |
| 10 | 9 | 1 | 0 | 0 | 0 | 0 | L_3 | q_{10} | 0 |
| 11 | 10 | 1 | 0 | 0 | 0 | $-\pi/2$ | 0 | q_{11} | 0 |
| 12 | 7 | 1 | 0 | 0 | L_1 | $-\pi/2$ | L_5 | q_{12} | $L_4/2$ |
| 13 | 12 | 1 | 0 | 0 | 0 | $\pi/2$ | 0 | $\pi/2 + q_{13}$ | 0 |
| 14 | 13 | 1 | 0 | 0 | 0 | $\pi/2$ | 0 | q_{14} | L_6 |
| 15 | 14 | 1 | 0 | 0 | 0 | $-\pi/2$ | 0 | q_{15} | 0 |
| 16 | 15 | 1 | 0 | 0 | 0 | $\pi/2$ | 0 | q_{16} | L_7 |
| 17 | 16 | 1 | 0 | 0 | 0 | $-\pi/2$ | 0 | $-\pi/2 + q_{17}$ | 0 |
| 18 | 17 | 1 | 0 | 0 | 0 | $-\pi/2$ | 0 | q_{18} | 0 |
| 19 | 7 | 1 | 0 | 0 | L_1 | $-\pi/2$ | L_5 | q_{19} | $-L_4/2$ |
| 20 | 19 | 1 | 0 | 0 | 0 | $\pi/2$ | 0 | $\pi/2 + q_{20}$ | 0 |
| 21 | 20 | 1 | 0 | 0 | 0 | $\pi/2$ | 0 | q_{21} | L_6 |
| 22 | 21 | 1 | 0 | 0 | 0 | $-\pi/2$ | 0 | q_{22} | 0 |
| 23 | 22 | 1 | 0 | 0 | 0 | $\pi/2$ | 0 | q_{23} | L_7 |
| 24 | 23 | 1 | 0 | 0 | 0 | $-\pi/2$ | 0 | $-\pi/2 + q_{24}$ | 0 |
| 25 | 24 | 1 | 0 | 0 | 0 | $-\pi/2$ | 0 | q_{25} | 0 |
| 26 | 25 | 0 | 2 | 0 | 0 | $\pi/2$ | L_8 | 0 | $-L_9$ |
| 27 | 18 | 0 | 2 | 0 | 0 | $\pi/2$ | L_8 | 0 | $-L_9$ |